THE UNIVERSITY OF WESTERN ONTARIO DEPARTMENT OF CIVIL AND ENVIRONMENTAL ENGINEERING

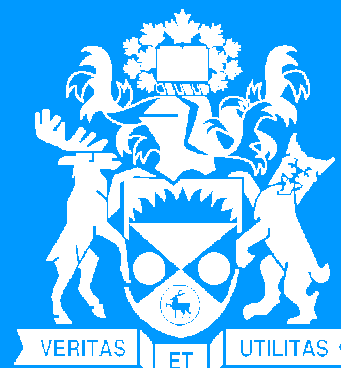## Water Resources Research Report

An Integrated System Dynamics Model for Analyzing Behaviour of the Social-Economic-Climatic System: Model Description and Model Use Guide

By:
Evan G. R. Davies
and
Slobodan P. Simonovic

An Integrated System Dynamics Model for Analyzing Behaviour of the Social-Economic-Climatic System: Model Description and Model Use Guide

by

Evan G. R. Davies and Slobodan P. Simonovic

Email: (edavies7, simonovic)@uwo.ca

Faculty of Engineering Science
The University of Western Ontario
London, Ontario, Canada

April 10, 2008

ABSTRACT

The society-biosphere-climate model described here takes an integrated assessment approach to simulating global change. It consists of eight individual sectors that reproduce the main characteristics of the climate, carbon cycle, economy, land use, population, surface water flow, and water demand and water quality sectors at a global scale, each of which is described individually in the report, both in terms of the theoretical foundation and mathematical basis, and then connected through *feedbacks* to other sectors in order to recreate the whole system. Several of the sectors build on previous modelling work, but their manner of integration is novel, as are the water sectors in particular.

The resulting model is implemented in a system dynamics modelling interface called *Vensim DSS* (Ventana Systems, 2003), which emphasizes the roles of nonlinearity and feedback in determining system behaviour. Both the diagrammatic and mathematical bases of Vensim are described in detail, as are the adjustable components of the model. Several sample experiments are conducted to illustrate the use of Vensim and the analytical tools it provides. The appendices list the model code – as mathematical equations – that forms the basis of the numerical simulations executed with the model, as well as the contents of a CD-ROM version of the model available from the authors, and previous reports in the series.

Key Words: Integrated assessment model; society-biosphere-climate model; model description; system dynamics; Vensim DSS; model code

i

ACKNOWLEDGEMENTS

TABLE OF CONTENTS

LIST OF TABLES

LIST OF FIGURES

1. INTRODUCTION

This report describes a new integrated assessment model of the society-biosphere-climate system, and provides a guide for its use by means of a system dynamics simulation package called *Vensim DSS* (Ventana Systems, 2003). Related publications analyze the general patterns of model behaviour and apply the model to improve both an understanding of nonlinear feedback connections within the modelled and real-world systems, and of their effects on tested socio-economic policy options. This report has many sections in common with Davies (2007), which provides the most complete description of the model and the most detailed analysis of its behaviour and its application to policy development. Davies and Simonovic (2006) represents the first journal publication dealing with the model, and both it and Simonovic and Davies (2006) explain the rationale that underlies the modelling approach. Finally, two companion articles describe and analyze the basic model behaviour (Davies and Simonovic, 2008a) and apply it to water resources policy development (Davies and Simonovic, 2008b).

Chapter 2 of this report discusses individually each of the eight sectors that make up the model, in terms of the theory behind each particular model component and its mathematical basis. Each of these eight, separate accounts describes the basic scientific or socio-economic theory behind the sectoral representation, other models that are similar to the chosen version, and the mathematics and theory that underlie the equations. Next follows a description, again in terms of both theory and mathematics, of the feedback linkages that unite these individual model components into one system. The third section of the chapter highlights novel aspects of the model and of the modelling approach in comparison with other models from the literature, while the fourth section explains the model validation process and compares the model's performance with observed data and with the results of other models.

Chapter 3 describes the implementation of the model in *Vensim DSS*, the program interface and its important features, and the experimental procedure. The first section deals with Vensim's approach to model organization, which consists of two parts: the

qualitative, diagrammatic representation of the modelled system, and the quantitative mathematical equations that determine model behaviour. This diagrammatic component of Vensim illustrates the causal linkages between system components and arranges system components into four fundamental variable types, while the mathematical portion of the model is generally hidden from view (although easily accessible), but determines the quantitative manner in which model elements interact. The second section explains the system dynamics approach toward model calibration and validation and lists adjustable parameters, while the third section discusses the experimentation procedure in system dynamics models and introduces many of the analytical tools available in Vensim.

The first appendix, Appendix A, lists the Vensim code for the model by sector. It also shows the diagrammatic component of each sector for easier replication of the model. Appendix B describes the contents of a model CD-ROM, which contains the model itself, as well as the experiments described in Davies (2007). The CD-ROM is available from the authors by request. Finally, Appendix C lists other reports in this series.

2. MODEL DESCRIPTION

This model reproduces the main characteristics of the climate, carbon cycle, economy, land-use, water demand, water quality, natural hydrological cycle, and population subsystems of the larger society-biosphere-climate system. All of the key processes and characteristics of these sectors, whether socio-economic or physical, are modelled at the global scale, so that simulated values should be understood as broad-scale, aggregate behaviours. This global scale means that caution is required in extrapolating simulated aggregate behaviour to smaller scales and to the real-world – clearly, global population, economic growth, temperature change, and atmospheric carbon dioxide concentration figures, among others, have value, but they do not resolve important regional or national differences. Therefore, any experiments conducted with the model should be understood to represent products of concerted, international action or investigations of uncertainties in large-scale physical processes – see Davies (2007) and the other publications listed in Chapter 1 for examples of such experiments.

At the sectoral, or single-component, level, the model replicates the relevant dynamics of individual elements of the system. At the intersectoral level, the individual model sectors are linked through mathematical feedbacks in order to reproduce important dynamics of the Earth-system. Covering the period from 1960-2100, the model operates at an annual scale, so that it provides a long-term view of the feedback effects of global change, but disregards variations at seasonal or shorter timescales. Several components of the model build on models created by other researchers, while other components are original. Individual sectors are described in the first section below, with a focus on the important internal processes; the theoretical and mathematical basis of each *intersectoral feedback* is then provided in the second section.

In the third section, novel aspects of the model are highlighted, which include original representations of several individual sectors and new approaches to their interconnection. The model is also compared, through intersectoral feedbacks, with a variety of climate

models, integrated assessment models, climate-economy models, hydrological models, and water supply and demand models from the literature.

The last topic of the chapter is model validation. The performance of the model in replicating historical observations is described and compared with the results of other modelling studies, and simulated future values are compared with predictions both from other models and from international organizations, such as the Intergovernmental Panel on Climate Change and the United Nations.

2.1 Individual Model Sectors

Because of the focus on the importance of feedback between model components, individual model sectors are at a level of complexity that captures the major processes and elements that characterize their behaviour. The representation of each component follows a *structural approach*, replicating the important elements or processes of the physical system in question rather than simulating its behaviour through a mathematical, pattern-matching type of behaviour. This structural approach is well-suited to an exploration of feedback-effects between elements of the overall system, because it allows an attribution of system behaviour to real-world characteristics and to the effects of particular feedback relationships within the model.

Since each sector is zero- to one-dimensional, its level of complexity provides both advantages and disadvantages. Here, *dimensionality* refers to the degree of aggregation in a sector, so that zero-dimensional sectors model important characteristics and processes at a global-aggregate level, while one-dimensional sectors have resolution in one spatial direction only – for example, the economy and population sectors produce single, global-aggregate values, and so are considered zero-dimensional, while the oceans are modelled as vertical layers in the carbon cycle and climate system, and terrestrial biomes are separated into six components, and so are one-dimensional representations of these real-world elements. *Lower-resolution models*, such as the individual sectors of this model, produce dynamic behaviour that is relatively easy to understand, and allow

the explicit representation of model feedbacks. Furthermore, they capture the critical elements of each sector and neglect components that have little effect on that sector's behaviour. However, because these models simplify complex systems, and because they often have low spatial resolution, their results are harder to verify against observations, and they run the risk of neglecting important intrasectoral feedbacks or features.

The model described in this report has eight components – climate, carbon cycle, economy, land-use, population, hydrological surface flow, water demand, and water quality – that range in comprehensiveness from the relative simplicity of the population and land-use sectors, to the more complex climate, carbon cycle, and water-related sectors. These sectors, shown in Figure 1, are described below, individually. Details of the figure are described in the subsequent section on intersectoral feedbacks.
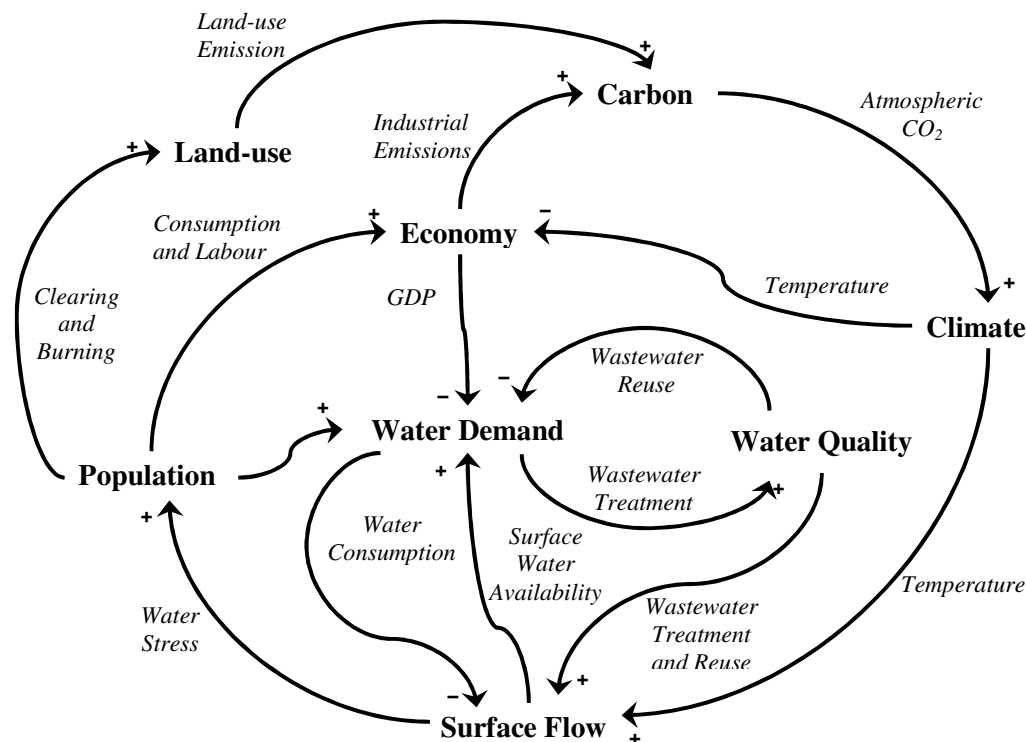
Figure 1: Model feedback structure (after Davies, 2007)

2.1.1 The Climate Sector

In this model, the climate sector simulates the atmospheric and oceanic temperature changes that result from changing atmospheric concentrations of CO_2 caused by human activities. The climate sector is an *upwelling-diffusion energy-balance model* (UD/EBM) that replicates the Box Advection-Diffusion (BAD) model of Harvey and Schneider (1985). Similar to well-known, earlier upwelling-diffusion or box-diffusion models, the BAD model focuses on the role of the oceans in determining the global surface temperature response to climatic forcings, such as changes in anthropogenic greenhouse gas (GHG) emissions. McGuffie and Henderson-Sellers (2005) describe the principles behind energy balance models and box-models in detail.

The BAD model includes the important solar and terrestrial radiative energy exchanges between outer space, the atmosphere, and the oceanic surface layer; the infrared radiative, and latent and sensible heat flows between the earth's surface and the atmosphere; and the diffusive and advective energy transfers within the ocean. As a one-dimensional model, BAD calculates energy transfers, and thus temperature differences, between the atmosphere, ocean surface (or mixed layer), and various ocean depths. The temperature profile it generates at steady state – when external forcings are assumed to equal zero – matches that of the observed oceanic profile quite well. The BAD model also generates good matches to global surface temperature changes predicted by GCMs and other complex models under climatic forcings (Harvey and Schneider, 1985). For example, this reproduction of BAD has a climate sensitivity of roughly 1.8°C for an atmospheric doubling of CO_2, or *2xCO$_2$*, concentrations, and uses a value of 4 W m^{-2} for radiative forcing at 2xCO$_2$. This climate sensitivity lies near the middle of a 1.0°C-4.1°C temperature-change spectrum (Forster and Gregory, 2006). Therefore, if necessary, the forcing response in the climate sector can be adjusted easily through the model's reaction to radiative forcing. For example, the climate sensitivity becomes 2.0°C for a radiative forcing value of 4.37 W m^{-2}, as used in the IPCC SAR, or 1.7°C for forcings of 3.7 W m^{-2} or 3.80 ± 0.33 W m^{-2}, as recommended by the IPCC TAR (Houghton et al., 2001), and the IPCC AR4 (Meehl et al., 2007), respectively.

The version of BAD used in this research applies the constant values of oceanic thermal diffusivity, *K*, and advection velocity, *w*, suggested by Harvey and Schneider (1985). There is one important difference between this reproduction of the model and the original: the system dynamics-based stock-and-flow structure of the model necessitates the conversion of the climate sector from Harvey and Schneider's (1985) temperature-based equations, using *dT/dt*, to an energy-based approach, with energy *stocks* and *flows*, or *E* and *dE/dt*, measured in Joules, and Joules yr^{-1}. Other modifications to the structure of the climate sector are possible, and can lead to different model behaviours. Several modifications to *K* and *w* are described in Harvey and Schneider (1985), while structural changes exist in other upwelling-diffusion models (see Harvey and Huang, 2001, and Joos et al., 1997, for example). However, they are significantly more complicated than BAD and prove essentially irrelevant to the behaviour of the model as a whole, as determined by a Monte Carlo sensitivity analysis described in Davies (2007) and Davies and Simonovic (2008a).

2.1.1.1 Mathematical Representation of the Climate Sector

The major equations for the climate system, and the values of their associated parameters, are provided in this section, beginning with the atmosphere. Again, the equations here are based on the work of Harvey and Schneider (1985), as described above.

For the heat content of the *atmosphere*, the governing equation is,

$$H_A = \int \left(Q_A^* + L_\uparrow - L_\downarrow - L_{out} + H + LE + F \right) \cdot dt \tag{1}$$

where H$_A$ is the heat content of the atmosphere measured in Joules, with an initial value given by $R_A \cdot SA_E \cdot T_{A,0}$, or the atmospheric heat capacity, 1.02 x 10^7 J m^{-2} K^{-1}, multiplied by the surface area of the Earth, 5.1 x 10^{14} m^2, and the initial temperature of the atmosphere, 287.5 K. The other variables are the shortwave (solar) radiation absorbed by the atmosphere, Q$_A^*$, the upward emitted surface longwave (planetary) radiation, L$_\uparrow$, the downward emitted longwave radiation, L$_\downarrow$, the longwave radiation emitted to space from

the top of the atmosphere, L_{out}, and the turbulent sensible and latent heat fluxes, H and LE, respectively. The value used for the shortwave radiation is a constant 66.9 W m^{-2}, while the other flows are calculated according to the following equations. All flows are measured in J yr^{-1}. Note that the last term, F, represents the radiative forcing from anthropogenic greenhouse gases, given by,

$$F = S\left(\frac{C_A}{C_{A0}}\right) - S \tag{2}$$

where F is the climate forcing in W m^{-2}, S is a sort of 'climate sensitivity' constant that relates the change in atmospheric CO_2 concentrations to F, and is set to 4 W m^{-2}, and C_A and C_{A0} represent the current and initial atmospheric carbon dioxide concentrations, respectively. Since equation (2) represents an *intersectoral* feedback, its full explanation is provided in the intersectoral feedback section, below.

For the downward longwave radiation emitted by the atmosphere, Harvey and Schneider (1985) use the Angström formula, which has the following form,

$$L_{\downarrow} = \sigma T_A^{4}\left[0.89 - 0.2\left(10^{-0.07e_a}\right)\right] \tag{3}$$

where σ is the Stefan-Boltzman constant, 5.67 x 10^{-8} J m^{-2} K^{-2}, T_A is the current atmospheric temperature in Kelvin, and e_a is the atmospheric vapour pressure, measured in mbar.

The upward longwave radiation calculation is modelled as the blackbody radiation from the Earth's surface,

$$L_{\uparrow} = \sigma T_S^{4} \tag{4}$$

where T_S is the surface temperature, also referred to as an 'equivalent mixed layer', since the entire planetary surface is treated as a 30 m-deep layer of water – an averaging of the

oceanic 70 m-deep mixed-layer with the thermal inertia of the land surface, which approximates a layer of water 1.7 m deep.

The longwave radiation to space is given by,

$$L_{out} = A + B \cdot T_A - C \cdot F_{CL} \cdot \Delta T_{S,CL} \tag{5}$$

which is a parameterization of the more complex blackbody form. Here, A is set to -251 W m^{-2}, B equals 1.8 W m^{-2} K^{-1}, C is 1.73 W m^{-2} K^{-1}, F_{CL} represents the area-weighted mean annual cloud amount, set to 0.531, and $\Delta T_{S,CL}$ is the surface to cloud-top temperature difference, set to 32.34 K.

The sensible and latent heat fluxes are based on drag laws, and have the following form,

$$H = C_1(T_S - T_A) \tag{6}$$

$$LE = C_2(e_s - e_a) \tag{7}$$

where C_1 equals 12.57 W m^{-2} K^{-1}, C_2 is 11.75 W m^{-2} mbar^{-1}, e_s is the surface saturation vapour pressure at surface temperature T_S, and e_a is the atmospheric vapour pressure using a fixed relative humidity of 0.71. The vapour pressures, e_s and e_a, are multiplied by factors of 1.39 and 1.31, respectively, to account for nonlinearity in the Clausius-Clapeyron relation. Base values for the two vapour pressures were taken from the "Goff-Gratch exact results" for the Clausius-Clapeyron relation, as listed by Lowe (1977).

The equation that governs the *mixed-layer* in the model differs slightly from the equation provided in Harvey and Schneider (1985), although the effect is the same. The heat balance of the mixed-layer is given by,

$$H_M = \int \left(Q_S^* - L_\uparrow + L_\downarrow - H - LE + F_{adv} - F_{diff} \right) \cdot dt \tag{8}$$

where H_M is the heat content of the mixed-layer measured in Joules, with an initial value given by $\rho \cdot c_p \cdot SA_O \cdot h_M \cdot T_{S,0}$, or the density of sea water, 1030 kg m^{-3}, multiplied by the specific heat capacity of water at constant pressure, 4218 J kg^{-1} K^{-1}, the surface area of the ocean, 3.8 x 10^{14} m^2, the equivalent mixed-layer depth, 30 m, and the initial surface temperature, 289.1 K. The new flows included in the equation are the solar radiation absorbed at the Earth's surface, Q_S^*, with a constant value of 168.95 W m^{-2}, the upward advective heat flow in the oceans, F_{adv}, and the downward diffusive heat flow in the oceans, F_{diff}.

In the oceans, advective heat flow represents global water upwelling, while the diffusive flow carries heat downwards into colder parts. Essentially, diffusive flow would homogenize the temperature of the oceans over a long period of time, so that the bottom and surface water would eventually have the same temperature, while advection maintains a temperature gradient between the surface and the bottom of the ocean. Both advective and diffusive heat transfers decrease with depth as the temperature gradient between isothermal oceanic 'layers' becomes less steep.

The heat balance for each *ocean* layer in the model is given by,

$$H_O(h) = \int \left[\left(F_{adv} - F_{diff}\right)_{h+1} + \left(F_{diff} - F_{adv}\right)_{h-1} \right] \cdot dt \tag{9}$$

where $H_O(h)$ is the heat content of the selected oceanic layer, h, while the subscripts on the brackets around the pairs of flows on the right-hand side represent heat outflows from the current layer, h, to the colder, deeper layer, h+1, and heat inflows to the current layer, h, from the warmer, shallower layer, h-1. Recall that advective flows carry heat upwards in the ocean, while diffusive flows transport it downwards.

Advective flows between adjacent isothermal layers take the following general form,

$$F_{adv}(h) = \rho \cdot c_p \cdot SA_O \cdot w \cdot \left(\theta(h) - \theta_B\right) \tag{10}$$

where w is the constant advection velocity, which is set to 4 m yr^{-1}, $\theta(h)$ is the oceanic temperature at the current depth, h, and θ_B is the constant temperature of 'bottom water', set to 274.35 K. Note that a constant advection velocity is assumed in most other upwelling-diffusion models as well – see, for example, Hoffert et al. (1981) and Siegenthaler and Joos (1992).

Diffusive flows between adjacent isothermal layers occur according to the following equation,

$$F_{diff}(h) = -K \cdot SA_O \cdot \frac{(\theta(h+1) - \theta(h))}{d(h)} \tag{11}$$

where K is a diffusivity constant modified from the version of κ used by Harvey and Schneider (1985) and set here to 2000 m^2 yr^{-1} – the K used here equals $\rho \cdot c_p \cdot \kappa$, or 8.224 x 10^9 W m^{-1} K^{-1} – while $\theta(h+1)$ is the oceanic temperature in Kelvin for the adjacent, colder, deeper oceanic layer, $\theta(h)$ is the temperature of the current layer, and d(h) is the depth of the current layer, which is variable, as explained below. Note that equation (11) must be multiplied by the number of seconds per year for correct units.

For calculation purposes, the ocean was broken into twenty layers. Where the temperature gradient was steepest, near the ocean surface, the isothermal layers were made very thin; in the deep ocean, where the temperature change between isothermal layers was small, the layers were left much thicker. Thus, the mixed layer and the next four layers were each 30 m deep, the sixth layer was 50 m deep, bringing the depth to 200 m so far, and then eight layers of 100 m depth followed. From 1000 m-depth, there were two layers of 250 m, three layers of 500 m, and a final layer of 792 m, which gave a total oceanic depth of 3792 m. The behaviour of the diffusion and advection schemes, as modelled here and provided above, was tested against an ocean with eighty, equal-thickness, isothermal layers to ensure that the equations used did not result in inaccurate oceanic temperatures.

Finally, temperature values are expressed in Kelvin, and their calculations for the atmosphere and the oceans take the following forms. For the atmosphere, temperature is given by,

$$T_A = \frac{H_A}{R_A \cdot SA_E} \qquad (12)$$

while the equation for the mixed-layer and oceanic temperatures is given by,

$$\theta(h) = \frac{H_O(h)}{c_p \cdot m_O(h)} \qquad (13)$$

where $\theta(0)$ equals T_S, and $m_O(h)$ is the mass of the current oceanic layer, calculated from $\rho \cdot SA_O \cdot d(h)$.

The initial temperatures for the atmosphere and for each of the ocean layers are given in Table 1, below. The temperature values are given in degrees Celsius for convenience, and depth measurements are in meters.

Table 1: Initial temperatures and configuration of oceanic layers (°C and m, respectively)

Layer	T_A	T_S	$\theta(1)$	$\theta(2)$	$\theta(3)$	$\theta(4)$	$\theta(5)$	$\theta(6)$	$\theta(7)$	$\theta(8)$	$\theta(9)$
Temperature	14.35	15.90	15.04	14.23	13.47	12.75	11.87	10.44	8.86	7.56	6.48
Depth (top)	N/A	0	30	60	90	120	150	200	300	400	500
Depth (bottom)	N/A	30	60	90	120	150	200	300	400	500	600

Layer	$\theta(10)$	$\theta(11)$	$\theta(12)$	$\theta(13)$	$\theta(14)$	$\theta(15)$	$\theta(16)$	$\theta(17)$	$\theta(18)$	θ_B
Temperature	5.59	4.85	4.23	3.72	3.07	2.44	1.90	1.52	1.32	1.20
Depth (top)	600	700	800	900	1000	1250	1500	2000	2500	3000
Depth (bottom)	700	800	900	1000	1250	1500	2000	2500	3000	3792

2.1.2 The Carbon Sector

Carbon cycle models often include both the oceans and the land surface, although many earlier models focused primarily, or exclusively, on the oceanic component. Terrestrial models have become important in carbon cycle modelling more recently because of the likely role of the terrestrial biosphere as a *carbon sink* (Keeling et al., 1996) in the short term, or possibly as a *carbon source* in the longer term (Friedlingstein et al., 2001; Scheffer et al., 2006). Such terrestrial models range in scale from single trees to the entire globe (see, for example, Harvey, 2000). At the global scale, carbon cycle models come in a relatively simple form that represents carbon exchange processes within and between the oceans and terrestrial biomes, while a more complex form of model, called a Dynamic Global Vegetation Model (DGVM), focuses exclusively on the terrestrial biosphere and includes a large number of biomes at high resolution. DGVMs are often designed for incorporation into complex climate models (Cramer et al., 2001).

This research builds on the carbon cycle model developed by Goudriaan and Ketner (1984), with a modified oceanic sector developed by Fiddaman (1997; 2002). It simulates carbon flows between the atmosphere, the terrestrial biosphere, and the oceans, focussing on atmosphere-mixed ocean layer interactions, and on carbon storage in soil, the terrestrial biosphere, and the deep oceans. The terrestrial biosphere includes six biomes: tropical and temperate/boreal forests, grasslands and agricultural lands, deserts/tundra, and settled areas. It divides living biomass into four components, leaves, branches, stems, and roots, and dead biomass into three soil-carbon pools, litter, humus, and charcoal/decay-resistant humus. Important biological processes simulated by the carbon cycle include biomass growth, litter fall, and litter and soil decomposition. The model also includes the effects of increased atmospheric carbon dioxide concentrations on biomass growth rates, through the somewhat controversial CO_2-fertilization, or β-factor, approach.

Note that, in any model of the carbon cycle, significant uncertainties in the carbon cycle come into play (Falkowski et al., 2000; Geider et al., 2001). Although frequently included in carbon cycle models in the form of Q_{10} factors (Harvey, 2000), the effects of

climate change on soil decomposition rates are also controversial, and the model does not by default include the influences of temperature change on microbial respiration – a feedback to the climate sector – in keeping with the approach used by Goudriaan and Ketner (1984). Note that a Monte Carlo sensitivity analysis run with the model, which tested different Q_{10}-effect strengths, revealed the greater importance of other factors in determining simulation results. See Davies (2007) and Davies and Simonovic (2008a) for information on sensitivity analyses.

2.1.2.1 Mathematical Representation of the Carbon Cycle Sector

All of the equations for the carbon cycle, and the values for their associated parameters, are provided in this section, beginning with the atmosphere. Again, the equations for the terrestrial biosphere and for the atmosphere are based on Goudriaan and Ketner (1984), while the oceanic carbon absorption is based on Fiddaman (1997; 2002).

All of the reservoirs of carbon, or the *carbon stocks*, in the model are measured in gigatons (10^9 t) of carbon, which is written as Gt C. The corresponding measurement for the carbon flows is therefore Gt C yr^{-1}. To translate the mass of carbon into a parts-per-million-volume (ppmv, or more simply *ppm*) measurement, the following equation is used,

$$C_A = 0.4754\, N_A \tag{14}$$

where C_A is the carbon dioxide concentration in the atmosphere, in ppm, and N_A is the mass of carbon in the atmosphere, in Gt C.

The accumulation of carbon in the atmosphere is governed by the following equation,

$$N_A = \int \left(D_B + D_L + D_H + D_K - NPP + B_B + B_L + E - F_O \right) \cdot dt \tag{15}$$

where D_B, D_L, D_H, and D_K are the releases of organic matter from the terrestrial biomass, litter, humus, and charcoal, respectively, to the atmosphere through decomposition, NPP is the net primary productivity (the difference between photosynthesis and respiration, and always positive in value), B_B and B_L are the biomass burning from land-use and land-use change – these two variables are also involved in an intersectoral feedback equation, as described in the intersectoral feedback section below – E is the industrial emissions as a result of economic activity, and F_O is the carbon absorption by the oceans.

Industrial emissions are calculated in the economic sector of the model, according to the following equation,

$$E = (1 - \mu) \cdot \sigma \cdot Q \tag{16}$$

where E is the industrial emission level in Gt C yr^{-1}, μ represents the effects of emissions control measures, such as carbon taxes, and is expressed as a fraction, σ is the ratio of emissions to output, also called the emissions intensity, measured in t/\$1000, and Q is the global-aggregate economic output, in $\$10^{12}$ yr^{-1}. Further information on industrial emissions is provided in the *intersectoral feedbacks* section, below.

The equations for the terrestrial biosphere are the most complicated in the carbon cycle model, since they incorporate the processes of net primary productivity, litter fall, decomposition, and land-use and land-use change. Net primary productivity drives the model according to the following equation,

$$NPP_{jk} = p_{jk} \cdot \sigma(NPP_j) \cdot A_j \big/ 1 \times 10^{15} \tag{17}$$

where NPP_{jk} refers to the biome type (j) and the biomass component (k), p_{jk} is the fraction of biomass partitioned to component k of biome j, where $\sum_{k=1}^{4} p_{jk} = 1$, $\sigma(NPP_j)$ is the surface density of net primary productivity in biome type j, measured in g C m^{-2} yr^{-1}, and A_j is the current area of biome j, measured in m^2. The last term, 1 x 10^{15} converts

between grams and gigatons. In other words, the equation specifies the amount of the total NPP allotted to each component k of each biome j, so that NPP_{jk} has twenty-four components. Biomass partition values, p_{jk}, along with other parameters of the carbon flows through the terrestrial biosphere, are given in Table 2 below, which has been reproduced from Table 1 in Goudriaan and Ketner (1984: 178).

Table 2: Parameters of the flow through the terrestrial biosphere

	Tropical Forest	Temperate Forest	Grassland	Agricultural Land	Human-Settled Area	Tundra and Semi-desert
Partitioning (p_{jk})						
Leaf	0.3	0.3	0.6	0.8	0.3	0.5
Branch	0.2	0.2	0	0	0.2	0.1
Stem	0.3	0.3	0	0	0.3	0.1
Root	0.2	0.2	0.4	0.2	0.2	0.3
Life Span (τ)						
Leaf	1	2	1	1	1	1
Branch	10	10	10	10	10	10
Stem	30	60	50	50	50	50
Root	10	10	1	1	10	2
Litter	1	2	2	1	2	2
Humus	10	50	40	25	50	50
Charcoal	500	500	500	500	500	500
Humification Factor (λ)	0.4	0.6	0.6	0.2	0.5	0.6
Carbonization Factor (φ) upon Decomposition	0.05	0.05	0.05	0.05	0.05	0.05
Carbonization factor (ε_k) on burning of leaves is 0.05, of branches 0.1, of stems 0.2, and of litter (ε_L) is 0.1						

To represent the contentious issue of CO_2-fertilization, Goudriaan and Ketner (1984) modify a base $\sigma(NPP)$ value for each biome according to the current atmospheric carbon dioxide concentration as compared with the initial value. The equation used for the variable surface density of net primary productivity in each biome, $\sigma(NPP_j)$, is,

$$\sigma(NPP_j) = \sigma(NPP_j)_0 \times \left(1 + \beta \ln\left(C_A / C_{A0}\right)\right) \tag{18}$$

where $\sigma(NPP_j)_0$ is the base surface density of net primary productivity for biome j, β is the CO_2-fertilization factor, set to 0.5, and C_A and C_{A0} are the current and initial carbon

dioxide concentrations in the atmosphere, respectively. Values for $\sigma(NPP_j)_0$ are given in Table 3, below.

In the same fashion as NPP_{jk}, biomass has twenty-four components, in the form of carbon stocks, which consist of the four biomass components in each of the six biome types. The accumulation of biomass in each of these twenty four stocks has the following form,

$$B_{jk} = \int \left(NPP_{jk} - FL_{B\,jk} - FH_{B\,jk} - FK_{B\,jk} - B_{B\,jk} - UB_{jk} \right) \cdot dt \qquad (19)$$

where B_{jk} is the biomass in each of components, k, of each of the biomes, j, FL_{Bjk} is the amount of litter falling from biomass to the litter layer of the soil, FH_{Bjk} is the direct decay of biomass material to humus, FK_{Bjk} is the burning of biomass directly to charcoal, B_{Bjk} is the burning of biomass from human land-use and land-use change, and UB_{jk} is the unburned remainder of biomass after land-use change that becomes part of the humus layer of soil.

The litter stock has only six components, with one component for each of the different biomes. Its equation is given by,

$$L_j = \int \left(\sum_{k=1}^{4} FL_{B\,jk} - D_{L\,j} - FH_{L\,j} - B_{L\,j} - FL_{K\,j} \right) \cdot dt \qquad (20)$$

where L_j is the mass of litter in each of the six terrestrial biomes, ΣFL_{Bjk} is the total litter fall from all four components, k, of biome j to litter stock j (some of these flows are clearly zero, since roots do not create leaf litter, for example), D_{Lj} is the flow of carbon from litter to the atmosphere through decomposition, FH_{Lj} is the decomposition of litter into humus, B_{Lj} is the carbon flow from litter to the atmosphere through litter burning as a result of land-use and land-use change, and FL_{Kj} is the carbon flow from litter directly to charcoal through litter burning, again as a result of land-use and land-use change.

The humus stock also has six components, and its equation is given by,

$$H_j = \int \left(\sum_{k=1}^{4} FH_{B\,jk} + FH_{L\,j} - FK_{H\,j} - D_{H\,j} + \sum_{k=1}^{4} UB_{jk} + FH_{H\,j} \right) \cdot dt \qquad (21)$$

where H_j is the mass of humus in each of the six terrestrial biomes, ΣFH_{Bjk} is the direct decay of biomass to humus, FH_{Lj} is the decomposition of litter to humus, FK_{Hj} is the decomposition of humus to charcoal, D_{Hj} is the decay of humus to the atmosphere, ΣUB_{jk} is the unburned remainder of biomass after land-use change that becomes part of the humus layer of soil, and FH_{Hj} is an internal flow of humus from one biome to another that results from land-use change, since humus remains in the soil after a portion of one biome has become part of another biome.

Finally, the stable humus and charcoal stock (generally referred to here as the 'charcoal stock') has six components as well, and its equation has the following form,

$$K_j = \int \left(FK_{H\,j} - D_{K\,j} + \sum_{k=1}^{4} FK_{B\,jk} + FK_{L\,j} + FK_{K\,j} \right) \cdot dt \qquad (22)$$

where K_j is the mass of charcoal in each of the six biomes, FK_{Hj} is the flow of carbon from humus to charcoal, D_{Kj} is the decay of charcoal to the atmosphere through decomposition, ΣFK_{Bjk} is the burning of biomass directly to charcoal, FK_{Lj} is the carbon flow from litter directly to charcoal through litter burning, and FK_{Kj} is an internal flow of charcoal from one biome to another that results from land-use change, since charcoal remains in the soil after a portion of one biome has become part of another biome. Initial values for each of the terrestrial stocks are provided in Table 3, below, which also gives the base surface density of net primary productivity values from Table 2 of Goudriaan and Ketner (1984: 178).

Table 3: Initial carbon stock and base surface density of NPP, σ(NPP_j)_0, values

	Tropical Forest	Temperate Forest	Grassland	Agricultural Land	Human-Settled Area	Tundra and Semi-Desert
Biomass (Gt C)						
Leaves	8.34	5.2	6.43	5.98	0.06	1.04
Branches	55.6	17.3	0	0	0.4	2.08
Stems	250.2	156.1	0	0	3.0	10.4
Roots	55.6	17.3	4.29	1.5	0.4	1.25
Litter (Gt C)	22.23	13.87	12.86	5.99	0.32	2.94
Humus (Gt C)	111.19	260.1	257.18	37.41	5.0	63
Charcoal (Gt C)	277.97	130.05	160.74	37.41	5.0	31.5
Base Surface Density of NPP (g C m^{-2} yr^{-1})	770	510	570	430	100	70

Equations (19) to (22) deal with the terrestrial biosphere stocks, and list the flows that change these stock values. The equations for the carbon cycle in the oceans are provided later in this section; first, however, the equations for the terrestrial flows are provided. Where the subscripts on the flows are both j and k, the flows have twenty-four components; however, when only the subscript j is present, there are six flows associated with the equation – one for each of the six biomes.

The equation for NPP in equation (19) was provided in equation (17). The presentation of the remainder of the flows that affect the terrestrial biomass in equation (19) begins with litter fall, FL_{Bjk}, which has the form,

$$FL_{Bjk} = B_{jk} \Big/ \tau(B_{jk}) \tag{23}$$

where B_{jk} is the amount of biomass in component k of biome j, and $\tau(B_{jk})$ is the life-span, or 'residence time', for biomass component k of biome j. Note that roots, the fourth component of biomass, do not generate litter, so FL_{Bj4} is 0 Gt C yr^{-1}. The values for $\tau(B_{jk})$ are provided in Table 2, above.

The equation for the direct decay of biomass material to humus, FH_{Bjk}, is the same as equation (23) above,

$$FH_{B\,jk} = \frac{B_{jk}}{\tau(B_{jk})} \tag{24}$$

except that FH_{Bjk} for all above-ground biomass components ($k = 1, 2, 3$) is 0 Gt C yr^{-1}, and only the decay of roots ($k = 4$) generates humus directly – in other words, all other biomass components become humus through litter, as in equation (23).

The next member of equation (19), the burning of biomass directly to charcoal, or FK_{Bjk}, is more complicated than the other flows, because it involves a land-use 'transfer matrix'. This matrix, TM_{ij}, represents clearing and burning *within* a terrestrial biome, and land-use *conversions* that establish new land-cover in the place of the previous vegetation. A brief description of TM_{ij} follows, although more information is provided in the intersectoral feedbacks section, below.

In TM_{ij}, the subscripts represent rows $= i$ and columns $= j$, where column headings j mean '*from* biome type' and row headings i mean '*to* biome type'. Clearing and burning within a particular biome is represented in equation (25) by the diagonal matrix entries, $i = j$, while land-use conversions are represented by the remainder of the entries. Since there are six terrestrial biomes, the transfer matrix has 6 x 6 = 36 entries. Its equation is given in algorithm form as,

$$\frac{dTM_{ij}}{dt} = \quad for\ all\ (i,\ j):$$
$$if\ (i = j), \tag{25}$$
$$r^{1/2} \cdot TM_{ij},$$
$$else(r \cdot TM_{ij});$$

where TM_{ij} is measured in Mha yr^{-1}, and r is the annual global-aggregate population growth rate. Again, since the transfer matrix connects the carbon cycle, land-use and population sectors, further details are provided in the next section, below.

Now the biomass-to-charcoal equation can be presented. It takes this form,

$$FK_{B\,jk} = \varepsilon_k \cdot \sigma(B_{jk}) \cdot \sum_{i=1}^{6} TM_{ji} \cdot 1 \times 10^{-5} \tag{26}$$

where ε_k is the carbonization fraction of component k on burning, which has a non-zero value for $k \neq 4$, $\sigma(B_{jk})$ is the surface density of biomass component k of biome j, which is measured in g C m^{-2} yr^{-1}, ΣTM_{ji} represents a flow of burned biomass from all biomes i to the current biome, j, as a result of biomass burning. In other words, the idea is that some fraction of the biomass that was part of any of the previous biomes $i \neq j$ prior to their conversion to the new biome, j, burns because of land-use change. The final constant, 1 x 10^{-5}, results from the conversion of g to Gt and m^2 to Mha.

Each $\sigma(X)$ term – for $\sigma(B_{jk})$, $\sigma(L_j)$, $\sigma(H_j)$, and $\sigma(K_j)$, in their respective equations – is a calculated value, which is based on the following equation,

$$\sigma(X_{j(k)}) = {X_{j(k)}}\Big/{A_j} \cdot 1 \times 10^{-5} \tag{27}$$

where $\sigma(X)$ is the surface density of a B, L, H, or K component of the terrestrial biosphere, measured in g C m^{-2} yr^{-1}, $X_{j(k)}$ is a carbon stock that has either six (L, H, and K) or twenty-four parts (B), and A_j is the current area of biome j, in Mha here. The constant is for unit conversion.

The biomass burning, B_{Bjk}, is related to equation (26), and takes the form,

$$B_{B\,jk} = (1 - \varepsilon_k) \cdot \sigma(B_{jk}) \cdot \sum_{i=1}^{6} TM_{ji} \cdot 1 \times 10^{-5} \ for \ k = 1,2$$

$$B_{B\,j3} = (1 - \varepsilon_3 - 0.5) \cdot \sigma(B_{j3}) \cdot \sum_{i=1}^{6} TM_{ji} \cdot 1 \times 10^{-5} \tag{28}$$

$$B_{B\,j4} = 0$$

where the fraction of biomass that does not become charcoal (actually much higher than the fraction that does burn to charcoal – see Table 2) burns and is released to the atmosphere for $k = 1$ and 2, or the 'leaves and branches'. Variables in the equation include the carbonization fraction, ε_k, from equation (26), the surface density, $\sigma(B_{jk})$, which is based on equation (27), and the transfer matrix ΣTM_{ji} function as in equation (25). In the case of the stems, $k = 3$, some fraction (ε_k) burns to charcoal, another fraction is released to the atmosphere through this equation $(1 - \varepsilon_k - 0.5)$, and the last half (0.5) of the stems is left on the land surface after the land-use change and becomes humus. The last biomass component, which is the roots ($k = 4$), does not burn, but is instead transferred directly to the humus pool of the new biome as in equation (29), below.

The last flow in equation (19) pertains to the portion of biomass that does not burn in a land-use change from one biome to another. This unburned biomass, UB_{jk}, is calculated from the following equation,

$$UB_{jk} = 0 \ for \ k = 1,2$$

$$UB_{j3} = 0.5 \cdot \sigma(B_{j3}) \cdot \sum_{i=1}^{6} TM_{ji} \cdot 1 \times 10^{-5} \qquad (29)$$

$$UB_{j4} = \sigma(B_{j4}) \cdot \sum_{i=1}^{6} TM_{ji} \cdot 1 \times 10^{-5}$$

where all leaves and branches ($k = 1$ and 2) are burned and released to either the atmosphere or to the charcoal layer of the soil, and so the unburned fraction is zero, whereas the unburned fraction (0.5) of the stems ($k = 3$), as well the entire mass of the roots, become humus.

The first flow in equation (20), for the litter stock, is the litter fall from equation (23). The next flow in equation (20) is the decay of litter to the atmosphere, D_{Lj}, which is given by,

$$D_{Lj} = \left(1 - \lambda_j\right) \cdot {L_j}\Big/{\tau(L_j)} \tag{30}$$

where λ_j is the humification fraction – or the fraction of litter that becomes humus – for biome j, and $\tau(L_j)$ is the turnover time, or 'residence time', for litter in biome j, which typically has a value of only one to two years. See Table 2 for the values for $\tau(L_j)$.

The equation for the decomposition of litter to humus, FH_{Lj}, is the complement to equation (30), and is given by,

$$FH_{Lj} = \lambda_j \cdot {L_j}\Big/{\tau(L_j)} \tag{31}$$

where the same variable and constant definitions apply as in equation (30).

The carbon flow from litter to the atmosphere as a result of litter burning via land-use and land-use change is analogous to equation (28), for the burning of biomass. For the burnt litter flow, B_{Lj}, the equation is,

$$B_{Lj} = \left(1 - \varepsilon_L\right) \cdot \sigma(L_j) \cdot \sum_{i=1}^{6} TM_{ji} \cdot 1 \times 10^{-5} \tag{32}$$

where ε_L is the carbonization fraction of litter upon burning, $\sigma(L_j)$ is the surface density of litter in biome j, as defined in equation (27), and ΣTM_{ji} represents the transfer matrix measured in Mha, where land-use change results in a flow of burned litter from the area of all the biomes i that was converted to the current biome, j. The final constant is, again, the result of a unit conversion.

The last flow in equation (20), FL_{Kj}, represents the carbon flow from litter directly to charcoal through litter burning, again as a result of land-use and land-use change. Its equation is,

$$FL_{K_j} = \varepsilon_L \cdot \sigma(L_j) \cdot \sum_{i=1}^{6} TM_{ji} \cdot 1 \times 10^{-5} \qquad (33)$$

which is the complement to equation (32). In other words, the small amount of litter that is not released directly to the atmosphere through burning joins the charcoal stock instead.

Several of the flows associated with the humus stock, as listed in equation (21), have already been provided above: FH_{Bjk}, FH_{Lj}, and UB_{jk}. Equations for the remaining flows are provided below, beginning with the decomposition of humus to charcoal, FK_{Hj},

$$FK_{H_j} = \phi_j \cdot \frac{H_j}{\tau(H_j)} \qquad (34)$$

where φ_j is the carbonization fraction of humus through decomposition, and $\tau(H_j)$ is the turnover time, or 'residence time', for humus in biome j.

Decomposition of humus and its release to the atmosphere, D_{Hj}, is the complement to equation (34), so that,

$$D_{H_j} = (1 - \phi_j) \cdot \frac{H_j}{\tau(H_j)} \qquad (35)$$

where the same variable and constant definitions apply as in equation (34).

The final flow in equation (21) is FH_{Hj}, which represents an internal flow of humus from one biome to another as a result of land-use change. It equation is given by,

$$FH_{H_j} = \sigma(H_j) \cdot \left[\sum_{i=1}^{6} TM_{ji} - \sum_{i=1}^{6} TM_{ij} \right] \cdot 1 \times 10^{-5} \quad \forall \, i \neq j \qquad (36)$$

where $\sigma(H_j)$ is the surface density of humus in biome j, as defined in equation (27), $\Sigma_i TM_{ji}$ is the sum of all land-use conversions from biome i to j, and $\Sigma_i TM_{ij}$ is the sum of all land-use conversions from biome j to different biomes i. In other words, the expression in the brackets determines the net change in biome area over the past time step – for tropical forests and some others, the change will be negative, while for agricultural land and others, the change will be positive. The constant is for unit conversions, and the logical statement (for all $i \neq j$) ensures that only land-use conversions are considered here.

In the case of the final stock, charcoal and stable humus from equation (22), only two equations have not been provided. The equation for the decomposition of charcoal to the atmosphere is similar to the other equations for decomposition, and is given by,

$$D_{K_j} = K_j \big/ \tau(K_j) \tag{37}$$

where $\tau(K_j)$ is the turnover time, or 'residence time', for charcoal in biome j.

The more complicated equation for FK_{Kj}, which is an internal flow of charcoal from one biome to another that results from land-use change and is analogous to FH_{Hj} in equation (36), takes the following form,

$$FK_{K_j} = \sigma(K_j) \cdot \left[\sum_{i=1}^{6} TM_{ji} - \sum_{i=1}^{6} TM_{ij} \right] \cdot 1 \times 10^{-5} \quad \forall\, i \neq j \tag{38}$$

where $\sigma(K_j)$ is the surface density of charcoal in biome j, as calculated in equation (27), and the rest of the terms are the same as in equation (36).

The equations for the *oceanic* component of the carbon cycle are based on work by Fiddaman (1997), and are broken into two parts: the *mixed-layer*, and the *deep oceans*.

For the mixed-layer carbon stock, the equation is,

$$C_{ML} = \int \left(FO_A - DF_O(0) \right) \cdot dt \qquad (39)$$

where C_{ML} is the amount of carbon in the oceanic mixed-layer, with an initial value of 769 Gt C, FO_A is the absorption of carbon dioxide by the mixed-layer from the atmosphere, and $DF_O(0)$ is the diffusive flow of carbon dioxide to the deep ocean. As was the case for the terrestrial biosphere, the oceanic flows are measured in Gt C yr^{-1}.

For the absorption of carbon dioxide from the atmosphere, the equation is,

$$FO_A = \left(C_{ML\,eq} - C_{ML} \right) / \tau_{ML} \qquad (40)$$

where C_{MLeq} is the equilibrium mixed-layer carbon content, C_{ML} is given by equation (39), and τ_{ML} is the 'mixing time' for the mixed-layer, set to 1.5 yr.

The equation for the diffusive flows takes the following form,

$$
\begin{aligned}
DF_O(0) &= \frac{2\delta_e \cdot \left(C_{ML}\big/ d_{ML} - conc(0) \right)}{d_{ML} + d(0)} \quad \textit{for mixed layer} \\
DF_O(h) &= \frac{2\delta_e \cdot \left(conc(h+1) - conc(h) \right)}{d(h+1) + d(h)} \quad \textit{for } h > 0
\end{aligned} \qquad (41)
$$

where the top equation calculates the diffusive flow from the mixed-layer to the first deep ocean layer, *layer 0*, and the bottom equation governs carbon flows between deep ocean layers. Therefore, in equation (41), δ_e is the eddy diffusivity coefficient, which is set to of 4000 m^2 yr^{-1}, d_{ML} is the depth of the mixed-layer, which is 75 m, C_{ML}/d_{ML} is the concentration of carbon in the mixed-layer, conc(0) is the concentration of carbon in the first deep ocean layer, calculated by $C_O(0)/d(0)$, and the denominator (with the '2' moved to the numerator) determines the average distance of heat diffusion from the centre of one

oceanic stock to the next. For the bottom equation, conc(h+1) is the concentration of carbon in the layer above the current layer, h, conc(h) is the concentration in the current layer, and d(h+1) and d(h) are the thicknesses of the two layers. Again, the concentrations are calculated by C_O(h)/d(h).

The equilibrium mixed-layer carbon content, C_{MLeq}, is calculated according to the following equation,

$$C_{MLeq} = C_{ML0} \cdot (C_A/C_{A0})^{1/\xi} \tag{42}$$

where C_{ML0} is the pre-industrial mixed-layer carbon content, set to the initial value for C_{ML}, C_A is the current atmospheric carbon dioxide concentration, from equation (14), and C_{A0} is the initial carbon dioxide concentration, from equation (18). The buffer factor, ξ, is also a calculated value, and comes from the following equation,

$$\xi = \xi_0 + \xi_c \cdot \ln(C_A/C_{A\xi}) \tag{43}$$

where all the terms are parameters, except for C_A. The reference buffer value, ξ_0, is set to 10, while buffer coefficient, ξ_c, is set to 4.05. Finally, the reference carbon dioxide in the atmosphere at the base buffer value, $C_{A\xi}$, is 760 Gt C.

For the *deep ocean* carbon stock, the equation is,

$$C_O(h) = \int [DF_O(h) - DF_O(h+1)] \cdot dt \tag{44}$$

where C_O(h) represents the carbon content of ocean layer h, DF_O(h) is the diffusive flow of carbon from the layer above to the current layer, and DF_O(h+1) is the diffusive flow to the layer below from the current layer – see equation (41), above. In this model of the ocean based on Fiddaman (1997), there are ten layers of unequal depth, with each of the

top five layers having a thickness of 200 m, and the bottom five layers having a thickness of 560 m each.

2.1.3 The Economic Sector

Computer-based economic models, or computable general-equilibrium (CGE) models, are used for a wide variety of economic policy evaluations (Shoven and Whalley, 1984), including the analysis of climate change policy, where the focus is generally on the impact of policy changes on 'intertemporal' social welfare. Different modelling approaches are available. Most of the economic studies of climate change policy have focussed on cost-effectiveness. However, several studies, including the model used here, incorporate estimates of the benefits of climate stabilization as well (Dowlatabadi and Morgan, 1993b). Such cost-benefit analysis approaches aim to maximize economic efficiency by determining optimal policies (Bürgenmeier et al., 2006). Note that, while cost-benefit analysis of climate change policy is now widely accepted, it is not without criticism, as explained below.

The economic sector of this model is an adaptation of a well-known climate-economy model called DICE (Nordhaus, 1992), or the "Dynamic Integrated model of Climate and the Economy", which was more recently updated to DICE-99 in Nordhaus and Boyer (2000). DICE models the global aggregate economic output (GDP, or gross domestic product) using a Cobb-Douglas production function that includes total factor productivity (often termed technological progress), capital, labour, and surface temperature change as inputs. Through *carbon taxes*, it measures the effects of climate change policies on the global economy. DICE also calculates industrial emissions, which are influenced by taxation levels, as a product of economic activity and climate change policy. In this work, the starting date for DICE-99 has been reset to 1960 from 1995, and this new version has a continuous time step, rather than the original discrete, decadal time step.

Note that the use of CGE models for policy development is not without criticism, and that DICE-99 in particular, despite its wide acceptance, was recently the subject of a specific

critique (see Füssel, 2007). In terms of the broader CGE approach, Peters et al. (1999: 501) explain that economics should not play a pivotal role in policy making, since "most economic policy models, in their current forms, are biased against non-marginal policy changes…" – a significant danger, because potentially large socio-economic changes are required to deal with climate change. They argue, furthermore, that the basic assumption in economic theory that every profitable opportunity is exploited is simply false, because people are not boundlessly rational, and that monetary tools should not serve as the fundamental metric for policy evaluation. Bürgenmeier et al. (2006) and Füssel (2007) describe the problems inherent in 'discounting practices', such as those employed by DICE, which are used by all 'intertemporal welfare maximization' schemes (which are also widely recognized as problematic), and are crucial in determining *optimal* economic policies. The problem with discounting, according to Bürgenmeier et al. (2006: 147) is that "the choice of discount rate [has] a decisive impact on the optimality of a given climate policy" – for example, large discount rates artificially shorten the time horizon used for planning. In terms of DICE itself, certain social welfare functions used by different versions of DICE are internally inconsistent, its climate sector is flawed, and several DICE-99 versions provided by Nordhaus (2006) on his website differ appreciably (Füssel, 2007). The version used here is the preferred, Excel implementation of DICE-99 (Nordhaus and Boyer, 1999).

Criticisms of the CGE approach certainly apply to the use of DICE-99 in this work. However, concerns about welfare maximization do not apply to this research, because the analysis undertaken here does not rely on the social welfare functions criticized by Füssel (2007). Instead, the economic analysis below focuses on changes in economic output and consumption per capita over time, rather than as a current, or 'intertemporal', value. In other words, the focus here is on Earth-system simulation, as opposed to economic *optimization*. Note too that more complex economic models are available instead of DICE, including a regionalized model called RICE, which divides the world into eight regions that produce a single commodity used for either consumption or investment. RICE also includes energy use, which is represented, in addition to labour and capital, as an input to production. International trade – an important element of the model – occurs

in terms of 'carbon emission permits', and the effects of several climate change policies are then analyzed in terms of this trade (Nordhaus and Boyer, 2000). However, DICE is particularly attractive because its global scale matches that of the rest of the model, and because it is "arguably the most widely used global climate-economy model" (Füssel, 2007: 162).

2.1.3.1 Mathematical Representation of the Economic Sector

Major equations for the DICE-99 economic sector are provided here, along with the values of important parameters, particularly those that required change in order to reset the starting date for DICE from 1995 to 1960. Equations for utility-based calculations are not given here, since they are rarely used in the model; however, should they be required, readers can find them in the Excel version of DICE (Nordhaus and Boyer, 1999). All equations listed below are based on Nordhaus and Boyer (2000) and Nordhaus and Boyer (1999).

The basis of the economic sector is *output*, or yearly production. The theory behind DICE is apparent from the following equation, although note that the equation is not actually used explicitly in the model,

$$Q = C + I - \tau(\Pi - E) \tag{45}$$

where Q represents the yearly economic output, in trillions of 1990 U.S. dollars at market exchange rates, C is the yearly consumption and I is the yearly investment, both of which are also measured in 10^{12} \$$_{1990\ \text{U.S.}}$ yr^{-1}, τ represents an *industrial emission permit price* or a *carbon tax*, which is expressed in \$/kt, Π is the current number of emissions permits in Gt C yr^{-1}, and E is industrial emissions, also measured in Gt C yr^{-1}.

Equation (45) basically states that yearly output is the sum of consumption and investment (the normal form of the equation) less the effects of global emissions (the new addition in DICE). The main message here is that carbon emissions represent a sort of

negative capital. There are, however, two important notes about equation (45): 1) the units do not match exactly – the carbon tax would have to be measured in \$1000/t, as in Nordhaus and Boyer (2000), which then creates scale mismatches in the rest of the model, and 2) several of the symbols here are close to symbols in other sectors of the model (C and τ). The mismatch of units is not important, because the equation is provided for illustrative purposes only here. In other words, equation (45) is not actually used in the model. In terms of the second point, the similarity of these variables with variables in other sectors is unavoidable, since readers may wish to compare the equations provided in this work with the equations in their sources. Furthermore, in the case of the economic sector equations, many of the symbols used here are common to all macroeconomic models, and so they have been retained; however, some caution is clearly advised in interpreting the variables used here.

The second output equation is actually used in the model, and so will receive greater attention in this section; it takes the following form,

$$Q = \Omega \cdot \left(1 - b_1 \cdot \mu^{b_2}\right) \cdot \left(A \cdot K^{\gamma} \cdot L^{1-\gamma}\right) \tag{46}$$

which is a modification of the standard Cobb-Douglas production function,

$$Q = z \cdot K^{\gamma} \cdot L^{1-\gamma} \tag{47}$$

where Q represents the net economic output per year, or GDP, measured in trillions of 1990 U.S. dollars per year, z is the total factor productivity, also called A in equation (46), which represents *technological progress*, K is the capital stock in trillions of 1990 U.S. dollars, γ is an elasticity parameter, set to 0.3, and L is labour, or the global aggregate population, referred to as P elsewhere, and measured here in millions of people. Equation (46) adds two terms on the left of the more basic equation (47): the climate damage multiplier, Ω, to account for the effects of climate change on production, and $\left(1 - b_1 \cdot \mu^{b_2}\right)$ to account for the effects of industrial emissions reductions on economic production. The second term represents the cost of emissions abatement, and includes b_1,

a variable "coefficient on the control rate in the abatement cost function" in DICE, μ, the industrial emission control rate, and b_2, a simple, constant exponent on the emissions control rate, set to 2.15.

The climate damage multiplier, Ω, is based on a temperature damage function,

$$D = \theta_1 \cdot \Delta T_S + \theta_2 \cdot \Delta T_S^2 \qquad (48)$$

where D is the percentage damage to the economy as a function of changing surface temperature, measured as a percentage loss of GDP per year, θ_1 and θ_2 are parameters, set to -0.0045 and 0.0035 respectively – an explanation for these values can be found in Chapter 4 of Nordhaus and Boyer (2000) – and ΔT_S is the surface temperature change from pre-industrial levels. Based on D, the climate damage multiplier, Ω, takes the following form,

$$\Omega = \frac{1}{(1 + D/100)} \qquad (49)$$

where Ω is a unitless multiplier with an initial value of one. Since D and Ω link the climate and economic sectors, see the *intersectoral feedbacks* section for further information.

According to Nordhaus and Boyer (1999), the industrial emission control rate, μ, measured in percent yr^{-1}, is generated as follows,

$$\mu = \frac{100(\tau/1000) \cdot \sigma \cdot (1 + D/100)}{b_1 b_2^{1/(b_2 - 1)}} \qquad (50)$$

where σ represents the variable "base case ratio of industrial emissions to output", measured in t \$1000^{-1}, τ is the *carbon tax* in \$ kt^{-1}, and D is defined in equation (48).

Neither Nordhaus and Boyer (1999) nor Nordhaus and Boyer (2000) explain this equation.

The total factor productivity, A, is prescribed in DICE through the following two equations,

$$A = \int g^a dt$$

$$g^a = \frac{A \cdot g^a{}_0 \cdot e^{-\delta_a t}}{10}$$

(51a)

where $g^a{}_0$ is set to 3.8% decade^{-1}, δ_a is a parameter set to 1 x 10^{-6} % decade^{-1}, and t is the current year. The equation is divided by 10 to make the change a yearly, rather than decadal, value. This approach yields total factor productivity values from 1995-2100 that are less than 3% lower than those of Nordhaus and Boyer (1999) in 1995, and the difference in values decreases over time to 0.8% by 2095. The initial 1995-value for A is set to 0.01685.

For calibration to 1960 values, several additional changes to A were required. The initial approach to modelling changes in total factor productivity in the 1960-start DICE-99 model was to back-cast linearly to a 1960 value of 0.01475 from the 1995 value of 0.01685 provided in Nordhaus and Boyer (2000). This approach caused a significant problem: it created a discontinuity in both economic output and capital formation between the DICE values and the 1960-start version of DICE at the year 1995. The best approach to fix this discontinuity was to alter values of A from 1960 to 1995. Essentially, since actual historical values for total factor productivity are unknown, it is possible to change A values within the 1960-1995 period as a calibration tool to achieve the following goals:

1. The ratio of $K(t):Q(t)$ can be kept close to the desired 2:1 – 3:1 values;
2. Annual savings rates can be used both pre- and post-1995, instead of switching between continuous and annual sets of values at the 1995 discontinuity;

3. Depreciation can be maintained as a constant value over the whole simulation period;

4. Both *K(t)* and *Q(t)* curves can be made to have nearly constant slope, while matching the DICE-99 spreadsheet values closely; and finally,

5. Since A is unknown, a linear back-cast to 1960 is unlikely to be correct either.

The recalibration of A was achieved as follows. The initial configuration of the total factor productivity curve resulted in a nearly linear growth in A over the course of the simulation. To change this curve in a gradual way (to avoid introducing additional discontinuities) until it converges with the post-1995 values used in DICE, a negative-feedback based multiplier was used. The recalibrated A equation therefore takes this form, as modified from equation (*51a*),

$$A = a_{mult} \cdot \int g^a \, dt$$

$$g^a = \frac{A \cdot g^a{}_0 \cdot e^{-\delta_a t}}{10}$$

$$a_{mult} = \int a_{incr} \, dt$$

$$a_{incr} = \alpha \left(a_{goal} - a_{mult} \right)$$

(51)

where the change in a_{mult}, the negative-feedback based multiplier value, is determined by the difference between the goal, a_{goal}, of 1.0 and the current value, a_{mult}, multiplied by a rate term, $\alpha = 0.06$, that controls the convergence of the multiplier with its goal.

The accumulation of capital, K, is governed by the following equation,

$$K = \int (I - \delta) \cdot dt$$

(52)

where I is the yearly investment and δ is the yearly depreciation, which is a fixed percentage of the capital, set to 6.45% yr^{-1}. The derivation of the depreciation term is accomplished according to the following logic. Nordhaus and Boyer (2000) set depreciation at 10% yr^{-1}, which is compounded decadally rather than continuously, as it

is here. This means that the depreciation term, δ, when evaluated at a decadal time scale, is $(0.9)^{10} = 0.3486$, so that only 34.9% of the previous time step's capital remains after one decade. The loss of capital is therefore $1 - 34.9$, or 65.1%, and turning this value into a yearly rate by matching it to the depreciation values in the discrete version of DICE-99 yields a depreciation rate of 6.45% yr^{-1}. The initial value for capital in 1960 is set to $\$5.75 \times 10^{12}$.

Investment is given by,

$$I = S/100 \cdot Q \tag{53}$$

where S is the savings percentage, which is prescribed in DICE from 1995 onwards. For values prior to the 1995 start-date of DICE, savings rates are available from the *World Development Indicators* online database (The World Bank Group, 2007) from 1971 through 2003 – see the "gross savings (percentage of GDP)" data – and set to a linear increase from 1960, at 22%, to the first year of data availability at the global level, which is 1971, at 24.71%.

Finally, carbon policies can be enacted through changes in the carbon tax variable, τ, through the following equation,

$$\tau = MIN\left\{c, \quad \frac{1000 \cdot b_1 b_2}{(1 + D/100) \cdot \sigma}\right\} \tag{54}$$

which uses the minimum of two values in the curly braces. The left-hand side represents a specified value, c, that would be assigned by international policy-makers. The right hand side calculates the tax required for 100% of industrial emissions to be controlled, so that any value less than this value is used directly, while any value greater is replaced by the calculated value corresponding to $\mu = 100\%$. In the case of the experiments in Davies (2007), carbon tax values are taken from Nordhaus and Boyer (2000).

2.1.4 The Land-use Sector

Land-use change plays a key role in determining atmospheric carbon dioxide levels over the long term. In fact, it is estimated that, while anthropogenic greenhouse gas emissions contributed 6.7 gigatons (Gt) (Marland et al., 2007) of carbon dioxide in 2000 to the atmosphere, land-use change, involving conversion of forests to agricultural lands among other things, added an extra 1.6 ± 0.8 Gt C/year (Watson et al., 2000) to the atmosphere in the 1990s.

This model represents land-use and land-use change in the same fashion as Goudriaan and Ketner (1984). The *transfer matrix* given in equation (25) simulates both conversions of one of the six biome-types to another, such as the conversion of tropical forest to agricultural land, and human interference within a single biome type, such as forest fire or burning of grassland or agricultural land after harvest. The transfer matrix approach is quite simple and straightforward: it assumes that ecosystems are fundamentally resilient (Cumming et al., 2005); thus, only human interventions, and not changing biological or climatic factors, cause decreases (or increases) in biome areas. The transfer matrix does not include actual spatial data, modelling simply the total extent of one biome and its change over time in an abstract fashion. Finally, it also does not specify the actual cause of changes in biome area, modelling any change simply as a result of population change – an *intersectoral* feedback. However, despite its simplicity, the approach models human impacts on biome extent acceptably, given the limited understanding of the direct causes of land-use change (Lambin et al., 2001; Veldkamp and Lambin, 2001).

The version used here has the initial values for the transfer matrix and biome areas shown in Table 4, since model simulations begin in 1960 rather than in 1780. Note that these values result in a match with the 1980 values in Tables 2 and 4 in Goudriaan and Ketner (1984: 178, 180), when the model incorporates a feedback, discussed in the intersectoral feedback section below, between the population and land-use sectors.

Table 4: Transfer Matrix values in 1960 (Mha/yr) and initial total area (Mha)

From: / To:	Tropical Forest	Temperate Forest	Grassland	Agricultur-al Land	Human Area	Semi-Desert and Tundra
Tropical Forest	11.30	0	0	0	0	0
Temperate Forest	0	1.507	0	0	0	0
Grassland	4.023	0.670	301.5	0	0	0
Agricultural Land	4.023	0	0	301.5	0	1.341
Human Area	0.335	0.335	0.670	0.670	0	0
Semi-Desert and Tundra	0	0	0	0	0	0
1960 Area	3815	1730	1780	1630	15	3000

2.1.5 The Population Sector

The structure of the population sector is based on one presented in Fiddaman (1997), who adapted the sector from Nordhaus (1992). According to the model, global population grows asymptotically at a steadily decreasing growth rate, beginning at a growth rate of 2.24%/year in 1960. During the historical period of the simulation, from 1960-2004, the population growth simulated by our model matches UN figures (UNESA, 2006). The rate of decrease in population growth is determined by an *intersectoral* feedback, and will be discussed below.

Note that other, more flexible approaches to modelling endogenous population growth are available, such as those used by the World3 model (Meadows et al., 2004) and TARGETS (Rotmans et al., 1997), which can simulate population growth and decline. The simpler asymptotic approach was used in this research to ensure model stability during the simulation runs – the effects of this decision are described in detail in Davies (2007).

2.1.6 The Water Sectors

The water sectors of the model simulate the natural hydrological cycle, human water demand, water quality, and many of the factors that control them. Like the rest of the model, the water sectors simulate the natural hydrological cycle, water demand, and water quality on a yearly basis, and as a global aggregate.

Other models of the global hydrological cycle and human demand exist. For example, Alcamo et al. (2003a) have developed a high-resolution global hydrological model, called WaterGAP2, that resolves individual river basins, Vörösmarty (2002) and Vörösmarty et al. (2000) have developed a similar model, called the Water Balance Model, as has Arnell (1999a) with a third model, called Macro-PDM. In addition to describing his globally-averaged, system dynamics-based expansion on the World3 model (Meadows et al., 1992), Simonovic (2002) also details several other approaches towards modelling the global hydrological cycle; however, none of these other models are dynamic in nature, since they do not integrate other physical sectors, relying instead on external driving scenarios.

The following sections describe a series of original models that combine to create a linked natural-anthropogenic water sector in our model. The first component of the water sector is the natural hydrological cycle. The next two components replicate quantitative and qualitative aspects of anthropogenic water demand, beginning with water withdrawals and consumption, and then progressing to water quality. Water quality components of the water sector include the generation of water pollution and its impact on surface water availability, and wastewater treatment and reuse as approaches to reduce water scarcity. The water sector also includes groundwater withdrawals and desalination as approaches to increase surface water availability, while embedded economic and power-generation sectors affect the degree to which possible solutions to surface water scarcity are adopted.

2.1.6.1 The Natural Hydrological Cycle

The natural portion of the hydrological cycle includes the reservoirs of gaseous, liquid, and solid forms of water, as well as water transfers between these states. Water reservoirs in the global hydrological cycle include the oceans, the land surface, groundwater, ice sheets, and the atmosphere, which can be separated into marine and terrestrial components (Chahine, 1992). Transfers between these reservoirs include the processes of evaporation and evapotranspiration, advection, precipitation (both solid and

liquid), melting, groundwater percolation into, and baseflow from, aquifers, and surface runoff to the oceans (Chahine, 1992; Gleick, 2000b; Shiklomanov, 2000). The structure of the natural hydrological cycle is modified from earlier work at the University of Western Ontario, and focuses on the cycle's steady-state behaviour: the average annual amounts of water in each reservoir as well as average annual flows from one reservoir to another.

Since humans withdraw water from surface water resources, especially from lakes, rivers, and streams, the simulated global-average annual runoff from the land surface – and its variability as a result of intersectoral feedbacks, discussed below – is the most important issue for the purposes of this research. Shiklomanov (2000) estimates this annually renewable runoff at 42750 km^3 yr^{-1}, which is therefore the runoff value this model has been calibrated to yield.

The model reaches a steady-state at the reservoir and flow values given in Table 5 and Table 6, which lie within the range of values provided by Shiklomanov and Rodda (2003: 13), Gleick (2000b: 21) and Chahine (1992). Table 5 compares the range of reservoir values provided in the literature with the values used in the model; where values differ between the sources, the most recent figures available have been used.

Table 5: Major reservoirs of water, and values used in model (in km^3)

Name of Stock	Literature Value	Model Values
Marine Atmosphere	9.4-11 x 10^3	9.4 x 10^3
Terrestrial Atmosphere	4.0-4.5 x 10^3	4.0 x 10^3
Oceanic Water Content	1338 x 10^6	1338 x 10^6
Land Surface Water	118-360 x 10^3	200 x 10^3
Ice and Permanent Snow	24-43 x 10^6	24.5 x 10^6
Groundwater Content	10.5-23.4 x 10^6	10.6 x 10^6

The initial, steady-state flow values used in the model simulations are generally close to the values in the literature, as shown in Table 6; where no values are available, the flow in question is marked as *not available.*

Table 6: Hydrological flows and initial flow values used in model (in km^3 yr^{-1})

Name of Flow	Literature Value	Model Value
Rainfall over Land	107000-180151	117500
(Terrestrial) Evapotranspiration	71000-126631	72125
Snowfall over Ice Sheets	2474	2625
Advection (Marine to Terrestrial)	36000-53520	45375
Precipitation over Oceans	398000-481680	489825
Evaporation from Oceans	434000-535200	535200
Melting of Ice Sheets (to Oceans)	2474	2625
Percolation to Groundwater	*Not available*	2000
Groundwater Discharge	*Not available*	2000
Streamflow	36000	40750
Total Renewable Flow	42750	42750

Note that the most sensitive values in the model are the base *flows* rather than reservoir values; however, the *terrestrial atmosphere* is an exception, since it has the smallest volume of any of the stocks, and is affected by very large flow values. Particularly uncertain values in the model involve groundwater recharge and baseflow, although ice melt and snowfall over ice sheets are also uncertain.

Mathematical Form of the Natural Hydrological Cycle

The major details of the natural hydrological cycle are provided above. This section lists the major stock and flow equations for the sector.

The equations for the marine and terrestrial atmospheric components are given by,

$$A_M = \int (E_M - Adv - P_O) \cdot dt \qquad (55)$$

and,

$$A_L = \int (Adv + ET - P_R - P_S) \cdot dt \qquad (56)$$

where A_M and A_L are the atmospheric water contents over the ocean and land, respectively, measured in km^3 and with initial values given in Table 5, E_M is the evaporation from the oceans to the marine atmosphere, Adv is the advective flow of

moisture from the marine atmosphere to the terrestrial atmosphere, P_O is precipitation over the oceans, ET is evapotranspiration from the land surface to the terrestrial atmosphere, P_R is precipitation over land in the form of rain, and P_S is precipitation in the form of snow, which accumulates on ice sheets and in glaciers.

The equation for the land surface has the following form,

$$LS = \int (P_R - ET - SF - GP) \cdot dt \tag{57}$$

where LS represents the water storage in the terrestrial environment, SF is the surface flow of water to the oceans, and GP is percolation of water from the land surface into longer-term storage in groundwater.

The oceans are governed by the following equation,

$$O = \int (SF + GD + P_O + M - E_M) \cdot dt \tag{58}$$

where O is the water storage in the oceans, GD is the discharge of groundwater to surface flow, which then flows to the oceans, and M is the melting of ice sheets into the oceans.

Groundwater storage, GS, is determined by,

$$GS = \int (GP - GD) \cdot dt \tag{59}$$

and ice storage, IS, is given by,

$$IS = \int (P_S - M) \cdot dt \tag{60}$$

Equations for the flows that determine changes in water storage in each of the components given in equations (55) to (60) are provided next, beginning with the flows

in equation (55). For the evaporation from the ocean to the marine atmosphere, the equation is,

$$E_M = E_{M0} \cdot T_{feedback} \tag{61}$$

where E_{M0} is the initial evaporation, set to 535200 km^3 yr^{-1}, as in Table 6, and $T_{feedback}$ is a multiplier that represents the effect of climate change on the global hydrological cycle. $T_{feedback}$ increases evaporation, evapotranspiration, snowfall, and melting rates within the natural hydrological sector by a fixed percentage for every degree of warming, and its value is based on two equations,

$$T_{feedback} = 1 + \left(P_{mult} \middle/ 100 \right) \tag{62}$$

$$P_{mult} = P_{mult,base} \cdot \Delta T_S \tag{63}$$

where $T_{feedback}$ is the temperature multiplier, and P_{mult} is the percentage increase calculated by equation (63), in which $P_{mult, base}$ is its base value, set to 3.4% K^{-1}. Clearly, P_{mult} depends on the change in surface temperature between initial and current conditions, which is represented by the ΔT_S term and is calculated in the model's climate sector. Since these two equations represent the effects of *intersectoral feedbacks* in the model, they are described in greater detail below.

The equation for advection from the marine atmosphere to the terrestrial atmosphere is given by,

$$Adv = Adv_0 \cdot \left(1 + \delta_{adv} / 100\right) \tag{64}$$

where Adv_0 is the initial advection value, set to 45375 km^3 yr^{-1}, as in Table 6, and δ_{adv} is the percentage change in advection because of changes in the gradient that drives

moisture from the marine atmosphere into the terrestrial atmosphere. The calculation for the percentage change in advection, δ_{adv}, is given by,

$$\delta_{adv} = 100 \cdot \frac{\left[\left(A_M/SA_{O\%} - A_L/SA_{L\%}\right) - \left(A_{M0}/SA_{O\%} - A_{L0}/SA_{L\%}\right)\right]}{\left(A_{M0}/SA_{O\%} - A_{L0}/SA_{L\%}\right)} \tag{65}$$

where A_{M0} and A_{L0} are the initial water contents of the marine and terrestrial atmospheres, respectively, as in Table 5, $SA_{O\%}$ is the percentage of the Earth's surface that is covered by oceans, and is set to 67%, while $SA_{L\%}$ is the remaining percentage that is land.

The equation that governs precipitation over the oceans, P_O, is,

$$P_O = P_{O0} \frac{A_M}{A_{M0}} \tag{66}$$

where P_{O0} is the initial precipitation over the oceans, given in Table 6.

From the flows in equation (56), the equation for evapotranspiration, ET, is,

$$ET = ET_0 \cdot \frac{LS}{LS_0} \cdot T_{feedback} + E_{res} + C_{wa} \tag{67}$$

where ET_0 is the initial evapotranspiration from the Earth's surface, given in Table 6, LS_0 is the initial water content of the land surface, given in Table 5, $T_{feedback}$ is given by equation (62), E_{res} is the evaporation from human-made reservoirs, explained below, and C_{wa} is the evaporation from consumptive water uses to the atmosphere, also explained in this section, below.

Precipitation over the land surface is broken into three components, P_R, P_S, and total precipitation, P_L. Precipitation in the form of rain over the land surface is governed by the following equation,

$$P_R = P_L - P_S + C_{wl} \tag{68}$$

where P_L is the total precipitation over land, given by equation (69), and C_{wl} is the addition to the land surface because of irrigation-based water-logging – note that C_{wl} is added to P_R for convenience only and is not intended to represent a component of the actual physical process of precipitation (recall that stocks can be influenced only through their flows). The total precipitation over land is given by,

$$P_L = P_{L0} \cdot {A_L}/{A_{L0}} \tag{69}$$

where the initial total precipitation over land, P_{L0}, is given in Table 6. Finally, the equation for precipitation in the form of snow is,

$$P_S = \left(P_{S0} \cdot {P_L}/{P_{L0}} \right) / T_{feedback} \tag{70}$$

where P_{S0} is the initial precipitation in the form of snow, which is given in Table 6, and $T_{feedback}$ is explained in the intersectoral feedbacks section, below. The effect of climate change here – division by $T_{feedback}$ rather than multiplication – is to decrease the amount of snow that falls as snow.

Several flows to and from the land surface, in equation (57), have already been provided. The surface flow equation is more complicated than most in this section, and takes the form,

$$SF = SF_0 \cdot \left({LS}/{LS_0} \right)^2 - E_{res} - C_{wa} - C_{gw} - C_{wl} - C_{loss} \tag{71}$$

where SF_0 is the initial surface flow, given in Table 6, the land surface content comparison is raised to the exponent 2 to model a non-linear increase in surface flow to the oceans as land storage increases, C_{gw} represents the seepage of withdrawn surface water to groundwater, and C_{loss} is the long-term, or permanent, loss of water from the hydrological cycle because of its incorporation into manufactured goods, and so on. The other consumptive flows, C_{wa} and C_{wl}, are explained in equations (67) and (68), respectively.

The last flow in equation (57) models the percolation of water from the land surface into groundwater storage. The equation for percolation is given by,

$$GP = GP_0 \cdot {LS}/{LS_0} + C_{gw} \tag{72}$$

where GP_0 is the initial percolation of land surface water into groundwater, which is given in Table 6, and C_{gw} was explained in equation (71).

Several of the flows that affect the oceanic water content, as provided in equation (58), have already been given. The remaining flows are groundwater discharge, GD, and melting, M. The equation for groundwater discharge is,

$$GD = GD_0 \cdot {GS}/{GS_0} + GW \tag{73}$$

where GD_0 is the initial groundwater discharge from Table 6, GS_0 is the initial groundwater storage from Table 5, and GW is the groundwater withdrawal, explained below. Note that, like C_{wl} in equation (68), GW is added to GD for convenience only and is not intended to represent a component of the actual physical process of groundwater discharge (again, recall that stocks can be influenced only through their flows).

Melting of ice occurs according to the following equation,

$$M = M_0 \cdot IS\Big/IS_0 \cdot T_{feedback}{}^2 \qquad\qquad (74)$$

where M_0 is the initial rate of ice melt, given in Table 6, IS_0 is the initial water content of ice sheets and glaciers, given in Table 5, and the $T_{feedback}$ is explained in the intersectoral feedbacks section, below. Note that the exponent on $T_{feedback}$ means that melting accelerates with changing temperature.

Finally, the flows for the groundwater and ice sheet storage of water, equations (59) and (60), have already been given in equations (70), (72), (73), and (74).

2.1.6.2 Human Water Withdrawals and Consumption

Since anthropogenic water withdrawals and consumption depend on overall surface water availability, the first requirement in developing an anthropogenic water use sector is the determination of a *stable*, or *steady-state*, runoff value, which occurs at some fraction of the total average runoff. Shiklomanov (2000: 18) sets this steady-state value at 37% of the total volume, while Simonovic (2002) and Alcamo et al. (2003a) use similar values of 33% and 32%, respectively. In this model, the *available surface water* is set to 37% of the total runoff, giving a base value of roughly 16000 km^3 yr^{-1}, as in Shiklomanov (2000).

The available surface water can be allocated to two forms of human water use: water withdrawals and water consumption. These two terms require definitions because of differences in terminology from one study to another. According to Gleick (2000b: 41), the term *withdrawal* "refers to water removed from a source and used for human needs. Some of this water may be returned to the original source with changes in the quantity and quality of the water." Water *consumption* "refers to water withdrawn from a source and made unusable for reuse in the same basin", through evaporation, seepage to a saline sink, or through contamination (Gleick, 2000b: 41). In other words, water *withdrawal* is the sum of water *consumption* and *returnable waters*. Note that the water returned after use to the surface flows, or the *returnable waters*, may cause surface water to become

polluted, which has important effects on the availability of surface water (Shiklomanov, 2000; Simonovic, 2002).

Both water withdrawals and water consumption have three components – domestic, industrial, and agricultural – as in other hydrological models, such as those developed by Alcamo et al. (2003a), Simonovic (2002), and Vörösmarty et al. (2000). Each of these components has different *drivers*, which are related to the quantitative elements of anthropogenic water demand and are explained next, while the values for several *prescribed* drivers are given in Table 7, below. Note that the structural change curve for the industrial sector does not have an inflection point; instead, it simply has the three points listed in the table.

In the case of the **domestic sector**, water demand is modelled on a *per capita* basis, which provides a connection to the *population* and *economic* sectors. Drivers of change in the domestic sector are *technological change* and changes in the *standard of living* and in the *municipal water system efficiency*. These last two drivers affect either water withdrawals or water consumption, and stem from what Alcamo et al. (2003a) term *structural change*. Here, structural change has two components because withdrawals depend on the standard of living, including the use of water-requiring household appliances, and so on (Alcamo et al., 2003a), while consumption depends on the efficiency of the water distribution and sewage systems (Shiklomanov, 2000).

For the **industrial sector**, the drivers include, 1) ongoing changes in the approach to cooling power generation plants, in an effect called *structural change*, and 2) changes in water-use efficiency per unit of energy required for industrial production via *technological change* (Alcamo et al., 2003a). Industrial water demand is modelled on an *energy-intensity* basis (m^3_{water} MWh_{energy}^{-1}), which provides a connection to a simple power generation sector in the model, while the level of structural change is driven by the economic sector – the equation for structural change in the industrial sector is therefore given in the intersectoral feedback section, below. In terms of the first industrial sector driver, water use depends on the transition from once-through flow to circulating water

supply systems for power generation, and on the development of dry technologies in the manufacturing industries (Shiklomanov, 2000). The most important result of a switch from once-through flow to circulating water systems for industrial cooling is that water withdrawals decrease strongly, while water consumption levels increase. *Technological change*, the second driver, "almost always leads to improvements in the efficiency of water use and a decrease in water intensity" (Alcamo et al., 2003a: 322), unlike structural changes which can either increase or decrease water intensity.

For the **agricultural sector**, the main drivers are *total irrigated area* and *technological change*. Climate change, through an *intersectoral* feedback, also plays an important role in determining irrigation water requirements, since the rate of evapotranspiration from irrigated areas will rise as the surface temperature increases. In terms of the first driver, the global irrigated area expanded rapidly during the 1950s-1970s; however, since that time it has slowed considerably in both developed and developing countries, because of the very high cost of irrigation system construction, soil salinization, depletion of water sources, and problems of environmental protection. According to Postel (1999: 60), "irrigation has simply begun to reach diminishing returns. In most areas, the best and easiest sites are already developed." For simulating future irrigation expansion, figures from Simonovic (2002) are used. The second agricultural driver, *technological change*, affects the specific water intake value, or base irrigation water requirement per hectare of irrigated land (Shiklomanov, 2000), used in the model. To model the effects of technological change, it is important to recognize that the overall efficiency of irrigation worldwide may be as low as 40% presently, and that certain advanced irrigation techniques can increase efficiency quite strongly (Gleick, 2000a).

Table 7: Water-use sectors, drivers, and prescribed changes over time (fractional)

| Sector | Driver | 1960 | Inflection Point | | 2100 | Source |
			Year	Value		
Domestic	Municipal Efficiency	1.0	2025	0.75	0.6	Based on Gleick (2000a)
Industrial	Structural Change	0.91	1995	0.89	0.7	Based on Shiklomanov (2000)
Agricultural	Technology	1.0	2025	0.85	0.7	Based on Gleick (2000a)

Note that, while technological change in the agricultural sector is prescribed in Table 7, technological change in the domestic and industrial sectors occurs according to the total factor productivity, equation (51), simulated by the economic sector. The transformation of A into a water sector *driver* occurs according to the following equation,

$$A_w = A / A_0 \qquad\qquad\qquad (75)$$

where A is the current total factor productivity and A_0 is its initial value.

Finally, humans affect the global water balance in one additional way. Over the course of the past century, and especially since 1960, a considerable number of reservoirs have been constructed worldwide. On an annual basis, reservoirs increase both evaporation from the land surface and seepage to groundwater, and reduce surface runoff to the oceans. Their combined effects make reservoirs "one of the largest freshwater users" (Shiklomanov, 2000: 17). To model evaporative losses from reservoirs, termed E_{res} in equation (67), above, historical figures are taken from Table 5 of Shiklomanov (2000: 24), while in terms of future development, new construction is likely to be limited by a lack of suitable sites (Simonovic, 2002).

2.1.6.3   Water Pollution and Water Stress

Having discussed the quantitative modelling of anthropogenic water demand, the next issue is simulating **water quality** and its effects on surface water availability. Wastewater results from domestic water use, industrial processes, and irrigation projects. It causes pollution of receiving waters, and in many cases, makes that water unsuitable for further use, especially for drinking-water supply. According to Shiklomanov (2000), every cubic meter of contaminated wastewater discharged into water bodies and streams renders eight to ten cubic meters of pure water unsuitable for use. Yet, although other authors recognize its importance – see Falkenmark (2005), Miller (2006), and Gleick (2000a), for example – the effect of wastewater on surface water availability is included in only one of the three hydrological models cited above. Simonovic (2002: 263), who

includes wastewater effects in his model, states that "the main conclusion of [his] research is that water pollution is the most important future water issue on the global scale."

To include the effects of wastewater on surface water availability, it is important to separate the water-use sectors, since each has different characteristics. In the domestic sector, *all* returnable waters require treatment (Gleick, 2000b), while in the industrial sector, only the wastewater from manufacturing processes requires treatment, since thermal power plants do not generate chemical pollution (Vassolo and Döll, 2005). In the agricultural sector, returnable waters come from broadly distributed fields and cannot be treated, despite the presence of fertilizers and toxic chemicals (Postel, 1999). As it stands now, the model draws no distinction between highly- and minimally-polluted water: all untreated wastewater uses the same *dilution factor* of one part wastewater to nine parts pure water. This simplification is probably acceptable, since Simonovic (2002) found that changing dilution factor values caused no significant change in the overall *WorldWater* model behaviour. Wastewater treatment parameters, as presented in Table 9, below, are set to match figures in WHO and UNICEF (2005).

Since the effect of untreated wastewater on global surface water withdrawals is to greatly increase, by the dilution factor, the amount of surface water appropriated for human use, the modelling of untreated wastewater effects on total surface water availability involves conversion of the *actual* surface water withdrawal into an *effective* withdrawal. This conversion is affected through multiplication of the wastewater volume by the dilution factor given by Shiklomanov (2000), and then addition of the resulting volume to the initial withdrawal. In other words,

$$W_{SW} = W_{SW,desired} + (\delta_{dil} - 1)W_{SW\ untreated} \tag{76}$$

where W_{SW} represents the effective withdrawal of surface water in $km^3\ yr^{-1}$, $W_{SW,\ desired}$ is the total volume of surface water required each year for domestic, industrial, and agricultural purposes, δ_{dil} is the dilution factor, set to 9, and $W_{SW\ untreated}$ is the untreated

volume of wastewater. The (δ_{dil} – 1) term avoids double-counting, since $W_{SW, desired}$ represents the total water requirement.

Clearly, as the effective withdrawal approaches the value of the total surface water availability, water scarcity issues will become increasingly important. Water scarcity is often measured via an indicator called *water stress*, which "is a measure of the degree of pressure put on water resources (including its quantity and ecosystems) by users of the resources, including municipalities, industries, power plants and agricultural users" (Alcamo and Henrichs, 2002: 353). The most commonly used indicator of water stress is the "annual withdrawals-to-availability (wta)" ratio, although *per capita* measures are also possible (Arnell, 1999b). Alcamo and Henrichs (2002) write that *wta* values of 0.2 indicate 'mid-stress' and that values of 0.4 and higher indicate 'severe stress', and Vörösmarty et al. (2000) use a similar scale. Indicator values of 0.2 or higher suggest that water stress is likely to limit development (Arnell, 1999b).

According to the usual ratio approach, water stress equals the total *withdrawal* over the surface water *availability*, or,

$$wta = W\big/(SF + GD) \tag{77}$$

where W is the *actual* surface water withdrawal and (SF + GD) is the total surface runoff available for human use; however, Hoekstra et al. (1997) argue that this total-runoff approach leads to overestimation of surface water availability. They recommend instead that water availability be considered some portion of the total runoff.

Therefore, in this research, water stress is altered in two ways to take water pollution into account by using the *effective*, rather than *actual*, withdrawal, as explained above, and a reduced fraction of the total runoff, called A_S. This modification gives water stress the following form,

$$wta = W_{SW} \big/ A_S \qquad\qquad (78)$$

where wta is now the *effective* surface water withdrawal, W_{SW}, as defined by equation (76), divided by the available runoff volume, A_S. The result is a much higher value of water stress than is calculated in the general fashion. Note that an equation for A_S is provided in the intersectoral feedbacks section, below.

Note that the concept of water scarcity is most meaningful at the watershed or sub-watershed level, and that even at national levels, identifying water-stressed nations may not be overly meaningful. Here, we apply the concept of water stress to the *entire globe*, because of the aggregation of all other sectors into single global values. The results of this aggregation demonstrate that water stress at a global scale does have meaning in a model of this type, as described below, although the global value does not apply to a particular local or regional level. Furthermore, the inclusion of water pollution in this model renders the results unique, and supports the view that water pollution may be a larger issue than is generally recognized.

2.1.6.4 Water Reuse

Water reuse offers a means to reduce water stress, as many of regions of the world, such as the United States, Southern Africa, Israel, and the Middle East have discovered (Gleick, 2000a; Gleick, 2000b; Simonovic, 2002). As clean surface water becomes scarcer, there is greater incentive to treat larger volumes of wastewater and then to reuse a portion of that treated wastewater. Thus, an increasing *water stress* indicator value in the model causes both the treated wastewater volume and the wastewater reuse fraction to increase over time. For example, when the water stress is low (below 0.2), increases in the level of wastewater treatment and reuse are unlikely; however, moderate to high water stress (values above 0.4) will almost certainly drive an increase in wastewater treatment and reuse, after some delay.

In the model, the amount of treated wastewater reused increases over time, with the rate of increase dependent on the level of global water stress and on a parameter that represents a real-world infrastructure or decision-based delay. The effect of water reuse is to reduce the *desired* surface water withdrawal volume in each water-use sector by the volume of treated wastewater used. According to Gleick (2000b), irrigation generally receives the most treated wastewater for reuse, followed by industrial and domestic uses. Unfortunately, wastewater reuse figures are generally anecdotal, so it is difficult to determine actual usage, particularly at a global level – the values in Table 8 are assumed to be representative, at present.

Table 8: Allocations to water-use sectors

Parameter Name	Sector			Source
	Domestic	Industrial	Agricultural	
Treated Wastewater Reuse	10%	30%	60%	Based on Gleick (2000b)

Note that, because of the form of calculation for the domestic and industrial treatment percentages, the values for wastewater treatment begin quite low, and then grow exponentially over long periods to a final value of 100% treatment. In other words, the growth in treatment percentage *does not slow*, as is the case with logistic growth, as it approaches 100%. Whether the final value should be 100% is an issue open to debate, but such a high value is unlikely to occur in reality. The likely cause of this behaviour is that economic considerations have no effect on the increase in wastewater treatment rates, as the model now stands. The equations for wastewater treatment and reuse are provided in the intersectoral feedbacks section, below.

2.1.6.5   Alternative Water Sources

Water scarcity also drives a search for alternative water sources, with additional water supply coming in the form of desalination and groundwater pumping. The question is how much water can come from these sources, and what is the trigger and rate of increase?

In this model, groundwater pumping refers to the extraction of non-renewable groundwater resources, where growth in groundwater use depends on the degree of water scarcity, and grows at an exponential rate until it reaches a maximum value, given by Simonovic (2002). Little information on the allocation of groundwater to different uses is available (Gleick, 2000b; Postel, 1999). It is therefore assumed that irrigation receives *all* the water from groundwater mining, which is a simplification, but not an unreasonable one, given the relatively large water demands of the agricultural sector. A feedback connection to the natural hydrological cycle is also necessary, since groundwater withdrawals are either consumed or return to surface water flows.

Currently, the best approach to modelling desalination is similar to the modelling of groundwater withdrawals; however, there are some important distinctions between groundwater mining and desalination that should eventually be taken into consideration: desalination requires a great deal of energy, is expensive, and causes pollution (the creation of a great deal of solid salt or highly-saline brine). Gleick (2000a: 135) provides information on worldwide desalination capacity growth, and suggests that the domestic sector is the primary destination of desalinated water. This model follows the logistic growth-based desalination expansion of Simonovic (2002).

Equations for both groundwater pumping and desalination are provided in the intersectoral feedbacks section, below.

2.1.6.6 Power Generation Components

Water use in the industrial sector depends on the total level of power generation, since industrial structural water intensity is measured in m^3 MWh^{-1}. Electricity production capacity is included in the water demand sector.

The growth in power generation capacity is modelled according to figures from the U.S. Department of Energy (Energy Information Administration (EIA), 2006), which is a source also used by Vassolo and Döll (2005); however, note that global electricity

production figures are available only from 1980-2005 (EIA, 2006). From 1960-1980, electricity production is assumed to grow linearly at 251.3 x 10^6 MWh yr^{-1}, and then at 357.2 x 10^6 MWh yr^{-1} from 2005 to 2100. These 'rate values' yield a linear increase in electricity production over the entire simulation period.

The equation used for the growth in electricity production is,

$$
\begin{aligned}
P_{elec} &= \int r_{elec} \cdot dt, \quad where, \\
r_{elec} &= 251.3 \; x \; 10^6 \; MWh \; yr^{-1} \; for \; 1960 - 1980, \\
r_{elec} &= EIA \; (2006) \; data \; for \; 1980 - 2005, \; and \\
r_{elec} &= 251.3 \; x \; 10^6 \; MWh \; yr^{-1} \; for \; 2005 - 2100.
\end{aligned}
\tag{79}
$$

2.1.6.7   Water Sector Calibration

Once the individual natural and anthropogenic water supply and demand components described above have been coupled together to create the water sector, the overall behaviour of the sector must be investigated. Parameter and initial values are also required in order to recreate the water sector model; values for the important characteristics of the anthropogenic withdrawal and consumption elements of the water sector are given in Table 9.

Table 9: Values for model parameters, and initial values for variables

Sector	Parameter/Variable Name	Initial Value (1960)	Notes
Domestic	Treated Wastewater Percentage	25%	Yields good match to WHO and UNICEF (2005) figures
	Delay in Establishing Treatment	30 yr	
	Min. Structural Water Intensity	17.5 m^3 cap^{-1} yr^{-1}	Parameter in Alcamo et al. (2003a)
	Max. Structural Water Intensity	220 m^3 cap^{-1} yr^{-1}	Parameter in Alcamo et al. (2003a)
	Curve Parameter, γ_d	2.2 x 10^{-8}	Parameter in Alcamo et al. (2003a)
Industrial	Max. Polluted Returnable Waters	42%	Based on returnable water ratio in Vassolo and Döll (2005)
	Treated Wastewater Percentage	40%	Yields good match to WHO and UNICEF (2005) figures
	Delay in Establishing Treatment	75 yr	
	Min. Structural Water Intensity	15 m^3 MWh^{-1}	Parameter in Alcamo et al. (2003a)
	Max. Structural Water Intensity	100 m^3 MWh^{-1}	Else ISWI $\rightarrow \infty$ when GDP $\approx$ GDP_0
	Curve Parameter, γ_i	6.5 x 10^{-6} MWh m^{-3} $\$^{-1}$	Based on Alcamo et al. (2003a)

Agricultural	Specific Water Intake	10500 m^3 ha^{-1}	Shiklomanov (2000: 22)
	Pollution of Returnable Waters	80%	
All	Wastewater Reuse Percentage	5%	
	Wastewater Reuse Increase Rate	0.09% yr^{-1}	
	Infrastructure/Policy Delay	20 yr	
Sources	Max. Groundwater Extraction	8.4 km^3 yr^{-1}	Simonovic (2002)
	Max. Desalination Capacity	4.2 km^3/yr^{-1}	Simonovic (2002)

Historical water use figures are available in Shiklomanov (2000), Shiklomanov and

Rodda (2003), and Chapter 3 of Gleick (2000b), that allow a comparison between model-

generated values and the historical water use figures. In Table 10, the historical water

use figures in Shiklomanov (2000) for 1960-2000 are replicated over the model

calibration period and compared with model simulations using the full, interconnected

water sector as described above – overall, the model results closely match the historical

figures. Other water sector figures are provided below, under Model Validation, and in

Davies (2007).

Table 10: Withdrawal and consumption values from Shiklomanov (2000) versus model results (km^3 yr^{-1})

	Assessment					Forecast
Year	1960	1970	1980	1990	1995	2000
Total Withdrawals	1968	2526	3175	3633	3788	3973
Total Consumption	1086	1341	1686	1982	2074	2182
Modelled Withdrawals	1961	2542	3122	3632	3759	3874
Modelled Consumption	1120	1390	1682	1997	2077	2145

2.2 Intersectoral Feedbacks in the Model

To examine the feedbacks involved in shaping Earth-system behaviour over the next

century, the model connects the natural and socio-economic sectors described above

through a series of *intersectoral feedbacks*. This section explains the theoretical and

mathematical basis of those feedbacks, which are depicted in Figure 1 of section 3.1,

above.

Clearly, the model represents the society-biosphere-climate system as a set of linked,

closed-loop structures, each of which can affect the other sectors and loops in a *causal*

fashion. All of the major elements of the system are *endogenous*, or included explicitly,

so that the dynamic behaviour of the model arises from the system structure rather than from input data or driving functions. Recall that from a modelling perspective, the advantage of an endogenous approach is that it allows a direct, simulation-based exploration of changes in behaviour that result from adjustments to the model structure and the rules of interaction. In other words, the dynamics of these models change as a modeller prescribes new arrangements between the *represented* variables and processes in the model (Sterman, 2000). As opposed to the system dynamics approach, models based on driving functions and *exogenous* relationships explain the dynamics of important variables in terms of other variables whose behaviour has been assumed.

In Figure 1, the positive or negative polarity associated with each arrow indicates the direction of change one model component imposes on the next. Positive relationships represent change in the same direction, where an increase/decrease in one sector causes an increase/decrease in the next sector, while negative relationships mean that change occurs in the opposite direction, so that an increase/decrease in one sector causes a decrease/increase in the next sector. The figure also presents the manner in which one model component influences the next: each arrow-connection between two model sectors bears the name of the sectoral element whose change causes a related change in the next model sector. As in Figure 1, the model feedbacks described below therefore include connections between,

- The *carbon* and *climate* sectors through atmospheric CO_2 concentrations;
- The *climate* and *surface flow* sectors through surface temperature change;
- The *climate* and *economy* sectors through surface temperature change;
- The *surface flow* and *water demand* sectors through surface water availability, and also through water consumption;
- The *surface flow*, (*water demand*) and *population* sectors through water stress;
- The *surface flow* and *water quality* sectors through wastewater treatment and reuse;
- The *water demand* and *water quality* sectors through wastewater treatment and reuse;
- The *population* and *water demand* sectors through population;

- The *population* and *land-use* sectors through forest and grassland clearing and burning;
- The *population* and *economy* sectors through consumption per capita and labour;
- The *economy* and *carbon* sectors through industrial emissions;
- The *economy* and *water demand* sectors through economic output (GDP); and,
- The *land-use* and *carbon* sectors through land-use emissions.

The following description of feedback equations has two parts, based on *water-* and *non-water* sectors – since the water demand, water quality, and surface flow (natural hydrological cycle) sectors are interdependent and essentially inseparable, their interconnections are described separately from the rest of the intersectoral connections. The non-water sectors, climate, carbon cycle, economy, land-use, and population are described first.

2.2.1 Feedbacks in the Non-Water Sectors

The **carbon cycle-climate** sector feedback depends on the atmospheric CO_2 concentration as determined by the carbon sector, and uses a *forcing equation* to translate the atmospheric concentration into a radiative forcing, which then leads to an increase in surface temperature. A doubling of CO_2 causes an equilibrium surface temperature increase of 1.8°C. The forcing equation is linear – meaning that 4xCO_2 will result in 2x1.8°C, or 3.6°C, of surface temperature change at equilibrium – and has this form, which is repeated from the climate sector equations, above,

$$F = S\left(C_A \middle/ C_{A0}\right) - S \qquad (2)$$

Recall that F is the climate forcing in W m^{-2}, S is a 'climate sensitivity' constant, also in W m^{-2}, and C_A and C_{A0} represent the current and initial atmospheric carbon dioxide concentrations, respectively, as explained in equations (13) and (16), above.

The **climate and surface flow** sectors are connected via the surface temperature change. Since increased surface temperature will likely increase the intensity of the hydrological cycle as well as amplify precipitation volumes, the model includes a *temperature multiplier* equation that increases evaporation, evapotranspiration, snowfall, and melting rates within the natural hydrological sector by a fixed percentage for every degree of warming. For calculation of the *temperature multiplier*, Huntington (2006) explains that global precipitation is energy rather than moisture limited, and so precipitation is expected to rise by *3.4%* per 1°C surface temperature increase. Note, however, that such values are still uncertain, as the overall effect of climate change on the global hydrological cycle remains unclear. Therefore, as given above, the equations for the temperature and precipitation multipliers are,

$$T_{feedback} = 1 + \left(P_{mult} \Big/ 100 \right) \qquad (62)$$

$$P_{mult} = P_{mult,base} \cdot \Delta T_S \qquad (63)$$

where $T_{feedback}$ is the temperature multiplier described above, which takes its value from P_{mult}, the precipitation multiplier calculated by equation (63). $P_{mult,\,base}$ is the multiplier base value, $3.4\%\ K^{-1}$. Again, P_{mult} depends on the change in surface temperature, ΔT_S, measured in Kelvin, which is calculated in the model's climate sector.

In a similar fashion to the climate-surface flow feedback, two elements of the **water use** sector have connections to changes in the surface temperature as simulated by the **climate** sector. Agricultural water demand and reservoir evaporation both increase with temperature change because of greater evaporation with increasing surface temperature. To model the effects of climate change on irrigation water requirements, the "per hectare water withdrawals" and "per hectare water consumption" are multiplied by the same *temperature multiplier*, equation (62), as in the surface flow sector.

The **climate** influences the **economy** through two equations: 1) a temperature damage function, *D*, developed by Nordhaus and Boyer (2000), based on an extensive literature review of the economic impacts of climate change, and 2) a climate damage multiplier, *Ω*, which is derived from D. Recall that these two variables, D and Ω, were introduced above as equations (48) and (49). Again, the temperature damage function takes this form (Nordhaus and Boyer, 2000: 23)

$$D = \theta_1 \cdot \Delta T_S + \theta_2 \cdot \Delta T_S^{\,2} \tag{48}$$

where D is the percentage damage to the economy as a function of changing surface temperature, θ_1 and θ_2 are parameters, and ΔT_S is the surface temperature change from pre-industrial levels. Note that the units Nordhaus and Boyer (2000) assign to D are erroneous, but the Excel version of DICE-99 (Nordhaus and Boyer, 1999) has the correct *percentage* units. Füssel (2007) details additional unit inconsistencies between DICE versions.

Based on equation (48), the climate damage multiplier affects the Cobb-Douglas production function used by DICE, equation (46), above, and takes this form (Nordhaus and Boyer, 2000: 23),

$$\Omega = {1}\big/{(1 + D/100)} \tag{49}$$

where, again, Ω is a unitless multiplier with an initial value of one.

The **surface flow, water demand and population** sectors are connected through global water stress levels. The reasoning behind this connection runs as follows: water availability determines agricultural output, economic growth, and power generation; water scarcity limits all three, and severe water scarcity results in lower fertility rates, or even famine and increased mortality rates. Therefore, water stress essentially serves as a *proxy* for many other aspects of population growth. The effect of this assumption is

examined in Davies (2007). As the model is configured presently, increased water stress simply reduces the levels of population growth that might otherwise have occurred with greater surface water availability; however, see Simonovic (2002) for a more dramatic example of this connection. For the population to surface flow connection in this model, the form of the equation is simply,

$$g = b \cdot wta \tag{80}$$

where g represents the decline in the population growth rate – a second-order, deceleration-like term – and wta is the water stress level, taking pollution effects into consideration, from equation (78), above. The parameter b is an arbitrary, dimensionless constant that matches simulated values with historical population figures from UNESA (2006), and has a value of 0.025 for most model simulations.

Note that the *wta* of equation (78) is not used directly to drive other variables; instead, a modification of the base wta calculation is used, called *water stress effects*, which slightly reduces high values of water stress. The reasoning here is that the effects of water scarcity are likely to drive change fairly quickly as water stress increases, but that their effects will begin to saturate at a certain point as other socio-economic factors come into play. The form of 'water stress effects' is a natural logarithm-based curve, with an asymptote at 1, and water stress effects values begin to diverge from the base value for wta above 0.6. In this chapter, references to equation (78) are actually references to the related 'water stress effects' variable.

To obtain the growth rate for the global population, the form of the equation is,

$$\frac{dr}{dt} = r \cdot g \tag{81}$$

where r is the population growth rate, and g is the decline in the population growth rate, as defined in equation (80). Finally, the change in population per year follows the same format as equation (81), such that,

$$\frac{dP}{dt} = P \cdot r \tag{82}$$

Equations (80), (81), and (82) are solved by numerical integration (see Appendix B), since none of the relevant variables (wta, g, and r) are constant – recall that wta depends on water availability, demand, and pollution, all of which are variable and are subject to model feedbacks.

The **economy, water demand, and population** sectors use a set of equations developed by Alcamo et al. (2003a: 321, 322) that relate economic performance, as modelled in the economy sector, to water use levels in the domestic and industrial sectors of the water use sector. These equations calculate values for *domestic* and *industrial structural water intensities*, or DSWI and ISWI, that depend on *absolute* and *relative* measures of gross domestic product, respectively. The DSWI curve also depends on global population, since domestic water demand is modelled on a *per capita* basis, while ISWI also depends on electrical power generation, as described above. The equations for DSWI and ISWI are therefore

$$DSWI = DSWI_{min} + DSWI_{max} \cdot \left(1 - e^{-\gamma_d \left(Q/P \right)^2} \right) \tag{83}$$

$$ISWI = \frac{1}{\gamma_i \cdot \left(Q/P - Q_0/P_0 \right)} + ISWI_{min} \tag{84}$$

where DSWI is the domestic structural water intensity in m^3 person^{-1} yr^{-1}, DSWI$_{min}$ is the base amount, DSWI$_{max}$ is the maximum amount, γ_d is a curve parameter (all three, DSWI$_{min}$, DSWI$_{max}$, γ_d, are calibrated values), Q is the total annual economic output from

the economic sector of the model, given by equation (46), above, and P is the current global population from the model's population sector, based on equation (82), above. In equation (84), the situation for ISWI, $ISWI_{min}$, Q and P is similar, γ_i is a curve parameter, Q_0 is the initial global output, and P_0 is the initial global population. ISWI is measured in m^3 MWh^{-1} yr^{-1}, and parameter values for equations (83) and (84) are provided in Table 9, above.

In a similar fashion, the **population and economy** sectors are connected through an important element of the DICE model's Cobb-Douglas production function. Although DICE modifies the equation somewhat – see equation (46) above, or Nordhaus and Boyer (2000: 181) – to take climate damage and carbon tax policies into account, Cobb-Douglas functions typically take the form of equation (47), repeated here,

$$Q = z \cdot K^{\gamma} \cdot L^{1-\gamma} \tag{47}$$

where Q represents the net economic output per year, or GDP, z is the total factor productivity, called A in equation (51), which represents *technological progress*, K is the capital stock, γ is an elasticity parameter, and L is labour, or the global aggregate population, P, of equation (82), above. Nordhaus and Boyer (2000) include the climate damage multiplier, Ω – see equation (49), above – to account for the effects of climate change on production.

The calculation of **industrial emission levels** is a component of the DICE model, which, as explained above, depends on the economic output calculated by equation (46) as well as a ratio of emissions to output or *emissions intensity*, σ, and emissions control measures, μ, such as carbon tax policies – see equations (50) and (54), above, or Nordhaus and Boyer (2000: 181, and 185-6). Note that in order to match the 1960-1995 emissions values from the model to historical emissions from Marland et al. (2007), modification to the σ equation was necessary. As given above, the equation for industrial emissions is,

$$E = (1 - \mu) \cdot \sigma \cdot Q \tag{16}$$

The **population and carbon sectors** are linked through the land-use sector, following the approach of Goudriaan and Ketner (1984), who model CO_2 emissions from clearing and burning *within* a terrestrial biome, and from land-use *conversions* that establish new land-cover in the place of the previous vegetation. Yearly conversions from one biome type to another grow proportionally to the global population, while burning and clearing within a biome occurs in proportion to the square-root of the population growth (Goudriaan and Ketner, 1984: 180).

As explained above, the land-use sector equations use a 6x6 *transfer matrix*, TM_{ij}, with row $= i$ and column $= j$ subscripts, where column headings j mean '*from* biome type' and row headings i mean '*to* biome type'. Thus, TM_{11} means a transfer of land-use *from* tropical forest *to* tropical forest (in other words, cultivation and burning *within* the tropical biome), TM_{31} means a change in land-use from tropical forest to grassland, and TM_{46} means a change in land-use from semi-desert and tundra to agricultural area. Transfer matrix entries, of which there are 6 x 6 = 36, can be either zero (24 in total) or non-zero (12 in total) and are measured in biome area use or transfer of Mha yr^{-1}. The initial values used for the model are presented in Table 4, above.

To determine changes in the land area of a biome, then, there are two equations. For all $i = j$ (the diagonal members for cultivation and burning *within* the tropical biome, in other words),

$$\frac{dTM_{ii}}{dt} = r^{1/2} \cdot TM_{ii} \tag{25a}$$

while for all $i \neq j$ (which represents a change of biome area from type j to type i),

$$\frac{dTM_{ij}}{dt} = r \cdot TM_{ij} \tag{25b}$$

In equations (*25a*) and (*25b*), dTM$_{ii}$/dt and dTM$_{ij}$/dt represent the change in the annual cultivation and burning within a biome and change in biome area, respectively, while r is the annual population growth rate defined in equation (78), above. Written in logical form, the equation takes the form presented above and repeated here:

$$\frac{dTM_{ij}}{dt} = \quad for \; all \; (i, \, j):$$
$$if \, (i = j),$$
$$r^{1/2} \cdot TM_{ij},$$
$$else(r \cdot TM_{ij}); \tag{25}$$

The 'for' condition requires equation (25) to run thirty-six times, once for each separate combination of *i* and *j*, since i x j = 36.

In terms of the carbon fluxes to the atmosphere, which cause a change in the atmospheric carbon dioxide levels, there are three important equations that all rely on equation (25). Essentially, land-use via shifting cultivation and burning results in the burning of a large fraction of biomass and litter and its direct release to the atmosphere. Land transfer to a different biome is treated in basically the same way, but also includes the redirection of stem and root material either to the atmosphere through decomposition or to soil humus via the same process. See equations (28), (29), and (32), above. Adding the direct effects of land-use change together yields the total flux of carbon from the terrestrial biosphere to the atmosphere,

$$LU_C = B_B + B_L \tag{85}$$

where LU_C is the carbon dioxide flux in Gt C yr^{-1} from land-use and land-use change, and B_B and B_L represent the annual total biomass burned and the annual total litter burned. The decomposition of root material resulting from land transfer is an important

component of land-use change, but is not included in equation (85) because it is not an immediate transfer.

2.2.2 Feedbacks in the Water Sectors

The **surface flow, water demand, and water quality** sectors form a closed loop, interacting with one another via water stress, surface water availability, water withdrawals and consumption, wastewater treatment, and treated wastewater reuse. Feedbacks between elements of the water sectors include:

- The basis of the majority of the water sector in the calculation of *water stress* from water withdrawals versus surface water availability; and,
- The construction of reservoirs and the resulting increase in evaporation from the land surface, with a corresponding reduction in surface flows;
- The withdrawal of groundwater and the resulting increase in surface flows and decrease in both surface water withdrawal and groundwater volume;
- The effects of desalination on the global volume of surface water withdrawal;
- The effects of water withdrawal (and use) on the production of wastewater;
- The effects of water stress on the wastewater treatment percentage;
- The effects of wastewater treatment on water stress; and,
- The reuse of treated wastewater and the corresponding decrease in surface water withdrawal.

Since the interactions between the water sectors are actually somewhat more complicated than is apparent from Figure 1, an additional feedback diagram that focuses specifically on important elements of the three water sectors is presented in Figure 2. Feedbacks that connect the water sectors with the non-water components, in regular type, are included as dashed lines. Note that the three water sectors are best represented by one or more of the variables listed, although the listed variables are not complete representations of the water sectors. 'Withdrawal' fits in the water demand sector, as would water consumption, for example, if it were included in Figure 2. 'Surface Flow' represents one component of the larger natural hydrological cycle. Finally, wastewater reuse and

wastewater treatment fit within the water quality sector. The other variables either result from a combination of values from separate water sectors (water stress and wastewater volume, for example), or function as intermediaries, since their value is affected by one sector, and then serves as input to a different water sector.

Figure 2: Interactions of important characteristics of the water sectors, with connections to other sectors (after Davies, 2007)

As explained above, **water stress** is a measure of *water scarcity*, and is calculated in this research as the *effective* withdrawal over the *available* surface runoff – recall that the *effective* withdrawal incorporates water pollution in the water stress calculation by considering every 1 m^3 of polluted water as the equivalent of 8-10 m^3 of pure water (Shiklomanov, 2000). The equation for the modified water stress calculation is given in equation (78), and repeated here,

$$wta = {W_{sw}}/{A_S} \qquad\qquad (78)$$

where W_{sw} represents the total – domestic, industrial, and agricultural – effective global surface water withdrawal and A_S is the total surface water availability for human use, as explained above.

The **total surface runoff**, of which A_S is a relatively small component, is simply the sum of the surface flow plus the groundwater discharge, so that,

$$Q_S = SF + GD$$
$$= \left(SF_0 \cdot \left(LS / LS_0 \right)^2 - E_{res} - C_{wa} - C_{gw} - C_{wl} - C_{loss} \right) + \left(GD_0 \cdot GS / GS_0 + GW \right) \quad (86)$$

where Q_s is the global total annual surface runoff, measured in km^3 yr^{-1}, and SF and GD are the annual surface flow and groundwater discharge, from equations (71) and (73), above. There are two important notes here: 1) the similarity in symbols between Q_s in equation (86) and Q in equation (46) is purely coincidental, and 2) the difference between Q_S and A_S is important, and is given by this equation,

$$A_S = f_s \cdot Q_S \quad (87)$$

where f_s is the *stable*, usable fraction of global run-off, set to 0.37 (Shiklomanov, 2000).

Reservoir construction is prescribed according to historical data and the corresponding evaporation values are taken directly from Shiklomanov (2000), while future construction slows over the 21st century so that evaporation reaches a maximum base value of 305 km^3 yr^{-1} by 2100, according to the figures used by Simonovic (2002). Since reservoir evaporation is affected by the degree of global climate change, its equation is,

$$E_{res} = E_{res0} \cdot T_{feedback} \quad (88)$$

where E_{res} is the annual evaporation from reservoir surfaces, measured in km^3 yr^{-1}, E_{res0} is the base evaporation, and $T_{feedback}$ is the temperature feedback term, from equation (62).

The term '**groundwater withdrawal**' pertains only to the withdrawal of non-renewable – or *fossil* – groundwater for human use. Its annual use is capped at 8.4 km^3 yr^{-1}, as in Simonovic (2002), and depends on the current demand for fresh water versus the current level of water scarcity. The modelling of groundwater withdrawal from deep aquifers is quite straightforward and has two parts,

$$\frac{dGW_{fraction}}{dt} = \begin{array}{l} if\left(GW_{fraction} < 1\right), \\ \left(wta \cdot GW_{fraction}\right)/t_{pump} \\ else\left(GW_{fraction} = 1\right); \end{array} \tag{89}$$

where equation (89) is written in logical form, with $GW_{fraction}$ as the current fraction (0.0-1.0) of the global maximum of groundwater withdrawal, wta the same as in equation (78), and t_{pump} the delay in establishing additional groundwater pumps, set to 10 yr. Equation (89) causes groundwater withdrawals to increase exponentially, since the basic form is a positive feedback – the growth of $GW_{fraction}$ depends on its current value, in other words. The second part of the groundwater pumping relationship is

$$G_w = GW_{fraction} \cdot G_{w,\max} \tag{90}$$

where G_w is the annual volume of groundwater pumping, $GW_{fraction}$ comes from equation (89), and $G_{w,max}$ is the capped-maximum value given above.

Once the groundwater is withdrawn from the aquifer, it reduces the desired *surface water* withdrawals for agriculture, and is no longer present in the groundwater pool. The result of groundwater pumping, reduction of the desired surface water withdrawal, is straightforward to model – whatever water comes from groundwater pumping need not come from surface water bodies:

$$W_a = T_{feedback} \cdot W_{a,\,desired_0} - G_w - Q_{ww\,reuse,\,a} \tag{91}$$

where W_a is the total agricultural water withdrawal from *surface water sources*, $W_{a,desired0}$ is the *base total required* agricultural water withdrawal, which is modified by climate change according to $T_{feedback}$ from equation (62), G_w is from equation (90), and $Q_{ww\,reuse,a}$ is the volume of treated wastewater used for irrigation purposes. Note that agriculture is the only water sector affected directly by changing global surface temperatures.

Desalination is modelled in a similar fashion to groundwater withdrawal, with the increase in annual desalinated volume based on water scarcity and with a capped maximum annual production volume. However, while the groundwater withdrawal is modelled in terms of the fraction of the maximum withdrawal, desalination is modelled as an annual volumetric desalination capacity, and the capacity growth is modelled using an S-curve, so that

$$\frac{dDC}{dt} = wta/t_{desalinate} \cdot \left(DC - DC^2/DC_{max} \right) \qquad (92)$$

where DC is the global yearly desalination capacity in $km^3\ yr^{-1}$, wta is defined in equation (78), DC_{max} is set to 32.4 $km^3\ yr^{-1}$, and $t_{desalinate}$ is the time required to plan, construct, and bring new desalination facilities into use, set to 5 yr. DC is of course the integral of dDC/dt. Another important issue is the overall capacity usage of desalination plants worldwide, which is estimated as 50% in the model in order to create a match between figures in Gleick (2000a; 2000b) with Simonovic (2002).

Once seawater is desalinated, it is used exclusively by the domestic water sector, so that an equation similar to (91) results

$$W_d = W_{d,desired} - DC - Q_{ww\,reuse,d} \qquad (93)$$

where W_d is the total domestic water withdrawal from *surface water sources*, $W_{d,desired}$ is the *total required* domestic water withdrawal, DC is from equation (92), and $Q_{ww\ reuse,\ d}$ is the volume of treated wastewater used for domestic purposes.

All domestic, manufacturing, and agricultural water uses produce **wastewater**. The model determines the wastewater volumes produced by each sector per year according to three simple equations, one for each of the water use sectors. The equation form is,

$$Q_{ww}[\sec tor] = (\pi[\sec tor]/100) \cdot Q_{ret}[\sec tor] \qquad (94)$$

where Q_{ww}[sector] is the total wastewater volume for each of the domestic, industrial, or agricultural sectors, π[sector] represents the *polluted percentage*, which has possible values of 0-100%, and Q_{ret}[sector] is the returnable water volume for the sector in question. The '[sector]' term represents a three-member array of domestic, industrial, and agricultural wastewater production values, so that the total wastewater production, Q_{ww}, equals the sum of the three sectoral values, or $Q_{ww} = Q_{ww}$[dom] + Q_{ww}[ind] + Q_{ww}[agr], in other words. The polluted percentage, π[sector], has a different, fixed value for each sector: 100% for the domestic sector (Gleick, 2000b), 42% for the industrial sector (Vassolo and Döll, 2005), and 80% for the agricultural sector. The final variable, returnable water volume, or Q_{ret}[sector], is simply the difference between the water withdrawals and consumption for each sector, both of which change each year, as explained above.

Unlike wastewater production, the **wastewater treatment percentage** has only two components, *domestic* and *industrial* – since agricultural wastewater is untreatable – which depend on the global water stress level. Each component follows computational logic similar to that used for groundwater withdrawal, as in equation (89), which generates the same sort of exponential growth because of positive feedback. To calculate the wastewater treatment percentage, then, the following logic is used:

$$\frac{d\tau_{ww\% \, d/i}}{dt} = \quad if\left(\tau_{ww\% \, d/i} < 100\right),$$
$$\left(wta \cdot \tau_{ww\% \, d/i}\right)/t_{treat \, d/i} \qquad (95)$$
$$else\left(\tau_{ww\% \, d/i} = 100\right);$$

where $\tau_{ww\% \, d/i}$ represents the global wastewater treatment percentage for the domestic *or* industrial sector, rather than division of one by the other, wta is defined in equation (78), and $t_{treat \, d/i}$ is the time required to plan, construct, and bring new domestic or industrial wastewater treatment facilities into use. Clearly, higher water scarcity levels lead to higher rates of wastewater treatment facility construction, while lower water stress decreases the rate of establishment of water treatment infrastructure.

The treated, returnable wastewater volume in km^3 yr^{-1} is then given by this equation,

$$Q_{treated \, ww} = \tau_{ww\% \, d} \cdot Q_{ww}[dom] + \tau_{ww\% \, i} \cdot Q_{ww}[ind] \qquad (96)$$

where $Q_{ww}[dom]$ and $Q_{ww}[ind]$ are the total volumes in km^3 yr^{-1} of domestic and industrial wastewater from equation (94), while the wastewater treatment percentage, $\tau_{ww\% \, d/i}$, is from equation (95).

The **reuse of treated wastewater** depends on the global water stress level, follows the same computational logic as the wastewater treatment percentage (95), and generates the same sort of exponential growth. To calculate the treated wastewater reuse, then, the following logic is used:

$$\frac{d\tau_{ww \, reuse \, \%}}{dt} = \quad if\left(\tau_{ww \, reuse \, \%} < 100\right),$$
$$\left(wta \cdot \tau_{ww \, reuse \, \%}\right)/t_{reuse} \qquad (97)$$
$$else\left(\tau_{ww \, reuse \, \%} = 100\right);$$

where $\tau_{ww\ reuse\ \%}$ represents the global percentage of treated wastewater reuse, wta is defined in equation (78), and t_{reuse} is the time required to plan and institute treated wastewater reuse programs, set to 20 yr. Clearly, higher water scarcity levels encourage higher rates of wastewater reuse, while lower water stress levels decrease the necessity of wastewater reuse.

Treated wastewater for reuse must be allocated to the domestic, industrial, or agricultural sector, since each can make use of some treated wastewater. Based on anecdotal information from the literature (see above), the percentage allocation to each sector is therefore set to 10%, 30%, and 60% for the domestic, industrial, and agricultural sectors respectively. The actual volume of treated wastewater reused creates the feedback of interest here, where wastewater reuse is calculated according to

$$Q_{ww\ reuse}[\sec tor] = \left(\tau_{ww\ reuse\ \%} / 100\right) \cdot \left(\tau_{ww\ \%\ by\ \sec tor}[\sec tor]/100\right) \cdot Q_{treated\ ww} \qquad (98)$$

where the amount of treated wastewater allocated to each sector is $Q_{ww\ reuse}$[sector], in $km^3\ yr^{-1}$, with the '[sector]' term again representing a three-member array of domestic, industrial, and agricultural uses, $\tau_{ww\ reuse\ \%}$ is from equation (97), $\tau_{ww\ \%\ by\ sector}$[sector] takes the values of 10%, 30%, and 60%, as explained above, and $Q_{treated\ ww}$ is from equation (96).

Equation (98) reduces the overall required surface water withdrawals through equations (91) and (93), which are for W_a and W_d, respectively. Along the same lines, industrial surface water withdrawals can be written as,

$$W_i = W_{i,\ desired} - Q_{ww\ reuse,\ i} \qquad (99)$$

following the notation used for W_a and W_d. From these three equations, the result of wastewater reuse is clearly to lower the total actual surface water withdrawal and thus to decrease global water stress levels.

2.2.3 Summary

The descriptions and equations above provide the theoretical and mathematical basis of the feedbacks between different sectors of the model – note that further information is provided in Appendix B. Figure 1 shows the basic feedbacks for the whole model in a causal loop with labelled arrows, while the similar Figure 2 focuses on the key elements of the three water sectors. To summarize both figures and descriptions, a third figure has been created that ties together the important variables in the equations above as a set of feedback loops. The resulting Figure 3 clarifies the overall information flows in the model, and so serves as a complement to the other means of explanation.

In Figure 3, there is no indication of polarities as in a standard causal loop diagram, because it is not intended to be read in terms of reinforcing/balancing loop behaviour. It should instead be understood as a means of tracing the effects of changes in one variable on the other key variables in the model – the flow of information from one sector to the next. It also serves as a sort of index to the equations provided above. As in a causal loop diagram, arrows denote causality, so that change in one variable causes change in the next variable. In other words, $x \rightarrow y$ means a change in x causes a change in y.

For ease of reference to the equations above, equation numbers are provided in Figure 3, in round brackets above each arrow.

Figure 3: Major intersectoral information flows and feedbacks (after Davies, 2007)

2.3 Novel Aspects of the Model

Individual sectors of the model contain novel features, both in terms of the connections
between different variables and the mathematical expressions of those variables, while
the model structure as a whole, despite similarities with a variety of different models and
model types, has several unique elements.

At the level of individual sectors, the model introduces new representations of the global
water demand and water quality sectors, and modifies a version of the hydrological sector
based on earlier work at the University of Western Ontario. Other sectors of the model,
as shown in Figure 1, come from previous work by other researchers either directly, or
with slight modification, as is the case with the implementation of an endogenous driver

for the population sector, and a change in the start date and time-step for the DICE-99 economic sector.

The model as a whole replicates key feedbacks between a set of sectors that also exist, to various degrees, in integrated assessment models, climate-economy models, and water supply and demand models. For example, the model contains the same representation of the macro-economic system that is present in climate-economy models like DICE (Nordhaus and Boyer, 2000), and FREE (Fiddaman, 1997) – note that, like DICE, this model omits an energy sector, and that, like DICE and FREE, it also neglects food production. Furthermore, the majority of the sectors present in integrated assessment models like ICAM-1 (Dowlatabadi and Morgan, 1993a), IMAGE 2.0 (Alcamo et al., 1994), and TARGETS (Rotmans and de Vries, 1997) are present in this model as well, although clearly each model is different. Finally, the model simulates water supply and demand like the more complicated WaterGAP2 model (Alcamo et al., 2003a), as well as surface flows and water scarcity, like WaterGAP2, Macro-PDM (Arnell, 1999b), and WBM (Vörösmarty et al., 2000); and in a similar fashion to TARGETS and WorldWater (Simonovic, 2002), the model also simulates water quality issues.

Clearly, many of the models listed above have much higher spatial resolution and a higher level of complexity. IMAGE 2.0 (Alcamo et al., 1994) operates at high resolution on a global grid and includes a variety of important socio-economic and natural components and processes. With a similarly high resolution, WaterGAP2 (Alcamo et al., 2003a) simulates both water demand and supply. TARGETS (Rotmans and de Vries, 1997) has a similar resolution to this model, but includes a variety of nutrient cycles, agricultural production, and human health, while WorldWater (Simonovic, 2002) models persistent pollution and population growth in greater detail. RICE (Nordhaus and Boyer, 2000) improves on DICE substantially, and divides the world into eight economic regions. However, IMAGE 2.0 does not include water supply or demand, WaterGap2 models water supply and use, but not water quality, TARGETS prescribes economic behaviour in scenario-form, WorldWater neglects climate change, nutrient cycles, and land-use, and DICE and RICE ignore water and land-use, model population exogenously,

and simplify the climate system and carbon cycles dramatically. In other words, modelling involves trade-offs, and so each of these models has a different focus. The resulting variations between models have important effects on simulated behaviour: in this model, both the novel water sectors and the endogenous representation of population growth combine to yield unanticipated behavioural patterns and novel insights into Earth-system feedbacks, as explained in Chapter 4 of Davies (2007).

To explore the differences between the model presented here and other models in the literature in greater detail, Table 11, below, provides the important output of each intersectoral feedback equation listed above and displayed in Figure 3, the other variables it affects, model types that contain similar feedbacks, and specific examples of such models, and a brief comparison of this model with examples from the literature. Note that equation numbers in **bold** type, with an asterisk beside them, mark novel connections in the model.

Table 11: Intersectoral equations, their outputs and feedbacks, and inter-model comparison

Equation	Output Variable	Affected Variables	Model Comparison	Model Names	Comments
2	F	ΔT	GCM, EMIC, Simple model, IAM	Any climate, climate-economy, or integrated assessment model	Essentially any models that translate atmospheric greenhouse gas concentrations into a radiative forcing – which then drives climatic change – use this kind of equation.
16	E	$\Delta[CO_2]_{atm}$	IAM, Climate-economy models, SRES	DICE, RICE, FREE, ICAM-1, IMAGE 2.0, TARGETS	Many Integrated Assessments and Climate-Economy models take this approach. Most GCMs and EMICS use scenarios, like the SRES scenarios of Nakicenovic and Swart (2000), for changes in atmospheric CO_2.
25	TM_{ij}	LU_C	IAM, SRES	Goudriaan and Ketner (1984), IMAGE 2, TARGETS	The matrix-based approach used here, and its global scale, is from Goudriaan and Ketner (1984). However, Klein Goldewijk et al. (1994) and Rotmans and de Vries (1997) include land-use change and its effect on emissions.
46*	Q	E; W_{sw}	IAM, Climate-Economy models; and Water supply & demand models	DICE, RICE, FREE, IMAGE 2.0; ICAM-1, TARGETS, WaterGAP2, WorldWater	The approach taken for emissions is the same as in Nordhaus and Boyer (2000). Dowlatabadi and Morgan (1993a) and Fiddaman (1997) also calculate economic growth and emissions endogenously. Alcamo et al. (1994) calculate emissions from exogenous economic growth. Rotmans and de Vries (1997) and Alcamo et al. (2003a) generate water demand from economic scenarios, while Simonovic (2002) generates water demand endogenously. However, only this model includes an endogenously-calculated economic output as a driver for both emissions and water demand.
48	D	Ω	IAM, Climate-Economy models	DICE, RICE, FREE, ICAM-1, IMAGE 2, TARGETS	The approach used here is from Nordhaus and Boyer (2000). Both climate-economy models and IAMs include effects of climate change on macro-economics, and so the connection is common.
49	Ω	Q	IAM, Climate-economy models	DICE, RICE	The specific formulation used here is from Nordhaus and Boyer (2000).
62	$T_{feedback}$	E_{res}, W_a	IAM, Hydrological models, and Water supply and demand	IMAGE 2, Macro-PDM, TARGETS, WBM, and	The hydrological models developed by Arnell (1999b), Vörösmarty et al. (2000), and Alcamo and Henrichs (2002) use GCM or IAM climate outputs as driving fields; no *feedbacks* exist between climate and surface

			models	WaterGAP2	flow in these models. Alcamo et al. (1994) and Hoekstra (1997) explicitly model the effects of climate change on the hydrological system, as in this model.
63	P_{mult}	$T_{feedback}$	Hydrological models	See (62) above	Temperature feedback effects on the hydrological system are common, but are not global in extent as in this model, except in Hoekstra (1997).
78*	wta	P, DC, GW, $\tau_{ww\,\%}$, $\tau_{ww\,reuse\,\%}$	Water supply & demand models, Hydrological models, IAM, Climate-economy models	DICE, RICE, FREE, TARGETS, WorldWater. Macro-PDM, WaterGAP2, WBM	The approach taken to calculate water stress, which includes pollution effects, is unique. Alcamo et al. (2003a) and Vörösmarty et al. (2000) calculate water stress at the watershed or river system level, while Arnell (1999b) and this research calculate water stress at the national and global scales, respectively. The use of wta as the *only* driver of population growth is also unique – and is tested, in Davies (2007) – although Rotmans and de Vries (1997) and Simonovic (2002) calculate water pollution and use it as one factor that affects population growth. Again, the structure used for population growth is from Nordhaus and Boyer (2000) and Fiddaman (1997).
80*	g	r	IAM, Climate-economy models	DICE, FREE, TARGETS, World3, WorldWater	The asymptotic approach to calculating population is taken from Nordhaus and Boyer (2000) and Fiddaman (1997); however, *wta* as input to *g* is unique.
81	r	P	IAM, Climate-economy models	DICE, FREE	The asymptotic approach to calculating population is taken from Nordhaus and Boyer (2000) and Fiddaman (1997).
82	P	Q; W_{SW}; TM_{ij}	IAM, Climate-economy models, and Water supply and demand models	DICE, RICE, FREE, ICAM-1, IMAGE 2, TARGETS, WaterGAP2, World3, WorldWater, and Goudriaan and Ketner (1984)	See comments for equation (81). All models that include socio-economic factors include population. Climate-Economy models use population to drive their economic sector, Integrated Assessment Models use population to drive land-use and land-use change, and water supply and demand models use population to drive water demand. Several authors, including Rotmans and de Vries (1997), Meadows et al. (2004), and Simonovic (2002) use population as a driver for more than one of these sectors. Note that population generally serves as an exogenous driver in most models – the SRES (Nakicenovic and Swart, 2000) scenarios are a good example of this approach. However, Meadows et al. (2004), Rotmans and de Vries (1997), and Simonovic (2002) also calculate population

					growth endogenously.
83	DSWI	W_d	IAM, Water supply & demand models	WaterGAP2, TARGETS, WorldWater	The approach taken here is from Alcamo et al. (2003a). Simonovic (2002) and Hoekstra (1997) also model domestic demand endogenously.
84	ISWI	W_i	IAM, Water supply & demand models	WaterGAP2, TARGETS, WorldWater	The approach taken here is from Alcamo et al. (2003a). Simonovic (2002) and Hoekstra (1997) also model industrial demand endogenously.
85	LU_C	$[CO_2]$	IAM, SRES	Goudriaan and Ketner (1984), DICE, RICE, FREE, ICAM-1, IMAGE 2, TARGETS	The approach taken for emissions is the same as in Goudriaan and Ketner (1984). However, the connection between land-use change and atmospheric $[CO_2]$ is common to most climate change studies. Nordhaus and Boyer (2000) and Fiddaman (1997) use an exogenous approach, and climate model-based studies have used emissions scenarios like SRES (Nakicenovic and Swart, 2000).
86	Q_s	A_s	IAM, Water supply & demand models, Hydrological models	Macro-PDM, TARGETS, WaterGAP2, WBM, WorldWater	Surface flows in individual watersheds are calculated by Alcamo et al. (2003a), Arnell (1999b), and Vörösmarty et al. (2000). Hoekstra (1997), Simonovic (2002), and this model simulate surface water flows at the global level – in other words, flows are not regionally resolved.
87	A_s	wta	IAM, Water supply & demand models, Hydrological models	Macro-PDM, WaterGAP2, WBM, WorldWater	All models that calculate water stress include an equation of this sort, although Alcamo et al. (2003a), Arnell (1999b), and Vörösmarty et al. (2000) use the entire surface water flow, Q_s, rather than the available flow, A_s. Hoekstra et al. (1997) argue that this total-runoff approach leads to *overestimation* of surface water availability, and so use an A_s-like term in TARGETS; however, they do not calculate water stress. Simonovic (2002) uses stable annual runoff, or A_s, to determine water scarcity; however, A_s is constant, since climate change effects are not included.
88	E_{res}	Q_S	IAM, Climate models, Hydrological models	Many	Evaporation is an important process in the natural hydrological cycle, and is therefore included in all higher-resolution climate models, such as GCMs and EMICs, as well as in some IAMs (Alcamo et al., 1994; Hoekstra, 1997); however, hydrological models do not feed back to

					climate models via evaporation, since they use GCM or other climatic data as input. Note that Simonovic (2002) and Hoekstra (1997) include reservoir evaporation, but it is unclear whether purely hydrological models, like those of Alcamo et al. (2003a), Arnell (1999b), and Vörösmarty et al. (2000), do so as well.
89	$GW_{fraction}$	GW	IAM	WorldWater	The approach taken here is basically the same as in Simonovic (2002), although the use of water stress as a driver is unique to this model. Hoekstra (1997) prescribes groundwater pumping by policy scenario. Alcamo et al. (2003a) also plan to include groundwater pumping.
90	GW	W_a	IAM	WorldWater	See comments for equation (89). Note too that the allocation, in this model, of groundwater purely to irrigated agriculture is unusual.
91	W_a	W_{sw}	IAM, Water supply & demand models, Hydrological models	Macro-PDM, TARGETS, WaterGAP2, WBM, WorldWater	Any models that simulate water supply and demand include agricultural water demand, since agricultural water use is the highest of all the water use sectors. This is a very common, and necessary, connection. However, fewer models calculate agricultural demand endogenously – those that do include Alcamo et al. (2003a), Hoekstra (1997), Simonovic (2002), and this model.
92	DC	W_d	IAM	WorldWater	The approach taken here is basically the same as in Simonovic (2002), although the maximum desalinated volume is higher. Note, however, that the use of water stress as the driver of facility expansion is unique to this model. Hoekstra (1997) prescribes desalinated volumes by policy scenario. Alcamo et al. (2003a) also plan to include desalination.
93	W_d	W_{sw}	IAM, Water supply & demand models, Hydrological models	Macro-PDM, TARGETS, WaterGAP2, WBM, WorldWater	As was the case for equation (91), any models that simulate water supply and demand include domestic water demand. This is a very common, and necessary, connection. However, fewer models calculate domestic demand endogenously – those that do include Alcamo et al. (2003a), Hoekstra (1997), Simonovic (2002), and this model.
94	Q_{ww}	$Q_{treated\ ww}$	IAM, Water supply	TARGETS,	Other models, such as those of Hoekstra (1997) and Simonovic (2002)

			& demand models	WorldWater	also include wastewater production. Wastewater generation in Simonovic (2002) is a function of a base value and a variable pollution index, while Hoekstra (1997) states that wastewater generation is a function of water use.
95*	$\tau_{ww\ \%}$	$Q_{treated\ ww}$	IAM, Water supply & demand models	TARGETS, WorldWater	The approach taken here, where water stress drives expansion in wastewater treatment, is unique. However, Hoekstra (1997) and Simonovic (2002) also include wastewater treatment. Hoekstra (1997) makes wastewater treatment a function of the discharged volume and of a 'policy parameter'. Simonovic (2002) has wastewater treatment depend on *all* persistent pollution treatment.
96*	$Q_{treated\ ww}$	$Q_{ww\ reuse}$	IAM, Water supply & demand models	TARGETS, WorldWater	The approach taken here, where water stress drives an increase in wastewater reuse, is unique. However, Simonovic (2002) allows for some wastewater reuse, once water demand exceeds surface and groundwater supply. Hoekstra (1997) considers some portion of all returnable waters to be reusable, but provides few details on the reuse calculations or the feedbacks involved.
97*	$\tau_{ww\ reuse\ \%}$	$Q_{ww\ reuse}$	IAM, Water supply & demand models	TARGETS, WorldWater	The approach taken here, where the reuse percentage is driven by water stress and is variable, is unique. However, see comments on other models under equation (95).
98*	$Q_{ww\ reuse}$	W_d, W_i, and W_a	IAM, Water supply & demand models	TARGETS, WorldWater	See comments for equation (95). In this model, any wastewater designated for reuse is assigned to water use sectors at a fixed ratio.
99	W_i	W_{sw}	Water supply & demand models	Macro-PDM, TARGETS, WaterGAP2, WBM, WorldWater	As was the case for equation (91), any models that simulate water supply and demand include industrial water demand. This is a very common, and necessary, connection. However, fewer models calculate industrial demand endogenously – those that do include Alcamo et al. (2003a), Hoekstra (1997), Simonovic (2002), and this model.

2.4 Model Performance

By now, models of many different elements of the society-biosphere-climate system have been developed independently, verified against observations of the real-world, and then used to test understanding of the Earth-system, to develop policy suggestions, and/or to predict the effects of current practices on society, the environment, and so on. Many of these models were described in the previous section.

This research takes several of these independent sectors, or groups of sectors, and integrates them with several newly developed sectors to make a more comprehensive, feedback-based model of the full society-biosphere-climate system, as explained above. This section demonstrates that the 'integrating approach' used here can produce good results, with the advantage that they arise from model interactions rather than from imposed, exogenous trends. Through analysis of the model's 'base run' – or the set of simulation results generated using the *default model settings* – it becomes apparent that this comprehensive model can,

- Match historical global water use data and model water use reasonably into the future;
- Match historical global population data and model population growth into the future;
- Match historical global economic data and model economic behaviour into the future;
- Match historical global industrial emissions and model emissions into the future; and,
- Match historical physical data (atmospheric CO_2 levels, global surface temperatures, and terrestrial net primary productivity) and obtain similar behaviour to that predicted by other models for these variables into the future.

An examination and explanation of the model's behaviour is found in Davies (2007); this section provides a comparison of data and simulations, as well as simulated future values.

Before generating 'base run' results, model calibration and validation are necessary steps. However, calibration in the context of global change research faces a key limitation: there is only one Earth, and therefore only one set of globally-aggregated data available. Model calibration therefore proceeded in several steps here: 1) parameters were adjusted in individual sectors first, 2) the individually-calibrated sectors were checked against historical data and against data from other models, and 3) the sectors were integrated and model output was again tested against other sources. Since many of the model sectors are based on previous modelling work, they use the same parameter values as other models. Furthermore, where parameters were based on well-established, quantifiable, and measurable characteristics, the values obtained here were checked against real-world data. However, when the parameters had no strong physical basis, the effects of parameter variations on whole-model behaviour were checked through sensitivity analysis, in a manner described in Davies (2007).

Model validation was the next requirement. In interpreting the following performance results, note that the model is not intended to be used for predictions of Earth-system behaviour. Instead, the validation, below, which consists of a comparison between 'base run' model results, real world observations, and results from other models, demonstrates that the model can generate believable historical values for each important model sector. Reasonable historical accuracy then suggests that future conditions generated by model simulations have some validity, at least in terms of granting a deeper insight into the society-biosphere-climate system being modelled. In other words, models of this sort are primarily tools used to increase understanding of the system under study. Davies (2007) discusses the extension of model results to the real world in greater detail. See Chapter 3 for more information on the calibration and validation procedure; for further discussion of validation approaches for system dynamics models, see for example Shreckengost (1985), Sterman (1984), and Sterman (2000).

2.4.1 Water Use

Shiklomanov (2000) and Shiklomanov and Rodda (2003) provide data on both global and regional water demands over the past century, split into domestic, industrial, and agricultural demands; because the values in the two studies are very similar, only the values from Shiklomanov (2000) are listed below. After calibration, the model matches historical water withdrawals and consumption figures from Shiklomanov (2000) very closely – compare the actual withdrawal of 3788 km^3 yr^{-1} in 1995 with both the modelled withdrawal of 3759 km^3 yr^{-1}, and the value of 3572 km^3 yr^{-1} from Alcamo et al. (2003b), for example. The following tables compare these historical water use figures, first as a global total (Table 12), and then in terms of domestic, industrial, and agricultural use (Table 13).

Table 12: Global withdrawals and consumption for Shiklomanov (2000) vs. 'Base Run' (in km^3 yr^{-1})

	Assessment					Forecast
Year	1960	1970	1980	1990	1995	2000
Total Withdrawals (Data)	1968	2526	3175	3633	3788	3973
Total Consumption (Data)	1086	1341	1686	1982	2074	2182
Modeled Withdrawals	1961	2542	3122	3632	3759	3874
Modeled Consumption	1120	1390	1682	1997	2077	2145

Table 13: Global water withdrawals and consumption by water-use sector (in km^3 yr^{-1})

	Assessment					Forecast
Year	1960	1970	1980	1990	1995	2000
Shiklomanov (2000) Data						
Domestic Withdrawals	118	160	219	305	344	384
Domestic Consumption	20.6	28.5	38.3	45.0	49.8	52.8
Industrial Withdrawals	339	547	713	735	752	776
Industrial Consumption	30.6	51.0	70.9	78.8	82.6	87.9
Agricultural Withdrawals	1481	1743	2112	2425	2504	2605
Agricultural Consumption	1005	1186	1445	1691	1753	1834
Simulated Values						
Domestic Withdrawals	98	161	235	305	339	384
Domestic Consumption	15.8	25.3	36.3	46.4	51.3	57.7
Industrial Withdrawals	344	546	706	750	755	764
Industrial Consumption	31.1	52.5	72.1	81.2	84.3	92.7
Agricultural Withdrawals	1489	1759	2050	2410	2476	2527
Agricultural Consumption	1043	1236	1443	1701	1752	1795

Several more sources project water use into the future: Shiklomanov (2000) provides predictions of water use until 2025; Alcamo et al. (2003b: 343) provides regional and global surface water withdrawal values for 2025 based on a total increase in irrigated area

of only 1.5% over 1995 values; Simonovic (2002: 265) provides values for total global withdrawals in all major water use sectors in 2025; and Cosgrove and Rijsberman (2000: 26) provide two future scenarios based on previous work by Shiklomanov (1999) and Alcamo et al. (1999) – projections from the latter study are detailed. Table 14, below, compares these values with the predictions of the model.

Table 14: Water-use figures from different sources and from 'Base Run' simulation (in km^3 yr^{-1})

	Forecast and Simulation				
Year	2010	2025	2050	2075	2100
Shiklomanov (2000) Data					
Total Withdrawals	*4431*	*5235*	–	–	–
Total Consumption	*2399*	*2764*	–	–	–
Domestic Withdrawals	472	607	–	–	–
Domestic Consumption	60.8	74.1	–	–	–
Industrial Withdrawals	908	1170	–	–	–
Industrial Consumption	117	169	–	–	–
Agricultural Withdrawals	2817	3189	–	–	–
Agricultural Consumption	1987	2252	–	–	–
Alcamo et al. (2003b)					
Total Withdrawals	–	*4091.5*	–	–	–
Simonovic (2002)					
Total Withdrawals	–	*5073*	–	–	–
Domestic Withdrawals	–	723	–	–	–
Industrial Withdrawals	–	520	–	–	–
Agricultural Withdrawals	–	3554	–	–	–
Reservoir Withdrawals	–	276	–	–	–
Cosgrove and Rijsberman (2000)					
Total Withdrawals	–	*4300*	–	–	–
Total Consumption	–	*2100*	–	–	–
Domestic Withdrawals	–	900	–	–	–
Domestic Consumption	–	100	–	–	–
Industrial Withdrawals	–	900	–	–	–
Industrial Consumption	–	120	–	–	–
Agricultural Withdrawals	–	2300	–	–	–
Agricultural Consumption	–	1700	–	–	–
Reservoir Withdrawals	–	200	–	–	–
Simulated Values					
Total Withdrawals	*4096*	*4262*	*4253*	*4188*	*4328*
Total Consumption	*2263*	*2400*	*2550*	*2692*	*2826*
Domestic Withdrawals	462	559	695	811	925
Domestic Consumption	65.6	70.5	84.1	92.7	96.3
Industrial Withdrawals	819	830	780	686	642
Industrial Consumption	116	147	198	243	280
Agricultural Withdrawals	2594	2623	2491	2387	2440
Agricultural Consumption	1860	1932	1979	2050	2124
Reservoir Consumption	221	250	287	303	321

2.4.2 Global Population

The United Nations Department of Economic and Social Affairs (UNESA, 2006) provides global population values over the initial period of simulation, from 1960-2005, as well as a projection of values into the future. Scenarios used for global change, such as Nakicenovic and Swart (hereafter, IPCC 2000), provide figures of population growth into the future, as do certain integrated assessment models like IMAGE 2.0 (Alcamo et al., 1994), and climate economy models like DICE (Nordhaus and Boyer, 2000) and FREE (Fiddaman, 2002). Note that DICE and FREE prescribe (exogenous) population growth percentages over the duration of their simulations, while IMAGE 2.0 uses population scenarios developed by the IPCC (1992).

Table 15, below, compares the population values from UNESA (2006) with the simulated values from the model from 1960-2000, while Table 16 compares predicted values from UNESA (2006), various IPCC scenarios, and other model simulations, with those obtained from our model. Note that, because values provided by IPCC (2000) are for years 1990, 2020, 2050, and 2100, a weighted average is used to calculate the value for 2025 in Table 16 and Table 18, below. Furthermore, DICE (Nordhaus and Boyer, 2000) operates on a decadal time-scale, so values are available for years ending in '5' only. Where the year ends in a '0', values have been averaged between the nearest half-decades.

Table 15: UN population data *versus* endogenously simulated population values (in 10^9 people)

Year	1960	1965	1970	1975	1980	1985	1990	1995	2000	2005
UNESA (2006)	3.02	3.34	3.70	4.08	4.45	4.86	5.30	5.72	6.12	6.51
Simulated Population	3.02	3.37	3.74	4.12	4.51	4.91	5.31	5.70	6.09	6.47

Table 16: Comparison of population projections with simulated change into the future (in 10^9 people)

Year	2010	2025	2050	2075	2100
UNESA (2006)	6.91	8.01	9.19	–	–
IPCC (2000) Scenario A1	–	7.74	8.70	–	7.06
IPCC (2000) Scenario A2	–	8.81	11.3	–	15.1
IPCC (2000) Scenario B2	–	8.01	9.37	–	10.4
Alcamo et al. (1996), Base A	7.11	–	10.1	–	11.5
Alcamo et al. (1996), Base B	6.70	–	7.84	–	6.43
Fiddaman (1997)	7.23	8.41	9.98	11.1	11.8
Nordhaus and Boyer (2000)	6.88	7.96	9.29	10.2	10.7
Simulated Population	6.84	7.87	9.36	10.6	11.7

2.4.3 Global Economic Performance

The most authoritative sources of historical economic output (GDP) data, at both national and global levels, are Maddison (2001; 2003), and the WDI Online database (The World Bank Group, 2007). Note, however, that economic data use different base years and international aggregation approaches – for example, Nordhaus and Boyer (2000) and IPCC (2000) use *1990 US$ at market exchange rates* while other studies use *1990 international Geary-Khamis dollars* (Maddison, 2003) or *constant 2000 US$* (The World Bank Group, 2007) – and so their values are seldom directly comparable. Furthermore, these values are generally uncertain, particularly those farther in the past, and so the values should be read with some caution. See Table 17 below for historical GDP data.

Projections of economic growth into the future are available from the two climate-economy models (DICE and FREE), where they are calculated as an endogenous feature of the model, as well as from exogenous approaches, including the trend-based socio-economic scenarios of the IPCC (2000) and the projections used for other models like IMAGE 2.0 (Alcamo et al., 1996). Future economic output from these sources is provided in Table 18. Note that Fiddaman (1997: 82) presents a graph of GDP which provides no specific numbers; therefore, his numbers in Table 18 are approximate.

Table 17: Historical economic output, or GDP (in 10^{12} dollars)

Year	1960	1970	1980	1990	1995	2000	2005
Maddison (2003)	8.44	13.77	20.05	27.12	30.57	36.50	–
WDI Online (2007)	7.29	12.20	17.62	23.96	26.93	31.78	36.41
Nordhaus and Boyer (2000)	–	–	–	–	22.58	–	29.63
Simulated GDP	5.45	10.07	15.26	20.45	23.09	26.39	29.67

Table 18: Economic output according to scenario projections and simulations (in 10^{12} dollars)

Year	2010	2020	2045	2050	2055	2075	2095	2100
IPCC (2000) Scenario A1	–	56.5	–	181.3	–	–	–	528.5
IPCC (2000) Scenario A2	–	40.5	–	81.6	–	–	–	242.8
IPCC (2000) Scenario B2	–	50.7	–	109.5	–	–	–	234.9
Alcamo et al. (1996), Base A	39.77	–	–	95.95	–	–	–	244.21
Alcamo et al. (1996), Base B	33.29	–	–	51.51	–	–	–	67.19
Fiddaman (1997)	~45	~60	~90	~100	~110	~160	> 200	> 200
Nordhaus and Boyer (2000)	–	–	54.97	–	61.16	73.62	86.39	–
Simulated GDP	32.80	39.04	54.95	58.31	61.74	76.36	92.56	96.87

2.4.4 Industrial Emissions

The rate of increase or decrease in industrial emissions plays an important role in determining the degree of climate change, since industrial and land-use emissions are responsible for the climatic forcing that causes changes in global surface temperatures. The most widely cited industrial emissions data come from the Carbon Dioxide Information Analysis Center (CDIAC) and are available from Marland et al. (2007) – this set of CDIAC data is among the two data sets listed by the IPCC AR4 (Forster et al., 2007). Table 19 compares industrial emissions generated by the model with the data from Marland et al. (2007).

Table 19: Historical industrial emissions, 1960-2004 (in Gt C yr^{-1})

Year	1960	1970	1980	1990	1995	2000	2004
IPCC (2000) Scenario A1	–	–	–	6.0	–	–	–
IPCC (2000) Scenario A2	–	–	–	6.0	–	–	–
IPCC (2000) Scenario B2	–	–	–	6.0	–	–	–
Marland et al. (2007)	2.58	4.08	5.35	6.20	6.49	6.98	7.91
Simulated Values	2.47	3.92	5.11	5.96	6.32	6.77	7.11

Note that although the observed values are always higher than the simulated values in Table 19, a graphical comparison (not shown here) reveals that the observed values oscillate over time and are often below the simulated values. As a result, the cumulative observed and simulated industrial emissions are quite close in value in 2000, and much closer than Table 19 suggests. The difference in cumulative industrial emissions is only 2.7 Gt C, or 1.2%, over 40 years: 198.4 Gt C for the data from Marland et al. (2007) *versus* 196.1 Gt C for the simulated emissions.

In terms of future projections, three IPCC SRES emissions scenarios (2000), A1B, A2, and B2, are used in the IPCC Fourth Assessment Report for global climate projections (Forster et al., 2007). Their industrial emissions projections, along with the model-generated values of Alcamo et al. (1996), Goudriaan and Ketner (1984), Nordhaus and Boyer (2000) and this model, are listed in Table 20 below.

Table 20: Industrial emissions according to scenario projections and simulations (in Gt C yr^{-1})

Year	2010	2020	2030	2045	2050	2055	2075	2095	2100
IPCC (2000) Scenario A1	–	12.1	–	–	16.0	–	–	–	13.1
IPCC (2000) Scenario A2	–	11.0	–	–	16.5	–	–	–	28.9
IPCC (2000) Scenario B2	–	9.0	–	–	11.2	–	–	–	13.8
Alcamo et al. (1996), Base A	11	13	14	–	15.5	–	18	–	22
Alcamo et al. (1996), Base B	8	10	9.5	–	9	–	8	–	8
G&K (1984), Low Emissions	–	–	8.9	–	–	–	–	–	–
G&K (1984), High Emissions	–	–	16.2	–	–	–	–	–	–
Nordhaus and Boyer (2000)	–	–	–	9.17	–	9.51	9.92	9.79	–
Simulated Values	7.54	8.19	8.82	9.78	10.11	10.46	11.93	13.55	13.98

2.4.5 Physical Characteristics

The previous sections dealt with the reproduction of historical socio-economic behaviour and its projection into the future. The model clearly generates reasonable behaviour in terms of water withdrawals and consumption, population growth, economic output, and industrial emissions.

The next sections investigate how well the model reproduces historical observations of physical aspects of the Earth-system, and assess how closely it matches projections of the physical behaviour into the future. Physical elements examined below include the global climate (surface temperature), the global carbon cycle (atmospheric [CO_2]), and global net primary productivity.

2.4.5.1 Surface Temperature Change

Historical global climatic data is difficult to compile, and existing global averages are consequently not overly reliable. Such data suffer from the generally insufficient spatial and temporal coverage of weather records and monitoring stations, with earlier records particularly incomplete (Brohan et al., 2006). Hansen et al. (2006) estimate uncertainty in global temperature values at 0.05°C by the last several decades, and at roughly 0.1°C in the early 20th century, while Smith and Reynolds (2005) estimate uncertainty in the 20th century at a much higher ±0.30°C.

A recent study of satellite data by Vinnikov et al. (2006) states that global surface temperatures changed by 0.2°C decade[-1] between 1978-2004, while similar studies of surface records find a warming rate of 0.17°C decade[-1]. These values are generally consistent with the studies by Brohan et al. (2006) and Smith and Reynolds (2005) used in Table 21 below for model validation. Other approaches and studies of the same sort are available – see, for example, Alexander et al. (2006), New et al. (1999), which provide a greater variation of climatic variables, but do not present long-term temperature anomalies.

Brohan et al. (2006) and Smith and Reynolds (2005) calculate temperature anomalies based on the deviation, in degrees Celsius, from a long-term 1961-1990 temperature average. For the simulated values, the temperature anomaly was calculated based on the difference between simulated values for the years in question (1960, 1970, and so on) from the simulated 1961-1990 average surface temperature. Nordhaus and Boyer (2000) calculate their temperature anomaly based on the pre-industrial average surface temperature, so that their *starting, 1995-value* for the temperature anomaly is 0.43°C. In Table 21, their anomaly is corrected by subtracting 0.15°C from their calculated values, since 1960 was roughly 0.15°C warmer than 1900 (an approximate pre-industrial average, and the value available), according to figures from the US National Climatic Data Center (NCDC, 2006). The anomaly for this model is clearly considerably smaller than observations, likely because of the relatively small climate sensitivity (simulated as 1.7°C for a forcing at $2xCO_2$ of 3.7 W m^{-2}) of the climatic sector developed by Harvey and Schneider (1985), and also smaller than the anomaly calculated by Nordhaus and Boyer (2000) because, again, their climate sensitivity is considerably higher.

Table 21: Global surface temperature anomalies from 1960-2005 versus 'Base Run' values

Year	1960	1970	1980	1990	1995	2000	2005
Brohan et al. (2006)	-0.1°C	-0.1°C	0.05°C	0.15°C	0.25°C	0.35°C	0.45°C
Smith and Reynolds (2005)	-0.05°C	-0.1°C	0.1°C	0.18°C	0.25°C	0.38°C	0.45°C
Nordhaus and Boyer (2000)	–	–	–	–	0.28°C	–	0.34°C
Simulated Values	-0.03°C	-0.03°C	0.01°C	0.07°C	0.11°C	0.14°C	0.19°C

For comparison of the simulated values with those of other models into the future, a variety of studies are available. The most useful, because of the number of GCMs and other models included, is the Fourth Assessment Report of the IPCC (Meehl et al., 2007); however, its climate projection approach does not match that of the studies in Table 21. Instead, the IPCC results use an 'average climate period' of 1980-1999 and present 20-year averages of surface temperature anomalies over three periods of the 21st century: 2011-2030, 2046-2065, and 2080-2099.

Table 22 provides figures from Meehl et al. (2007: 763), Alcamo et al. (1996), Nordhaus and Boyer (2000) – corrected as much as possible given the differences in time scales – and from the 'base run' of the model. Figures from Fiddaman (1997) are omitted because FREE and DICE use the same climate sector. Again, the anomaly values simulated by our model are considerably smaller than those projected by other studies, possibly because of differences in climate sensitivity, but more likely because of differences in other sectors of the model – note that Nordhaus and Boyer (2000), despite a larger climate sensitivity than ours, also obtain lower values than Meehl et al. (2007). Note that Meehl et al. (2007) do not provide anomaly values for Scenario B2, so values for B1 are given in Table 22 instead; furthermore, Figure 27 of Alcamo et al. (1996) begins at year 1990, so a 1980-1999 'base anomaly' is not available. However, because values from 1980-1990 probably grew at roughly the same rate as from 1990-1999, it is reasonable to use an initial 1980-1999 period anomaly of 0°C.

Table 22: Future global surface temperature anomalies based on 1980-1999 average climate

Year	2011-2030	2046-2065	2080-2099
Meehl et al. (2007), SRES A2	0.64°C	1.65°C	3.13°C
Meehl et al. (2007), SRES A1B	0.69°C	1.75°C	2.65°C
Meehl et al. (2007), SRES B1	0.66°C	1.29°C	1.79°C
Alcamo et al. (1996), Base A	0.8°C	1.6°C	2.6°C
Alcamo et al. (1996), Base B	0.5°C	1.1°C	1.45°C
Nordhaus and Boyer (2000)	0.34°C	1.05°C	1.76°C
Simulated Anomaly	0.27°C	0.70°C	1.28°C

A final note: according to the IPCC TAR (Houghton et al., 2001), the global average surface temperature is roughly 15°C. More recent data from Smith and Reynolds (2005), cited by the National Climatic Data Center (NCDC 2006), states that the global average

surface temperature between 1880-2004 was actually 13.9°C, while Meehl et al. (2007) give a value of 13.6°C. Despite these lower figures, the model currently begins in 1960 with an average surface temperature of 15.9°C, which is the equilibrium/initial temperature used by Harvey and Schneider (1985).

2.4.5.2 Atmospheric Carbon Dioxide Concentrations

Historical atmospheric carbon dioxide concentration data are available from Mauna Loa, Hawaii, based on long-term records collected by Keeling and Whorf (2005). Other datasets of CO_2 concentrations collected in different areas of the globe are also available – see for example the IRI Data Library (International Research Institute for Climate and Society, 2007) – but they add little to the trend used here. Table 23 therefore compares the observed atmospheric carbon dioxide concentrations with modelled concentrations from Alcamo et al. (1994), Nordhaus and Boyer (2000), Goudriaan and Ketner (1984) – the source of the model's carbon and land-use sectors – and the model's 'base run' simulation from 1960-2004.

Table 23: Historical atmospheric carbon dioxide concentrations, 1960-2004 (in ppm)

Year	1960	1970	1980	1990	1995	2000	2004
Alcamo et al. (1994)	–	325	340	358	–	–	–
Goudriaan and Ketner (1984)	316	325	340	–	–	–	–
Keeling and Whorf (2005)	317	326	339	354	361	369	377
Nordhaus and Boyer (2000)	–	–	–	–	349	–	369
Simulated Values	309	310	322	337	345	354	361
Difference: Obs. – Simulated	*8*	*16*	*17*	*17*	*16*	*15*	*16*

Clearly, the model simulates lower CO_2 concentrations than the data and the other models; however, the overall behaviour of the model follows that of the data over a period of at least 34 years. Furthermore, attempts to recalibrate the carbon cycle to the observed values would have no effect on the rest of the model because of the use of a 'relative change' term in the GHG forcing equation, which compares the current CO_2 level with the initial value – in this case, 309 parts per million (ppm). Note that the model values here do not match those of Goudriaan and Ketner (1984), probably because of a difference in timescale: where G&K begins in 1780, our model begins in 1960 and 'equilibrates' over the first decade of the simulation.

Many studies are available for comparison of projected atmospheric CO_2 levels into the future; where possible, the same studies are used here as were used in the tables above. Table 24 includes two sets of projected CO_2 values (in ppm) from the IMAGE 2.1 model (Alcamo et al., 1996), from a coupled climate-carbon model called IPSL (Berthelot et al., 2002), which is driven by the A2 scenario (IPCC 2000), from Goudriaan and Ketner (1984), which is driven by older emissions scenarios developed by IIASA, and one set of values from the base run of Nordhaus and Boyer (2000). These values are compared with the values generated by the 'base run' simulation of the model. Note that the values for Berthelot et al. (2002) were obtained from their Figure 2 and converted to parts-per-million using the *Gt C to ppm* equation in Goudriaan and Ketner (1984), assuming a base atmospheric CO_2 content in 1860 of 595 Gt C (283 ppm). The match between the figures in Table 24 and the text of Berthelot et al. (2002) is not perfect, with 782 ppm obtained for the 'coupled' experiment value here while they calculated a value of 778 ppm, but it is close. Additional values are available in a coupled climate-carbon model study conducted by Cox et al. (2000), which calculated an atmospheric CO_2 concentration in 2100 of 980 ppm.

Table 24: Atmospheric concentrations according to scenario projections and simulations (in ppm)

Year	2010	2020	2030	2045	2050	2055	2075	2095	2100
Alcamo et al. (1996), Base A	400	425	460	495	510	530	610	710	745
Alcamo et al. (1996), Base B	390	410	420	440	450	460	480	505	515
Berthelot et al. (2002), Coupled	383	414	445	492	502	525	616	747	782
Berthelot et al. (2002), Fertilization	373	397	426	468	485	497	573	673	700
G&K (1984), Low Emission	–	–	431	–	–	–	–	–	–
G&K (1984), High Emission	–	–	482	–	–	–	–	–	–
Nordhaus and Boyer (2000)	–	–	–	448	–	467	502	534	–
Simulated Values	373	393	415	450	462	476	534	604	624

From Table 22, it is clear that our model generates a smaller temperature anomaly than the other studies cited. Table 24 provides at least a partial explanation for the lower anomaly: the carbon sector of the model calculates lower atmospheric CO_2 concentrations than do other models; then, in combination with the relatively low climate sensitivity of the climate sector from Harvey and Schneider (1985), the lower CO_2 levels result in less forcing and therefore less climate change.

2.4.5.3   Net Primary Productivity

Accurate figures on global net primary productivity (NPP), which is the net flux of carbon dioxide from the atmosphere into green plants, are relatively difficult to obtain – for example, the IPCC TAR (Houghton et al., 2001) cites two global studies, one of which was conducted in 1979 (Atjay et al., 1979) and is still used as a basis of comparison.

Many published NPP values come from Dynamic Global Vegetation Models (DGVM) – a sort of General Circulation Model for terrestrial biosphere dynamics – or comparisons of such models. Cramer et al. (1999) tested sixteen different DGVMs using long-term average monthly climate values and base atmospheric CO_2 concentrations of 340-360 ppm; they found simulated NPP values between 39.9-80.5 Pg C yr^{-1} with an average value of 54.9 Pg C yr^{-1}. In a similar study, Cramer et al. (2001) ran six DGVMs using climate data generated by the HadCM2-SUL climate model driven by the IPCC IS92a emissions scenario; they obtained NPP values of between 45-60 Pg C yr^{-1} during the initial period of the simulations. Berthelot et al. (2002) generated NPP figures of 57.5 ± 2.5 Gt C yr^{-1} using their IPSL model driven by a fixed climate and atmospheric CO_2 concentration of 286 ppm; values under climate change and other related scenarios are available in their Figure 3. Other NPP figures include 53 Gt C yr^{-1} (Cox et al., 2000; using a coupled carbon-climate model with fixed climate and atmospheric carbon dioxide of 290 ppm), and 58.5 Gt C yr^{-1} (Klein Goldewijk et al., 1994: 213; calculated 1970 model value).

Table 25 displays calculated net primary productivity values from four different studies conducted by Berthelot et al. (2002), Cramer et al. (2001), Goudriaan and Ketner (1984), and Klein Goldewijk et al. (1994), as well as historical values calculated by our model. All fit within the broad range of values given in the paragraph above, with our values closest to the majority of the studies. Values from Cramer et al. (2001) are approximations only, because of the nature of their Figure 4, and values are given only for several points in time. Comparisons with Nordhaus and Boyer (2000) and Fiddaman

(1997) are not possible because of differences in representation of the carbon cycle (Nordhaus and Boyer, 2000), or because NPP values are not explicitly presented (Fiddaman, 1997).

Table 25: Historical net primary productivity (NPP), 1960-2005 (in Gt C yr^{-1})

Year	1960	1970	1980	1990	1995	2000	2005
Berthelot et al. (2002), Coupled	61	62	63	65	66	67.5	67.5
Berthelot et al. (2002), Fertiliz^n	61	62	63	65	66	67.5	68
Cramer et al. (2001), $CO_2 + \Delta T$	56	–	–	–	–	61	–
Goudriaan and Ketner (1984)	–	–	61.9	–	–	–	–
Klein Goldewijk et al. (1994)	58.5	–	–	60.6	–	–	–
Simulated Values	57.6	57.5	58.1	59.0	59.4	59.9	60.3

Projections of net primary productivity figures associated with various models are available, but are not particularly common. Table 26 below provides NPP values from the same studies present in Table 25: Berthelot et al. (2002), Cramer et al. (2001), Goudriaan and Ketner (1984), Klein Goldewijk et al. (1994), and our model.

Table 26: Net primary productivity (NPP) according to simulations (in Gt C yr^{-1})

Year	2010	2025	2030	2050	2075	2100
Berthelot et al. (2002), Coupled	68	70	71	74	78	82
Berthelot et al. (2002), Fertiliz^n	68	72	73	79	85	94
Cramer et al. (2001), $CO_2 + \Delta T$	–	–	–	75	–	84
Goudriaan and Ketner (1984)	–	–	65.3	–	–	–
Klein Goldewijk et al. (1994)	–	–	–	82.5	–	–
Simulated Values	60.8	61.9	62.3	63.4	64.6	65.3

Note that our model predicts lower NPP values in the future than all other models, because only two other models (Goudriaan and Ketner, 1984; Klein Goldewijk et al., 1994) include land-use effects, which tend to reduce NPP through timber harvesting, the spread of urban land, and so on.

2.4.6 Discussion

The preceding comparisons of model-simulated values with historical observations and future projections demonstrated that the model produces good results. There is a clear advantage in the approach taken by this research: model results arise from feedback-based interactions rather than from imposed trends. Of course, each individual model sector is

calibrated to historical data, and so the match is not entirely unexpected; however, such sector-by-sector calibration need not result in close matches between the integrated model and historical data – divergent behaviour is a normal outcome of complex, non-linear systems.

The fact that simulated values closely approximate historical values therefore indicates that 1) the calibration worked, so that the model can reproduce historical behaviour in a variety of sectors, and 2) that the model *may* accurately reproduce important feedbacks in the real-world. Furthermore, comparable behaviour into the future between the 'base run' simulation and other model simulations and trend-based projections means that 1) the model is stable and reliable in its initial settings over the entire simulation period, and again suggests that 2) the model *may* accurately reproduce important feedbacks in the real-world, at least within the range of behaviour of other, higher-resolution but less-interlinked approaches. Note that the extension of model results to the real world is discussed in greater detail in Chapter 4 of Davies (2007).

2.5 Conclusions

The model described in this chapter has eight components, or sectors, which include representations at the global scale of the climate, the carbon cycle, the economy, land-use, population, the natural hydrological cycle, water demand, and water quality. Each of these sectors are either original to this work, in the case of two of the three water sectors, or stem from previous work by other researchers.

Feedbacks, in the form of mathematical equations, connect these individual components to generate a comprehensive, interlinked model of the society-biosphere-climate system – see Figure 1, above. All of the major elements of the consequent system are endogenous, or included explicitly, so that each sector of the model affects other sectors causally through feedbacks. As a result, the dynamic behaviour of the model arises from its system structure, rather than from assumptions in the form of exogenously imposed trends input to the model. The model can then be used to gain deeper insight into the

behaviour and interconnections within the model, and by extension, into the real world as well.

Of course, as illustrated by Table 11, many of the individual sectors and their interconnections in this model are common to integrated assessment models, climate-economy models, and water supply and demand models; however, other connections are either unique or are original versions of approaches taken by other models. Each model has a different focus, which has important effects on the simulated behaviour, and on the types of investigations possible with each model.

Finally, the model verification section demonstrates that the historical values for each important socio-economic and physical sector match observations and the results of other models closely. In other words, the 'fusing approach' used in this work can produce reasonable, believable results, with the advantage that they arise from model feedbacks rather than from imposed, exogenous trends.

3. MODEL USERS' GUIDE

This chapter serves as an introduction to model use through a system-dynamics-modelling software-package called Vensim (Ventana Systems, 2003). The model uses Vensim DSS, which is available for purchase from the Ventana Systems, Inc. website at http://www.vensim.com. *The model works best when simulated with Vensim DSS software*.

Ventana Systems also offers a 'Vensim Model Reader' at no cost, which can simulate a complete model and can be used to read data sets from previous model runs, but does not allow model modification. Note that data derived from simulations using the Model Reader differ slightly from the data produced by the Vensim DSS version because of a difference in numerical precision: although both the Model Reader and Vensim DSS use automatic Runge-Kutta 4 (RK4 auto) to run the model, Vensim DSS has double the precision of the Model Reader – see below for more details on numerical integration.

In terms of modelling software, note too that an introductory modelling package, called Vensim PLE, is available from Ventana Systems at no cost; however, because the model uses subscripts (or *arrays*), it cannot be run using Vensim PLE.

3.1 Chapter Outline

The intended audience for the completed model is presented first, while model use is described second, in terms of the software interface. The topics in the second section include model organization and Vensim's mathematical basis, experimentation with the model, and the interpretation tools available for analysis of the simulation results. The third section explains how the model can be applied to policy development, and provides a simulation example to demonstrate how the model simulates engineering-based policy.

3.2 Intended Audience

The 'systems thinking' that gave rise to this model emphasizes the interdependence of the system elements, and the feedbacks that connect them and that determine overall system behaviour. The model aims to improve an understanding of complex processes and feedbacks, and their effect on model behaviour, rather than to provide predictions of future conditions. In other words, the model is a learning tool.

Because of its temporal (annual) and spatial (global) resolution, this model focuses on large-scale developments in a relatively complete, highly-interconnected representation of the Earth system. Its use is therefore appropriate for academics, researchers, and students interested in modelling feedbacks in the society-biosphere-climate system, and in undertaking interdisciplinary modelling work at large scales, more generally. Both disciplinary and interdisciplinary modellers will find the new representations of the global water use and quality sectors, as well as the hydrological cycle, useful for comparison with their models. Policy-makers at the international level could use the model as a tool to increase their understanding of important interconnections in the Earth system, and how decisions pertaining to one sector affect not just that sector, but others as well.

The model is particularly useful from the perspective of water resources management, and therefore water resources managers can use the model to see the quantitative impacts of water quality on water availability, and the importance of clean water to the rest of the Earth system; they can also investigate factors that lead to increases or decreases in water demand. Engineers can identify potential effects of current and future policies – in terms of water use, wastewater treatment, land use change, and carbon emissions regulation – on the state of physical systems at the global level, and investigate the consequences of various potential policies or interventions on those systems.

3.3 How to Use the Model

This section describes a typical system dynamics model interface – this research uses Vensim DSS – in terms of the resulting model organization, through a user interface, and its mathematical basis. A typical approach towards simulation is then provided, as well as the analytical tools available.

3.3.1 Model Organization and Mathematical Basis

Mathematical models characterize important interconnections in the real world in terms of relationships between mathematical variables, which represent important real-world attributes or processes like global surface temperature, net primary productivity, average annual surface flow, population growth, economic output, wastewater volume, and so on. This mathematical basis can be readily apparent, as in computer code, or it can be concealed by a user interface.

In system dynamics models like this one, there are two levels of model representation: 1) a diagrammatic representation of the causal connections that constitute the system under study, and 2) the mathematical basis of those connections in the form of equations. Both of these levels are apparent in Chapter 2, which includes both causal loop diagrams, as in the figures of intersectoral feedbacks, and equations for the same feedbacks.

At the diagrammatic level, the model is broken into its individual sectors, which has two benefits. Model division by sector aids in organization, and it simplifies the modelling procedure. In terms of model organization, the division of a model into individual sectors is important both conceptually and practically. Conceptually, a sectoral view helps to draw boundaries around the processes of importance in that element of the model, since the included processes must produce the behaviour desired and nothing extraneous. For example, if the only requirement from the climate sector is the global average surface temperature, local to regional-scale processes like convective precipitation patterns (thunder storms) are irrelevant and should not be modelled. Practically, an organized model is both easier to use and easier to understand. The majority of variables in one

sector are not relevant to the rest of the model, and their number within an individual sector is generally significantly higher than the number of equations that connect the different sectors. From a modelling perspective, then, model partitioning into sectors also allows the addition of new sectors to a model or the transfer of developed sectors between different models, as well as the testing of independent sectors and simpler upgrading of deficient components. Ultimately, model division into subsystems separates the relevant from the irrelevant variables, so that only key variables – those involved in intersectoral feedbacks – are visible to the rest of the model.

In Vensim, this segregation of the model into subsystems is organized by 'views', which is the term applied to each representation of an individual subsystem. Therefore, in this model, each of the eight sectors described in Chapter 2, as well as their constituent subsectors, represents a 'view'. There are thirteen views in total, corresponding to the eight major sectors. These thirteen views can be accessed in the Vensim DSS model version through the 'view selector' at the bottom of the main screen, as shown in Figure 4, or by pressing the 'page up' and 'page down' keys. Further details about model 'views' are available in the Vensim User's Guide (Ventana Systems, 2006a), which is distributed with all Vensim versions.
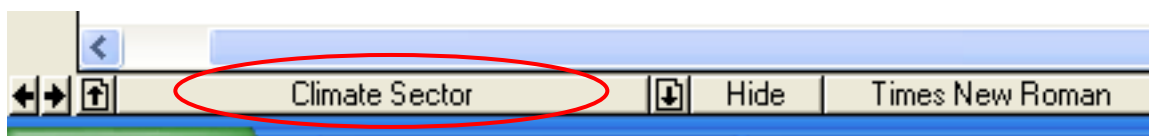
Figure 4: Location of 'View' selector in Vensim

The model views are displayed in Figure 5 through Figure 17, below, in the following order: climate, baseline climate, carbon cycle, baseline carbon cycle, economy, baseline economy, land-use, surface flow, water demand, water quality, population, industrial emissions, and baseline emissions.
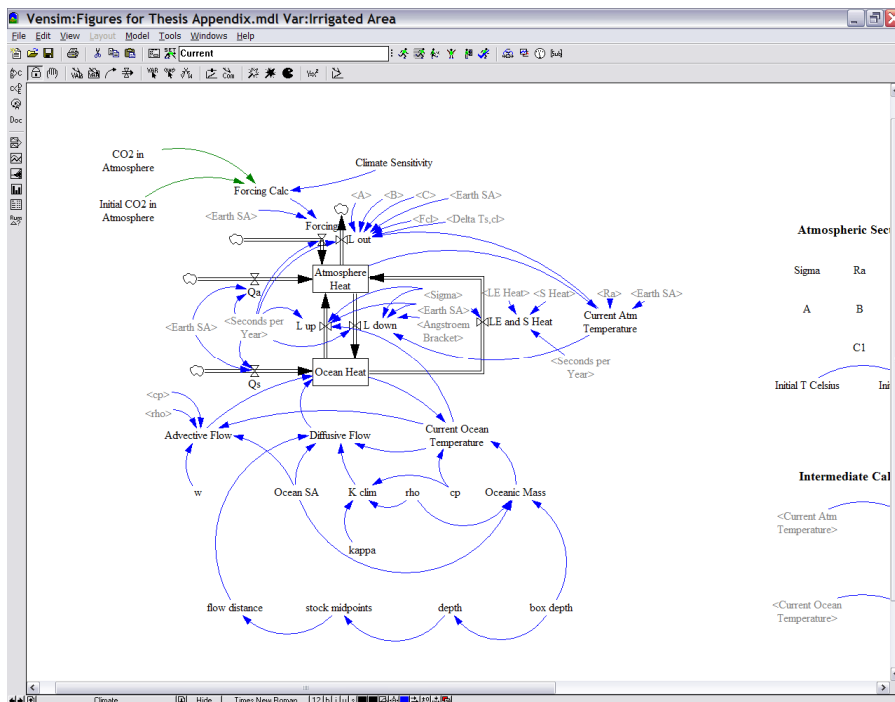
Figure 5: Illustration of the climate 'view'
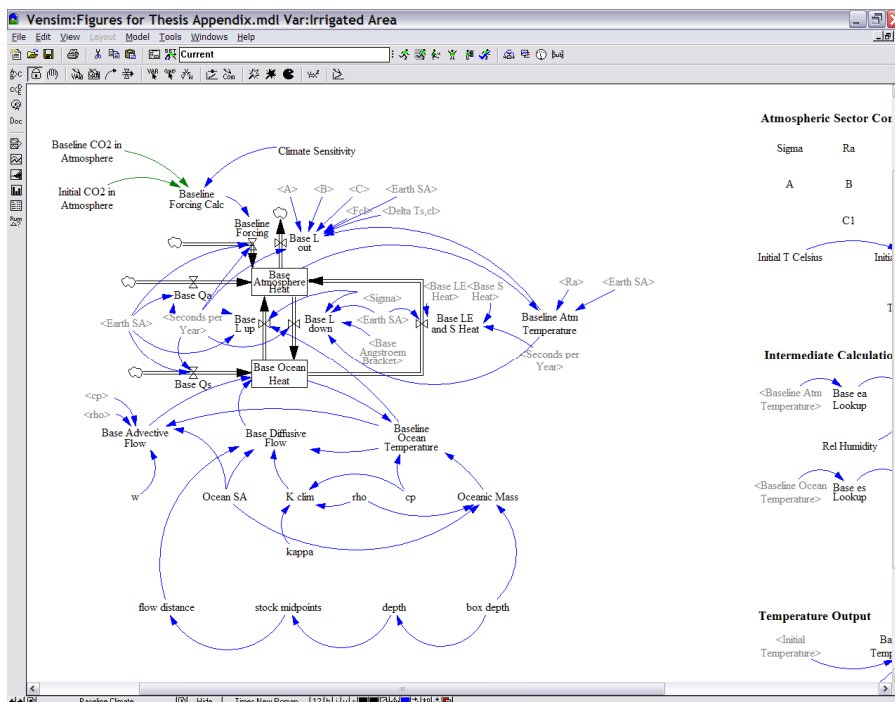
Figure 6: Illustration of the baseline climate 'view'
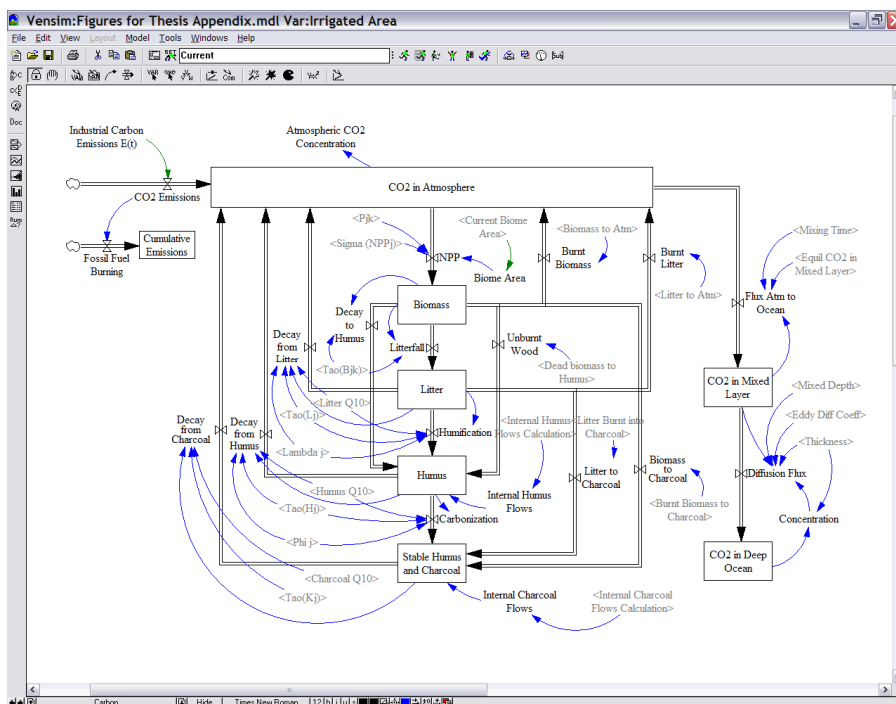
Figure 7: Illustration of the carbon cycle 'view'
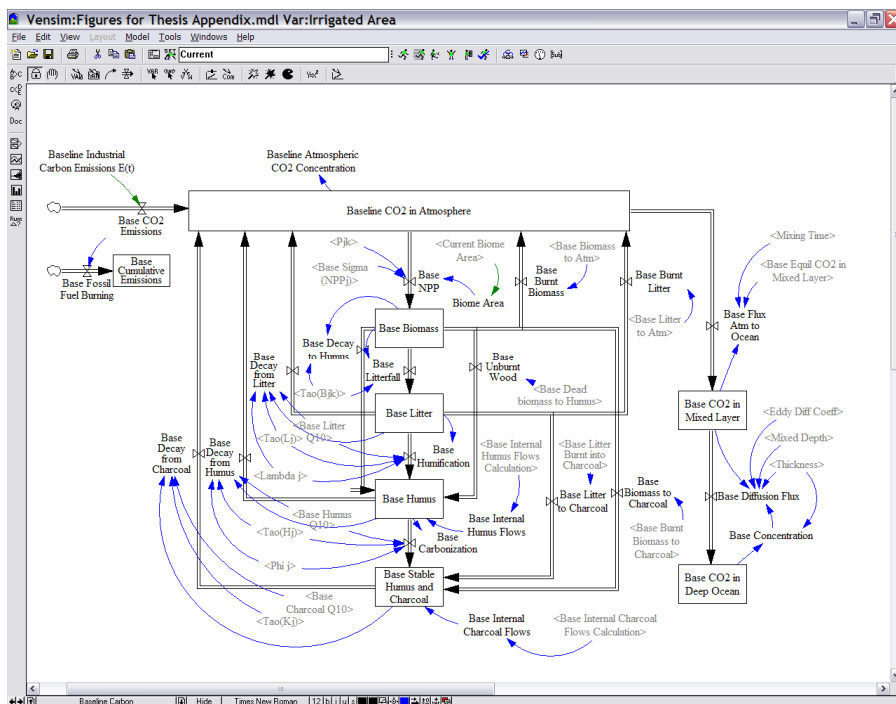
Figure 8: Illustration of the baseline carbon 'view'
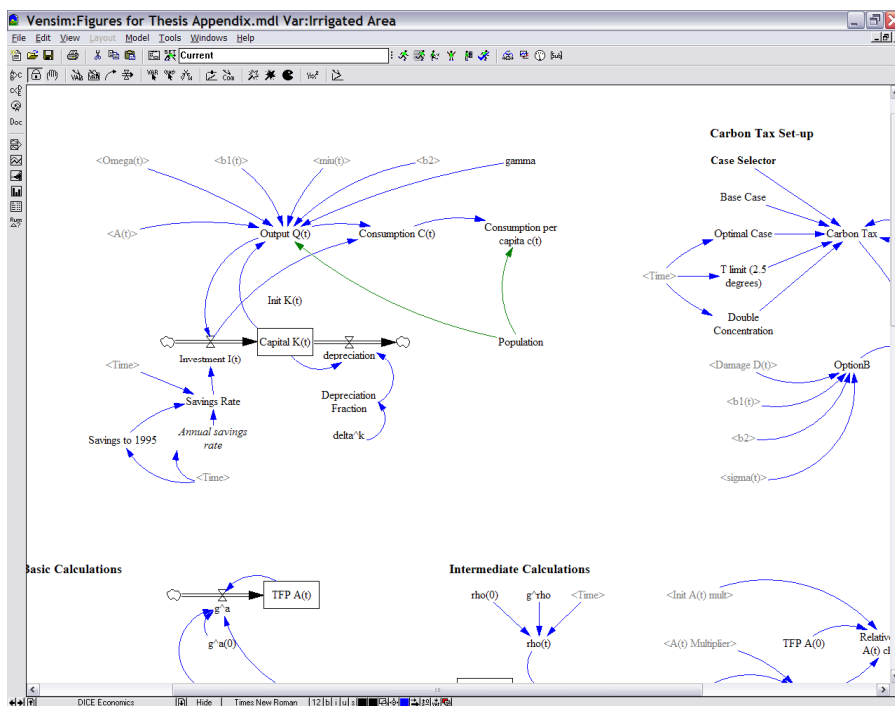
Figure 9: Illustration of the economy 'view'
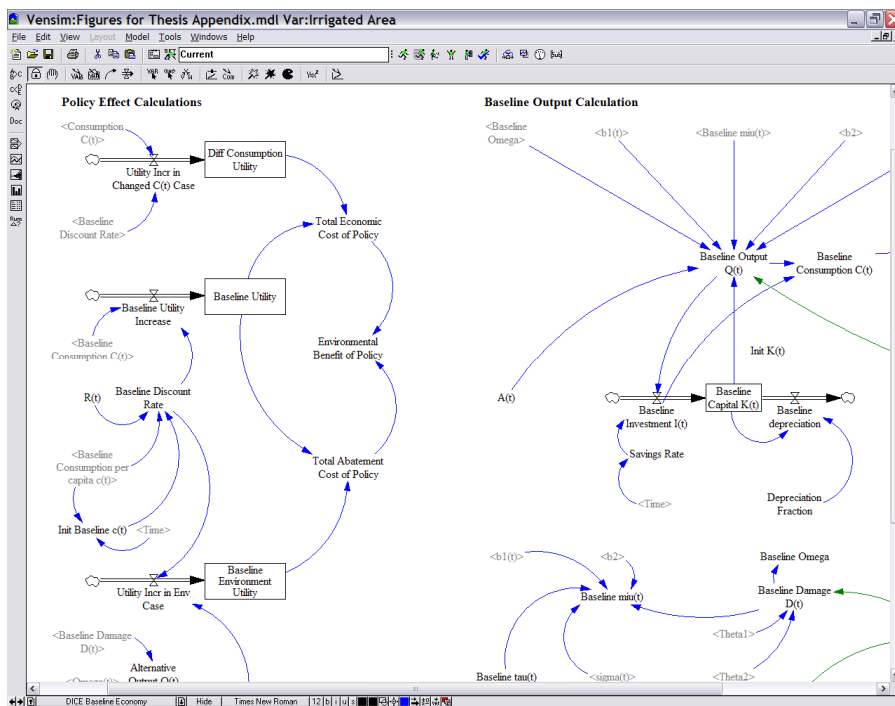
Figure 10: Illustration of the baseline economy 'view'
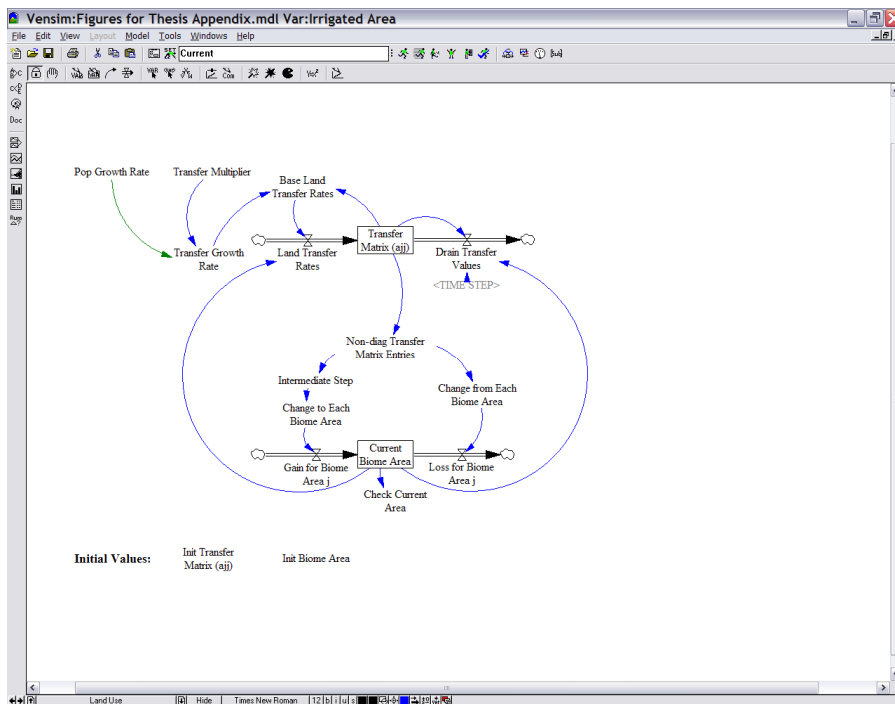
Figure 11: Illustration of the land-use 'view'
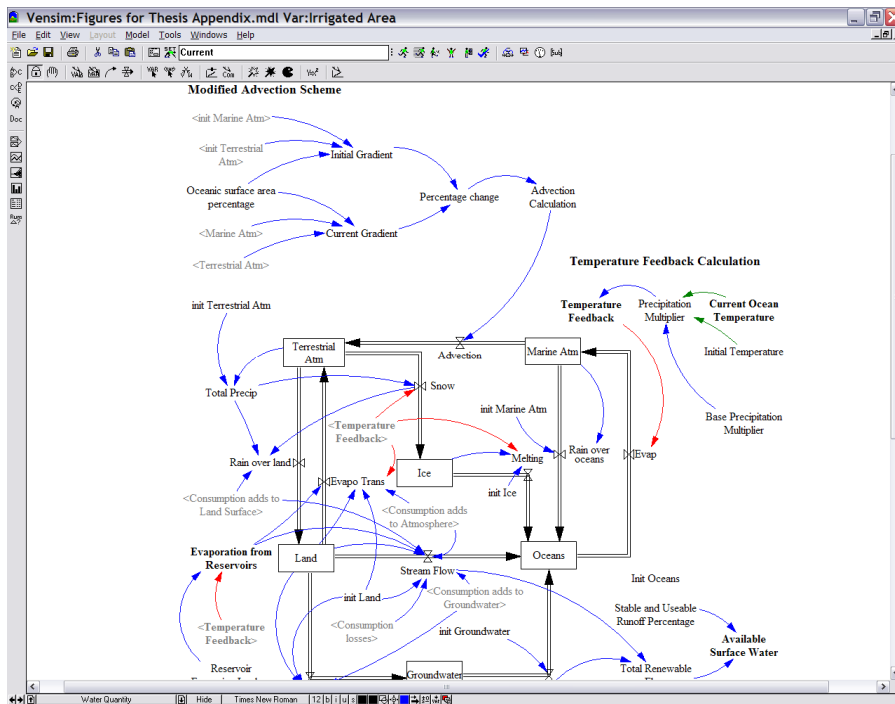
Figure 12: Illustration of the surface flow 'view'
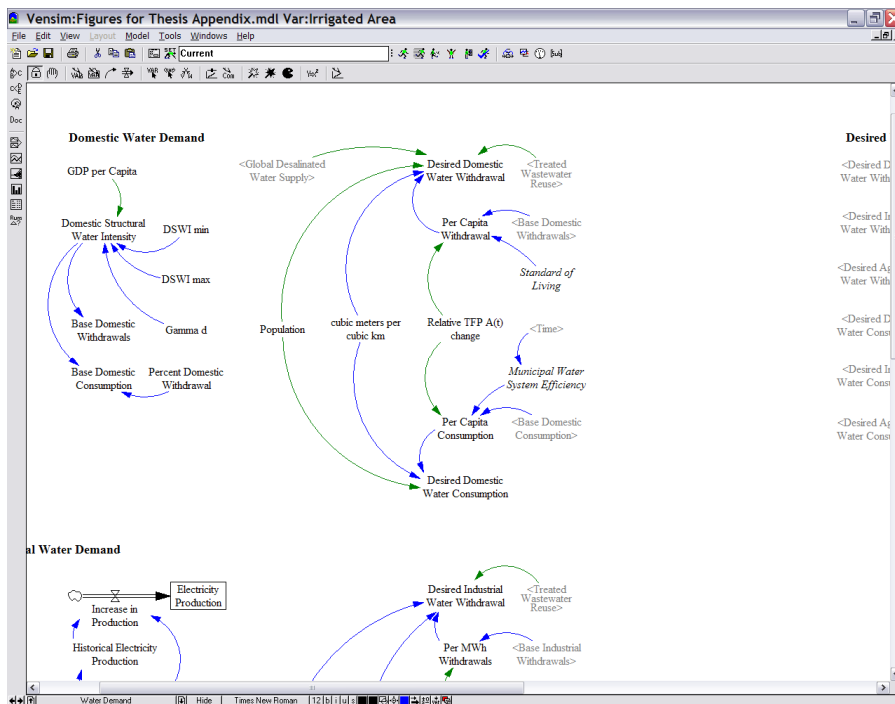
Figure 13: Illustration of the water demand 'view'
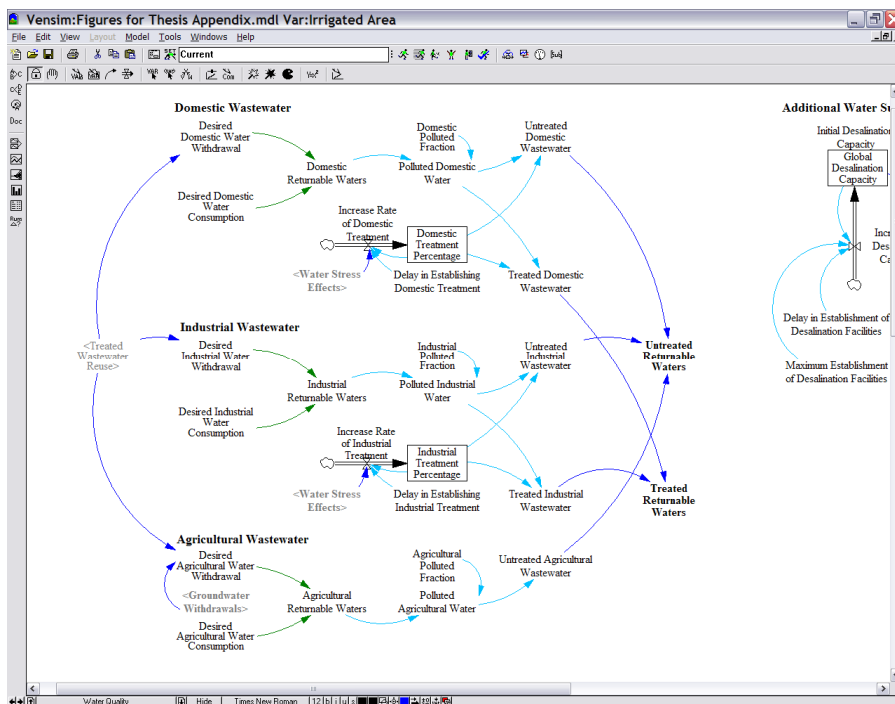
Figure 14: Illustration of the water quality 'view'
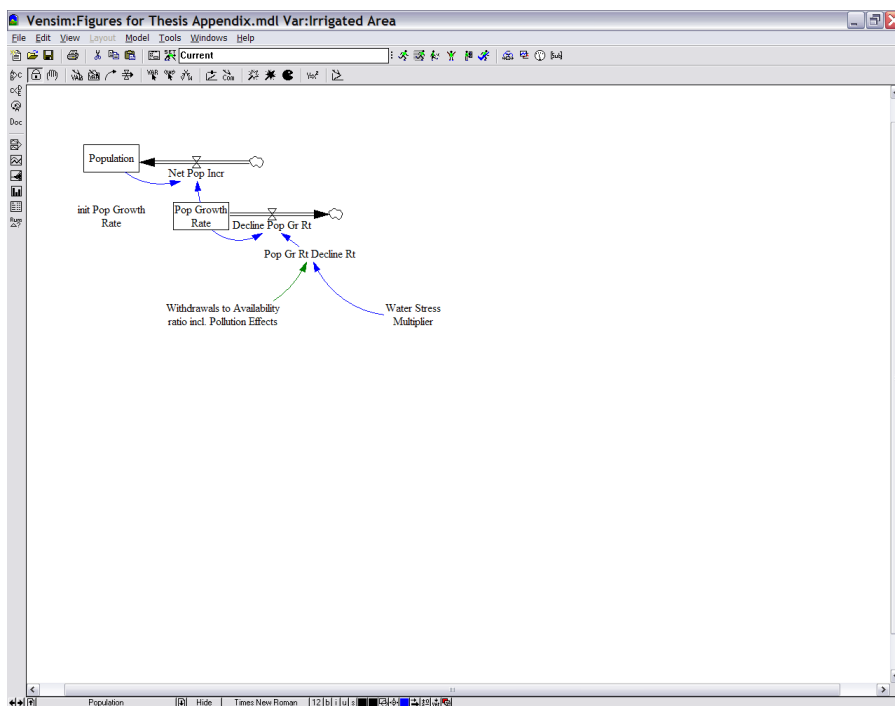
Figure 15: Illustration of the population 'view'
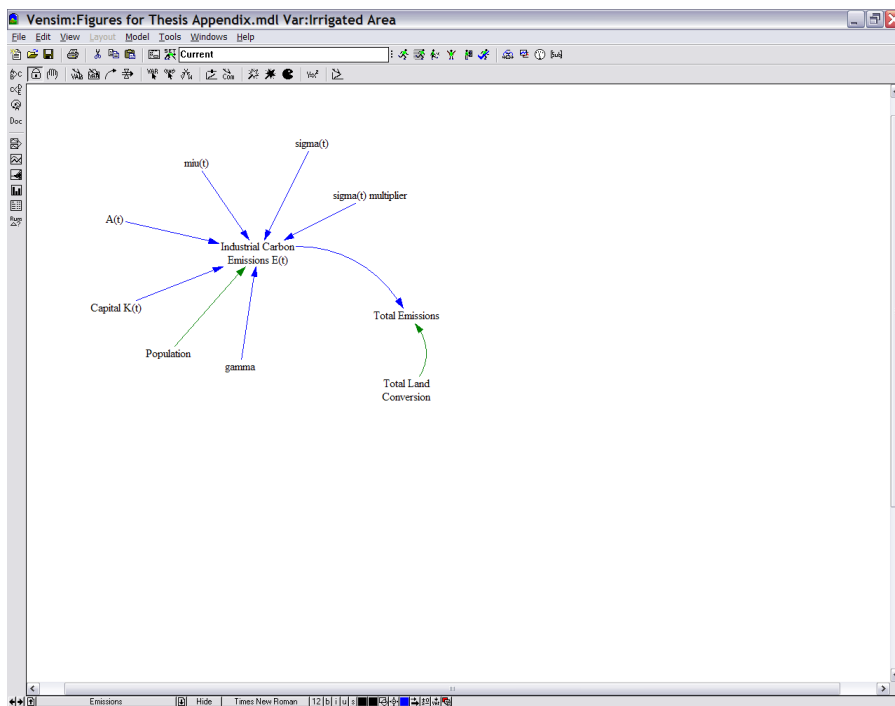
Figure 16: Illustration of the industrial emissions 'view'
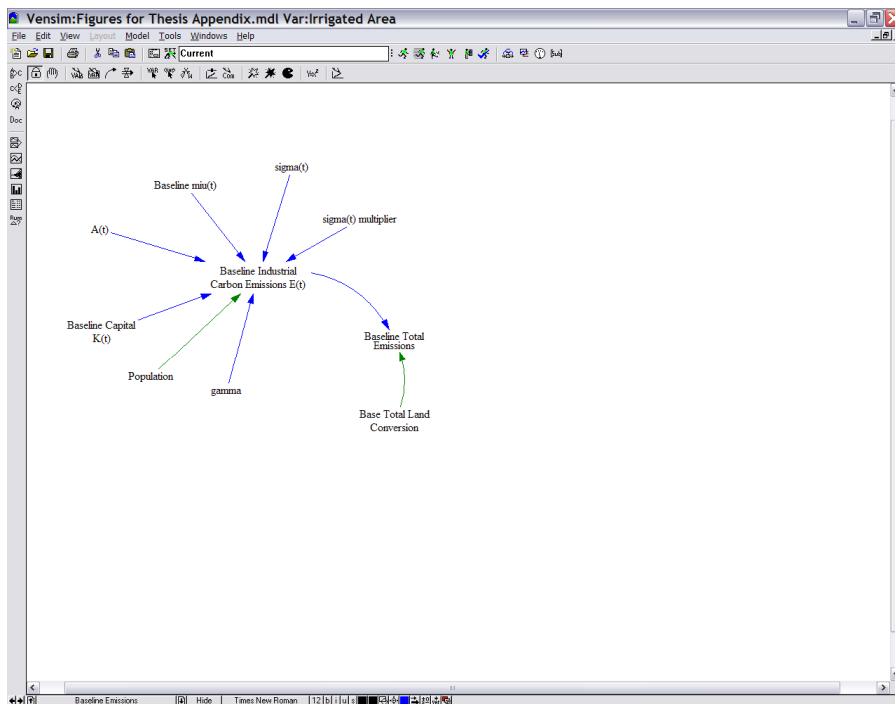
Figure 17: Illustration of the baseline industrial emissions 'view'

Note that these sectors are programmed in Vensim DSS, and so either Vensim DSS or the Model Reader is required to run the model. If the user has purchased a Vensim DSS license, the model can be run from the CD-ROM – see Appendix B – available from the authors by clicking on the 'run simulation' icon, which resembles a running person – see Figure 18, below. The same procedure is used to run the model with the Model Reader software, although the interface differs slightly.

Figure 18: How to run a simulation in Vensim DSS

The diagrammatic representations of each individual sector in Figure 5 through Figure 17 include variables, their connections with other variables, and parameters. Variables in system dynamics models have three forms: stocks, flows, and 'variables' (Ventana Systems, 2006a). Stocks represent accumulations of material or information, such as the

physical quantities of heat in the atmosphere, global capital, the total human population, or the global wastewater treatment capacity. They are associated with time-independent units, like Joules, dollars, people, or km^3. Flows are *rates* that add to, or subtract from, stocks, and take units of amounts per time. Therefore, the flows that correspond to the stocks listed above might include planetary longwave radiation, investment, the birth rate, and treatment plant construction. Connections between variables and parameters take the form of arrows or flows, where x → y can be interpreted either as "a change in x causes a change in y", or more simply as y = f(x). Flows and arrows differ in one important way: flows cause stocks to increase or decrease, while arrows represent a transfer of information that can affect flows and other variables, but never stocks. Stocks can only change in value through their inflows and outflows, which must have the same units, divided by time, as their associated stocks.

When a series of stocks and variables is connected through flows and arrows, such that a loop can be traced from one variable to the next, and eventually back to the element chosen first, a feedback is said to connect the variables. Note that feedback loops are not always easily identified in a system dynamics user interface, because a variable in one sector may be connected to another variable in a different sector, which is connected to a third variable in a third sector before a fourth variable connects back to the first variable in the first sector. Loop-tracing tools are therefore provided in Vensim, through the button indicated in Figure 19 – further details on loop-tracing are available in the Vensim User's Guide (Ventana Systems, 2006a).
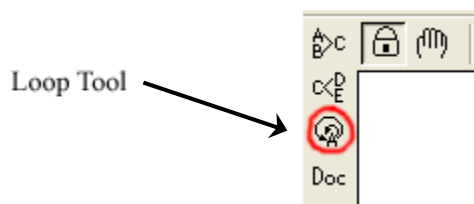
Figure 19: Loop-tracing tool in Vensim

Figure 20 serves as an example of the user interface described above – note that the structure below is simplified from the actual model for illustrative purposes. Here,

'Output Q(t)' represents the gross domestic product (GDP), which depends on total factor productivity (TFP), 'Population' (labour), 'Capital K(t)', and γ (gamma), according to the Cobb-Douglas production function. Capital and Population are stocks (accumulations), while 'Investment I(t)', Depreciation, and 'Population Decrease' are their flows. Thus, capital depends on investment (an *inflow*), which increases the value of capital, and depreciation (an *outflow*), which decreases the capital value, while population depends on the population decrease, which depends on the population, in turn – this is a simple *feedback*. A slightly more complicated feedback connects 'Capital K(t)' with 'Output Q(t)' through 'Investment I(t)'. The parameters in the figure, TFP, gamma, and the Savings Rate, are model *constants*, which do not change from their initial values – there are no arrows pointing to them, so nothing affects them over the course of a simulation.
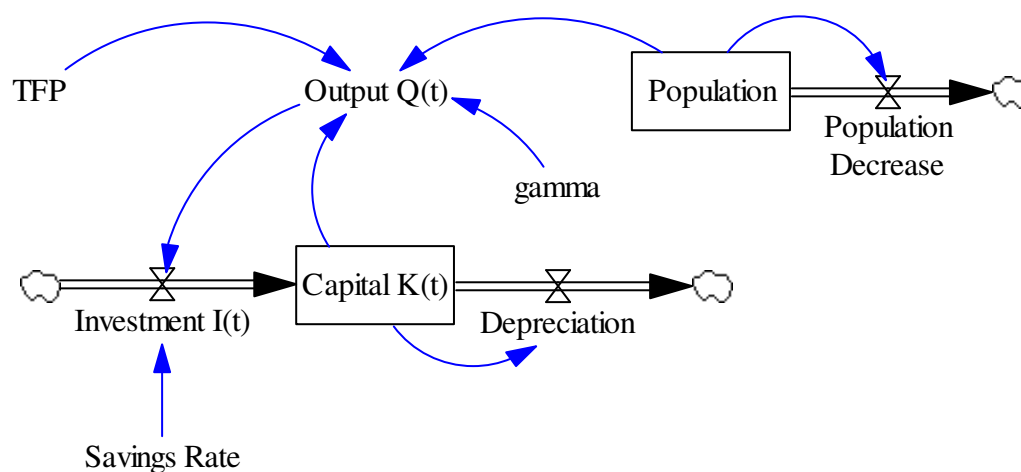
Figure 20: Example System Dynamics interface based on the economic sector

Note that Figure 20 lacks any mathematical equations that specify the manner in which a stock, flow, or variable affects another. It simply provides an illustration of the causal relationships between the model variables – for example, capital affects output, which affects investment, which affects capital, and so on. The equations and parameter values provided in Chapter 2 or Appendix A can be entered for each stock, flow, and variable, directly into the model through the user interface; however, the *mathematical level*, described next, provides the full mathematical basis of the model.

The mathematical level is much more straightforward from a computer coding perspective than the user interface, but is harder to analyze directly, because it consists only of a list of equations and their associated units, which can be organized in any fashion. The mathematics involved in a system dynamics model takes the form of first-order, ordinary differential equations, where stocks represent integrals of their inflows minus their outflows, and flows represent rates of change for their associated stocks.

The mathematical view is seldom accessed directly, but is crucial, of course, because it determines how the model actually functions – in other words, *how* capital affects output, and so on. The equations in the model are accessible through an icon labelled 'y=x^2' in the sketch toolbar in Vensim, just below the main toolbar, which displays the equation-editing interface shown in Figure 21 when clicked.
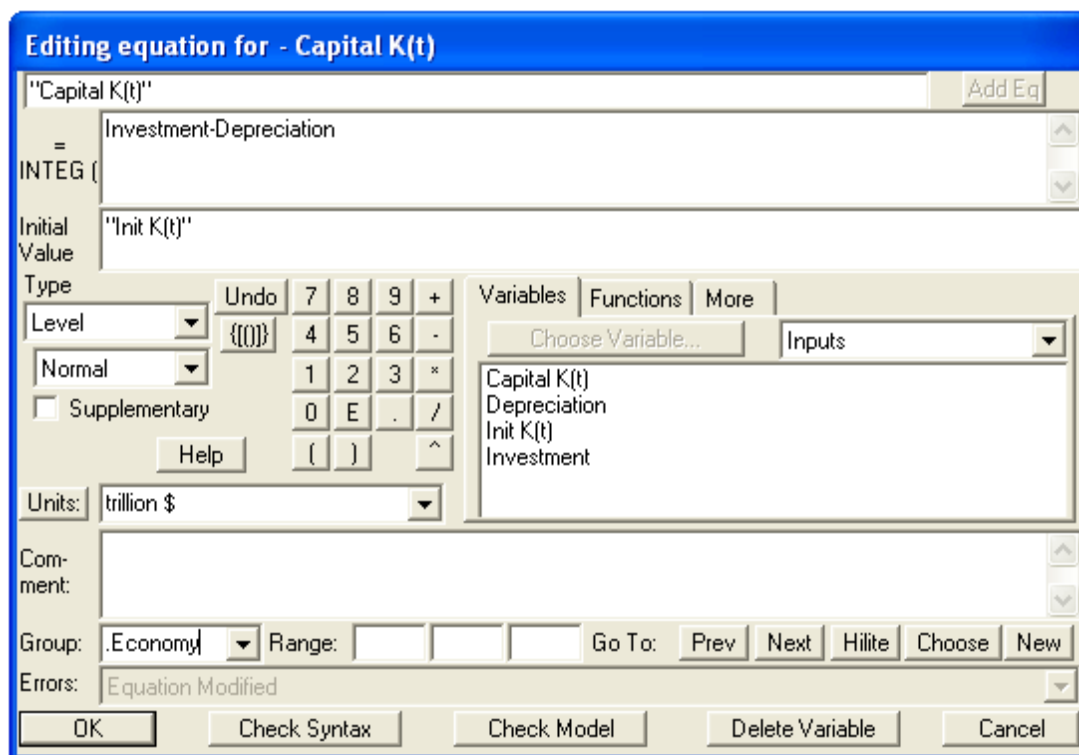
Figure 21: Equation Editor in Vensim

In software packages like Vensim DSS, actual computation of simulation results requires numerical integration (Ventana Systems, 2006b). Several different forms of numerical integration are available: Euler, Runge-Kutta, and difference equations. Euler integration is the fastest numerical method, but is less accurate than the Runge-Kutta method. Runge-Kutta is modification of Euler integration that improves accuracy substantially by checking derivatives between the set time-interval, without imposing a heavy computational burden. Several different Runge-Kutta intervals can be chosen in Vensim: fixed step sizes of one-half (fixed RK2) and one-quarter (fixed RK4), as well as automatic adjustments of step size, (RK2 auto and RK4 auto). The 'RK4 auto' calculations used in this research have the highest accuracy, but require significantly more computational effort than the other forms, and so RK4 auto is the slowest of the numerical integration techniques.

All numerical integration techniques require the selection of a discrete, finite 'time-step', at which solutions are calculated for each simulated variable. This time step has a significant effect on model behaviour, so its value must be chosen carefully to avoid the introduction of *integration error* into the simulated values. Since integration error depends on the rate at which flows change relative to the selected time step, faster rates of change in flows demand shorter time steps. The selection of an appropriate time step for system dynamics models involves the following considerations,

- Time steps should be divisible by 2, so that possible time step values are 1, 0.5, 0.25, 0.125, and so on;
- Time steps should be roughly one-quarter to one-tenth the size of the smallest time constant in the model.

To test the suitability of the chosen time step, run a model simulation and check its behaviour. Then halve the time step to check the results of a shorter integration interval – for example, change the time step from 0.25 to 0.125. If the model behaviour matches between the two simulations, the original time step is acceptable; however, if there is any change in behaviour, continue to halve the time step until no further change in behaviour between simulations arises (Simonovic, 2008).

3.3.2 Model Experimentation

A note is required here on the model calibration and validation procedure, which differs in system dynamics from the traditional simulation approach. System dynamics follows a structural approach to modelling, so that each individual sector is based on the current, best understanding of the real-world structure it represents. This structural approach means that equations used to drive the model are not based on a mathematical, data-matching methodology – which can yield excellent matches to historical data, but assumes a direct connection between past and future behaviour that likely does not exist under global change conditions – but rather on the level of scientific understanding of the underlying physical and informational (or decision-focussed) processes that give rise to observed behaviours. Importantly, the system dynamics approach makes these assumptions about real-world structure explicit and testable, both critically and through simulation studies.

Since the behaviour of a system dynamics model results from its structure rather than from best-fit equations, the calibration procedure concentrates primarily on the manipulation of uncertain structural elements through alterations to stock-and-flow and feedback structures. Parameter tuning constitutes a minor part of the calibration. However, where parameters are required in system dynamics models, modellers attempt to base their values on well-understood, real-world characteristics, so that they have actual physical meaning. Parameter values are chosen based on the available literature, and model performance (described below) is tested to see that the chosen values cause the model to behave as expected. In the unusual case that calibrated parameters differ significantly from real-world values, assumptions that led to their inclusion in the model and to their associated value are checked. For such parameter values, sensitivity analysis, as described in Davies (2007), is especially necessary.

For this particular model, the calibration procedure focussed first on individual model sectors to ensure that their internal structures caused the model to behave as anticipated. As the sectors were connected through feedbacks, combinations of sectors were tested together to ensure that the model responded as expected.

Model validation was the next step, and consisted of three parts: 1) performance testing, 2) functional analysis, and, 3) feedback tracing. The performance testing of Chapter 2 concerned the ability of the complete model to generate matches to historical observations and to the performance of the other models on which it was based (in the cases of the carbon, climate, and economic sectors), and to behave in an analogous fashion to other models. Functional analysis is described in Davies (2007), and determines the causes of the whole-model behaviour. Finally, feedback tracing reveals the feedback-basis of unanticipated simulation results. Taken together, these three steps result in a *process* that increases confidence in model behaviour. Such confidence is important, Sterman (1984: 51) argues, since the "ultimately subjective nature of all 'objective' tests means one can never validate a model in the sense of establishing its truth".

The model has already been run, calibrated, and validated, as described above and in Chapter 2. Model users will therefore be interested in using it to focus on 'what if' simulations – in other words, through simulations with the model, they will investigate outcomes of changes in chosen model parameters that represent either policy options or uncertain physical characteristics, such as carbon taxation rates, the delay in establishing wastewater treatment facilities, changes in the thermal diffusivity of the oceans, higher CO_2-fertilization factors, and any number of other options or combinations of options. The best parameters to manipulate include those representing policy variables or corresponding to uncertain natural characteristics. Thus, investigating the effects of changes in the solar constant would be less informative, since its value is reasonably well-known, than imposing changes in carbon taxation rates or in land use change rates, on the policy side, or changes in the CO_2-fertilization factor, initial net primary productivity values, or oceanic diffusivity constant values on the physical side, for example. The major physical and policy-related parameters are listed in Table 27, below, by sector. Logical switches are also included in the table, under the 'type' heading of 'Switch'.

Table 27: Controllable model parameters by sector

Sector	Parameter Name	Type	Reasonable to Modify	Description
Climate	Climate Sensitivity	Physical	Yes	Parameter represents climate system response to change in atmospheric CO_2.
	Advection (w)	Physical	Possibly	Value gives reasonable climate sector behaviour. Other approaches possible.
	Diffusivity (κ)	Physical	Possibly	See comment above.
	Initial Temperatures	Physical	No	No compelling reason to change initial temperature values.
	Solar Constant	Physical	No	Value for incident solar shortwave radiation is well-established.
	Turn On Oceanic Inertia	*Switch*	Yes	Logical switch that turns on (set to '1') or off (set to '0') oceanic inertial effects. Default setting is 'on'.
Carbon Cycle	CO_2-fertilization (β)	Physical	Yes	Value is not well-established. Model is sensitive to change.
	Q_{10} factors	Physical	Yes	Values are not well-established. Model is somewhat sensitive to changes.
	Residence Times (τ)	Physical	Possibly	These sets of values are uncertain. However, no other values are available.
	Base NPP [σ(NPP)]	Physical	Possibly	See comment above.
	Decay (λ, φ)	Physical	Possibly	See comment above.
	Carbonization (ε)	Physical	Possibly	See comment above.
	Biomass partition fractions (p_{jk})	Physical	Possibly	See comment above.
	Buffer factor	Physical	Possibly	This is an oceanic calculation that requires three parameter settings. Its constituent parameter values are uncertain, but no other values are available.
	Mixing Time	Physical	Possibly	This is an oceanic parameter. Its value is uncertain, but no other values are available.

	Eddy Diffusion Coefficient	Physical	Possibly	See comment above.
	Initial Stocks	Physical	No	No compelling reason to change initial carbon stock values.
	Turn On Human Emissions	*Switch*	Yes	Logical switch that turns on (set to '1') or off (set to '0') the carbon flow from industrial emissions to the atmosphere. Default setting is 'on'.
	Turn On Human Land Use	*Switch*	Yes	Logical switch that turns on (set to '1') or off (set to '0') effects of human activities on the biosphere. Default setting is 'on'. If switch turned off, land-use and land-use change are not modelled, so there are no land-use emissions, and the biome areas remain constant over the entire simulation.
	Turn On Oceanic CO2 Absorption	*Switch*	Yes	Logical switch that turns on (set to '1') or off (set to '0') oceanic CO_2 absorption. Allows isolation of biospheric from oceanic carbon absorption. Default setting is 'on'.
	Turn On Q10 Effects	*Switch*	Yes	Logical switch that turns on (set to '1') or off (set to '0') Q_{10} effects in the model. Default setting is 'off'.
Economy	Carbon Tax	Policy	Yes	A key policy variable in the form of a set of look-up tables and calculations. Several different carbon taxation schemes available – see the 'Case Selector', below.
	A(t)	Economic	Yes	Technological change, in the form of 'total factor productivity', plays an important role in economic output. However, its dynamics into the future are unclear, and historical values are not available. Several parameters are involved in determining A(t), including 'rate', 'goal', 'init A(t) mult', 'TFP A(0)', '$g^a(0)$', and 'δ^a'.
	Savings	Economic	Possibly	This parameter is actually composed of two look-up tables of year-wise values. Historical savings values are reasonably clear and are given in 'savings to 1995'. Future values, given in 'annual savings rate' are uncertain and come from DICE.
	Depreciation	Economic	Possibly	Depreciation fraction is set as constant. No compelling reason to change value.
	Initial Capital	Economic	No	This value is uncertain, but there is no other available value.

	DICE parameters	Variable	No	A variety of dynamic model parameters, which change in pre-determined manner over the course of the simulation, are used in DICE. These parameters include b_1, g^b, σ, g^σ, and R, among others. There is no compelling reason to change these values.
	Case Selector	*Switch*	Yes	Provides the means of selecting between different carbon tax policies. Default value is '1', which gives the 'base run'. Other possible values are '2' (the optimal tax), '3' (the temperature limit tax), '4' (the double [CO_2]), '5' (the constant tax), and '6' (the ramp tax). Note that other numerical values also give the 'ramp tax'.
	Ignore Climate Change in Output	*Switch*	Yes	Logical switch that turns on (set to '1') or off (set to '0') climate change effects on economic output. Default setting is 'on'.
Land-use	Base Transfer Rate	Policy	Yes	Land-use change set to match population change. Reasonable to change the proportionality constant (set generally to one).
	Initial Values	Physical	Possibly	These values are uncertain. However, no other values are available.
	Turn On Altered Land Use Pattern	*Switch*	Yes	Logical switch that turns on (set to '1') or off (set to '0') changes in the 'base transfer rate' proportionality constant. Default setting is 'off'. If set to 'on', the effects of land-use policy changes are simulated. Check the model code, as this switch is somewhat more complicated than most.
Surface Flow	Reservoir Expansion Rate	Policy	Yes	Reservoir expansion assumed to slow in future. Other expansion rates possible.
	Base Precipitation Multiplier	Physical	Possibly	This value is uncertain. However, no other value is available.
	Consumption Percentages	Policy	Possibly	These values are uncertain. However, no other values are available.
	Stable Runoff Percentage	Physical	Possibly	Value not well-established. Model is somewhat sensitive to change.
	Initial Values	Physical	No	No compelling reason to change initial values. Worth revisiting if new values become available.

	Turn On Anthropogenic Consumption Effects	*Switch*	Yes	Logical switch that turns on (set to '1') or off (set to '0') the effects of anthropogenic water consumption on the hydrological cycle. Default setting is 'on'.
	Turn On Climate Effects on Water	*Switch*	Yes	Logical switch that turns on (set to '1') or off (set to '0') temperature feedbacks on the hydrological cycle from climate change. Default setting is 'on'.
	Turn On Reservoir Evaporation	*Switch*	Yes	Logical switch that turns on (set to '1') or off (set to '0') effects of reservoir evaporation on the natural hydrological cycle. Default setting is 'on'. <u>Note</u>: if all three switches in this sector are turned 'off', the sector simulates an *equilibrium* surface flow.
Water Demand	Irrigation Expansion	Policy	Yes	Irrigation expansion assumed to slow in future. Other expansion rates are possible, and the model is sensitive to the rates chosen.
	Electricity Production	Policy	Yes	Increase in electricity production is assumed. Other rates of increase possible.
	$DSWI_{min}$, $DSWI_{max}$, γ_d	Validated	No	Model validated for these values. Changes are possible, but not advised.
	$ISWI_{min}$, γ_i	Validated	No	See comment above.
	Consumption Percentage	Validated	No	See comment above.
Water Quality	Delay in Instituting Wastewater Reuse	Policy	Yes	An important policy variable, whose value is not well-established. The model is sensitive to changes.
	Wastewater Reuse Breakdown by Sector	Policy	Possibly	These values are uncertain. However, no other values are available.
	Delay in Establishing Domestic Treatment	Policy	Yes	An important policy variable, whose value is not well-established. The model is sensitive to changes.
	Delay in Establishing Industrial Treatment	Policy	Yes	An important policy variable, whose value is not well-established. The model is somewhat sensitive to changes.

	Domestic Polluted Fraction	Physical	No	This value is reasonably well-established.
	Industrial Polluted Fraction	Physical	Possibly	This value is uncertain. However, no other value is available.
	Agricultural Polluted Fraction	Physical	Possibly	This value is uncertain. However, no other value is available.
	Dilution Requirement	Physical	Possibly	Value is not well-established. Model is somewhat sensitive to changes.
	Water Stress Effects	Look-up	Possibly	These pre-set values are uncertain. However, no other values are available.
	Desalination Parameters	Policy	Possibly	Parameters involved: "delay in establishment of desalination facilities", "maximum establishment of desalination facilities", and "fractional usage of desalination facilities". Desalination plays minor role in model only. However, if real-world importance of desalination grows significantly, changes would be reasonable here.
	Groundwater Withdrawal	Policy	Possibly	Parameters involved: "delay in establishing groundwater pumps", and "maximum groundwater withdrawal". Groundwater withdrawal plays minor role in model only, and since the groundwater modelled here is non-renewable, that small role is unlikely to become bigger.
	Turn On Desalination	*Switch*	Yes	Logical switch that turns on (set to '1') or off (set to '0') the desalinated water supply in the model. Default setting is 'on'.
	Turn on Groundwater Withdrawals	*Switch*	Yes	Logical switch that turns on (set to '1') or off (set to '0') groundwater withdrawals in the model. Default setting is 'on'.
	Turn On Wastewater Reuse	*Switch*	Yes	Logical switch that turns on (set to '1') or off (set to '0') the reuse of treated wastewater in the model. Default setting is 'on'.
Population	Turn On Pollution Effects on Population Growth	*Switch*	Yes	Logical switch that selects between the novel water stress definition, which includes the effects of water pollution on water scarcity (set switch to '1'), or

selects the traditional water stress definition, which neglects water quality effects on water scarcity (set switch to '0').

This is an important policy variable, because the choice of *wta* definition used in each simulation has a significant effect on model results.

For a more comprehensive look at the effects of parameter manipulation, sensitivity analysis is available. Sensitivity analysis, and a specific form available in Vensim (and in many other software tools) called Monte Carlo analysis, is described and applied in Davies (2007); however, a few details are also provided here. Sensitivity analysis allows a user to determine the effects on key variables in the model to changes in a parameter or group of parameters – sensitive parameters cause large variations in key variables for small parameter value changes. Monte Carlo analysis involves the automatic application of a selected probability distribution to uncertain parameters over one to several hundred simulation runs. Many forms of probability distributions are available in system dynamics software, including random normal, random Weibull, random uniform, random exponential, and so on.

Regardless of the simulation approach used, whether comparisons between individual model runs or more comprehensive sensitivity analysis, the aim of any experimentation is the exploration of model variable behaviours between different simulation runs. The desire is to see how the modelled system behaves normally, and then how changes in policies or physical parameters alter that behaviour. From a policy perspective, model sensitivity to a parameter change means that a 'high-leverage' point has been discovered – such parameter changes may represent useful intervention points in the real-world. For example, enacting a carbon tax policy that results in little economic cost, but large environmental benefits in the model may be an intelligent option. From a scientific perspective, less sensitivity in uncertain parameters is preferable, since this lower sensitivity means that the process or physical characteristic associated with that parameter does not affect model behaviour strongly. A lack of understanding of the physical system involved therefore changes neither the model results nor the conclusions drawn from model behaviour.

3.3.3 Interpretation

Experimentation involves selecting the parameters to manipulate in each simulation run. Once the chosen simulations have been run, the results must obviously be analyzed or

interpreted. Vensim, like other system dynamics software, has a variety of tools available for analyzing individual simulation runs, and for comparing the results of one simulation with one or more alternatives – see the Vensim User's Guide (Ventana Systems, 2006a) for further details. These tools are applied in Davies (2007) and the other publications listed in Chapter 1, but this section introduces the basic types available and their uses.

Certain analysis tools are primarily qualitative, while others are quantitative. Tables display actual simulated values to several decimal places for one or more selected variables. They are useful for comparison and validation purposes. Graphs show the qualitative behaviour of selected variables over time, and can be used to compare the results of several different simulation runs for the same variable, or to compare several different variables from the same simulation run. Other tools are more specialized to feedback analysis: the feedback loop tool, the 'causes tree' tool, the 'uses tree' tool, and the causes strip tool. The loop tool determines the number of feedback loops associated with a selected variable and specifies the feedback path from one variable to the next, until a full circle is completed for each loop. The causes tree and uses tree tools list the 'upstream' and 'downstream' variables associated with the chosen variable to a pre-selected distance from the chosen variable – examples of these tool outputs are provided in Figure 22. Note that the feedback loop tool, the 'causes tree' tool, and the 'uses tree' tool focus on model structure rather than on simulation results, so they will work without a model simulation loaded. All other tools apply to individual, or groups of, simulations.
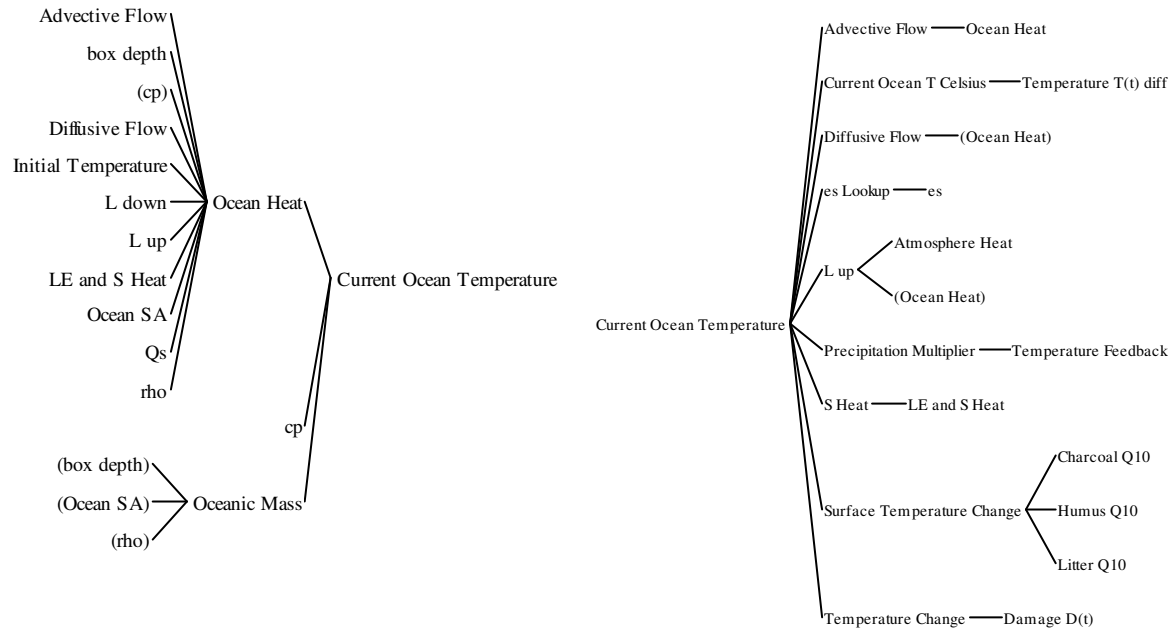
Figure 22: Example of the output from the 'Causes Tree' and 'Uses Tree' tools in Vensim

The causes strip tool shows the graph associated with the currently selected variable, as well as the individual graphs of all 'upstream', or causative, variables. Significant changes in the chosen variable can then be matched against causative changes in the other variables shown. For example, Figure 23 shows how a slight discontinuity in the desired surface water consumption around 1990 is a result of a change in the desired agricultural water consumption, rather than an outcome of changes in the much smaller domestic and industrial water consumption values.
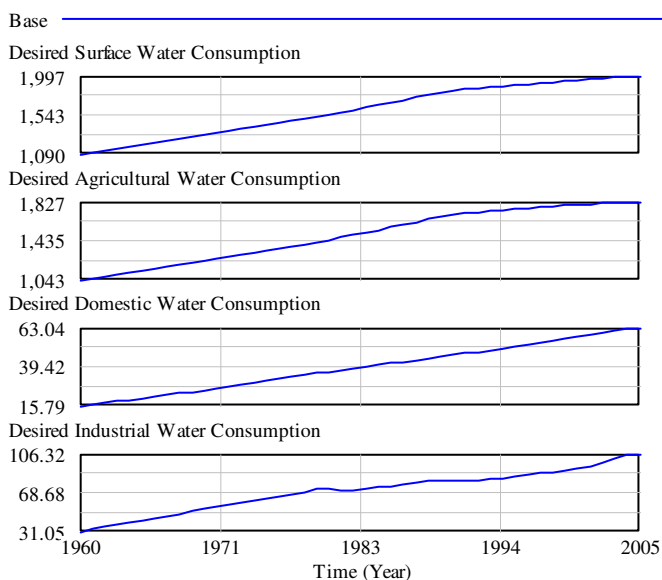
Figure 23: Example of the output from the 'Causes Strip' tool

Finally, sensitivity analysis has its own tools: histograms and graphs. The histogram tool displays the range of values simulated through Monte Carlo analysis for a selected variable at a chosen time. A sensitive variable will have a histogram with a wide variety of values spread over the one to several hundred simulation trials – the number of simulation trials is shown on the vertical axis – while an insensitive variable may have a graph with a single large peak that corresponds to all or most of the simulation trials, or the variation in the range of values on the horizontal axis may be small. Figure 24 shows these two histogram types, with the left histogram showing a sensitive variable (note the horizontal scale), and the right showing a relatively insensitive variable.
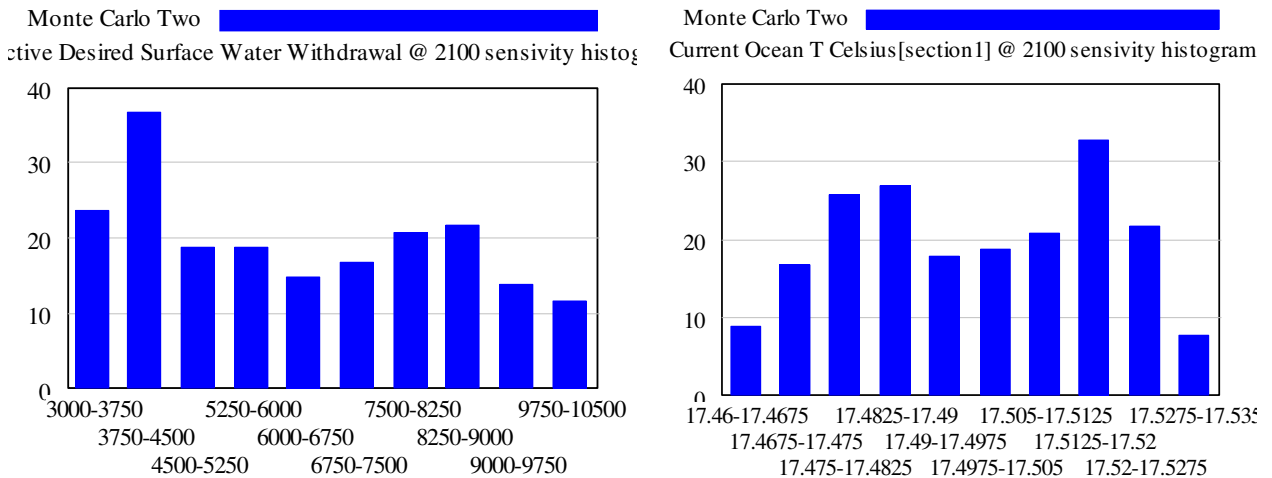
Figure 24: Example of the histogram tool output

Sensitivity graphs differ considerably from histograms, since they show the behaviour of the selected variable over the entire duration of the simulation, rather than at one particular time. Typical sensitivity graphs show either a divergence in the simulated values of the selected variable over the course of multiple simulation trials from a base value, so that the sensitivity graph resembles a trumpet-like, or similar, shape, or they may show a marked lack of divergence from the base value, in which case the chosen variable is insensitive to the imposed parameter changes. Figure 25 shows a sensitive variable on the left side, and an insensitive variable on the right side.
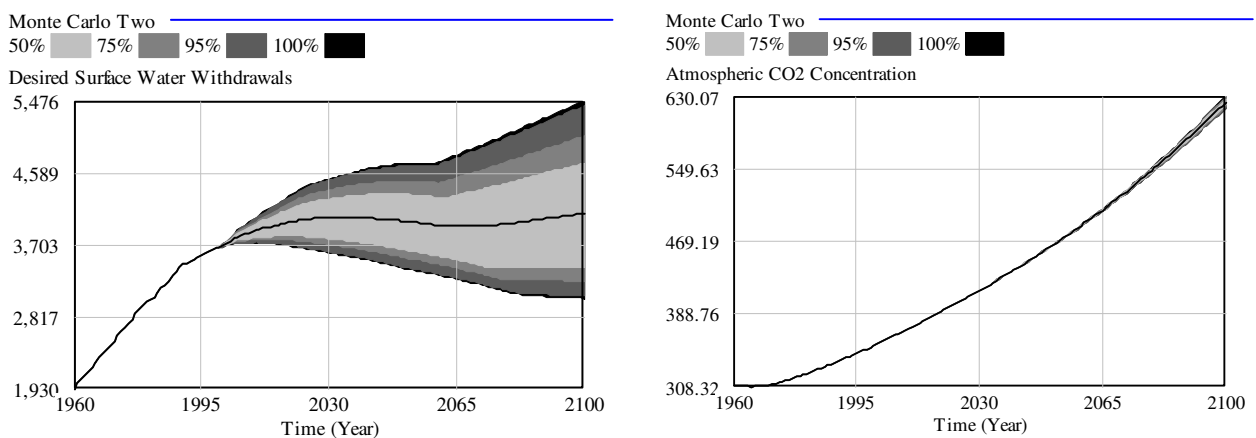
Figure 25: Example of the sensitivity graph output

In summary, the aim of the interpretation tools is to illustrate or clarify system behaviours by showing the results of changes in parameters, and particularly their effects on key variables either quantitatively or qualitatively. Interpretation tools are usually used in groups to trace the causes and effects of model feedbacks.

3.4 Policy Creation

Parameter changes in the socio-economic areas of the model relate to policy change, so that the model can be used to simulate the effects of changes in policies related to land use, water use and water quality, population growth, and carbon reduction, or combinations of these possibilities. Recall that all of the controllable parameters in the model are listed in Table 27, above.

This section focuses specifically on policy development in the context of engineering, and provides two examples. The first example of policy development deals with desalination levels, while the second implements measures to increase wastewater treatment and reuse volumes. Note that the results of these simulations are presented but not analyzed here – for such an analysis, see Davies (2007).

3.4.1 Desalination Policy

In this experiment, the effect on water scarcity levels of widespread desalination facility creation is modelled, but the possibility of treated wastewater reuse is neglected.

Several parameters in the *water quality* sector must be manipulated to simulate the proposed changes in desalination policy. The parameters associated with desalination and their settings for this experiment are,

- The fractional usage of desalination capacity = 0.6;
- The maximum establishment of desalination facilities = 100 km^3 yr^{-1}; and,
- Turn On Wastewater Reuse = 0.

Recall that in the 'base run' of the model, the desalination volume in the model is capped at 32.4 km^3 yr^{-1} with a fractional usage of 0.5, while the 'on/off' switch that disables wastewater reuse, called 'turn on wastewater reuse', has a default value of 1.

To enter these changes, go to the *water quality* sector of the model, click in the wide box visible in Figure 18, above, that reads 'Current', and enter a name for the simulation: 'Greater Desalination, No Reuse'. Naming the simulation allows a comparison between this model run and others, such as the base run. Then click on the button to the left of the simulation name box, called 'Set'. All of the controllable parameters will then be displayed as yellow type in a blue box – see Figure 26. Once 'Set' is clicked, it is replaced by 'Stop', which cancels the simulation run if selected.
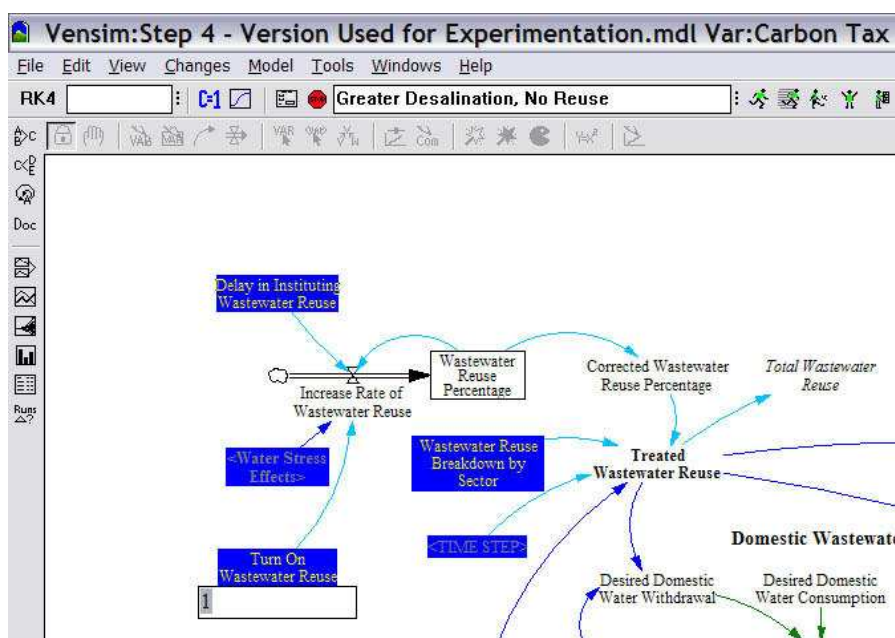
Figure 26: Partial screen-capture of experiment one setup

The parameter changes for this experiment are entered by clicking on the three parameters listed above, and changing the default values to the new values chosen. In Figure 26, for example, the 'turn on wastewater reuse' parameter has already been selected, and an editing box is visible below the parameter's blue box. After the parameters have their new values, click on the 'Run Simulation' button – again, see Figure 18 – to run the simulation, and store the data as 'Greater Desalination, No Reuse'.

Running the simulation will probably take several minutes in Vensim DSS, during which time a simulation progress will be displayed, as in Figure 27. Note that parameter changes can be made through the 'Set' button or through equation editor in Figure 21; however, parameter changes made through the equation editor are stored as the new default values and must be altered manually.

Figure 27: Simulation progress display

When the simulation run is complete, the progress display will disappear, and the model structure will reappear. Simulation results will then be available for analysis through the Vensim tools described above.

The best approach to analyzing the results of a policy experiment is to compare them with the results of the model's base run. Selection of the simulation runs to compare is accomplished through the control panel in Vensim DSS, which is shown in Figure 28. The figure shows that two sets of experimental data are loaded (on the right-hand side panel), and many more data sets are available (in the left-hand side panel). The arrows between the two panels are used to load and unload experimental data sets.
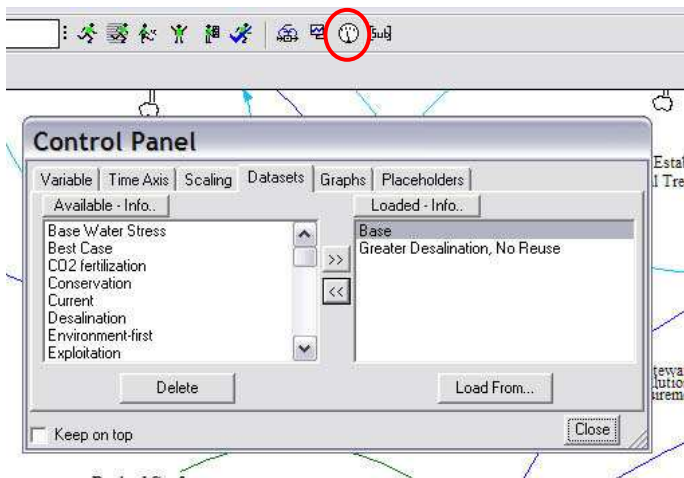
Figure 28: Partial screen-capture showing control panel and selected data sets

Note that if a 'base run' is not available from the control panel, it can be created by changing the text in the simulation name box to 'Base', and then clicking on the 'Run Simulation' button in Figure 18. The model will then be run with its default values, and the resulting data stored under the name 'Base'. Note that failure to enter a new simulation name will overwrite the 'Greater Desalination, No Reuse' data.

Once the two data sets are loaded through the control panel, the simulation results can be investigated and differences in model behaviour can be identified. As described above, a variety of tools are available, including tables of values, graphs, causes strips, causes and uses trees, and the loop and sensitivity tools. Another useful tool, called the 'runs compare' lists differences between the loaded data sets. Clicking on it, in this case, identifies the three parameter changes described above.

As an example of the experimental results, the Vensim graph tool output shows the effect of changes in desalination parameters on the total available desalinated volume, as well as on global water stress – see Figure 29, in which the top line in both graphs represents the results of the proposed desalination policy, while the bottom line represents the effects of the model's base run. To access these graphs, find the 'lock' button on the structure toolbar, as shown in Figure 30, and click on it so that subsequent clicking on model variables simply *selects* rather than *alters* them.

Global Desalinated Water Supply

Global Desalinated Water Supply : Base ————————	km*km*km/Year
Global Desalinated Water Supply : Desalination ————————	km*km*km/Year

Water Stress Effects

Water Stress Effects : Base ————————	Dimensionless
Water Stress Effects : Desalination ————————	Dimensionless
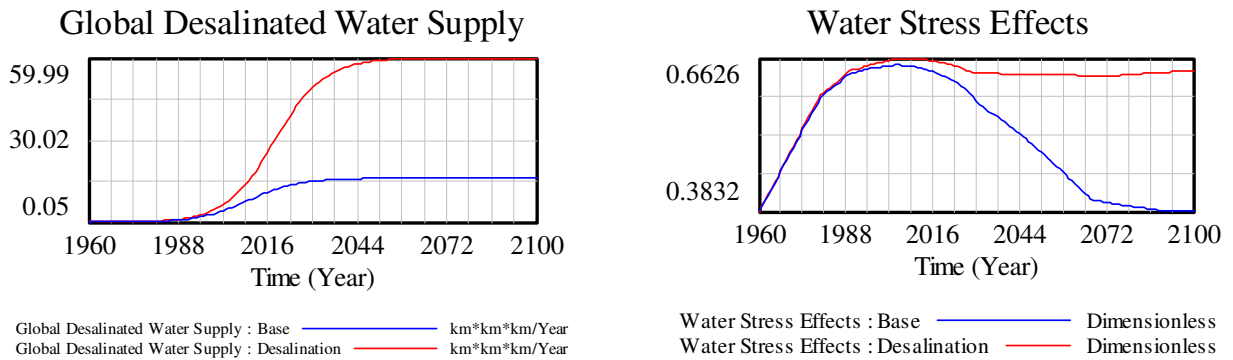
Figure 29: Effects of policy experiment one on the global desalination volume and global water stress value

Figure 30: Location of lock button in Vensim

Next, ensure that the current view is still *water quality*, and find the "global desalinated water supply variable". Click on it, and then select the graph tool shown in Figure 31. A graph that is either the same or very similar to the left-hand side of Figure 29 will appear. Clearly, the parameter changes have had an effect on the desalinated water supply volume. Close the first graph and click on the "water stress effects" variable, also in the *water quality* view, to show the graph visible on the right-hand side of Figure 29.
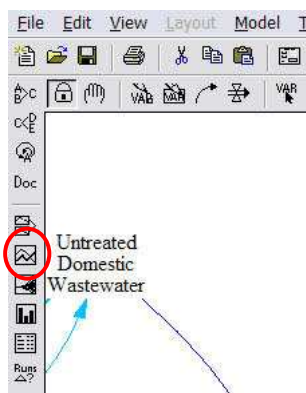
Figure 31: Location of graph tool, and of all other tools, in Vensim

Once these direct results of the parameter changes have been identified, the interpretation tools described above can be used to determine the effects of feedbacks on model behaviour as a whole, to identify which specific feedbacks cause these sorts of changes, and to discover how they operate. Most of this sort of analysis is left to the user; however, several examples follow.

From the model description of Chapter 2, it is clear that the change in water stress effects shown in Figure 29 will have effects on population, and then on the rest of the model through these population differences between experiments. Therefore, use the 'page down' key to switch to the *population* sector 'view', and, making sure the 'lock' button is still selected, click on the Population stock. Next, click on the graph button in Figure 31, and a graph like Figure 32 will appear, which shows that population is lower in this experiment than in the base run. To find the numerical difference, use the 'table' tool, also visible in Figure 31, to find that the final populations in 2100 are 11.73 and 11.03 billion people for the base run and the experiment, respectively – a difference of 700 million people.
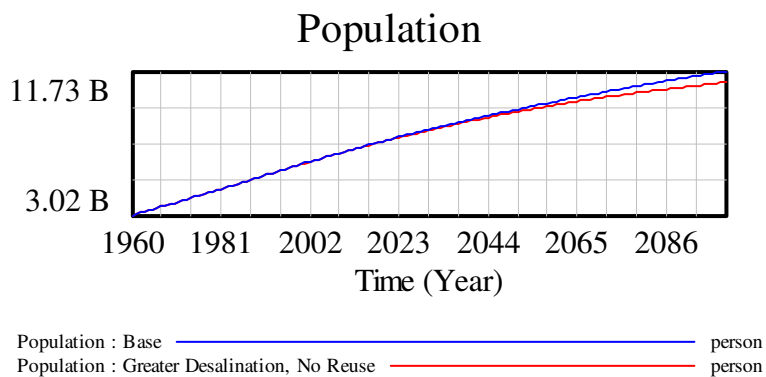
Figure 32: Population comparison between "Greater Desalination, No Reuse" and 'Base Run' simulations

As a final example of the analysis procedure, close any open graphs and tables, and use the 'page up' key to navigate to the *economy* 'view'. Make sure the 'lock' button is still selected, and then click on the 'Output Q(t)' variable and the 'causes strip' button visible

in Figure 31. Three windows of output will appear. Close two windows, but leave the
third, shown in Figure 33, open. The evolution of 'Output Q(t)' in both cases clearly
varies with 'Capital K(t)' and with 'Population'.
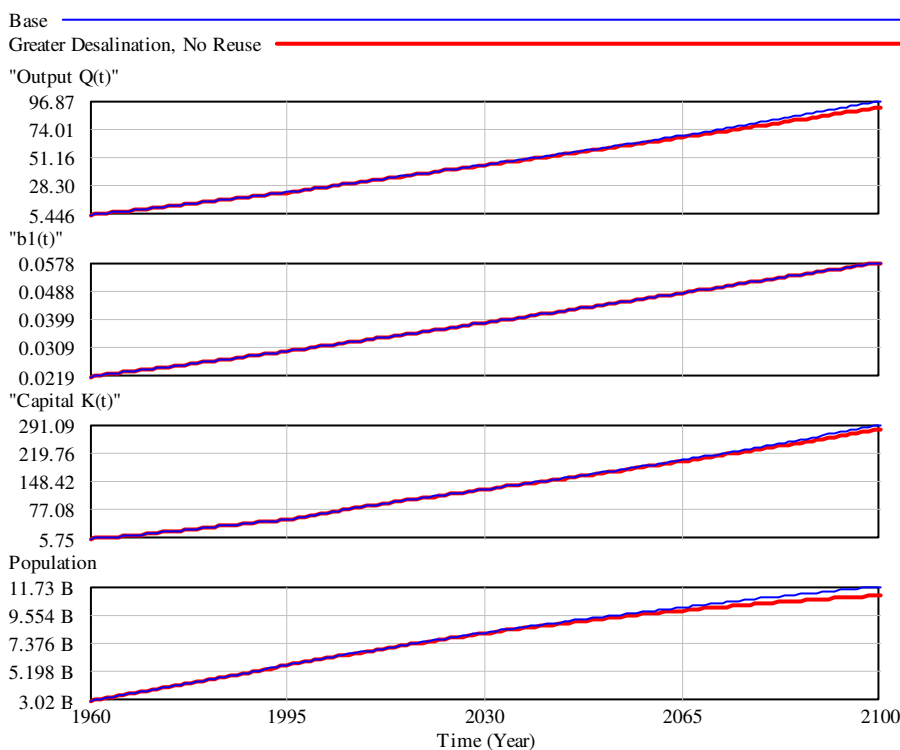
Figure 33: Experiment one results: 'Output Q(t)' and its causes

Many other analytical tools and approach are available in Vensim. The user is
encouraged to try some of them now to trace other effects of the changes in desalination
volumes and wastewater reuse – for example, it may be useful to determine whether the
changes in desalination volumes or in wastewater reuse had more impact on model
behaviour.

3.4.2 Wastewater Treatment and Reuse Policy

In this second policy change example, the wastewater treatment capacity will be
increased considerably from the 'base run', greater volumes of treated wastewater will be
reused, all of which will be devoted to agricultural production.

The parameters involved in the experiment are members of the *water quality* sector. They are,

- The delay in establishing domestic treatment;
- The delay in establishing industrial treatment;
- The delay in instituting wastewater reuse; and,
- The wastewater reuse breakdown by sector.

Since the policy is to come into effect at present, rather than from 1960 onwards, several equation changes must be made. Currently, the three delays involved in the experiment are simply constant values of 30, 75, and 20 years, respectively. To change their behaviour – rather than just their constant values, through the 'Set' button used in the previous experiment – the equation editor shown in Figure 21 must be used.

The first step in setting up the experiment is to modify the model structure slightly. In the *water quality* sector, locate the three delays listed above. Then add the 'Time' variable to the model structure near the delay variables, so that the delays can access the current time in the simulation run – note that, as an important control variable, 'Time' is present (but *hidden*) in all Vensim models.

The variable is made visible for direct use as follows. Click on the 'shadow variable' button on the 'structure toolbar', as shown in Figure 34, and then click in a white area of the model overview, near one of the delays. A list of variables will appear, as shown in Figure 35. Either enter the word 'Time' into the 'name or pattern' box, or scroll down to the 'Time' variable and select it in the list. After 'Time' is highlighted, click 'OK' to insert it in the model.
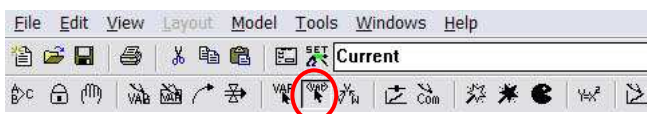
Figure 34: Shadow variable button location
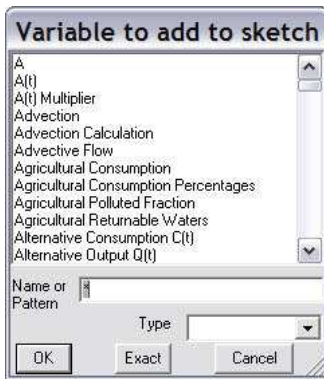
Figure 35: Shadow variable selection dialogue

Once 'Time' is visible near the first delay – it will appear in angle brackets, as <Time> – insert two more copies near the remaining two delays. Then, to indicate to Vensim that the three delay parameters *depend on* the current simulation time, each version of the 'Time' variable must be connected to the relevant delay using an *arrow*. The arrow tool is visible in Figure 34 as a curved arrow, three buttons to the left of the shadow variable button. Click on the arrow button, then click on one copy of the time variable, and finally click on the chosen delay. The three steps followed here are shown in Figure 36:

1. Appearance before modification;
2. Addition of 'Time' variable; and,
3. Addition of arrow to connect 'Time' to "delay in establishing domestic treatment".
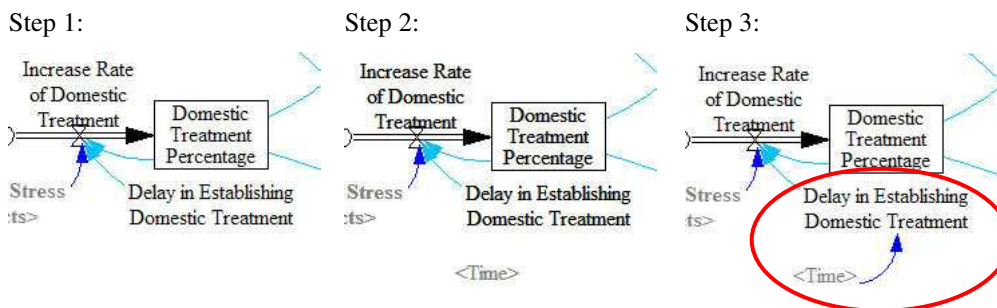
Figure 36: Addition of 'Time' variable and arrow to model structure

Note that any mistakes, like an incorrect *arrow* connection, can be fixed using the 'delete' button, which looks like a Pacman in Figure 34, above; however, be careful with

this tool, since misuse can eliminate model variables and introduce errors. The edit menu has an undo function, in case model variables are mistakenly erased.

Once the model has been modified to include three new instances of the 'Time' variable and its associated arrows, the equations for each delay must be altered slightly. Click on the 'y=x^2' button, beside the Pacman in Figure 34, to change the three delay equations. The addition of the 'Time' variable and arrows will cause Vensim to identify each of the delay equations as changed. The delays will be shown as black boxes with white text, as in Figure 37.
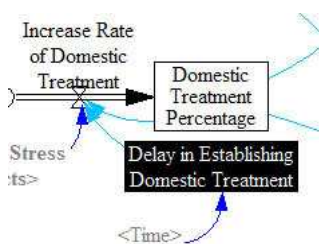
Figure 37: Modified equation identification in Vensim

Click on the first delay, called "delay in establishing domestic treatment" and modify it by entering the following text:

IF THEN ELSE(Time < 2005, 30, 15).

The actual equation for the variable will then be,

Delay in Establishing Domestic Treatment = IF THEN ELSE(Time < 2005, 30, 15)

This code tells Vensim that the delay before 2005 is 30 years, but in and after 2005 is 15 years. Now change the remaining two delays to read as follows:

Delay in Establishing Industrial Treatment = IF THEN ELSE(Time < 2005, 75, 37.5)

Delay in Instituting Wastewater Reuse = IF THEN ELSE(Time < 2005, 20, 10)

In summary, before running the simulation, equations are changed for the three delays by adding three instances of the 'Time' variable, connecting these variables to the three delay variables, and then changing the code for the delays by using the equation editor. The resulting parameter changes are,

- Delay in Establishing Domestic Treatment = 30 years from 1960-2004, and 15 years from 2005-2100;

- Delay in Establishing Industrial Treatment = 75 years from 1960-2004, and 37.5 years from 2005-2100; and,

- Delay in Instituting Wastewater Reuse = 20 years from 1960-2004, and 10 years from 2005-2100;

Finally, "wastewater reuse breakdown by sector" has default settings of 10%, 30%, and 60% for the domestic, industrial, and agricultural sectors, respectively. To change these percentages to 0, 0, and 100%, the two options are to use the '$y=x^2$' button, as explained above, and then to enter the new values in place of the old, or more simply to use the 'Set' button after the equation changes to the three delays are accomplished.

If the second option – using the 'Set' button – is chosen, the instructions from this point are similar to those of the first experiment, "Greater Desalination, No Reuse", above. The simulation run here will be called "Wastewater Treatment, Agricultural Reuse", so click 'Set' and then enter this name into the simulation name box shown in Figure 18. Next, click on the "wastewater reuse breakdown by sector" parameter, and set the values for the domestic, industrial, and agricultural sectors to 0, 0, and 100%, respectively. Finally, run the simulation by clicking on the 'Run Simulation' button in Figure 18.

When the simulation run is complete, the progress display dialogue, as in Figure 37, will disappear and the model structure will reappear. Simulation results will then be available for analysis through the Vensim tools described above.

Again, a comparison of the results of this experiment with the base run will allow the model user to determine the results of the proposed policies. See Figure 38, which displays the differences in wastewater treatment volumes between the base run and the proposed treatment and reuse policy, as well as the resulting changes in water stress levels. These graphs were displayed in Vensim using the 'graph' tool, as explained above. In this case, the wastewater policy change results in a greater treated volume on the left side, and a much lower water stress on the right side.
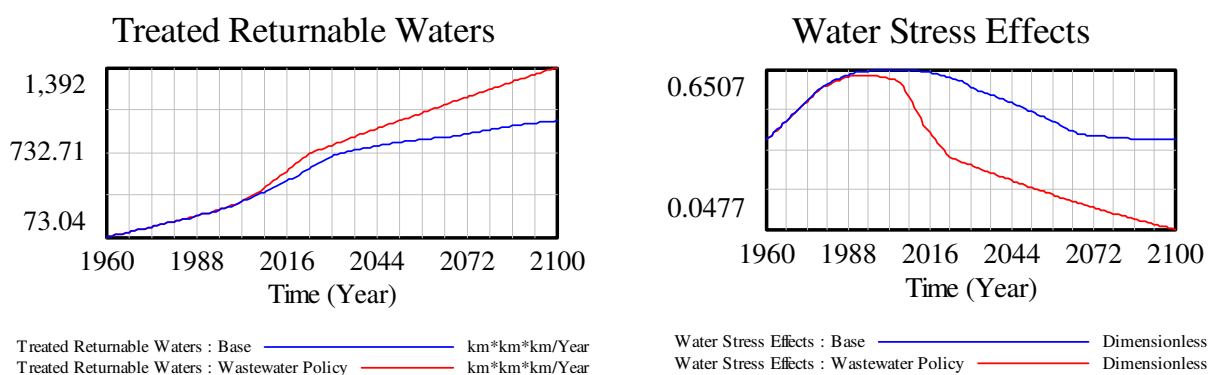
Figure 38: Effects of policy experiment two on the treated wastewater volume and global water stress value

Note that the new data set, "Wastewater Treatment, Agricultural Reuse", will be selected automatically in the Vensim control panel after running the simulation, and will be available for comparison with other experiments in subsequent uses of Vensim DSS. It is therefore best at this point to close Vensim without saving the equation and structural changes in the model, rather than manually undoing the changes through the equation editor. After closing Vensim without saving, and opening the program again, use the control panel, shown in Figure 28, to load the desired data sets.

3.5 Conclusions

This appendix introduced the modelling interface, Vensim, and its use both in analyzing the results of model simulations, and in designing and running policy experiments. The intended audience – academics, researchers, students, engineers, and policy-makers – for

the completed model was presented, and model use through the software interface was then described, in terms of the system dynamics approach towards model organization and mathematics, experimentation with system dynamics models, and interpretation of the obtained simulation results. The third and final section explained the application of the model to policy development, with two examples demonstrating the simulation of engineering-related policy.

4. REFERENCES

Alcamo, J., T. Henrichs and T. Roesch. (1999). *World water in 2025: Global modeling and scenario analysis for the World Commission on Water for the 21st Century.* Center for Environmental Systems Research, University of Kassel, Kassel, Germany.

Alcamo, J., G. J. J. Kreileman, J. C. Bollen, G. J. van den Born, R. Gerlagh, M. S. Krol, A. M. C. Toet and H. J. M. de Vries. (1996). Baseline scenarios of global environmental change. *Global Environmental Change,* 6: 261-303.

Alcamo, J., G. J. J. Kreileman, M. S. Krol and G. Zuidema. (1994). Modeling the global society-biosphere-climate system: Part 1: Model description and testing. *Water, Air and Soil Pollution,* 76: 1-35.

Alcamo, J., P. Döll, T. Henrichs, F. Kaspar, B. Lehner, T. Rösch and S. Siebert. (2003a). Development and testing of the WaterGAP 2 global model of water use and availability. *Hydrological Sciences Journal,* 48: 317-337.

Alcamo, J., P. Döll, T. Henrichs, F. Kaspar, B. Lehner, T. Rösch and S. Siebert. (2003b). Global estimates of water withdrawals and availability under current and future "business-as-usual" conditions. *Hydrological Sciences Journal,* 48: 339-348.

Alcamo, J. and T. Henrichs. (2002). Critical regions: A model-based estimation of world water resources sensitive to global changes. *Aquatic Sciences,* 64: 352-362.

Alexander, L. V., X. Zhang, T. C. Peterson, J. Caesar, B. Gleason, A. M. G. K. Tank, M. Haylock, D. Collins, B. Trewin, F. Rahimzadeh, A. Tagipour, K. R. Kumar, J. Revadekar, G. Griffiths, L. Vincent, D. B. Stephenson, J. Burn, E. Aguilar, M. Brunet, M. Taylor, M. New, P. Zhai, M. Rusticucci and J. L. Vazquez-Aguirre. (2006). Global observed changes in daily climate extremes of temperature and precipitation. *Journal of Geophysical Research,* 111, D05109, doi:10.1029/2005JD006290.

Arnell, N. W. (1999a). A simple water balance model for the simulation of streamflow over a large geographic domain. *Journal of Hydrology,* 217: 314-335.

Arnell, N. W. (1999b). Climate change and global water resources. *Global Environmental Change,* 9: S31-S49.

Atjay, G. L., P. Ketner and P. Duvigneaud. (1979). Terrestrial primary production and phytomass, in *The Global Carbon Cycle*, edited by B. Bolin, E. T. Degens, S. Kempe and P. Ketner, pp. 129-181, John Wiley and Sons, Chichester, U.K.

Berthelot, M., P. Friedlingstein, P. Ciais, P. Monfray, J. L. Dufresne, H. Le Treut and L. Fairhead. (2002). Global response of the terrestrial biosphere to CO2 and climate

change using a coupled climate-carbon cycle model. *Global Biogeochemical Cycles,* 16(4), 1084, doi:10.1029/2001GB001827.

Brohan, P., J. J. Kennedy, I. Harris, S. F. B. Tett and P. D. Jones. (2006). Uncertainty estimates in regional and global observed temperature changes: A new data set from 1850. *Journal of Geophysical Research,* 111, D12106, doi:10.1029/2005JD006548.

Bürgenmeier, B., A. Baranzini, C. Ferrier, C. Germond-Duret, K. Ingold, S. Perret, P. Rafaj, S. Kypreos and A. Wokaun. (2006). Economics of climate policy and collective decision making. *Climatic Change,* 79: 143-162.

Chahine, M. T. (1992). The hydrological cycle and its influence on climate. *Nature,* 359: 373-380.

Cosgrove, W. J. and F. R. Rijsberman. (2000). *World Water Vision: Making Water Everybody's Business*. Earthscan Publications Ltd., London, U.K.

Cox, P. M., R. A. Betts, C. D. Jones, S. A. Spall and I. J. Totterdell. (2000). Acceleration of global warming due to carbon-cycle feedbacks in a coupled climate model. *Nature,* 408: 184-187.

Cramer, W., A. Bondeau, F. I. Woodward, I. C. Prentice, R. A. Betts, V. Brovkin, P. M. Cox, V. Fisher, J. A. Foley, A. D. Friend, C. Kucharik, M. R. Lomas, N. Ramankutty, S. Sitch, B. Smith, A. White and C. Young-Molling. (2001). Global response of terrestrial ecosystem structure and function to CO_2 and climate change: Results from six dynamic vegetation models. *Global Change Biology,* 7: 357-373.

Cramer, W., D. W. Kicklighter, A. Bondeau, B. Moore, C. Churkina, B. Nemry, A. Ruimy and A. L. Schloss. (1999). Comparing global models of terrestrial net primary productivity (NPP): overview and key results. *Global Change Biology,* 5(Suppl. 1): 1-15.

Cumming, G. S., J. Alcamo, O. Sala, R. Swart, E. M. Bennett and M. Zurek. (2005). Are Existing Global Scenarios Consistent with Ecological Feedbacks? *Ecosystems,* 8: 143-152.

Davies, E. G. R. (2007). *Modelling Feedback in the Society-Biosphere-Climate System*. Doctoral Thesis. Department of Civil and Environmental Engineering, the University of Western Ontario, London, Ontario, Canada. Available from http://www.eng.uwo.ca/research/iclr/fids/publications/nserc-climate/Davies_Thesis.pdf. Last accessed April 10, 2008.

Davies, E. G. R. and S. P. Simonovic. (2006). Modeling feedback in the Society-Biosphere-Climate system. *Climatic Change*. (*under review*).

Davies, E. G. R. and S. P. Simonovic. (2008a). Insights from integrated assessment modelling of the society-biosphere-climate system. *Journal of Environmental Management* (*under review*).

Davies, E. G. R., and Simonovic, S. P. (2008b). Water resources management and feedback modelling. *Journal of Water Resources Planning and Management* (*under review*).

Dowlatabadi, H. and M. G. Morgan. (1993a). A Model Framework for Integrated Studies of the Climate Problem. *Energy Policy,* 21: 209-221.

Dowlatabadi, H. and M. G. Morgan. (1993b). Integrated Assessment of Climate Change. *Science,* 259: 1813-1932.

Energy Information Administration (EIA). (2006). *Official Energy Statistics from the U.S. Government* (on line), U. S. Department of Energy, Washington, D.C. Available from http://www.eia.doe.gov/emeu/international/contents.html. Last accessed Aug. 1, 2007.

Falkenmark, M. (2005). Water usability degradation – Economist wisdom or societal madness? *Water International,* 30: 136-146.

Falkowski, P., R. J. Scholes, E. Boyle, J. Canadell, D. Canfield, J. Elser, N. Gruber, K. Hibbard, P. Hoegberg, S. Linder, F. T. Mackenzie, B. Moore, III, T. Pedersen, Y. Rosenthal, S. Seitzinger, V. Smetacek and W. Steffen. (2000). The global carbon cycle: A test of our knowledge of Earth as a system. *Science,* 290: 291-296.

Fiddaman, T. S. (1997). *Feedback complexity in integrated climate-economy models.* Doctoral Thesis. Alfred P. Sloan School of Management, Massachusetts Institute of Technology, Boston, Massachusetts, U.S.A.

Fiddaman, T. S. (2002). Exploring policy options with a behavioral climate-economy model. *System Dynamics Review,* 18: 243-267.

Forster, P., V. Ramaswamy, P. Artaxo, T. Berntsen, R. Betts, D. W. Fahey, J. Haywood, J. Lean, D. C. Lowe, G. Myhre, J. Nganga, R. Prinn, G. Raga, M. Schultz and R. Van Dorland. (2007). Changes in Atmospheric Constituents and in Radiative Forcing, in *Climate Change 2007: The Physical Science Basis. Contribution of Working Group I to the Fourth Assessment Report of the Intergovernmental Panel on Climate Change*, edited by S. Solomon, D. Qin, M. Manning, Z. Chen, M. Marquis, K. B. Averyt, M. Tignor and H. L. Miller, pp. 129-234. Cambridge University Press, Cambridge, U.K.

Forster, P. M. d. F. and J. M. Gregory. (2006). The climate sensitivity and its components diagnosed from Earth radiation, *Journal of Climate,* 19: 39-52.

Friedlingstein, P., L. Bopp, P. Ciais, J. L. Dufresne, L. Fairhead, H. LeTreut, P. Monfray and J. Orr. (2001). Positive feedback between future climate change and the carbon cycle, *Geophysical Research Letters,* 28: 1543-1546.

Füssel, H.-M. (2007). Methodological and empirical flaws in the design and application of simple climate-economy models. *Climatic Change,* 81: 161-185.

Geider, R. J., E. H. Delucia, P. G. Falkowski, A. C. Finzi, J. P. Grime, J. Grace, T. M. Kana, J. La Roche, S. P. Long, B. A. Osborne, T. Platt, I. C. Prentice, J. A. Raven, W. H. Schlesinger, V. Smetacek, V. Stuart, S. Satyendranath, R. B. Thomas, T. C. Vogelmann, P. Williams and F. I. Woodward. (2001). Primary productivity of planet Earth: Biological determinants and physical constraints in terrestrial and aquatic habitats. *Global Change Biology,* 7: 849-882.

Gleick, P. H. (2000a). The changing water paradigm: A look at twenty-first century water resources development. *Water International,* 25: 127-138.

Gleick, P. H. (2000b). *The world's water: the biennial report on freshwater resources.* Island Press, Washington, D.C., U.S.A.

Goudriaan, J. and P. Ketner. (1984). A simulation study for the global carbon cycle, including man's impact on the biosphere. *Climatic Change,* 6: 167-192.

Hansen, J., M. Sato, R. Ruedy, K. Lo, D. W. Lea and M. Medina-Elizade. (2006). Global temperature change. *Proceedings of the National Academy of Sciences of the United States of America,* 103: 14288-14293.

Harvey, L. D. D. (2000). Box models of the terrestrial biosphere, in *The Carbon Cycle*, edited by T. M. L. Wigley and D. S. Schimel, pp. 238-247, Cambridge University Press, Cambridge, U.K.

Harvey, L. D. D. and Z. Huang. (2001). A quasi-one-dimensional coupled climate-change carbon-cycle model 1. Description and behaviour of the climate component. *Journal of Geophysical Research,* 106(C10): 22339-22353.

Harvey, L. D. D. and S. H. Schneider. (1985). Transient climate response to external forcing on 10^0-10^4 year time scales. Part I: Experiments with globally averaged, coupled, atmosphere and ocean energy balance models. *Journal of Geophysical Research,* 90(D1): 2191-2205.

Hoekstra, A. Y. (1997). The water submodel: AQUA, in *Perspectives on Global Change: the TARGETS approach*, edited by J. Rotmans and B. J. M. de Vries, pp. 107-134. Cambridge University Press, Cambridge, U.K.

Hoekstra, A. Y., A. H. W. Beusen, H. B. M. Hilderink and M. B. A. van Asselt. (1997). Water in crisis?, in *Perspectives on Global Change: The TARGETS Approach*, edited by J. Rotmans and B. de Vries, pp. 291-317. Cambridge University Press, Cambridge, U.K.

Hoffert, M. I., A. J. Callegari and C. T. Hsieh (1981). A box-diffusion carbon dioxide model with upwelling, polar bottom water formation and a marine biosphere, in *Carbon Cycle Modelling*, edited by B. Bolin, pp. 287-305. John Wiley and Sons, Chichester, U.K.

Houghton, J. T., Y. Ding, D. J. Griggs, M. Noguer, P. J. van der Linden, X. Dai, K. Maskell and C. A. Johnson. (2001). *Climate Change 2001: The Scientific Basis. Contribution of Working Group I to the Third Assessment Report of the Intergovernmental Panel on Climate Change*. Cambridge University Press, Cambridge, U.K.

Huntington, T. G. (2006). Evidence for intensification of the global water cycle: Review and synthesis. *Journal of Hydrology,* 319: 83-95.

International Research Institute for Climate and Society. (2007). *IRI/LDEO Climate Data Library* (on line). IRI Data Library, Columbia University. Last accessed: Nov. 1, 2007. Available from http://iridl.ldeo.columbia.edu.

Joos, F., J. C. Orr, and U. Siegenthaler. (1997). Ocean carbon transport in a box-diffusion versus a general circulation model. *Journal of Geophysical Research*, 102(C6): 12367-12388.

Keeling, C. D. and T. P. Whorf. (2005). Atmospheric CO2 records from sites in the SIO air sampling network, in *Trends: A Compendium of Data on Global Change, Carbon Dioxide Information Analysis Center*, Oak Ridge National Laboratory, U.S. Department of Energy, Oak Ridge, Tennessee, U.S.A.

Keeling, R. F., S. C. Piper and M. Heimann. (1996). Global and hemispheric CO_2 sinks deduced from changes in atmospheric O_2 concentration. *Nature,* 381: 218-221.

Klein Goldewijk, K., J. G. van Minnen, G. J. J. Kreileman, M. Vloedbeld and R. Leemans. (1994). Simulating the carbon flux between the terrestrial environment and the atmosphere. *Water, Air and Soil Pollution,* 76: 199-230.

Lambin, E. F., B. L. Turner, H. J. Geist, S. B. Agbola, A. Angelsen, J. W. Bruce, O. T. Coomes, R. Dirzo, G. Fischer, C. Folke, P. S. George, K. Homewood, J. Imbernon, R. Leemans, X. B. Li, E. F. Moran, M. Mortimore, P. S. Ramakrishnan, J. F. Richards, H. Skanes, W. Steffen, G. D. Stone, U. Svedin, T. A. Veldkamp, C. Vogel and J. C. Xu. (2001). The causes of land-use and land-cover change: moving beyond the myths. *Global Environmental Change,* 11: 261-269.

Lowe, P. R. (1977). An approximating polynomial for the computation of saturation vapour pressure. *Journal of Applied Meteorology,* 16: 100-103.

Maddison, A. (2001). *The World Economy: A Millennial Perspective*. OECD Development Centre Studies, Organisation for Economic Co-operation and Development, Paris, France.

Maddison, A. (2003). *The World Economy: Historical perspective*. Organisation for Economic Co-operation and Development, Paris, France.

Marland, G., T. A. Boden and R. J. Andres. (2007). Global, regional, and national CO2 emissions, in *Trends: A Compendium of Data on Global Change, Carbon Dioxide Information Analysis Center*, U.S. Department of Energy, Oak Ridge, Tennessee, U.S.A.

McGuffie, K. and A. Henderson-Sellers. (2005). *A Climate Modelling Primer, 3rd Edition*. John Wiley and Sons, Ltd., Chichester, U.K.

Meadows, D. H., D. Meadows and J. Randers. (1992). *Beyond the Limits: Confronting Global Collapse, Envisioning a Sustainable Future*. Chelsea Green Publishing Company, Mills, Vermont, U.S.A.

Meadows, D. H., J. Randers and D. Meadows. (2004). *Limits to Growth: The Thirty Year Update*. Chelsea Green Publishing Company, White River Junction, Vermont, U.S.A.

Meehl, G. A., T. F. Stocker, W. D. Collins, P. Friedlingstein, A. T. Gaye, J. M. Gregory, A. Kitoh, R. Knutti, J. M. Murphy, A. Noda, S. C. B. Raper, I. G. Watterson, A. J. Weaver and Z.-C. Zhao. (2007). Global climate projections, in *Climate Change 2007: The Physical Science Basis. Contribution of Working Group I to the Fourth Assessment Report of the Intergovernmental Panel on Climate Change*, edited by S. Solomon, D. Qin, M. Manning, Z. Chen, M. Marquis, K. B. Averyt, M. Tignor and H. L. Miller, pp. 747-846. Cambridge University Press, Cambridge, U.K.

Miller, G. W. (2006). Integrated concepts in water reuse: managing global water needs. *Desalination,* 187: 65-75.

Nakicenovic, N. and R. Swart. (2000). *IPCC Special Report on Emissions Scenarios*. Cambridge University Press, Cambridge, U.K.

National Climatic Data Center (NCDC). (2006). *Climate of 2005 - Annual Report* (on line). National Environmental Satellite, Data, and Information Service, U.S. Department of Commerce, Asheville, North Carolina. Available from http://www.ncdc.noaa.gov/oa/climate/research/2005/ann/global.html#Gtemp. Last Accessed July 10, 2007.

New, M., M. Hulme and P. Jones. (1999). Representing twentieth-century space-time climate variability. Part I: Development of a 1961-90 mean monthly terrestrial climatology. *Journal of Climate,* 12: 829-856.

Nordhaus, W. D. (2006). *RICE and DICE Models of Economics of Climate Change* (on line). Yale University, New Haven, Connecticut, U.S.A. Available from http://www.econ.yale.edu/~nordhaus/homepage/dicemodels.htm. Last Accessed Sept. 8, 2007.

Nordhaus, W. D. and J. Boyer. (1999). *DICE-99 as an Excel Spreadsheet* (on line). Yale University, New Haven, Connecticut, U.S.A. Available from http://www.econ.yale.edu/~nordhaus/homepage/dice99.xls. Last Accessed Aug. 15, 2007.

Nordhaus, W. D. (1992). *The "DICE" Model: Background and Structure of a Dynamic Integrated Climate-Economy Model of the Economics of Global Warming*. Cowles Foundation Discussion Papers 1009, Cowles Foundation, Yale University, New Haven, Connecticut, U.S.A.

Nordhaus, W. D. and J. Boyer. (2000). *Warming the world: Economic models of global warming*. The MIT Press, Cambridge, Massachusetts, U.S.A.

Peters, I., F. Ackerman and S. Bernow. (1999). Economic theory and climate change policy. *Energy Policy,* 27: 501-504.

Postel, S. (1999). *Pillar of Sand: Can the Irrigation Miracle Last?* W. W. Norton, New York, New York, U.S.A.

Rotmans, J. and B. de Vries. (1997). *Perspectives on Global Change: The TARGETS Approach.* Cambridge University Press, Cambridge, U.K.

Rotmans, J., M. B. A. van Asselt, B. J. M. de Vries, A. H. W. Beusen, M. G. J. den Elzen, H. B. M. Hilderink, A. Y. Hoekstra, M. A. Janssen, H. W. Köster, L. W. Niessen and B. J. Strengers. (1997). The TARGETS model, in *Perspectives on Global Change: The TARGETS Approach*, edited by J. Rotmans and B. de Vries, pp. 33-54. Cambridge University Press, Cambridge, U.K.

Scheffer, M., V. Brovkin and P. M. Cox. (2006). Positive feedback between global warming and atmospheric CO2 concentration inferred from past climate change. *Geophysical Research Letters,* 33, L10702, doi:10.1029/2005GL025044.

Shiklomanov, I. A. (2000). Appraisal and assessment of world water resources. *Water International,* 25: 11-32.

Shiklomanov, I. A. and J. Rodda. (2003). *World water resources at the beginning of the 21st century*. Cambridge University Press, Cambridge, U.K.

Shoven, J. B. and J. Whalley. (1984). Applied general equilibrium models of taxation and international trade: An introduction and survey. *Journal of Economic Literature,* 22: 1007-1051.

Shreckengost, R. C. (1985). Dynamic Simulation Models: How Valid Are They?, in *Self-Report Methods of Estimating Drug Use: Meeting Current Challenges to Validity*, edited by B. A. Rouse, N. J. Kozel and L. G. Richards, pp. 1-11. National Institute on Drug Abuse, Rockville, Maryland, U.S.A.

Siegenthaler, U. and F. Joos. (1992). Use of a simple model for studying oceanic tracer distributions and the global carbon cycle. *Tellus*, 44B: 186-207.

Simonovic, S. P. and E. G. R. Davies. (2006). Are we modelling impacts of climatic change properly? *Hydrological Processes,* 20: 431-433.

Simonovic, S. P. (2008). *Water for Our Children: System Methods and Tools for Better Management of Water Resources*. Earthscan, James and James, London, U.K. (*in press*).

Simonovic, S. P. (2002). World water dynamics: Global modeling of water resources, *Journal of Environmental Management,* 66: 249-267.

Smith, T. M. and R. W. Reynolds. (2005). A global merged land-air-sea surface temperature reconstruction based on historical observations (1880-1997), *Journal of Climate,* 18: 2021-2036.

Sterman, J. D. (1984). Appropriate summary statistics for evaluating the historical fit of system dynamics models. *Dynamica,* 10: 51-66.

Sterman, J. D. (2000). *Business dynamics: Systems thinking and modeling for a complex world*. The McGraw-Hill Companies, Ltd., Boston, Massachusetts, U.S.A.

The World Bank Group. (2007). *WDI Online, DDP Quick Query* (on line). World Development Indicators, The World Bank Group, Washington, D.C. Available from http://ddp-ext.worldbank.org/ext/DDPQQ/. Last accessed Apr. 18, 2007.

United Nations Department of Economic and Social Affairs (UNESA). (2006). *World Population Prospects: the 2006 Revision Population Database* (on line), UNESA Population Division, New York, New York, U.S.A. Available from http://esa.un.org/unpp. Last accessed Nov. 1, 2007.

Vassolo, S. and P. Döll. (2005). Global-scale gridded estimates of thermoelectric power and manufacturing water use, *Water Resources Research,* 41, W04010, doi:10.1029/2004WR003360.

Veldkamp, A. and E. F. Lambin. (2001). Predicting land-use change. *Agriculture, Ecosystems and Environment,* 85: 1-6.

Ventana Systems. (2003). *Vensim DSS Software* (on line). Ventana Systems, Inc., Harvard, Massachusetts, U.S.A. Available from http://www.vensim.com. Last accessed Nov. 1, 2007.

Ventana Systems. (2006a). *Vensim Modeling Guide*. Ventana Systems, Inc., Harvard, Massachusetts, U.S.A.

Ventana Systems. (2006b). *Vensim Reference Manual*. Ventana Systems, Inc., Harvard, Massachusetts, U.S.A.

Vinnikov, K. Y., N. C. Grody, A. Robock, R. J. Stouffer, P. D. Jones and M. D. Goldberg. (2006). Temperature trends at the surface and in the troposphere. *Journal of Geophysical Research,* 111, D03106, doi:10.1029/2005JD006392.

Vörösmarty, C. J. (2002). Global water assessment and potential contributions from Earth Systems Science. *Aquatic Sciences,* 64: 328-351.

Vörösmarty, C. J., P. Green, J. Salisbury and R. B. Lammers. (2000). Global water resources: Vulnerability from climate change and population growth. *Science,* 289: 284-288.

Watson, R. T., I. R. Noble, B. Bolin, N. H. Ravindranath, D. J. Verardo and D. J. Dokken. (2000). *Land Use, Land Use Change, and Forestry*. Cambridge University Press, Cambridge, U.K.

World Health Organization (WHO) and United Nations Children's Fund (UNICEF). (2005). *Sanitation Data at Global Level* (on line), Joint Monitoring Programme, Geneva, Switzerland and New York, New York, U.S.A. Available from http://www.wssinfo.org/en/32_san_global.html. Last accessed Nov. 1, 2007.

APPENDIX A: MODEL CODE FOR VENSIM DSS

This appendix provides all equations, parameter settings, and units in alphabetical order for the Vensim model described in this report. The equations below were generated by the Vensim documenting tool, and are not commented – comments are, however, provided on the CD-ROM version of the model, which is described in Appendix B and is available from the authors. For details on the Vensim modelling language, refer to Ventana Systems (2006a).

Following the notation in Vensim, model sector headings are boxed by asterisks. Furthermore, illustrations of the layout of each sector are provided at the top of each equation listing, along with pertinent notes. Equations have the following format:

```
Variable=
          Equation
    Units:
```

The organization in this appendix is as follows, by model sector and starting page:

Note that the carbon cycle, climate, and economic sectors actually consist of two separate parts in the *simulation model* (included on the CD-ROM described above):

      1. The variable, controllable part; and,

      2. The 'business-as-usual' part.

This two-part approach is based on the DICE model (Nordhaus and Boyer, 2000). The controllable part of each sector allows a user to implement different carbon tax policies in the economic sector and to view their outcomes in terms of abatement costs and environmental benefits. The 'business-as-usual' part serves as the basis for comparison, since the abatement costs and environmental benefits are based on the differences in economic performance between the 'business-as-usual', or 'base case', and the modified case of part 1. In terms of the code below, then, all equations for the carbon tax policy case (part 1) have normal names, while all 'business-as-usual' equations (part 2) have 'Base', or 'Baseline' in front of their names. Parameters are shared between the two parts, and so are not duplicated in Parts 1 and 2.

****

.Carbon

****

The equations for the model's carbon cycle sector follow a set of figures that illustrate the model layout in Vensim. The six figures below focus on,

- The variable, controllable 'Part 1':
    - Stocks, Flows, and Feedbacks (Figure A-1);
    - Parameter Layout and Intermediate Calculations (Figure A-2); and,
    - Land-use, Land-use Change, and Important Output (Figure A-3).
- The business-as-usual 'Part 2':
    - Stocks, Flows, and Feedbacks (Figure A-4);
    - Parameter Layout and Intermediate Calculations (Figure A-5); and,
    - Land-use, Land-use Change, and Important Output (Figure A-6).
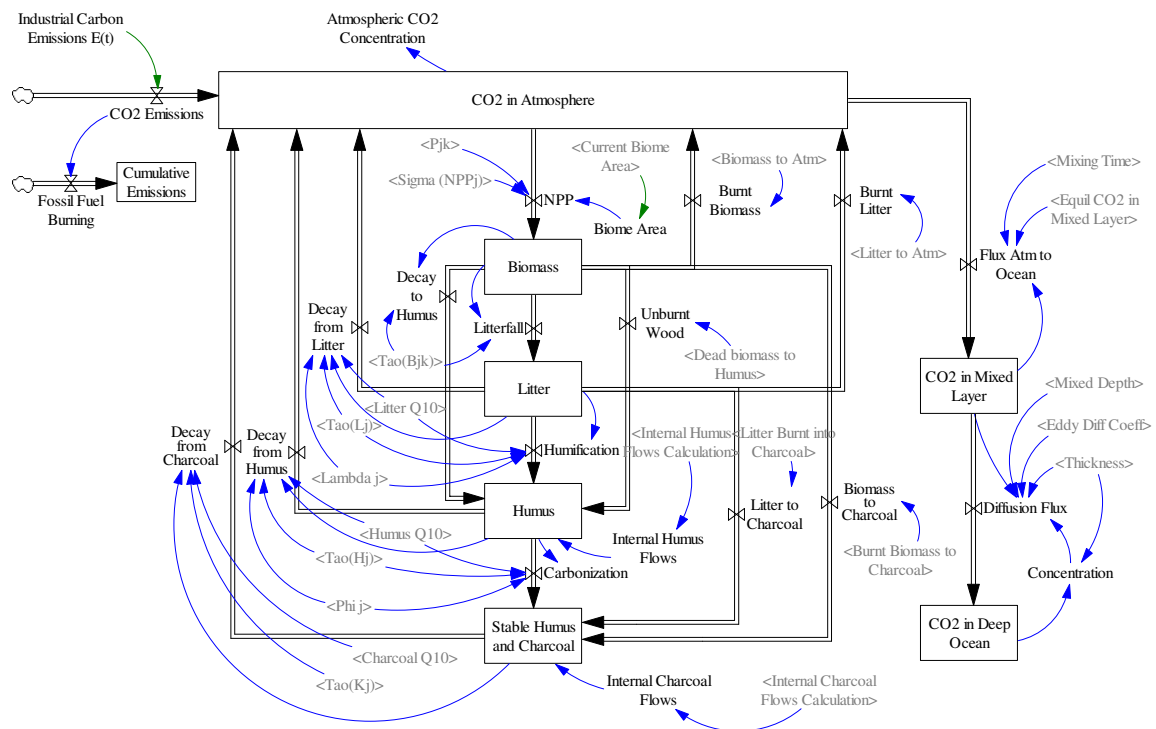
Figure A-1: Stocks, Flows, and Feedbacks in the Global Carbon Cycle – View of 'Part 1'
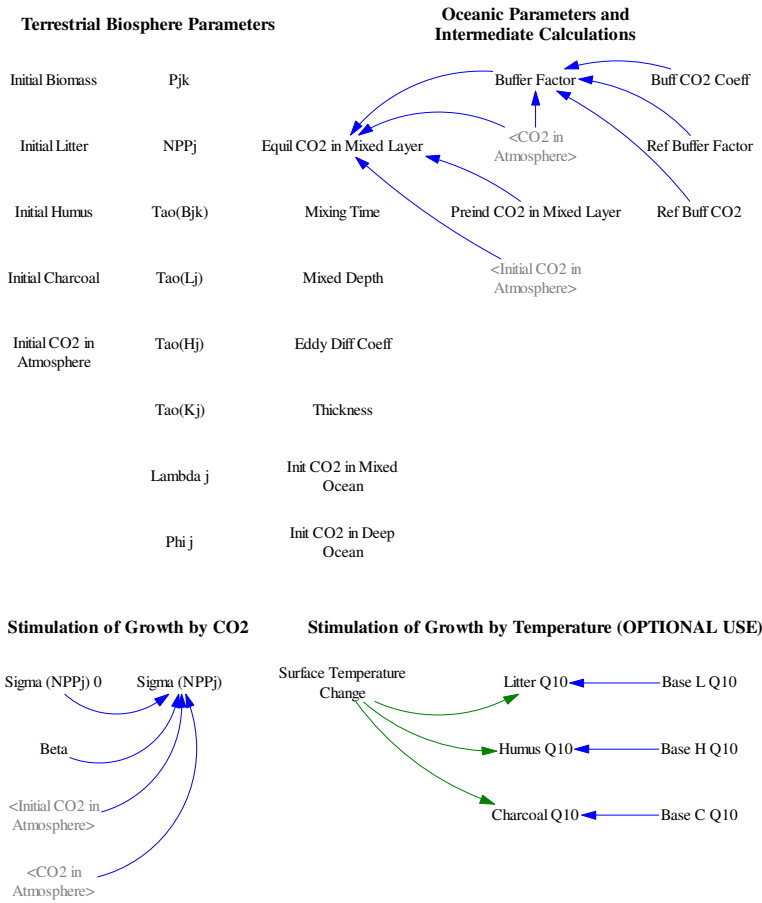
Figure A-2: Parameter Layout and Some Intermediate Variable Calculations from Carbon Cycle – View of 'Part 1'
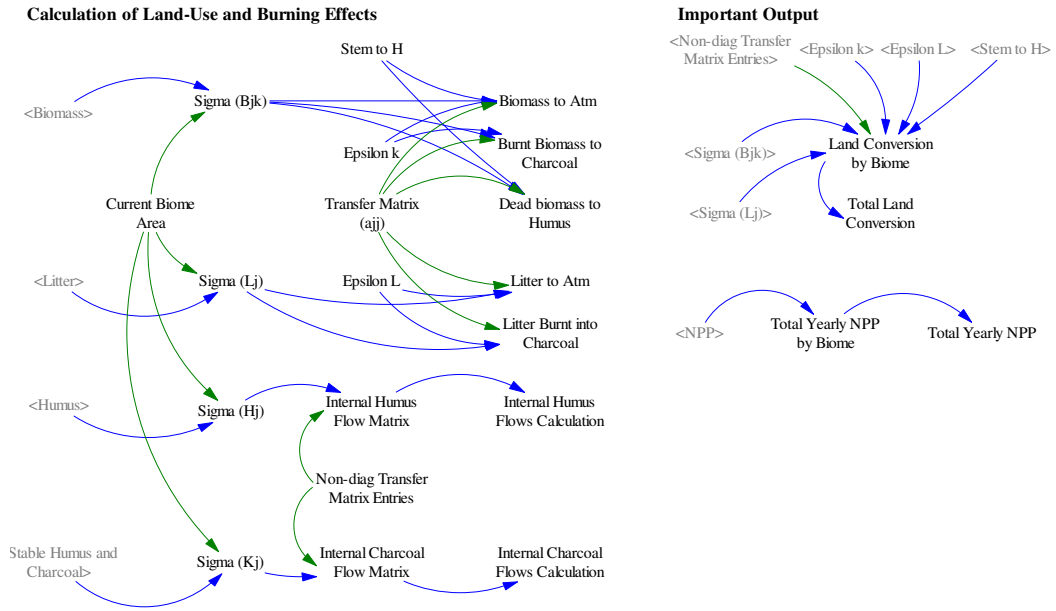
Figure A-3: Intermediate Calculations based on Land-use Change and Important Output – View of 'Part 1'
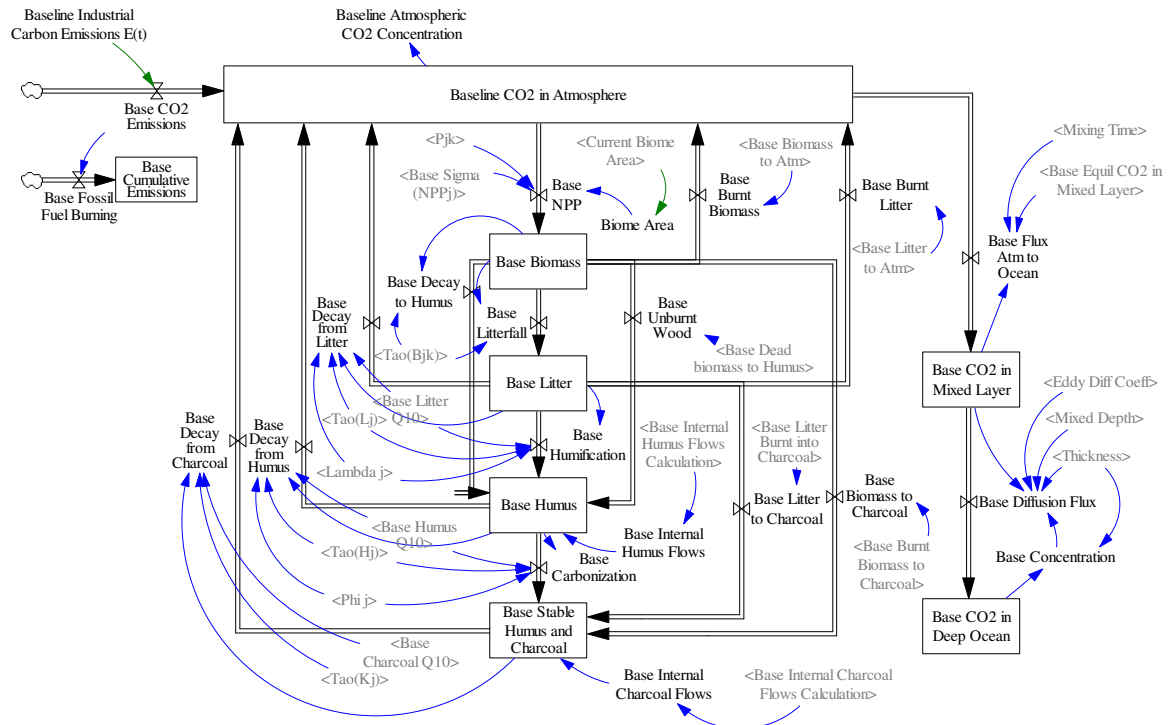
Figure A-4: Stocks, Flows, and Feedbacks in the Global Carbon Cycle – View of 'Part 2'

Oceanic Parameters and Intermediate Calculations

Stimulation of Growth by CO2

Stimulation of Growth by Temperature (OPTIONAL USE)
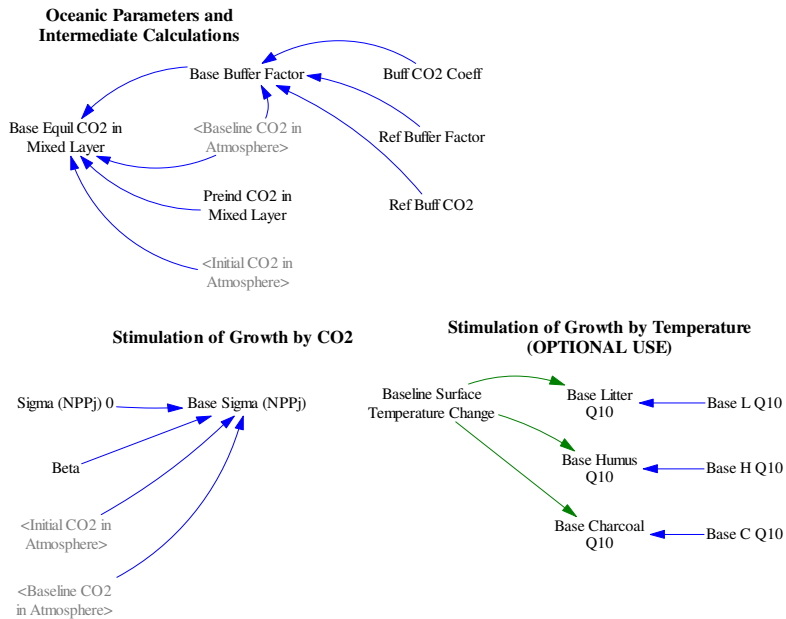
Figure A-5: Parameter Layout and Some Intermediate Variable Calculations from Carbon Cycle – View of 'Part 2'

Calculation of Land-Use and Burning Effects
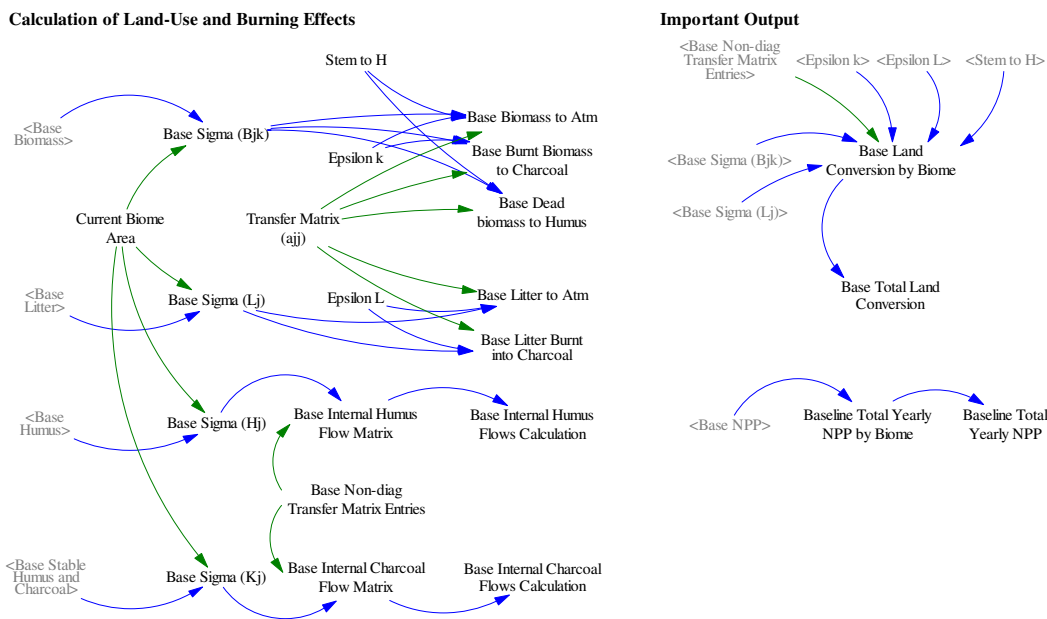
Important Output

Figure A-6: Intermediate Calculations based on Land-use Change and Important Output – View of 'Part 2'

```
Atmospheric CO2 Concentration=
          0.4754 * CO2 in Atmosphere
      Units: ppmv
```

```
Base Biomass[j,k]= INTEG (
            +Base NPP[j,k] – Base Decay to Humus[j,k] – Base
            Litterfall[j,k] – Base Biomass to Charcoal[j,k] – Base
            Burnt Biomass[j,k] – Base Unburnt Wood[j,k],
            Initial Biomass[j,k])
      Units: Gt C

Base Biomass to Atm[j,k1]=
            (1 – Epsilon k[k1]) * "Base Sigma (Bjk)"[j,k1] *
            SUM("Transfer Matrix (ajj)"[j,q!]) * 1e-005
Base Biomass to Atm[j,k2]=
            (1 – Epsilon k[k2]) * "Base Sigma (Bjk)"[j,k2] *
            SUM("Transfer Matrix (ajj)"[j,q!]) * 1e-005
Base Biomass to Atm[j,k3]=
            (1 – Epsilon k[k3] – Stem to H) * "Base Sigma (Bjk)"[j,k3]
            * SUM("Transfer Matrix (ajj)"[j,q!]) * 1e-005
Base Biomass to Atm[j,k4]=
            0
      Units: Gt C/Year

Base Biomass to Charcoal[j,k]=
            Base Burnt Biomass to Charcoal[j,k]
      Units: Gt C/Year

Base Buffer Factor=
            Ref Buffer Factor + Buff CO2 Coeff*LN(Baseline CO2 in
            Atmosphere/Ref Buff CO2)
      Units: Dimensionless

Base Burnt Biomass[j,k]=
            Base Biomass to Atm[j,k]
      Units: Gt C/Year

Base Burnt Biomass to Charcoal[j,k1]=
            Epsilon k[k1] * "Base Sigma (Bjk)"[j,k1] * SUM("Transfer
            Matrix (ajj)"[j,q!]) * 1e-005
Base Burnt Biomass to Charcoal[j,k2]=
            Epsilon k[k2] * "Base Sigma (Bjk)"[j,k2] * SUM("Transfer
            Matrix (ajj)"[j,q!]) * 1e-005
Base Burnt Biomass to Charcoal[j,k3]=
            Epsilon k[k3] * "Base Sigma (Bjk)"[j,k3] * SUM("Transfer
            Matrix (ajj)"[j,q!]) * 1e-005
Base Burnt Biomass to Charcoal[j,k4]=
            0
      Units: Gt C/Year

Base Burnt Litter[j]=
            Base Litter to Atm[j]
      Units: Gt C/Year

Base C Q10=
            1.1
      Units: Dimensionless

Base Carbonization[j]=
            Base Humus Q10 * Phi j[j] * Base Humus[j] / "Tao(Hj)"[j]
      Units: Gt C/Year
```

```
Base Charcoal Q10=
            Base C Q10^(Baseline Surface Temperature Change/10)
      Units: Dimensionless


Base CO2 Emissions=
            "Baseline Industrial Carbon Emissions E(t)"
      Units: Gt C/Year


Base CO2 in Deep Ocean[upper]= INTEG (
            Base Diffusion Flux[upper]-Base Diffusion Flux[lower],
            Init CO2 in Deep Ocean[upper])
Base CO2 in Deep Ocean[layer10]= INTEG (
            Base Diffusion Flux[layer10],
            Init CO2 in Deep Ocean[layer10])
      Units: Gt C


Base CO2 in Mixed Layer= INTEG (
            Base Flux Atm to Ocean-Base Diffusion Flux[layer1],
            Init CO2 in Mixed Ocean)
      Units: Gt C


Base Concentration[layers]=
            Base CO2 in Deep Ocean[layers]/Thickness[layers]
      Units: Gt C/Meter


Base Cumulative Emissions= INTEG (
            Base Fossil Fuel Burning, 0)
      Units: Gt C


Base Dead biomass to Humus[j,k1]=
            0
Base Dead biomass to Humus[j,k2]=
            0
Base Dead biomass to Humus[j,k3]=
            Stem to H*"Base Sigma (Bjk)"[j,k3] * SUM("Transfer Matrix
            (ajj)"[j,q!]) * 1e-005
Base Dead biomass to Humus[j,k4]=
            "Base Sigma (Bjk)"[j,k4] * SUM("Transfer Matrix
            (ajj)"[j,q!]) * 1e-005
      Units: Gt C/Year


Base Decay from Charcoal[j]=
            Base Charcoal Q10 * Base Stable Humus and Charcoal[j] /
            "Tao(Kj)"[j]
      Units: Gt C/Year


Base Decay from Humus[j]=
            Base Humus Q10 * (1 - Phi j[j]) * Base Humus[j] /
            "Tao(Hj)"[j]
      Units: Gt C/Year


Base Decay from Litter[j]=
            Base Litter Q10 * (1 - Lambda j[j]) * Base Litter[j] /
            "Tao(Lj)"[j]
      Units: Gt C/Year
```

```
Base Decay to Humus[j,kAboveGrnd]=
            0
Base Decay to Humus[j,k4]=
            Base Biomass[j,k4] / "Tao(Bjk)"[j,k4]
        Units: Gt C/Year


Base Diffusion Flux[layer1]=
            (Base CO2 in Mixed Layer/Mixed Depth-Base Concentration
            [layer1])*Eddy Diff Coeff*2/(Mixed Depth+Thickness[layer1])
Base Diffusion Flux[lower]=
            (Base Concentration[upper]-Base Concentration[lower])*Eddy
            Diff Coeff *2/(Thickness[upper]+Thickness[lower])
        Units: Gt C/Year


Base Equil CO2 in Mixed Layer=
            Preind CO2 in Mixed Layer * (Baseline CO2 in
            Atmosphere/Initial CO2 in Atmosphere)^(1/Base Buffer
            Factor)
        Units: Gt C


Base Flux Atm to Ocean=
            (Base Equil CO2 in Mixed Layer-Base CO2 in Mixed
            Layer)/Mixing Time
        Units: Gt C/Year


Base Fossil Fuel Burning=
            Base CO2 Emissions
        Units: Gt C/Year


Base H Q10=
            1.35
        Units: Dimensionless


Base Humification[j]=
            Base Litter Q10 * Lambda j[j] * Base Litter[j] /
            "Tao(Lj)"[j]
        Units: Gt C/Year


Base Humus[j]= INTEG (
            SUM(Base Decay to Humus[j,k!]) + Base Humification[j] -
            Base Carbonization[j] - Base Decay from Humus[j] + SUM(Base
            Unburnt Wood[j,k!]) + Base Internal Humus Flows[j],
            Initial Humus[j])
        Units: Gt C


Base Humus Q10=
            Base H Q10^(Baseline Surface Temperature Change/10)
        Units: Dimensionless


Base Internal Charcoal Flow Matrix[j,q]=
            "Base Sigma (Kj)"[j] * "Base Non-diag Transfer Matrix
            Entries"[j,q] * 1e-005
        Units: Gt C/Year


Base Internal Charcoal Flows[j]=
            Base Internal Charcoal Flows Calculation[j]
        Units: Gt C/Year
```

```
Base Internal Charcoal Flows Calculation[j]=
            -SUM(Base Internal Charcoal Flow Matrix[j,q!]) + SUM(Base
            Internal Charcoal Flow Matrix[j!,q])
        Units: Gt C/Year

Base Internal Humus Flow Matrix[j,q]=
            "Base Sigma (Hj)"[j] * "Base Non-diag Transfer Matrix
            Entries"[j,q] * 1e-005
        Units: Gt C/Year

Base Internal Humus Flows[j]=
            Base Internal Humus Flows Calculation[j]
        Units: Gt C/Year

Base Internal Humus Flows Calculation[j]=
            -SUM(Base Internal Humus Flow Matrix[j,q!]) + SUM(Base
            Internal Humus Flow Matrix[j!,q])
        Units: Gt C/Year

Base L Q10=
            2.2
        Units: Dimensionless

Base Litter[j]= INTEG (
            SUM(Base Litterfall[j,k!]) - Base Decay from Litter[j] -
            Base Humification[j] - Base Burnt Litter[j] - Base Litter
            to Charcoal[j], Initial Litter[j])
        Units: Gt C

Base Litter Burnt into Charcoal[j]=
            Epsilon L * "Base Sigma (Lj)"[j] * SUM("Transfer Matrix
            (ajj)"[j,q!]) * 1e-005
        Units: Gt C/Year

Base Litter Q10=
            Base L Q10^(Baseline Surface Temperature Change/10)
        Units: Dimensionless

Base Litter to Atm[j]=
            (1 - Epsilon L) * "Base Sigma (Lj)"[j] * SUM("Transfer
            Matrix (ajj)"[j,q!]) * 1e-005
        Units: Gt C/Year

Base Litter to Charcoal[j]=
            Base Litter Burnt into Charcoal[j]
        Units: Gt C/Year

Base Litterfall[j,kAboveGrnd]=
            Base Biomass[j,kAboveGrnd] / "Tao(Bjk)"[j,kAboveGrnd]
Base Litterfall[j,k4]=
            0
        Units: Gt C/Year

Base NPP[j,k]=
            (Pjk[j,k]*"Base Sigma (NPPj)"[j] * (Biome Area[j])) /
            1e+015
```

```
      Units: Gt C/Year


"Base Sigma (Bjk)"[j,k]=
          IF THEN ELSE(Base Biomass[j,k] > 0 :AND: Current Biome
          Area[j] > 0, Base Biomass[j,k] / Current Biome Area[j] *
          100000, 0)
      Units: g C/(Year*Meter*Meter)


"Base Sigma (Hj)"[j]=
          IF THEN ELSE(Base Humus[j] > 0 :AND: Current Biome Area[j]
          > 0, Base Humus[j] / Current Biome Area[j] * 100000, 0)
      Units: g C/(Year*Meter*Meter)


"Base Sigma (Kj)"[j]=
          IF THEN ELSE(Base Stable Humus and Charcoal[j] > 0 :AND:
          Current Biome Area[j] > 0, Base Stable Humus and
          Charcoal[j] / Current Biome Area[j] * 100000, 0)
      Units: g C/(Year*Meter*Meter)


"Base Sigma (Lj)"[j]=
          IF THEN ELSE(Base Litter[j] > 0 :AND: Current Biome Area[j]
          > 0, Base Litter[j] / Current Biome Area[j] * 100000, 0)
      Units: g C/(Year*Meter*Meter)


"Base Sigma (NPPj)"[j]=
          "Sigma (NPPj) 0"[j] * (1 + Beta * LN(Baseline CO2 in
          Atmosphere/Initial CO2 in Atmosphere))
      Units: g C/(Meter*Meter*Year)


Base Stable Humus and Charcoal[j]= INTEG (
          Base Carbonization[j] – Base Decay from Charcoal[j] +
          SUM(Base Biomass to Charcoal[j,k!]) + Base Litter to
          Charcoal[j] + Base Internal Charcoal Flows[j],
          Initial Charcoal[j])
      Units: Gt C


Base Unburnt Wood[j,k]=
          Base Dead biomass to Humus[j,k]
      Units: Gt C/Year


Baseline Atmospheric CO2 Concentration=
          0.4754 * Baseline CO2 in Atmosphere
      Units: ppmv


Baseline CO2 in Atmosphere= INTEG (
          SUM(Base Decay from Charcoal[j!]) + SUM(Base Decay from
          Humus[j!]) + SUM(Base Decay from Litter[j!]) – SUM(Base
          NPP[j!,k!]) + SUM(Base Burnt Biomass[j!,k!]) + SUM(Base
          Burnt Litter[j!]) + Base CO2 Emissions – Base Flux Atm to
          Ocean, Initial CO2 in Atmosphere)
      Units: Gt C


Beta=
          0.5
      Units: Dimensionless


Biomass[j,k]= INTEG (
```

```
                  +NPP[j,k] - Decay to Humus[j,k] - Litterfall[j,k] - Biomass
                  to Charcoal[j,k] - Burnt Biomass[j,k] - Unburnt Wood[j,k],
                  Initial Biomass[j,k])
          Units: Gt C


Biomass to Atm[j,k1]=
                  (1 - Epsilon k[k1]) * "Sigma (Bjk)"[j,k1] * SUM("Transfer
                  Matrix (ajj)"[j,q!]) * 1e-005
Biomass to Atm[j,k2]=
                  (1 - Epsilon k[k2]) * "Sigma (Bjk)"[j,k2] * SUM("Transfer
                  Matrix (ajj)"[j,q!]) * 1e-005
Biomass to Atm[j,k3]=
                  (1 - Epsilon k[k3] - Stem to H) * "Sigma (Bjk)"[j,k3] *
                  SUM("Transfer Matrix (ajj)"[j,q!]) * 1e-005
Biomass to Atm[j,k4]=
                  0
          Units: Gt C/Year


Biomass to Charcoal[j,k]=
                  Burnt Biomass to Charcoal[j,k]
          Units: Gt C/Year


bottom5 : (layer6-layer10)


Buff CO2 Coeff =
                  4.05
          Units: Dimensionless


Buffer Factor=
                  Ref Buffer Factor + Buff CO2 Coeff*LN(CO2 in Atmosphere/Ref
                  Buff CO2)
          Units: Dimensionless


Burnt Biomass[j,k]=
                  Biomass to Atm[j,k]
          Units: Gt C/Year


Burnt Biomass to Charcoal[j,k1]=
                  Epsilon k[k1] * "Sigma (Bjk)"[j,k1] * SUM("Transfer Matrix
                  (ajj)"[j,q!]) * 1e-005
Burnt Biomass to Charcoal[j,k2]=
                  Epsilon k[k2] * "Sigma (Bjk)"[j,k2] * SUM("Transfer Matrix
                  (ajj)"[j,q!]) * 1e-005
Burnt Biomass to Charcoal[j,k3]=
                  Epsilon k[k3] * "Sigma (Bjk)"[j,k3] * SUM("Transfer Matrix
                  (ajj)"[j,q!]) * 1e-005
Burnt Biomass to Charcoal[j,k4]=
                  0
          Units: Gt C/Year


Burnt Litter[j]=
                  Litter to Atm[j]
          Units: Gt C/Year


Carbonization[j]=
                  Humus Q10 * Phi j[j] * Humus[j] / "Tao(Hj)"[j]
          Units: Gt C/Year
```

```
Charcoal Q10=
            Base C Q10^(Surface Temperature Change/10)
      Units: Dimensionless


CO2 Emissions=
            "Industrial Carbon Emissions E(t)"
      Units: Gt C/Year


CO2 in Atmosphere= INTEG (
            SUM(Decay from Charcoal[j!]) + SUM(Decay from Humus[j!]) +
            SUM(Decay from Litter[j!]) - SUM(NPP[j!,k!]) + SUM(Burnt
            Biomass[j!,k!]) + SUM(Burnt Litter[j!]) + CO2 Emissions -
            Flux Atm to Ocean, Initial CO2 in Atmosphere)
      Units: Gt C


CO2 in Deep Ocean[upper]= INTEG (
            Diffusion Flux[upper]-Diffusion Flux[lower],
            Init CO2 in Deep Ocean[upper])
CO2 in Deep Ocean[layer10]= INTEG (
            Diffusion Flux[layer10],
            Init CO2 in Deep Ocean[layer10])
      Units: Gt C


CO2 in Mixed Layer= INTEG (
            Flux Atm to Ocean-Diffusion Flux[layer1],
            Init CO2 in Mixed Ocean)
      Units: Gt C


Concentration[layers] =
            CO2 in Deep Ocean[layers]/Thickness[layers]
      Units: Gt C/Meter


Cumulative Emissions= INTEG (
            Fossil Fuel Burning, 0)
      Units: Gt C


Dead biomass to Humus[j,k1]=
            0
Dead biomass to Humus[j,k2]=
            0
Dead biomass to Humus[j,k3]=
            Stem to H*"Sigma (Bjk)"[j,k3] * SUM("Transfer Matrix
            (ajj)"[j,q!]) * 1e-005
Dead biomass to Humus[j,k4]=
            "Sigma (Bjk)"[j,k4] * SUM("Transfer Matrix (ajj)"[j,q!]) *
            1e-005
      Units: Gt C/Year


Decay from Charcoal[j]=
            Charcoal Q10 * Stable Humus and Charcoal[j] / "Tao(Kj)"[j]
      Units: Gt C/Year


Decay from Humus[j]=
            Humus Q10 * (1 - Phi j[j]) * Humus[j] / "Tao(Hj)"[j]
      Units: Gt C/Year
```

```
Decay from Litter[j]=
          Litter Q10 * (1 - Lambda j[j]) * Litter[j] / "Tao(Lj)"[j]
     Units: Gt C/Year


Decay to Humus[j,kAboveGrnd]=
          0
Decay to Humus[j,k4]=
          Biomass[j,k4] / "Tao(Bjk)"[j,k4]
     Units: Gt C/Year


Diffusion Flux[layer1]=
          (CO2 in Mixed Layer/Mixed Depth-Concentration[layer1])*Eddy
          Diff Coeff*2/(Mixed Depth+Thickness[layer1])
Diffusion Flux[lower] =
          (Concentration[upper]-Concentration[lower])*Eddy Diff
          Coeff*2/(Thickness[upper]+Thickness[lower])
     Units: Gt C/Year


Eddy Diff Coeff =
          4000
     Units: Meter*Meter/Year


Epsilon k[k]=
          0.05, 0.1, 0.2, 0
     Units: Dimensionless


Epsilon L=
          0.1
     Units: Dimensionless


Equil CO2 in Mixed Layer=
          Preind CO2 in Mixed Layer * (CO2 in Atmosphere/Initial CO2
          in Atmosphere)^(1/Buffer Factor)
     Units: Gt C


Flux Atm to Ocean=
          (Equil CO2 in Mixed Layer-CO2 in Mixed Layer)/Mixing Time
     Units: Gt C/Year


Fossil Fuel Burning=
          CO2 Emissions
     Units: Gt C/Year


Humification[j]=
          Litter Q10 * Lambda j[j] * Litter[j] / "Tao(Lj)"[j]
     Units: Gt C/Year


Humus[j]= INTEG (
          SUM(Decay to Humus[j,k!]) + Humification[j] -
          Carbonization[j] - Decay from Humus[j] + SUM(Unburnt
          Wood[j,k!]) + Internal Humus Flows[j], Initial Humus[j])
     Units: Gt C


Humus Q10=
          Base H Q10^(Surface Temperature Change/10)
     Units: Dimensionless
```

```
Init CO2 in Deep Ocean[layers]=
        2054,2051,2050,2049,2048,5734,5733,5733,5733,5733
    Units: Gt C


Init CO2 in Mixed Ocean=
        767.8
    Units: Gt C


Initial Biomass[j,k]=
        8.34,55.6,250.2,55.6; 5.2,17.3,156.1,17.3; 6.43,0,0,4.29;
        5.98,0,0,1.5; 0.06,0.4,3,0.4; 1.04,2.08,10.4,1.25;
    Units: Gt C


Initial Charcoal[j]=
        277.97, 130.05, 160.74, 37.41, 5, 31.5
    Units: Gt C


Initial CO2 in Atmosphere=
        650
    Units: Gt C


Initial Humus[j]=
        111.19, 260.1, 257.18, 37.41, 5, 63
    Units: Gt C


Initial Litter[j]=
        22.23, 13.87, 12.86, 5.99, 0.32, 2.94
    Units: Gt C


Internal Charcoal Flow Matrix[j,q]=
        "Sigma (Kj)"[j] * "Non-diag Transfer Matrix Entries"[j,q] *
        1e-005
    Units: Gt C/Year


Internal Charcoal Flows[j]=
        Internal Charcoal Flows Calculation[j]
    Units: Gt C/Year


Internal Charcoal Flows Calculation[j]=
        -SUM(Internal Charcoal Flow Matrix[j,q!]) + SUM(Internal
        Charcoal Flow Matrix[j!,q])
    Units: Gt C/Year


Internal Humus Flow Matrix[j,q]=
        "Sigma (Hj)"[j] * "Non-diag Transfer Matrix Entries"[j,q] *
        1e-005
    Units: Gt C/Year


Internal Humus Flows[j]=
        Internal Humus Flows Calculation[j]
    Units: Gt C/Year


Internal Humus Flows Calculation[j]=
        -SUM(Internal Humus Flow Matrix[j,q!]) + SUM(Internal Humus
        Flow Matrix[j!,q])
    Units: Gt C/Year
```

```
j: (j1-j6) -> q

k: (k1-k4)

kAboveGrnd: (k1-k3)

Lambda j[j]=
          0.4, 0.6, 0.6, 0.2, 0.5, 0.6
     Units: Dimensionless

layers : (layer1-layer10)

Litter[j]= INTEG (
          SUM(Litterfall[j,k!]) - Decay from Litter[j] -
          Humification[j] - Burnt Litter[j] - Litter to Charcoal[j],
          Initial Litter[j])
     Units: Gt C

Litter Burnt into Charcoal[j]=
          Epsilon L * "Sigma (Lj)"[j] * SUM("Transfer Matrix
          (ajj)"[j,q!]) * 1e-005
     Units: Gt C/Year

Litter Q10=
          Base L Q10^(Surface Temperature Change/10)
     Units: Dimensionless

Litter to Atm[j]=
          (1 - Epsilon L) * "Sigma (Lj)"[j] * SUM("Transfer Matrix
          (ajj)"[j,q!]) * 1e-005
     Units: Gt C/Year

Litter to Charcoal[j]=
          Litter Burnt into Charcoal[j]
     Units: Gt C/Year

Litterfall[j,kAboveGrnd]=
          Biomass[j,kAboveGrnd] / "Tao(Bjk)"[j,kAboveGrnd]
Litterfall[j,k4]=
          0
     Units: Gt C/Year

lower : (layer2-layer10) -> upper

Mixed Depth =
          75
     Units: Meter

Mixing Time=
          1.5
     Units: Year

NPP[j,k]=
          (Pjk[j,k]*"Sigma (NPPj)"[j] * (Biome Area[j])) / 1e+015
     Units: Gt C/Year

NPPj[j]=
```

```
            27.8,8.7,10.7,7.5,0.2,2.1
        Units: Gt C/Year


Phi j[j]=
            0.05, 0.05, 0.05, 0.05, 0.05, 0.05
        Units: Dimensionless


Pjk[j,k]=
            0.3,0.2,0.3,0.2; 0.3,0.2,0.3,0.2; 0.6,0,0,0.4; 0.8,0,0,0.2;
            0.3,0.2,0.3,0.2; 0.5,0.1,0.1,0.3;
        Units: Dimensionless


Preind CO2 in Mixed Layer=
            767.8
        Units: Gt C


Ref Buff CO2=
            760
        Units: Gt C


Ref Buffer Factor =
            10
        Units: Dimensionless


"Sigma (Bjk)"[j,k]=
            IF THEN ELSE(Biomass[j,k] > 0 :AND: Current Biome Area[j] >
            0, Biomass[j,k] / Current Biome Area[j] * 100000, 0)
        Units: g C/(Year*Meter*Meter)


"Sigma (Hj)"[j]=
            IF THEN ELSE(Humus[j] > 0 :AND: Current Biome Area[j] > 0,
            Humus[j] / Current Biome Area[j] * 100000, 0)
        Units: g C/(Year*Meter*Meter)


"Sigma (Kj)"[j]=
            IF THEN ELSE(Stable Humus and Charcoal[j] > 0 :AND: Current
            Biome Area[j] > 0, Stable Humus and Charcoal[j] / Current
            Biome Area[j] * 100000, 0)
        Units: g C/(Year*Meter*Meter)


"Sigma (Lj)"[j]=
            IF THEN ELSE(Litter[j] > 0 :AND: Current Biome Area[j] > 0,
            Litter[j] / Current Biome Area[j] * 100000, 0)
        Units: g C/(Year*Meter*Meter)


"Sigma (NPPj)"[j]=
            "Sigma (NPPj) 0"[j] * (1 + Beta * LN(CO2 in
            Atmosphere/Initial CO2 in Atmosphere) )
        Units: g C/(Meter*Meter*Year)


"Sigma (NPPj) 0"[j]=
            770, 510, 570, 430, 100, 70
        Units: g C/(Meter*Meter*Year)


Stable Humus and Charcoal[j]= INTEG (
```

```
          Carbonization[j] - Decay from Charcoal[j] + SUM(Biomass to
          Charcoal[j,k!]) + Litter to Charcoal[j] + Internal Charcoal
          Flows[j], Initial Charcoal[j])
     Units: Gt C

Stem to H=
          0.5
     Units: Dimensionless

"Tao(Bjk)"[j,k]=
          1,10,30,10; 2,10,60,10; 1,10,50,1; 1,10,50,1; 1,10,50,10;
          1,10,50,2;
     Units: Year

"Tao(Hj)"[j]=
          10,50,40,25,50,50
     Units: Year

"Tao(Kj)"[j]=
          500,500,500,500,500,500
     Units: Year

"Tao(Lj)"[j]=
          1,2,2,1,2,2
     Units: Year

Thickness[top5] =
          200
Thickness[bottom5] =
          560
     Units: Meter

top5 : (layer1-layer5)

Total Yearly NPP=
          SUM(Total Yearly NPP by Biome[j!])
     Units: Gt C/Year

Total Yearly NPP by Biome[j]=
          SUM(NPP[j,k!])
     Units: Gt C/Year

Unburnt Wood[j,k]=
          Dead biomass to Humus[j,k]
     Units: Gt C/Year

upper : (layer1-layer9) -> lower
```

```
*******************************
    .Climate
*******************************
```

The equations for the model's climate sector follow a set of figures that illustrate the model layout in Vensim. The four figures below focus on,

- The variable, controllable 'Part 1':
    - Stocks, Flows, and Feedbacks (Figure A-7); and,
    - Parameter Layout, Intermediate Calculations and Output (Figure A-8).
- The business-as-usual 'Part 2':
    - Stocks, Flows, and Feedbacks (Figure A-9); and,
    - Intermediate Calculations and Output (Figure A-10).
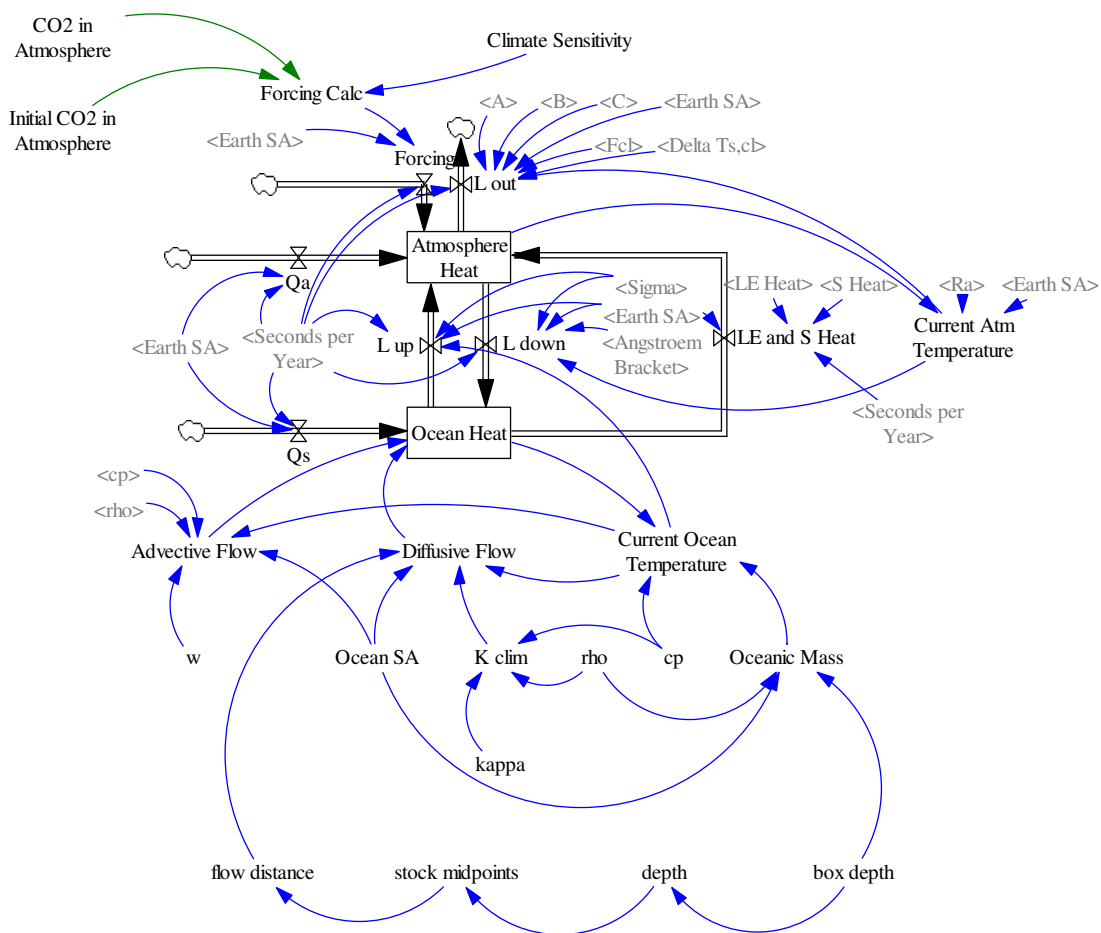
Figure A-7: Stocks, Flows, and Feedbacks in Global Climate System – View of 'Part 1'

Atmospheric Sector Constants

Sigma   Ra   Earth SA   Seconds per Year

A   B   Fcl   Delta Ts,cl

C1   C2   C

Initial T Celsius   Initial Temperature

Initial Atm
Temperature

Temperature Output

<Initial
Temperature>   Surface Temperature
Change

<Current Ocean
Temperature>   Current Ocean T
Celsius

<Current Atm
Temperature>   Current Atm T
Celsius

Intermediate Calculations

<Current Atm
Temperature>   ea Lookup   ea   ea Multiplier   <C2>

Rel Humidity   Angstroem
Bracket   LE Heat

<Current Ocean
Temperature>   es Lookup   es   es Multiplier

<Current Ocean
Temperature>   <Current Atm
Temperature>

<C1>   S Heat

Figure A-8: Parameter Layout, Intermediate Calculations, and Output Variables from Climate System – View of 'Part 1'

Figure A-9: Stocks, Flows, and Feedbacks in Global Climate System – View of 'Part 2'

Intermediate Calculations

Temperature Output
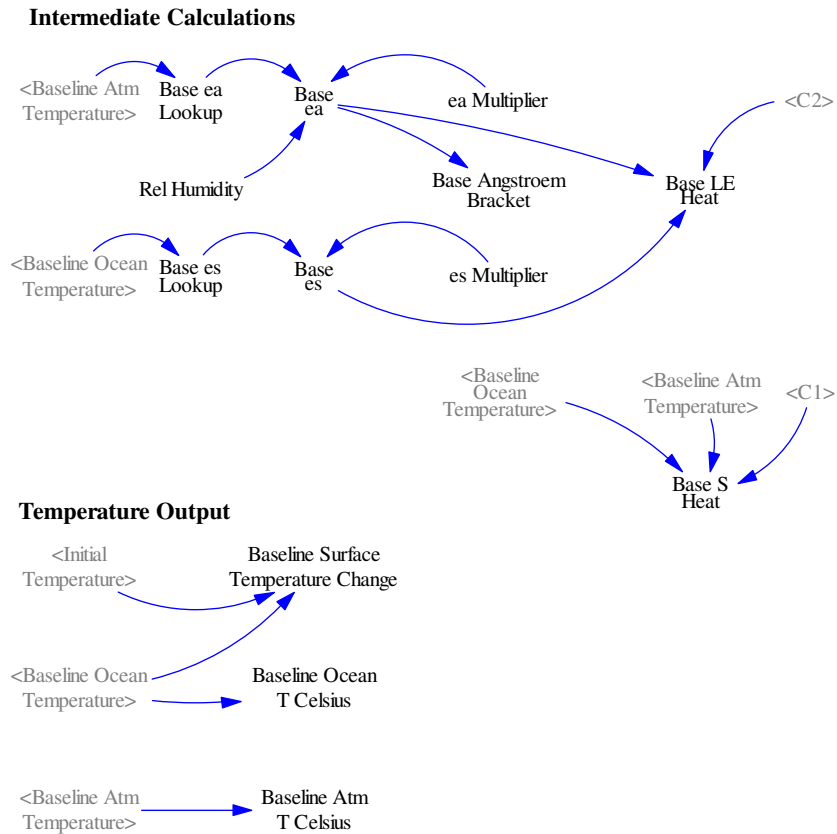
Figure A-10: Intermediate Calculations and Output Variables from Climate System – View of 'Part 2'

```
A=
            -251
      Units: Joules/(Meter*Meter*Second)

Advective Flow[LHsections]=
            rho * cp * Ocean SA * w * (Current Ocean
            Temperature[RHsections] - Current Ocean
            Temperature[section20])
Advective Flow[section19]=
            0
      Units: Joules/Year

Angstroem Bracket=
            10^(-0.07*ea)
      Units: Dimensionless

Atmosphere Heat= INTEG (
            Forcing+L up+LE and S Heat+Qa-L down-L out,
            Ra * Earth SA * Initial Atm Temperature)
      Units: Joules

B=
            1.8
```

```
        Units: Joules/(Meter*Meter*Kelvin*Second)


Base Advective Flow[LHsections]=
        rho * cp * Ocean SA * w * (Baseline Ocean
        Temperature[RHsections] – Baseline Ocean
        Temperature[section20])
Base Advective Flow[section19]=
        0
    Units: Joules/Year


Base Angstroem Bracket=
        10^(-0.07*Base ea)
    Units: Dimensionless


Base Atmosphere Heat= INTEG (
        Baseline Forcing+Base L up+Base LE and S Heat+Base Qa–Base
        L down–Base L out, Ra * Earth SA * Initial Atm Temperature)
    Units: Joules


Base Diffusive Flow[LHsections]=
        – K clim * Ocean SA * (Baseline Ocean
        Temperature[RHsections] – Baseline Ocean
        Temperature[LHsections]) / flow distance[LHsections]
Base Diffusive Flow[section19]=
        – K clim * Ocean SA * (Baseline Ocean
        Temperature[section20] – Baseline Ocean
        Temperature[section19]) / flow distance[section19]
    Units: Joules/Year


Base ea=
        ea Multiplier * (Rel Humidity * Base ea Lookup)
    Units: mbar


Base ea Lookup= WITH LOOKUP (
        Baseline Atm Temperature,([(220,0)-
        (340,150)],(0,0.06356),(223,0.06356),(228,0.11114),(233,0.1
        8914),(238,0.31387),(243,0.5088),(248,0.80697),(253,1.25401
        ),(258,1.91178),(263,2.8627),(268,4.21485),(273,6.1078),(27
        8,8.71922),(283,12.2723),(288,17.0438),(293,23.373),(298,31
        .6709),(303,42.4304),(308,56.2366),(313,73.7775),(318,95.85
        48),(323,123.4),(500,123.4) ))
    Units: mbar


Base es=
        es Multiplier * Base es Lookup
    Units: mbar


Base es Lookup= WITH LOOKUP (
        Baseline Ocean Temperature[section1],([(220,0)-
        (340,150)],(0,0.06356),(223,0.06356),(228,0.11114),(233,0.1
        8914),(238,0.31387),(243,0.5088),(248,0.80697),(253,1.25401
        ),(258,1.91178),(263,2.8627),(268,4.21485),(273,6.1078),(27
        8,8.71922),(283,12.2723),(288,17.0438),(293,23.373),(298,31
        .6709),(303,42.4304),(308,56.2366),(313,73.7775),(318,95.85
        48),(323,123.4),(500,123.4) ))
    Units: mbar
```

```
Base L down=
            (Sigma * Baseline Atm Temperature^4 * (0.89 – 0.2 * Base
            Angstroem Bracket) ) * Earth SA* Seconds per Year
      Units: Joules/Year


Base L out=
            (A + B*Baseline Atm Temperature –C*Fcl*"Delta Ts,cl") *
            Earth SA * Seconds per Year
      Units: Joules/Year


Base L up=
            (Sigma * Baseline Ocean Temperature[section1]^4) * Earth SA
            * Seconds per Year
      Units: Joules/Year


Base LE and S Heat=
            (Base S Heat + Base LE Heat) * Earth SA * Seconds per Year
      Units: Joules/Year


Base LE Heat=
            C2 * (Base es – Base ea)
      Units: Joules/(Meter*Meter*Second)


Base Ocean Heat[section1]= INTEG (
            (Base Qs + Base L down) – (Base L up + Base LE and S Heat)
            + (Base Advective Flow[section1] – Base Diffusive
            Flow[section1]), rho * cp * Ocean SA * box depth[section1]
            * Initial Temperature[section1])
Base Ocean Heat[RHsections]= INTEG (
            (Base Diffusive Flow[LHsections] + Base Advective
            Flow[RHsections]) – (Base Diffusive Flow[RHsections] + Base
            Advective Flow[LHsections]),rho * cp * Ocean SA * box
            depth[RHsections] * Initial Temperature[RHsections])
Base Ocean Heat[section20]= INTEG (
            Base Diffusive Flow[section19] – Base Advective
            Flow[section19],rho * cp * Ocean SA * box depth[section20]
            * Initial Temperature[section20])
      Units: Joules


Base Qa=
            Solar Constant change * 66.9* Earth SA * Seconds per Year
      Units: Joules/Year


Base Qs=
            Solar Constant change * (168.95 * Earth SA * Seconds per
            Year)
      Units: Joules/Year


Base S Heat=
            C1 * (Baseline Ocean Temperature[section1] – Baseline Atm
            Temperature)
      Units: Joules/(Meter*Meter*Second)


Baseline Atm T Celsius=
            Baseline Atm Temperature – 273.15
      Units: Celsius
```

```
Baseline Atm Temperature=
            Base Atmosphere Heat / (Ra * Earth SA)
      Units: Kelvin


Baseline Forcing=
            Baseline Forcing Calc * Earth SA * Seconds per Year
      Units: Joules/Year


Baseline Forcing Calc=
            (Climate Sensitivity/Initial CO2 in Atmosphere)*Baseline
            CO2 in Atmosphere – Climate Sensitivity)
      Units: Joules/(Meter*Meter*Second)


Baseline Ocean T Celsius[sections]=
            Baseline Ocean Temperature[sections] – 273.15
      Units: Celsius


Baseline Ocean Temperature[LHsections]=
            Base Ocean Heat[LHsections] / (cp * Oceanic
            Mass[LHsections])
Baseline Ocean Temperature[section20]=
            274.35
Baseline Ocean Temperature[section19]=
            Base Ocean Heat[section19] / (cp * Oceanic Mass[section19])
      Units: Kelvin


Baseline Surface Temperature Change=
            Baseline Ocean Temperature[section1] – Initial
            Temperature[section1]
      Units: Celsius


Baseline Temperature Change=
            (Baseline Ocean Temperature[section1] – Initial
            Temperature[section1]) + 0.2
      Units: degrees C


box depth[sections]=
            30, 30, 30, 30, 30, 50, 100, 100, 100, 100, 100, 100, 100,
            100, 250, 250,500, 500, 500, 792
      Units: Meter


C=
            1.73
      Units: Joules/(Meter*Meter*Kelvin*Second)


C1=
            12.57
      Units: Joules/(Meter*Meter*Kelvin*Second)


C2=
            11.75
      Units: Joules/(Meter*Meter*mbar*Second)


Climate Sensitivity=
            4
      Units: Joules/(Meter*Meter*Second) [0,10,1]
```

```
cp=
            4218
      Units: Joules/kg/Kelvin


Current Atm T Celsius=
            Current Atm Temperature - 273.15
      Units: Celsius


Current Atm Temperature=
            Atmosphere Heat / (Ra * Earth SA)
      Units: Kelvin


Current Ocean T Celsius[sections]=
            Current Ocean Temperature[sections] - 273.15
      Units: Celsius


Current Ocean Temperature[LHsections]=
            Ocean Heat[LHsections] / (cp * Oceanic Mass[LHsections])
Current Ocean Temperature[section20]=
            274.35
Current Ocean Temperature[section19]=
            Ocean Heat[section19] / (cp * Oceanic Mass[section19])
      Units: Kelvin


"Delta Ts,cl"=
            32.34
      Units: Kelvin


depth[section1]=
            box depth[section1]
depth[RHsections]=
            depth[LHsections] + box depth[RHsections]
depth[section20]=
            depth[section19] + box depth[section20]
      Units: Meter


Diffusive Flow[LHsections]=
            - K clim * Ocean SA * (Current Ocean
            Temperature[RHsections] - Current Ocean
            Temperature[LHsections]) / flow distance[LHsections]
Diffusive Flow[section19]=
            - K clim * Ocean SA * (Current Ocean Temperature[section20]
            - Current Ocean Temperature[section19]) / flow
            distance[section19]
      Units: Joules/Year


ea=
            ea Multiplier * (Rel Humidity * ea Lookup)
      Units: mbar


ea Lookup= WITH LOOKUP (
            Current Atm Temperature,([(220,0)-
            (340,150)],(0,0.06356),(223,0.06356),(228,0.11114),(233,0.1
            8914),(238,0.31387),(243,0.5088),(248,0.80697),(253,1.25401
            ),(258,1.91178),(263,2.8627),(268,4.21485),(273,6.1078),(27
            8,8.71922),(283,12.2723),(288,17.0438),(293,23.373),(298,31
```

```
                  .6709),(303,42.4304),(308,56.2366),(313,73.7775),(318,95.85
                  48),(323,123.4),(500,123.4) ))
          Units: mbar

ea Multiplier=
          1.39
      Units: Dimensionless

Earth SA=
          5.1e+014
      Units: Meter*Meter

es=
          es Multiplier * es Lookup
      Units: mbar

es Lookup= WITH LOOKUP (
          Current Ocean Temperature[section1],([(220,0)-
          (340,150)],(0,0.06356),(223,0.06356),(228,0.11114),(233,0.1
          8914),(238,0.31387),(243,0.5088),(248,0.80697),(253,1.25401
          ),(258,1.91178),(263,2.8627),(268,4.21485),(273,6.1078),(27
          8,8.71922),(283,12.2723),(288,17.0438),(293,23.373),(298,31
          .6709),(303,42.4304),(308,56.2366),(313,73.7775),(318,95.85
          48),(323,123.4),(500,123.4) ))
      Units: mbar

es Multiplier=
          1.31
      Units: Dimensionless

Fcl=
          0.544
      Units: Dimensionless

flow distance[LHsections]=
          stock midpoints[RHsections]-stock midpoints[LHsections]
flow distance[section19]=
          stock midpoints[section20]-stock midpoints[section19]
      Units: Meter

Forcing=
          Forcing Calc * Earth SA * Seconds per Year
      Units: Joules/Year

Forcing Calc=
          (Climate Sensitivity/Initial CO2 in Atmosphere)*CO2 in
          Atmosphere - Climate Sensitivity)
      Units: Joules/(Meter*Meter*Second)

Initial Atm Temperature=
          287.5
      Units: Kelvin

Initial T Celsius[sections]=
          15.9, 15.04, 14.23, 13.47, 12.75, 11.87, 10.44, 8.86, 7.56,
          6.48, 5.59, 4.85, 4.23, 3.72, 3.07, 2.44, 1.9, 1.52, 1.32,
          1.2
```

```
        Units: Celsius

Initial Temperature[sections]=
            Initial T Celsius[sections] + 273.15
        Units: Kelvin

K clim=
            (kappa * rho * cp)
        Units: Joules/(Meter*Kelvin*Second)

kappa=
            1893
        Units: (Meter*Meter)/Year

L down=
            (Sigma * Current Atm Temperature^4 * (0.89 - 0.2 *
            Angstroem Bracket ) ) * Earth SA* Seconds per Year
        Units: Joules/Year

L out=
            (A + B*Current Atm Temperature -C*Fcl*"Delta Ts,cl") *
            Earth SA * Seconds per Year
        Units: Joules/Year

L up=
            (Sigma * Current Ocean Temperature[section1]^4) * Earth SA
            * Seconds per Year
        Units: Joules/Year

LE and S Heat=
            (S Heat + LE Heat) * Earth SA * Seconds per Year
        Units: Joules/Year

LE Heat=
            C2 * (es - ea)
        Units: Joules/(Meter*Meter*Second)

LHsections: (section1-section18) -> RHsections

Ocean Heat[section1]= INTEG (
            (Qs + L down) - (L up + LE and S Heat) + (Advective
            Flow[section1] - Diffusive Flow[section1]), rho * cp *
            Ocean SA * box depth[section1] * Initial
            Temperature[section1])
Ocean Heat[RHsections]= INTEG (
            (Diffusive Flow[LHsections] + Advective Flow[RHsections]) -
            (Diffusive Flow[RHsections] + Advective Flow[LHsections]),
            rho * cp * Ocean SA * box depth[RHsections] * Initial
            Temperature[RHsections])
Ocean Heat[section20]= INTEG (
            Diffusive Flow[section19] - Advective Flow[section19], rho
            * cp * Ocean SA * box depth[section20] * Initial
            Temperature[section20])
        Units: Joules

Ocean SA=
            3.42e+014
```

```
         Units: Meter*Meter

Oceanic Mass[sections]=
         rho * Ocean SA * box depth[sections]
      Units: kg

Qa=
         66.9* Earth SA * Seconds per Year
      Units: Joules/Year

Qs=
         168.95 * Earth SA * Seconds per Year
      Units: Joules/Year

Ra=
         1.02e+007
      Units: Joules/(Meter*Meter*Kelvin)

Rel Humidity=
         0.71
      Units: Dimensionless

rho=
         1030
      Units: kg/(Meter*Meter*Meter)

RHsections: (section2-section19) -> LHsections

S Heat=
         C1 * (Current Ocean Temperature[section1] – Current Atm
         Temperature)
      Units: Joules/(Meter*Meter*Second)

Seconds per Year=
         60 * 60 * 24 * 365.25
      Units: Second/Year

sections: (section1-section20)

Sigma=
         5.67e-008
      Units: Joules/(Meter*Meter*Kelvin*Kelvin*Kelvin*Kelvin)

stock midpoints[section1]=
         depth[section1]/2
stock midpoints[RHsections]=
         (depth[RHsections]+depth[LHsections])/2
stock midpoints[section20]=
         (depth[section19]+depth[section20])/2
      Units: Meter

Surface Temperature Change=
         Current Ocean Temperature[section1] – Initial
         Temperature[section1]
      Units: Celsius

Temperature Change=
```

```
            (Current Ocean Temperature[section1] – Initial
            Temperature[section1]) + 0.2
       Units: degrees C

w=
            4
       Units: Meter/Year
```

****
.Control
****

            Simulation Control Parameters

```
FINAL TIME= 2100
       Units: Year

INITIAL TIME=
            1960
       Units: Year

SAVEPER=
            1
       Units: Year

TIME STEP=
            0.015625
       Units: Year
```


****
.Economy
****

The equations for the model's economic sector follow a set of figures that illustrate the model layout in Vensim. The nine figures below focus on,

- The variable, controllable 'Part 1':
    - Economic Output and Capital Growth (Figure A-11);
    - Carbon Tax Policy Selection (Figure A-12);
    - Parameter Layout and Basic Calculations (Figure A-13);
    - Intermediate Calculations (Figure A-14);

      o   Output Variables and Utility Calculation (Figure A-15); and,

      o   Industrial Emissions Calculation (Figure A-16).

- The business-as-usual 'Part 2':

      o   Economic Output, Capital Growth, and Intermediate Calculations (Figure A-17);

      o   Cost-Benefit Analysis Structure (Figure A-18); and,

      o   Industrial Emissions Calculation (Figure A-19).

Figure A-11: Economic Output and Capital Growth in Economic Sector – View of 'Part 1'

Carbon Tax Set-up

Case Selector

Base Case

Optimal Case   Carbon Tax   Random Tax   <INITIAL TIME>

<Time>   T limit (2.5 degrees)   Ramp Tax   <FINAL TIME>

Double Concentration   Ramp Slope

<Damage D(t)>   OptionB   tau(t)

<b1(t)>

<b2>

<sigma(t)>

Figure A-12: Carbon Tax Policy Selection in Economic Sector

Parameters and Basic Calculations
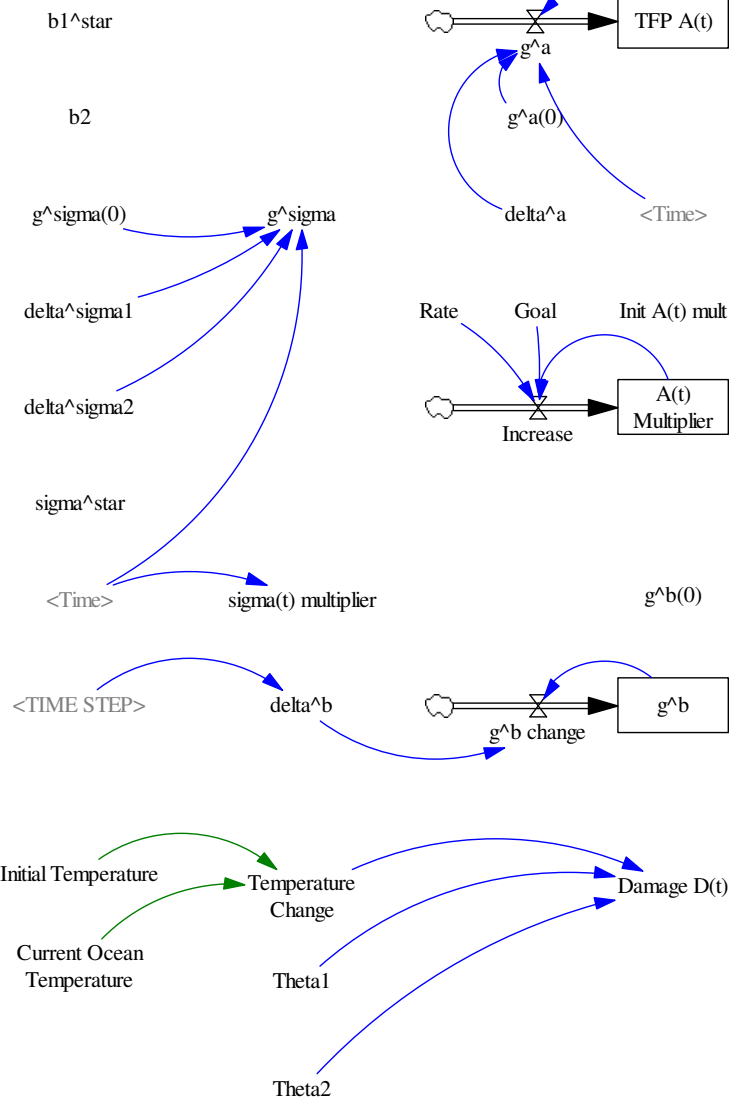
Figure A-13: Parameters and Basic Calculations in Economic Sector – View of 'Part 1'

Intermediate Calculations

Figure A-14: Intermediate Calculations in Economic Sector – View of 'Part 1'

Important Output
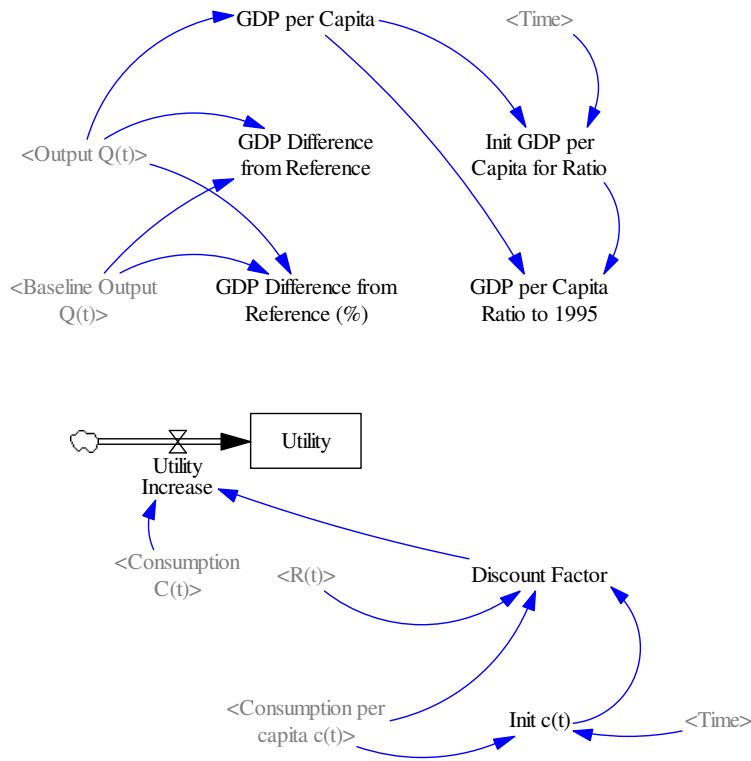
Figure A-15: Important Output Variables in Economic Sector and Utility Calculation – View of 'Part 1'
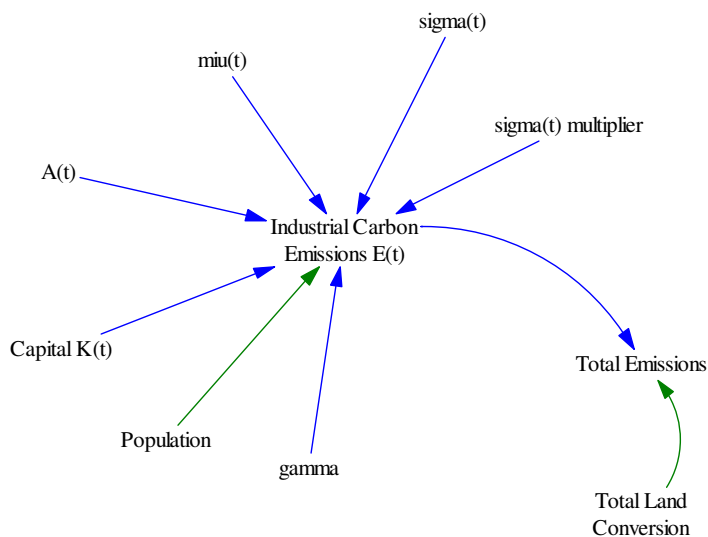
Figure A-16: Industrial Emissions Calculation in Economic Sector – View of 'Part 1'

Baseline Output Calculation
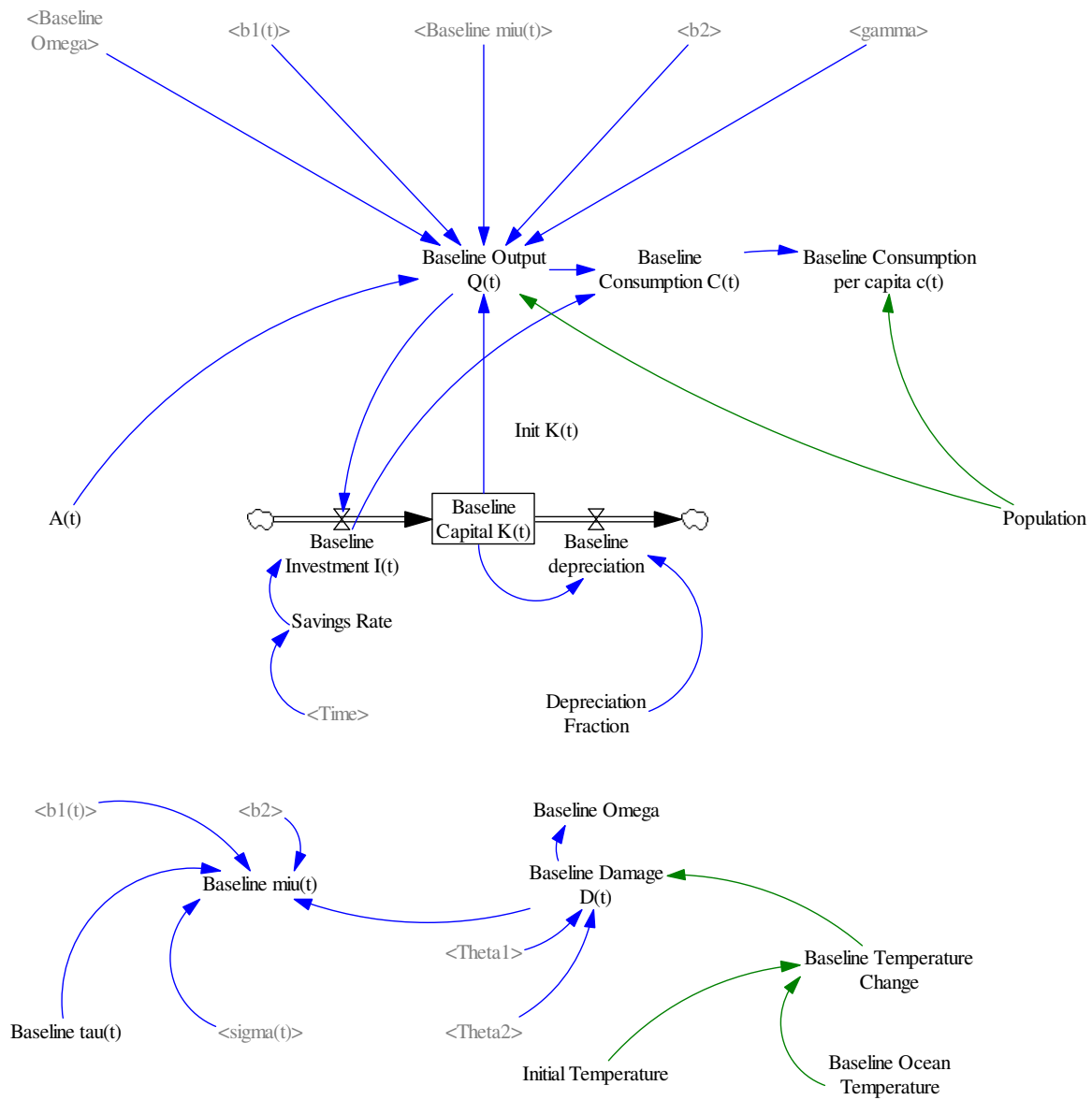
Figure A-17: Basic Structure of Baseline Economic Sector – View of 'Part 2'

Policy Effect Calculations
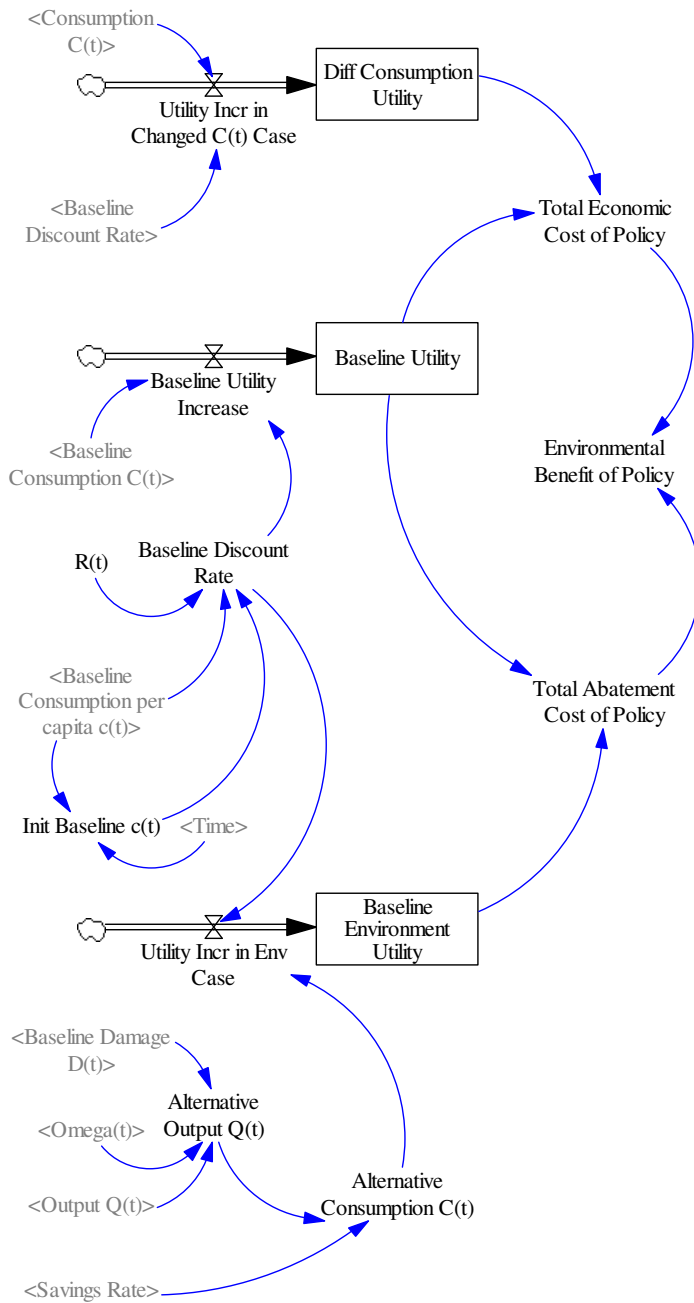
Figure A-18: Calculations of Carbon Tax Policy Effects (Abatement Costs, Environmental Benefits, and Total Economic Costs) – View of 'Part 2'
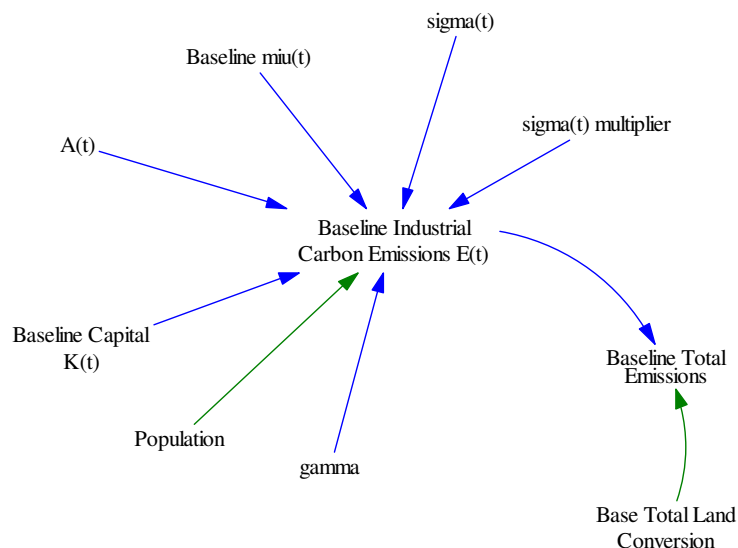
Figure A-19: Baseline Industrial Emissions Calculation in Economic Sector – View of 'Part 2'

```
"A(t)"=
            "A(t) Multiplier"*"TFP A(t)"
       Units: Dimensionless

"A(t) Multiplier"= INTEG (
            Increase,
            "Init A(t) mult")
       Units: Dimensionless

A Goal=
            1
       Units: Dimensionless

A Increase=
            Rate*(Goal-"A(t) Multiplier")
       Units: Dimensionless

"Abatement Cost (Excel Row 72)"=
            "b1(t)"*("miu(t)"/100)^b2
       Units: 1/Decade

"Alternative Consumption C(t)"=
            (1-Savings Rate/100)*"Alternative Output Q(t)"
       Units: trillion $/Year

"Alternative Output Q(t)"=
            ("Output Q(t)"/"Omega(t)")/(1+"Baseline Damage D(t)"/100)
       Units: trillion $/Year

Annual savings rate= WITH LOOKUP (
            Time,([(1960,0)-
            (2335,100)],(1995,25.3),(2004,25.3),(2005,24.02),(2014,24.0
            2),(2015,23.27),(2025,22.81),(2035,22.52),(2045,22.35),(205
```

```
            5,22.25),(2065,22.21),(2075,22.2),(2085,22.23),(2095,22.29)
            ,(2105,22.36),(2115,22.45),(2125,22.56),(2135,22.67),(2145,
            22.79),(2155,22.91),(2165,23.04),(2175,23.17),(2185,23.3),(
            2195,23.44),(2205,23.57),(2215,23.7),(2225,23.83),(2235,23.
            96),(2245,24.08),(2255,24.21),(2265,24.32),(2275,24.42),(22
            85,24.48),(2295,24.43),(2305,24.08),(2315,22.87),(2325,19.1
            2),(2335,6.05) ))
        Units: percent/Year


"b1(t)"= INTEG (
            "b1(t) change",
            "b1^star")
        Units: Dimensionless


"b1(t) change"=
            1/10*("b1(t)"/(1+"g^b"/100) - "b1(t)")
        Units: Dimensionless


"b1^star"=
            0.02196
        Units: Dimensionless


b2=
            2.15
        Units: Dimensionless


Base Case=
            0
        Units: Dimensionless


"Baseline Capital K(t)"= INTEG (
            +"Baseline Investment I(t)"-Baseline depreciation,
            "Init K(t)")
        Units: trillion $


"Baseline Consumption C(t)"=
            "Baseline Output Q(t)"-"Baseline Investment I(t)"
        Units: trillion $/Year


"Baseline Consumption per capita c(t)"=
            ("Baseline Consumption C(t)"*1e+012)/Population
        Units: trillion $/Year/person


"Baseline Damage D(t)"=
            (Theta1*Baseline Temperature Change+Theta2*Baseline
            Temperature Change*Baseline Temperature Change)*100
        Units: percent/Decade


Baseline depreciation=
            "Baseline Capital K(t)"*(1-Depreciation Fraction)
        Units: trillion $/Decade


Baseline Discount Rate=
            "R(t)"*(1/"Baseline Consumption per capita c(t)")*"Init
            Baseline c(t)"
        Units: Dimensionless
```

```
Baseline Environment Utility= INTEG (
            Utility Incr in Env Case,
            0)
      Units: trillion $

"Baseline Industrial Carbon Emissions E(t)"=
            (1-"Baseline miu(t)"/100)*("sigma(t)
            multiplier"*"sigma(t)")*("A(t)"*("Baseline Capital
            K(t)"^gamma)*((Population/1e+006)^(1-gamma)))
      Units: Gt C/Year

"Baseline Investment I(t)"=
            Savings Rate/100*"Baseline Output Q(t)"
      Units: trillion $/Year

"Baseline miu(t)"=
            100*(("Baseline tau(t)"/1000)*"sigma(t)"*(1+"Baseline
            Damage D(t)"/100)/("b1(t)"*b2))^(1/(b2-1))
      Units: percent/Decade

Baseline Omega=
            1/(1+"Baseline Damage D(t)"/100)
      Units: Dimensionless

"Baseline Output Q(t)"=
            Baseline Omega*(1-(100*"b1(t)"*("Baseline
            miu(t)"/100)^b2)/100)*"A(t)"*("Baseline Capital
            K(t)")^gamma*(Population/1e+006)^(1-gamma)
      Units: trillion $/Year

"Baseline tau(t)"=
            0
      Units: $/kton

Baseline Total Emissions=
            "Baseline Industrial Carbon Emissions E(t)"+Base Total Land
            Conversion
      Units: Gt C/Year

Baseline Utility= INTEG (
            Baseline Utility Increase,
            0)
      Units: trillion $

Baseline Utility Increase=
            "Baseline Consumption C(t)"*Baseline Discount Rate
      Units: trillion $/Year

"Capital K(t)"= INTEG (
            +"Investment I(t)"-depreciation,
            "Init K(t)")
      Units: trillion $

Carbon Tax=
            IF THEN ELSE(Case Selector = 1, Base Case, IF THEN
            ELSE(Case Selector = 2, Optimal Case , IF THEN ELSE(Case
            Selector= 3, "T limit (2.5 degrees)", IF THEN ELSE(Case
```

```
                Selector=4, Double Concentration, IF THEN ELSE(Case
                Selector=5, Random Tax, Ramp Tax)))))
        Units: $/kton

Case Selector=
                1
        Units: Dimensionless

"Consumption C(t)"=
                "Output Q(t)"-"Investment I(t)"
        Units: trillion $/Year

"Consumption per capita c(t)"=
                ("Consumption C(t)"*1e+012)/Population
        Units: $/person/Year

"Damage D(t)"=
                (Theta1*Temperature Change+Theta2*Temperature
                Change*Temperature Change)*100
        Units: percent/Decade

"delta^a"=
                1e-006
        Units: percent/Decade

"delta^b"=
                IF THEN ELSE(TIME STEP = 1, 0.475, 0.485)
        Units: percent/Year

"delta^k"=
                6.45
        Units: percent/Year

"delta^sigma1"=
                2.54
        Units: Dimensionless

"delta^sigma2"=
                -0.095
        Units: Dimensionless

depreciation=
                "Capital K(t)"*(1-Depreciation Fraction)
        Units: trillion $/Year

Depreciation Fraction=
                (1-"delta^k"/100)^1
        Units: 1/Year

Diff Consumption Utility= INTEG (
                "Utility Incr in Changed C(t) Case", 0)
        Units: trillion $

Discount Factor=
                "R(t)"*(1/"Consumption per capita c(t)")*"Init c(t)"
        Units: Dimensionless
```

```
Double Concentration= WITH LOOKUP (
          Time,([(1960,0)-
          (2335,5000)],(1960,0),(1994,0),(1995,2.79843),(2005,4.60428
          ),(2015,7.15395),(2025,10.82),(2035,16.0991),(2045,23.6169)
          ,(2055,34.3713),(2065,49.8148),(2075,71.4569),(2085,102.437
          ),(2095,146.101),(2105,209.739),(2115,307.874),(2125,437.01
          4),(2135,544.386),(2145,634.209),(2155,716.366),(2165,795.6
          12),(2175,874.911),(2185,956.5),(2195,1042.33),(2205,1134.3
          3),(2215,1234.65),(2225,1345.85),(2235,1470.98),(2245,1613.
          54),(2255,1776.88),(2265,1961.88),(2275,2159.94),(2285,2330
          .41),(2295,2331.02),(2305,1756.35),(2315,316.729),(2325,0.7
          31406),(2335,0) ))
     Units: $/kton

Environmental Benefit of Policy=
          Total Abatement Cost of Policy-Total Economic Cost of
          Policy
     Units: billion $

"g^a"=
          "TFP A(t)"*("g^a(0)"/10*EXP(-("delta^a"/100)*Time)/100)
     Units: Dimensionless

"g^a(0)"=
          3.8
     Units: percent/Decade

"g^b"= INTEG (
          "g^b change",
          "g^b(0)")
     Units: percent/Year

"g^b change"=
          "g^b"*-1*"delta^b"/100
     Units: percent/(Decade*Decade)

"g^b(0)"=
          -8.89
     Units: percent/Decade

"g^rho"=
          0.257
     Units: percent/Year

"g^sigma"=
          "g^sigma(0)"*EXP(-10*("delta^sigma1"/100)*((Time-1995)/10)
          - 10*("delta^sigma2"/100)*((Time-1995)/10)^2)
     Units: Dimensionless

"g^sigma(0)"=
          -15.8
     Units: Dimensionless

gamma=
          0.3
     Units: Dimensionless
```

```
GDP Difference from Reference=
            "Output Q(t)"-"Baseline Output Q(t)"
      Units: trillion $/Year

"GDP Difference from Reference (%)"=
            100*("Output Q(t)"-"Baseline Output Q(t)")/"Baseline Output
            Q(t)"
      Units: percent/Year

GDP per Capita=
            ("Output Q(t)"*1e+012)/Population
      Units: $/(Year*person)

GDP per Capita Ratio to 1995=
            IF THEN ELSE(Init GDP per Capita for Ratio > 0, GDP per
            Capita/Init GDP per Capita for Ratio, 0)
      Units: Dimensionless

"Industrial Carbon Emissions E(t)"=
            (1-"miu(t)"/100)*("sigma(t) multiplier" * "sigma(t)")
            *("A(t)" * ("Capital K(t)"^gamma) *
            ((Population/1e+006)^(1-gamma)))
      Units: Gt C/Year

"Init A(t) mult"=
            0.8
      Units: Dimensionless

"Init Baseline c(t)"=
            SAMPLE IF TRUE(  Time = 1995, "Baseline Consumption per
            capita c(t)", 0 )
      Units: trillion $/Year

"Init c(t)"=
            SAMPLE IF TRUE( Time = 1995, "Consumption per capita c(t)",
            0 )
      Units: $/(Year*person)

Init GDP per Capita=
            INITIAL(GDP per Capita)
      Units: $/(Year*person)

Init GDP per Capita for Ratio=SAMPLE IF TRUE(
            Time = 1995, GDP per Capita, 0)
      Units: $/(Decade*person)

"Init K(t)"=
            5.75
      Units: trillion $

"Init R(t)"=
            2.8035
      Units: Dimensionless

"Investment I(t)"=
            Savings Rate/100*"Output Q(t)"
      Units: trillion $/Year
```

```
"miu(t)"=
          100*(("tau(t)"/1000)*"sigma(t)"*(1+"Damage
          D(t)"/100)/("b1(t)"*b2))^(1/(b2-1))
     Units: percent/Decade

"Omega(t)"=
          IF THEN ELSE(Ignore climate change in output, 1,
          1/(1+"Damage D(t)"/100))
     Units: Dimensionless

Optimal Case= WITH LOOKUP (
          Time,([(1960,0)-
          (2335,200)],(1960,0),(1994,0),(1995,5.9),(2005,9.44),(2015,
          13.47),(2025,17.92),(2035,22.79),(2045,28.04),(2055,33.64),
          (2065,39.55),(2075,45.7),(2085,52.02),(2095,58.46),(2105,65
          .1),(2115,72.01),(2125,79.24),(2135,86.79),(2145,94.65),(21
          55,102.8),(2165,111.18),(2175,119.72),(2185,128.3),(2195,13
          6.77),(2205,144.9),(2215,152.47),(2225,159.05),(2235,164.18
          ),(2245,167.24),(2255,167.43),(2265,163.69),(2275,154.73),(
          2285,138.96),(2295,114.68),(2305,80.83),(2315,39.09),(2325,
          0),(2335,0) ))
     Units: $/kton

OptionB=
          1000*"b1(t)"*b2/((1+"Damage D(t)"/100)*"sigma(t)")
     Units: $/kton

"Output Gross (Excel Row 71)"=
          "A(t)"*(("Capital K(t)")^gamma)*((Population/1e+006)^(1-
          gamma))
     Units: trillion $

"Output Q(t)"=
          "Omega(t)"*(1-
          (100*"b1(t)"*("miu(t)"/100)^b2)/100)*"A(t)"*("Capital
          K(t)")^gamma*(Population/1e+006)^(1-gamma)
     Units: trillion $/Year

"R(t)"= INTEG (
          -"R(t) change",
          "Init R(t)")
     Units: Dimensionless

"R(t) change"=
          "R(t)" - "R(t)"*(1+"rho(t)")^-1
     Units: Dimensionless

Ramp Slope=
          2
     Units: $/kton

Ramp Tax=
          RAMP(Ramp Slope, INITIAL TIME+35, FINAL TIME)
     Units: $/kton

Random Tax=
```

```
                0
        Units: $/kton

Rate=
                0.06
        Units: Dimensionless

"Relative TFP A(t) change"=
                ("TFP A(0)"*"Init A(t) mult")/"A(t)"
        Units: Dimensionless

"rho(0)"=
                2.9
        Units: percent/Year

"rho(t)"=
                "rho(0)"/100)*EXP(-("g^rho"/100)*(Time-1995))
        Units: percent/Year

Savings Rate=
                IF THEN ELSE(Time <= 1995, Savings to 1995, Annual savings
                rate)
        Units: percent/Year

Savings to 1995= WITH LOOKUP (
                Time,([(1960,20)-
                (2003,30)],(1960,22),(1971,24.71),(1972,24.91),(1973,25.99)
                ,(1974,24.8),(1975,22.73),(1976,23.36),(1977,23.5),(1978,24
                .29),(1979,24.02),(1980,23.17),(1981,22.89),(1982,21.75),(1
                983,21.07),(1984,22.18),(1985,21.84),(1986,21.42),(1987,21.
                81),(1988,22.75),(1989,22.62),(1990,22.24),(1991,21.79),(19
                92,21.16),(1993,20.69),(1994,21.03),(1995,21.52),(1996,21.5
                6),(1997,22.3),(1998,22.11),(1999,21.95),(2000,22.17),(2001
                ,21.2),(2002,20.26),(2003,20.18) ))
        Units: percent/Year

"sigma(t)"= INTEG (
                -"sigma(t) change",
                "sigma^star")
        Units: tons/thousand $

"sigma(t) change"=
                1/10*("sigma(t)" - "sigma(t)"/(1-"g^sigma"/100))
        Units: tons/thousand $/Year

"sigma(t) multiplier"= WITH LOOKUP (
                Time,([(1960,0.8)-
                (2100,1)],(1960,0.8),(1970,0.9),(1980,0.96),(1990,0.99),(19
                95,1),(2100,1) ))
        Units: Dimensionless

"sigma^star"=
                0.56725
        Units: Dimensionless

"T limit (2.5 degrees)"= WITH LOOKUP (
```

```
            Time,([(1960,0)-
            (2335,5000)],(1960,0),(1994,0),(1995,7.57),(2005,12.35),(20
            15,19),(2025,28.44),(2035,41.91),(2045,61.13),(2055,88.41),
            (2065,126.92),(2075,180.88),(2085,255.82),(2095,358.2),(210
            5,492.76),(2115,650.49),(2125,766.04),(2135,819.54),(2145,8
            76.54),(2155,945.07),(2165,1021.07),(2175,1103.13),(2185,11
            91.88),(2195,1288.84),(2205,1396.2),(2215,1516.99),(2225,16
            55.5),(2235,1817.84),(2245,2012.87),(2255,2253.59),(2265,25
            58.28),(2275,2947.25),(2285,3422.56),(2295,3904.03),(2305,4
            066.55),(2315,3046.99),(2325,0),(2335,0) ))
        Units: $/kton

"tau(t)"=
            MIN(Carbon Tax, OptionB)
        Units: $/kton

"TFP A(0)"=
            0.01475
        Units: Dimensionless

"TFP A(t)"= INTEG (
            "g^a",
            "TFP A(0)")
        Units: Dimensionless

Theta1=
            -0.0045
        Units: %/K

Theta2=
            0.0035
        Units: %/K*K

Total Abatement Cost of Policy=
            1000*(Baseline Utility-Baseline Environment Utility)
        Units: billion $

Total Economic Cost of Policy=
            1000*(Baseline Utility - Diff Consumption Utility)
        Units: billion $

Total Emissions=
            "Industrial Carbon Emissions E(t)"+Total Land Conversion
        Units: Gt C/Year

Utility= INTEG (
            Utility Increase, 0)
        Units: trillion $

"Utility Incr in Changed C(t) Case"=
            "Consumption C(t)"*Baseline Discount Rate
        Units: trillion $/Year

Utility Incr in Env Case=
            "Alternative Consumption C(t)"*Baseline Discount Rate
        Units: trillion $/Year
```

```
Utility Increase=
        "Consumption C(t)"*Discount Factor
    Units: trillion $/Year
```

****

.Hydro

****

The equations for the model's natural hydrological (surface flow) sector follow a set of figures that illustrate the model layout in Vensim. The two figures below deal with,

- Stocks, Flows, and Feedbacks in the Natural Hydrological Cycle (Figure A-20); and,
- Water Consumption and Its Effects on the Cycle (Figure A-21).

Modified Advection Scheme
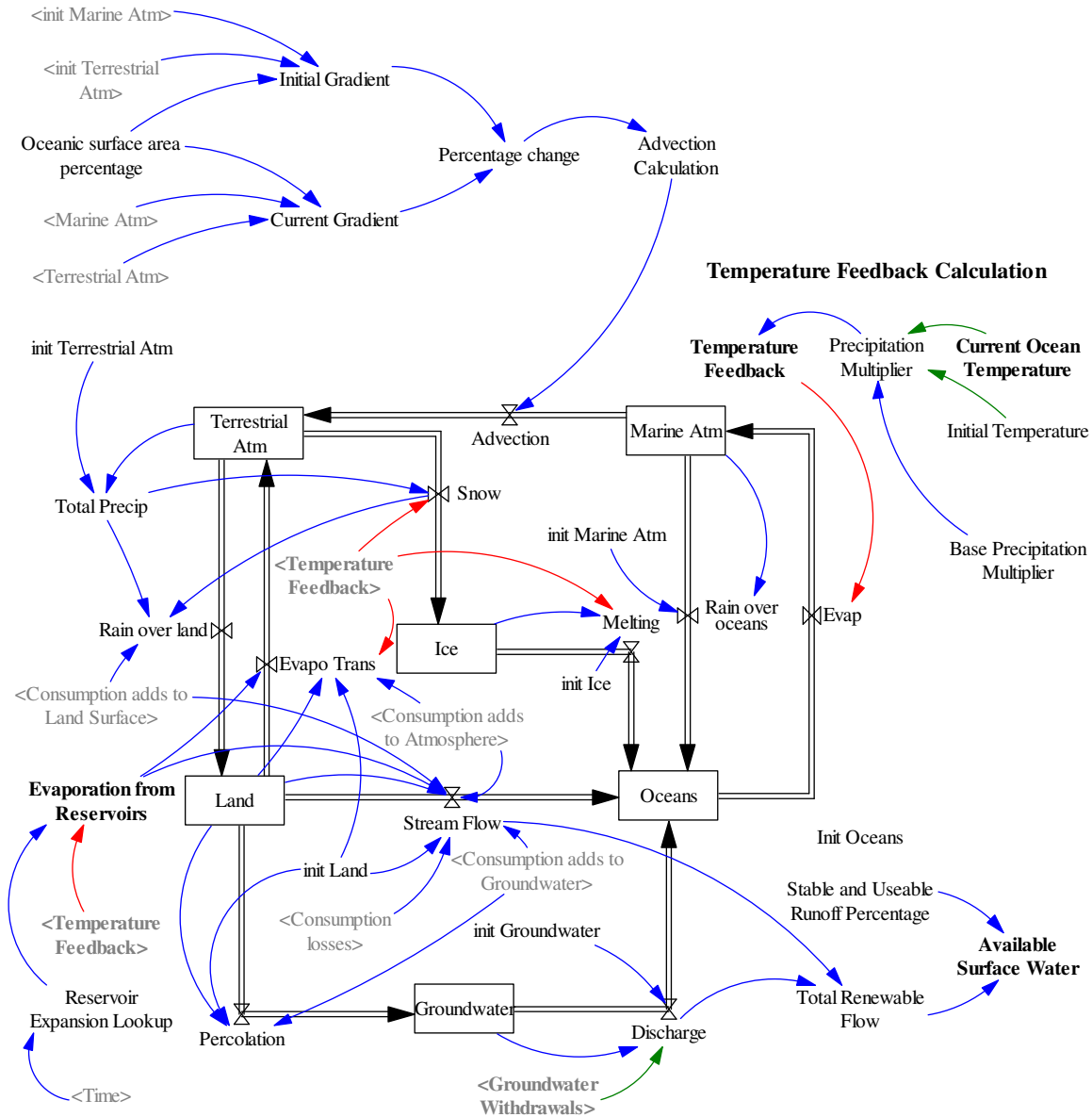
Figure A-20: Stocks, Flows, and Variables in the Natural Hydrological Cycle

Water Consumption

Desired Domestic
Water Consumption

Domestic Consumption
Percentages

Domestic
Consumption

Desired Industrial
Water Consumption

Industrial Consumption
Percentages

Industrial
Consumption

Desired Agricultural
Water Consumption

Agricultural Consumption
Percentages

Agricultural
Consumption

**Consumption adds
to Atmosphere**

**Consumption adds to
Land Surface**

**Consumption adds
to Groundwater**

**Consumption
losses**

Figure A-21: Water Consumption and Effects on Natural Hydrological Cycle

```
Advection=
          Advection Calculation
     Units: km*km*km/Year

Advection Calculation=
          45375*(1+Percentage change/100)
     Units: km*km*km/Year

Agricultural Consumption[destination]=
          (Agricultural Consumption
          Percentages[destination]/100)*Desired Agricultural Water
          Consumption
     Units: km*km*km/Year

Available Surface Water=
          (Stable and Useable Runoff Percentage/100) * Total
          Renewable Flow
     Units: km*km*km/Year

Base Precipitation Multiplier=
          3.4
     Units: percent/degrees C

Consumption adds to Atmosphere=
          (Domestic Consumption[atmosphere] + Industrial
          Consumption[atmosphere] + Agricultural
          Consumption[atmosphere])
     Units: km*km*km/Year

Consumption adds to Groundwater=
```

```
            (Domestic Consumption[subsurface] + Industrial
            Consumption[subsurface] + Agricultural
            Consumption[subsurface])
       Units: km*km*km/Year


Consumption adds to Land Surface=
            Agricultural Consumption[surface]
       Units: km*km*km/Year


Consumption losses=
            Industrial Consumption[lost]
       Units: km*km*km/Year


Current Gradient=
            (Marine Atm/Oceanic surface area percentage - Terrestrial
            Atm/(100-Oceanic surface area percentage))
       Units: km*km*km/surface area


destination: atmosphere, surface, subsurface, lost


Discharge=
            2000*(Groundwater/init Groundwater) + Groundwater
            Withdrawals
       Units: km*km*km/Year


Domestic Consumption[destination]=
            (Domestic Consumption Percentages[destination]/100)*Desired
            Domestic Water Consumption
       Units: km*km*km/Year


Evap=
            535200*Temperature Feedback
       Units: km*km*km/Year


Evapo Trans=
            72125*(Land/init Land)*Temperature Feedback + Evaporation
            from Reservoirs + Consumption adds to Atmosphere
       Units: km*km*km/Year


Evaporation from Reservoirs=
            Reservoir Expansion Lookup * Temperature Feedback
       Units: km*km*km/Year


Groundwater= INTEG (
            +Percolation-Discharge,
            init Groundwater)
       Units: km*km*km


Ice= INTEG (
            +Snow-Melting,
            init Ice)
       Units: km*km*km


Industrial Consumption[destination]=
            (Industrial Consumption
            Percentages[destination]/100)*Desired Industrial Water
            Consumption
```

```
          Units: km*km*km/Year

init Groundwater=
          1.06e+007
     Units: km*km*km

init Ice=
          2.45e+007
     Units: km*km*km

init Land=
          200000
     Units: km*km*km

init Marine Atm=
          9400
     Units: km*km*km

Init Oceans=
          1.338e+009
     Units: km*km*km

init Terrestrial Atm=
          4000
     Units: km*km*km

Initial Gradient=
          init Marine Atm/Oceanic surface area percentage - init
          Terrestrial Atm/(100-Oceanic surface area percentage)
     Units: km*km*km/surface area

Land= INTEG (
          +Rain over land-Evapo Trans-Percolation-Stream Flow,
          init Land)
     Units: km*km*km

Marine Atm= INTEG (
          +Evap-Advection-Rain over oceans,
          init Marine Atm)
     Units: km*km*km

Melting=
          2625*(Ice/init Ice)*Temperature Feedback^2
     Units: km*km*km/Year

Oceanic surface area percentage=
          67
     Units: percent

Oceans= INTEG (
          Discharge+Melting+Rain over oceans+Stream Flow-Evap,
          Init Oceans)
     Units: km*km*km

Percentage change=
          100*(Current Gradient - Initial Gradient)/Initial Gradient
     Units: percent
```

Percolation=
            2000*(Land/init Land) + Consumption adds to Groundwater
      Units: km*km*km/Year

Precipitation Multiplier=
            Base Precipitation Multiplier * (Current Ocean
            Temperature[section1] - Initial Temperature[section1])
      Units: percent

Rain over land=
            Total Precip-Snow + Consumption adds to Land Surface
      Units: km*km*km/Year

Rain over oceans=
            489825*(Marine Atm/init Marine Atm)
      Units: km*km*km/Year

Reservoir Expansion Lookup= WITH LOOKUP (
            Time, ([(1900,0)-
            (2100,400)],(1900,0.3),(1940,7),(1950,11.1),(1960,30.2),(19
            70,76.1),(1980,131),(1990,167),(1995,188),(2020,240),(2050,
            280),(2100,305)))
      Units: km*km*km/Year

Snow=
            2625*(Total Precip/117500)/Temperature Feedback
      Units: km*km*km/Year

Stable and Useable Runoff Percentage=
            37
      Units: percent

Stream Flow=
            40750*(Land/init Land)^2 - Evaporation from Reservoirs -
            Consumption adds to Atmosphere - Consumption adds to
            Groundwater - Consumption adds to Land Surface -
            Consumption losses
      Units: km*km*km/Year

Temperature Feedback=
            1 + Precipitation Multiplier/100
      Units: Dimensionless

Terrestrial Atm= INTEG (
            Advection+Evapo Trans-Rain over land-Snow,
            init Terrestrial Atm)
      Units: km*km*km

Total Precip=
            117500*(Terrestrial Atm/init Terrestrial Atm)
      Units: km*km*km/Year

Total Renewable Flow=
            Stream Flow + Discharge
      Units: km*km*km/Year

****
.HydroDemand
****

The equations for the model's water demand sector follow a set of figures that illustrate the model layout in Vensim. The four figures below deal with,

- Domestic Water Demand (Figure A-22);

- Industrial Water Demand (Figure A-23);

- Agricultural Water Demand (Figure A-24); and,

- Desired Withdrawal and Consumption, and Important Output (Figure A-25).

Domestic Water Demand
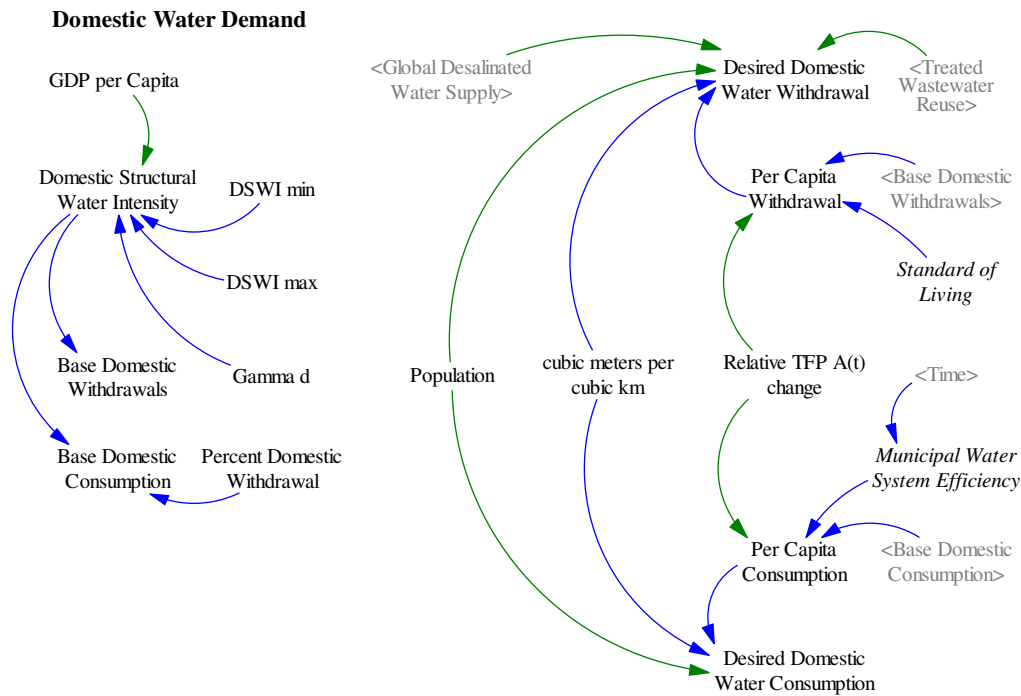
Figure A-22: Domestic Water Demand in Water Demand Sector

Industrial Water Demand
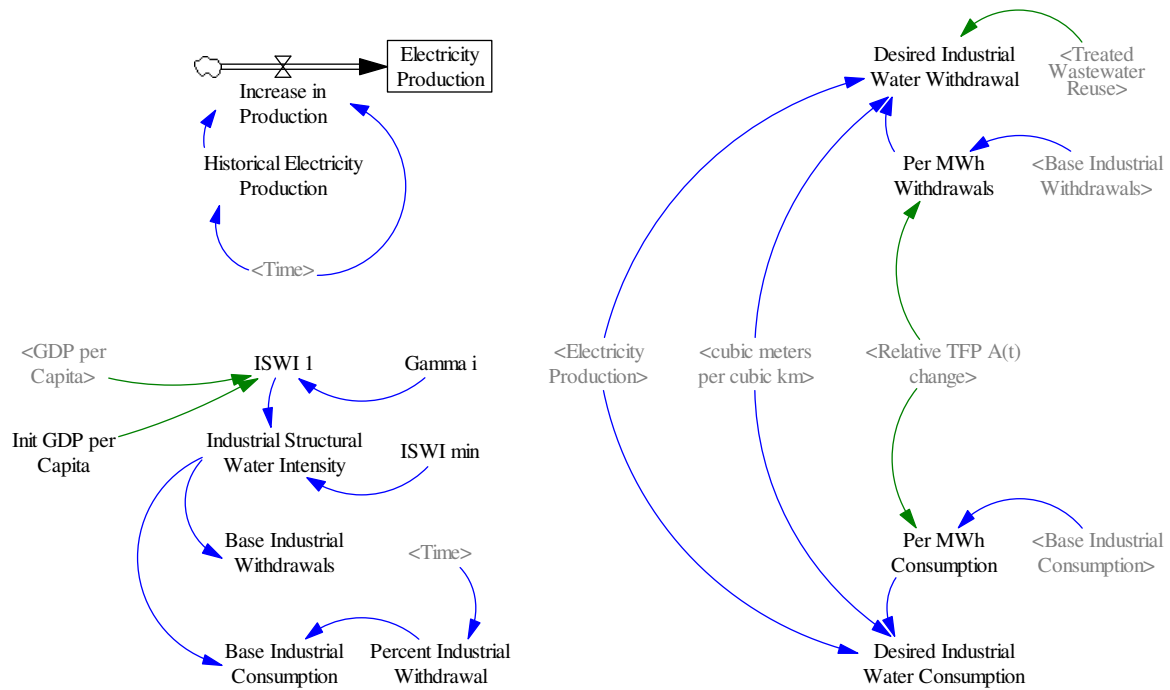
Figure A-23: Industrial Water Demand in Water Demand Sector

Agricultural Water Demand
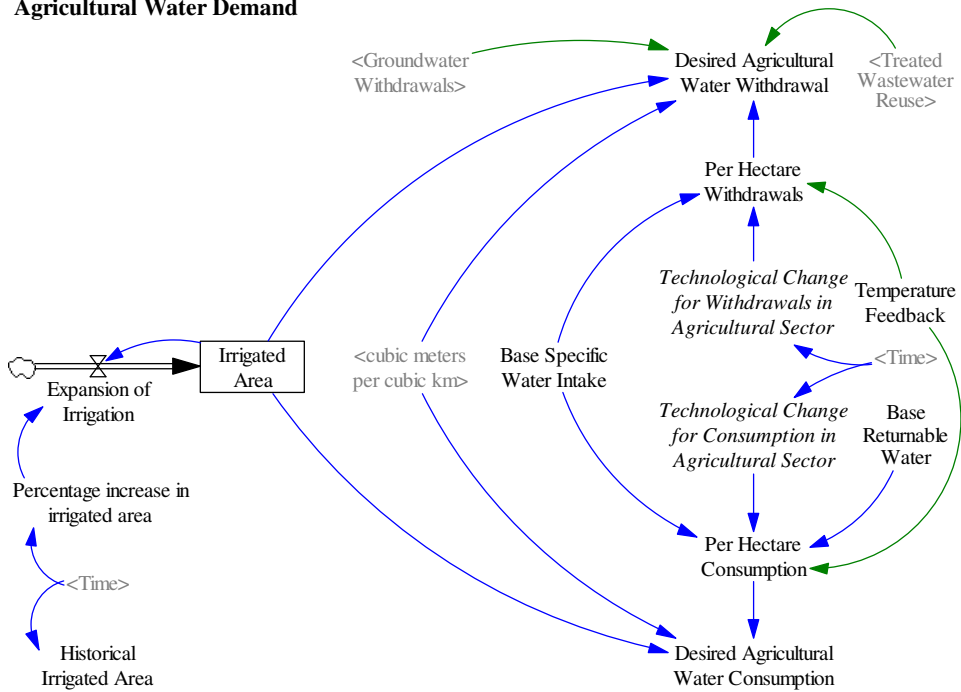
Figure A-24: Agricultural Water Demand in Water Demand Sector

Desired Withdrawals and Consumption

Comparison Variables
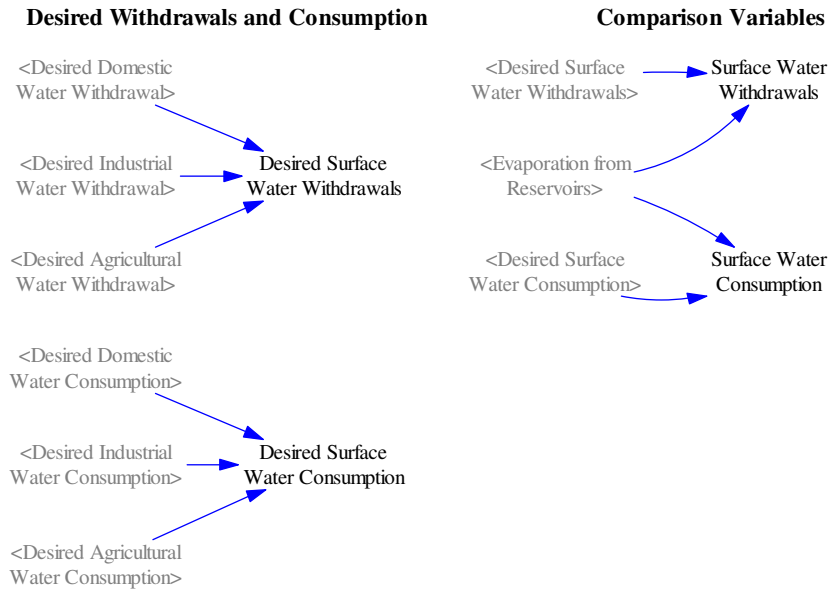
Figure A-25: Important Combination Variables and Comparison Variables in Water Demand Sector

```
Agricultural Consumption Percentages[destination]=
        70, 10, 20, 0
    Units: percent

Base Domestic Consumption=
        Domestic Structural Water Intensity*((100-Percent Domestic
        Withdrawal)/100)
    Units: m*m*m/person

Base Domestic Withdrawals=
        Domestic Structural Water Intensity
    Units: m*m*m/person

Base Industrial Consumption=
        Industrial Structural Water Intensity*(1- Percent
        Industrial Withdrawal/100)
    Units: m*m*m/MWh

Base Industrial Withdrawals=
        Industrial Structural Water Intensity
    Units: m*m*m/MWh

Base Returnable Water=
        30
    Units: percent

Base Specific Water Intake=
        10500
    Units: m*m*m/ha/Year

Base Water Stress=
        Desired Surface Water Withdrawals / Available Surface Water
```

```
        Units: Dimensionless

cubic meters per cubic km=
        1e+009
    Units: Liters/(km*km*km)

Delay in Establishing Groundwater Pumps=
        10
    Units: Year

Delay in Establishment of Desalination Facilities=
        5
    Units: Year

Desired Agricultural Water Consumption=
        Irrigated Area * Per Hectare Consumption / cubic meters per
        cubic km
    Units: km*km*km/Year

Desired Agricultural Water Withdrawal=
        Irrigated Area * Per Hectare Withdrawals / cubic meters per
        cubic km – Treated Wastewater Reuse[agr] – Groundwater
        Withdrawals
    Units: km*km*km/Year

Desired Domestic Water Consumption=
        Population * Per Capita Consumption/cubic meters per cubic
        km
    Units: km*km*km/Year

Desired Domestic Water Withdrawal=
        Population*Per Capita Withdrawal/cubic meters per cubic km
        – Treated Wastewater Reuse[dom] – Global Desalinated Water
        Supply
    Units: km*km*km/Year

Desired Industrial Water Consumption=
        (Electricity Production * 1e+006) * (Per MWh Consumption /
        cubic meters per cubic km)
    Units: km*km*km/Year

Desired Industrial Water Withdrawal=
        (Electricity Production * 1e+006) * (Per MWh Withdrawals /
        cubic meters per cubic km) – Treated Wastewater Reuse[ind]
    Units: km*km*km/Year

Desired Surface Water Consumption=
        Desired Agricultural Water Consumption + Desired Domestic
        Water Consumption + Desired Industrial Water Consumption
    Units: km*km*km/Year

Desired Surface Water Withdrawals=
        Desired Agricultural Water Withdrawal + Desired Domestic
        Water Withdrawal + Desired Industrial Water Withdrawal
    Units: km*km*km/Year

Domestic Consumption Percentages[destination]=
```

```
                        50, 0, 50, 0
        Units: percent

Domestic Structural Water Intensity=
                DSWI min + DSWI max*(1-EXP(-Gamma d*GDP per Capita*GDP per
                Capita))
        Units: m*m*m/person

DSWI max=
                220
        Units: m*m*m/person

DSWI min=
                17.5
        Units: (m*m*m)/person

Electricity Production= INTEG (
                Increase in Production,
                3000)
        Units: Billion kWh

Expansion of Irrigation=
                (y value*Percentage increase in irrigated area/100) *
                Irrigated Area
        Units: ha

Fractional Usage of Desalination Capacity= 0.5
        Units: Dimensionless

Gamma d=
                2.2e-008
        Units: Dimensionless

Gamma i=
                6.5e-006
        Units: MWh/Dollar/(m*m*m) [4e-006,1e-005,2.5e-007]

Global Desalinated Water Supply=
                Fractional Usage of Desalination Capacity * Global
                Desalination Capacity
        Units: km*km*km/Year

Global Desalination Capacity= INTEG (
                Increase of Desalination Capacity,
                Initial Desalination Capacity)
        Units: km*km*km/Year

Groundwater Withdrawal Fraction= INTEG (
                Increase Rate of Groundwater Withdrawal,
                0.1)
        Units: 1/Year

Groundwater Withdrawals=
                Max Groundwater Withdrawal * Groundwater Withdrawal
                Fraction
        Units: km*km*km/Year
```

Historical Electricity Production= WITH LOOKUP (
            Time,([(1980,0)-
            (2005,1000)],(1980,56.43),(1981,179.52),(1982,340.04),(1983
            ,492.59),(1984,381.6),(1985,202.45),(1986,443.49),(1987,431
            .39),(1988,522),(1989,246.23),(1990,232.13),(1991,86.5),(19
            92,265.66),(1993,273.48),(1994,444.21),(1995,385.53),(1996,
            335.36),(1997,336.12),(1998,335.83),(1999,578.29),(2000,204
            .01),(2001,542.48),(2002,541.28),(2003,715.58)))
        Units: Billion kWh/Year

Increase in Production=
            IF THEN ELSE(Time < 1980, 251.3, IF THEN ELSE(Time > 2004,
            357.17, Historical Electricity Production))
        Units: Billion kWh/Year

Increase of Desalination Capacity=
            ((Water Stress Effects/Delay in Establishment of
            Desalination Facilities)*Global Desalination Capacity -
            (Water Stress Effects/Delay in Establishment of
            Desalination Facilities)*(Global Desalination
            Capacity^2)/Maximum Establishment of Desalination
            Facilities)
        Units: km*km*km/Year/Year

Increase Rate of Groundwater Withdrawal=
            IF THEN ELSE(Groundwater Withdrawal Fraction < 1,
            Groundwater Withdrawal Fraction*Water Stress Effects/Delay
            in Establishing Groundwater Pumps, IF THEN ELSE(Groundwater
            Withdrawal Fraction > 1, 1 - Groundwater Withdrawal
            Fraction, 0))
        Units: Dimensionless

Industrial Consumption Percentages[destination]=
            70, 0, 15, 15
        Units: percent

Industrial Structural Water Intensity=
            IF THEN ELSE(ISWI 1 > 100, 100, ISWI 1) + ISWI min
        Units: m*m*m/MWh

Initial Desalination Capacity=
                0.1
        Units: km*km*km/Year

Irrigated Area= INTEG (
            Expansion of Irrigation,
            Historical Irrigated Area*1e+006)
        Units: ha

ISWI 1=
            1/ (Gamma i*(GDP per Capita-(Init GDP per Capita-1)))
        Units: MWh/(m*m*m*Dollar)

ISWI min=
            15
        Units: m*m*m/MWh

```
Last Water Stress=
            DELAY FIXED(Water Stress Effects, TIME STEP, 0.1)
      Units: Dimensionless


Max Groundwater Withdrawal=
            8.4
      Units: km*km*km


Maximum Establishment of Desalination Facilities= 32.4
Units: km*km*km/Year


Municipal Water System Efficiency= WITH LOOKUP (
            Time,([(1960,0)-
            (2100,1)],(1960,1),(2000,0.92),(2005,0.9),(2025,0.75),(2050
            ,0.7),(2100,0.6) ))
      Units: Dimensionless


Per Capita Consumption=
            Base Domestic Consumption * Municipal Water System
            Efficiency * "Relative TFP A(t) change"
      Units: m*m*m/(person*Year)


Per Capita Withdrawal=
            Base Domestic Withdrawals * Standard of Living * "Relative
            TFP A(t) change"
      Units: (m*m*m)/person/Year


Per Hectare Consumption=
            (1-Base Returnable Water/100) * Base Specific Water Intake
            * Technological Change for Consumption in Agricultural
            Sector * Temperature Feedback
      Units: m*m*m/ha/Year


Per Hectare Withdrawals=
            Base Specific Water Intake * Technological Change for
            Withdrawals in Agricultural Sector * Temperature Feedback
      Units: m*m*m/ha/Year


Per MWh Consumption=
            Base Industrial Consumption * "Relative TFP A(t) change"
      Units: m*m*m/MWh


Per MWh Withdrawals=
            Base Industrial Withdrawals * "Relative TFP A(t) change"
      Units: m*m*m/MWh


Percent Domestic Withdrawal=
            84
      Units: percent


Percent Industrial Withdrawal= WITH LOOKUP (
            Time,([(1960,60)-(2100,100)],(1960,91),(1995,89),(2100,70)
            ))
      Units: percent


Percentage increase in irrigated area= WITH LOOKUP (
```

```
            Time,([[(1960,0)-
            (2100,5)],(1960,1.74072),(1969.9,1.741),(1970,1.58368),(197
            9.9,1.584),(1980,2.04794),(1989.9,2.048),(1990,0.806561),(1
            994.9,0.8512),(1995,0.851192),(2000,0.6),(2024.9,0.6),(2025
            ,0.4),(2049.9,0.4),(2050,0.3),(2100,0.3) ))
        Units: percent

sector: dom, ind, agr

Standard of Living=
            1
        Units: Dimensionless

Surface Water Consumption=
            Desired Surface Water Consumption + Evaporation from
            Reservoirs
        Units: km*km*km/Year

Surface Water Withdrawals=
            Desired Surface Water Withdrawals + Evaporation from
            Reservoirs
        Units: km*km*km/Year

Technological Change for Consumption in Agricultural Sector= WITH
LOOKUP
            (Time,([[(1960,0)-
            (2100,1)],(1960,1),(1980,0.99),(1990,0.95),(2010,0.9),(2025
            ,0.85),(2050,0.78),(2100,0.7) ))
        Units: Dimensionless

Technological Change for Withdrawals in Agricultural Sector= WITH
LOOKUP
            (Time,([[(1960,0)-
            (2100,1)],(1960,1),(1980,0.99),(1990,0.95),(2010,0.9),(2025
            ,0.85),(2050,0.78),(2100,0.7) ))
        Units: Dimensionless

Water Stress Effects= WITH LOOKUP (
            Water Stress Function Chooser,
            ([(0,0)-
            (2,1)],(0,0),(0.2,0.2),(0.4,0.4),(0.6,0.6),(0.8,0.7),(1,0.7
            8),(1.5,0.85),(2,0.9) ))
        Units: Dimensionless

"Withdrawals to Availability ratio incl. Pollution Effects"=
            Effective Desired Surface Water Withdrawal / Available
            Surface Water
        Units: Dimensionless
```

****

.HydroTreatmt

****

The equations for the model's water quality sector follow a set of figures that illustrate the model layout in Vensim. The four figures below focus on,

- Wastewater Treatment and Returnable Waters (Figure A-26);
- Treated Wastewater Reuse and Water Stress Calculation (Figure A-27);
- Additional Water Sources (Figure A-28); and,
- Important Output (Figure A-29).
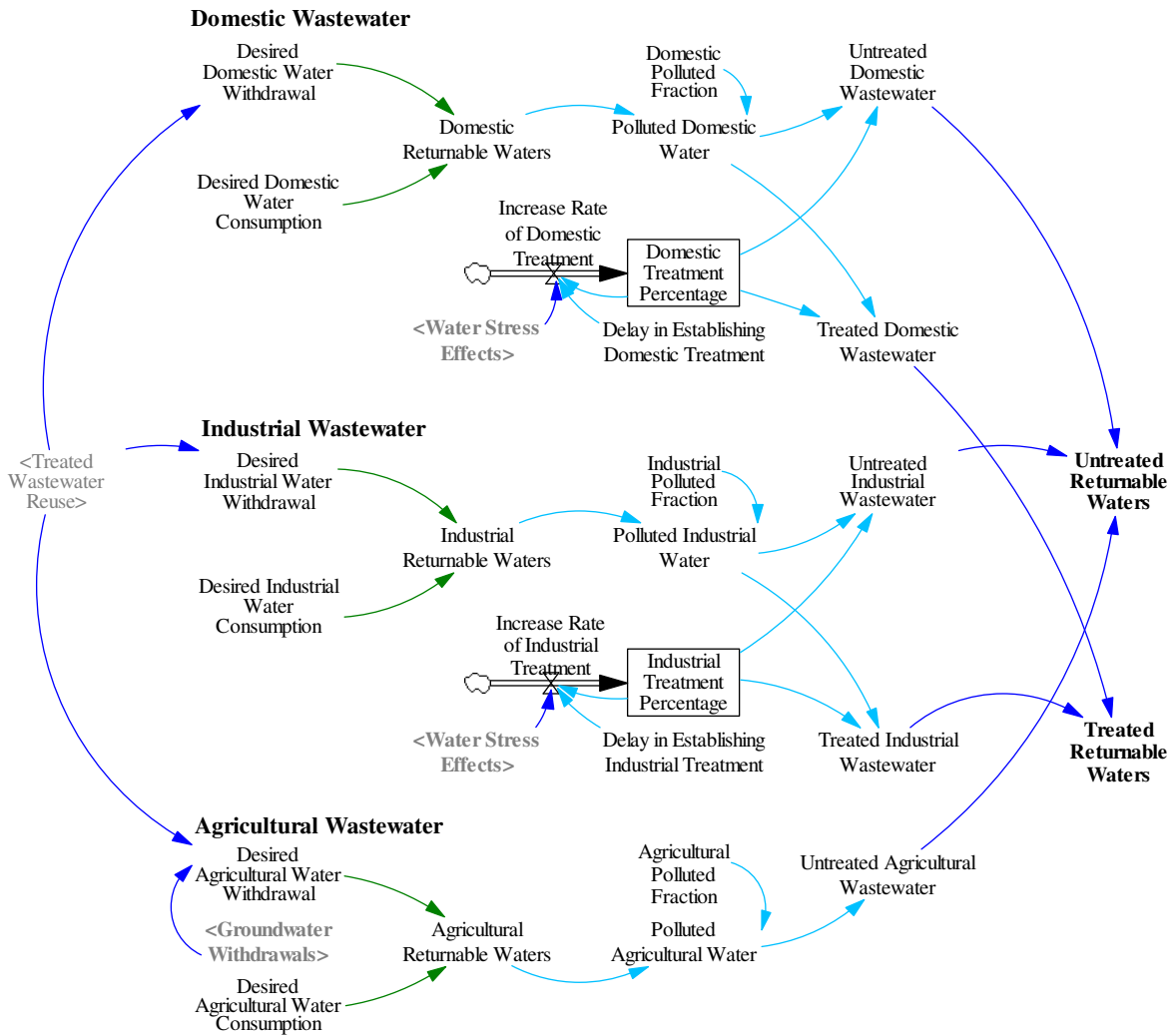
Figure A-26: Wastewater Treatment in Water Quality Sector

Wastewater Reuse Calculations

Delay in Instituting
Wastewater Reuse

Increase Rate of
Wastewater Reuse

Wastewater
Reuse
Percentage

Corrected Wastewater
Reuse Percentage

*Total Wastewater
Reuse*

<Water Stress
Effects>

Wastewater Reuse
Breakdown by
Sector

**Treated
Wastewater Reuse**

<TIME STEP>

<Treated
Returnable Waters>

Water Stress Calculation

Wastewater
Dillution
Requirement

**Effective Untreated
Returnable Waters**

<Untreated
Returnable Waters>

**Desired Surface
Water Withdrawals**

<Total Renewable
Flow>

**Available
Surface Water**

**Effective Desired
Surface Water
Withdrawal**

<Stable and Useable
Runoff Percentage>

<Desired Surface
Water
Withdrawals>

Base Water Stress

*Withdrawals to
Availability ratio incl.
Pollution Effects*

<Available Surface
Water>

**Water Stress
Effects**

Figure A-27: Wastewater Reuse and Water Stress Calculations in Water Quality Sector

Additional Water Supply

Initial Desalination
Capacity

Global
Desalination
Capacity

Fractional Usage of
Desalination Capacity

Increase of
Desalination
Capacity

**Global Desalinated
Water Supply**

Groundwater
Withdrawal
Fraction

Max Groundwater
Withdrawal

Increase Rate of
Groundwater
Withdrawal

**Groundwater
Withdrawals**

Delay in Establishment of
Desalination Facilities

<Water Stress
Effects>

Delay in Establishing
Groundwater Pumps

<Water Stress
Effects>

Maximum Establishment
of Desalination Facilities

**Figure A-28: Additional Water Sources in the Water Quality Sector: Desalination and Groundwater
Pumping**

Useful Output
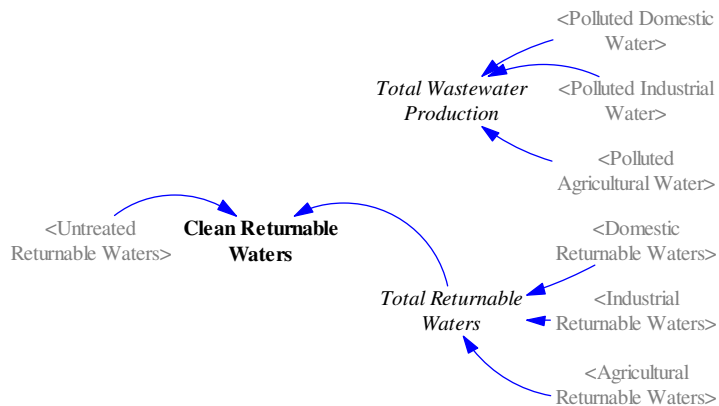
Figure A-29: Useful Output from Water Quality Sector

```
Agricultural Polluted Fraction=
          80
     Units: percent

Agricultural Returnable Waters=
          Desired Agricultural Water Withdrawal – Desired
          Agricultural Water Consumption
     Units: km*km*km/Year

Clean Returnable Waters=
          Total Returnable Waters – Untreated Returnable Waters
     Units: km*km*km/Year

Corrected Wastewater Reuse Percentage=
          IF THEN ELSE(Wastewater Reuse Percentage <= 100, Wastewater
          Reuse Percentage, 100)
     Units: percent

Delay in Establishing Domestic Treatment=
          IF THEN ELSE(Time >= 2005, Dom Treat Delay, 30)
     Units: Year

Delay in Establishing Industrial Treatment=
          IF THEN ELSE(Time >= 2005, Ind Treat Delay, 75)
     Units: Year

Delay in Instituting Wastewater Reuse=
          20
     Units: Year

Domestic Polluted Fraction=
          100
     Units: percent

Domestic Returnable Waters=
```
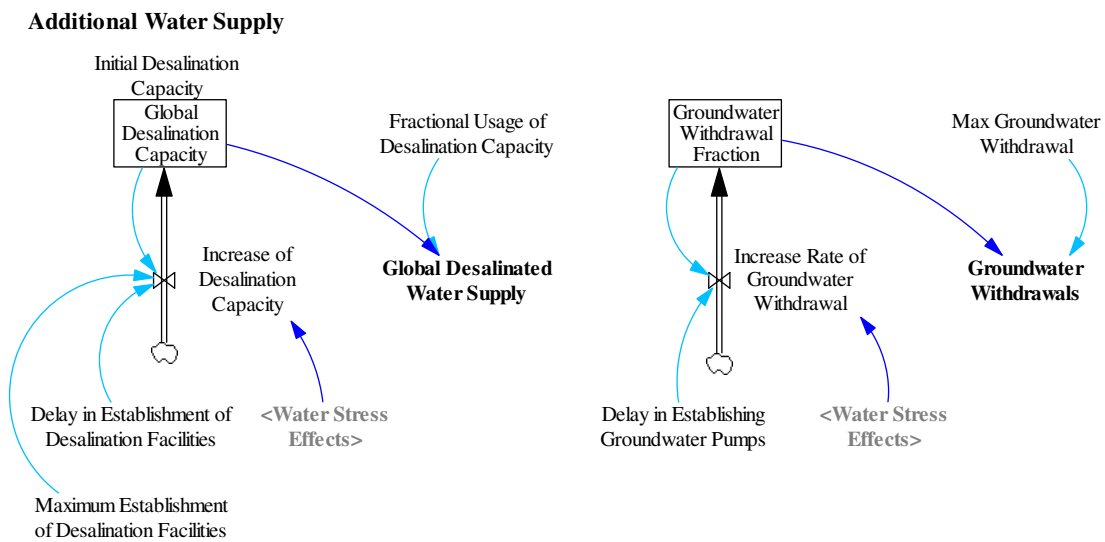
```
            Desired Domestic Water Withdrawal – Desired Domestic Water
            Consumption
     Units: km*km*km/Year


Domestic Treatment Percentage= INTEG (
            Increase Rate of Domestic Treatment,
            25)
     Units: percent


Effective Desired Surface Water Withdrawal=
            Desired Surface Water Withdrawals – Untreated Returnable
            Waters + Effective Untreated Returnable Waters
     Units: km*km*km/Year


Effective Untreated Returnable Waters=
            Wastewater Dillution Requirement * Untreated Returnable
            Waters
     Units: km*km*km/Year


Increase Rate of Domestic Treatment=
            IF THEN ELSE(Domestic Treatment Percentage < 100, Domestic
            Treatment Percentage*Water Stress Effects/Delay in
            Establishing Domestic Treatment, IF THEN ELSE(Domestic
            Treatment Percentage > 100, 100 – Domestic Treatment
            Percentage, 0))
     Units: percent/Year


Increase Rate of Industrial Treatment=
            IF THEN ELSE(Industrial Treatment Percentage < 100,
            Industrial Treatment Percentage*Water Stress Effects/Delay
            in Establishing Industrial Treatment, IF THEN
            ELSE(Industrial Treatment Percentage > 100, 100 –
            Industrial Treatment Percentage, 0))
     Units: percent/Year


Increase Rate of Wastewater Reuse=
            IF THEN ELSE(Wastewater Reuse Percentage < 100, Wastewater
            Reuse Percentage*Water Stress Effects/Delay in Instituting
            Wastewater Reuse, IF THEN ELSE(Wastewater Reuse Percentage
            > 100, 100 – Wastewater Reuse Percentage, 0))
     Units: percent/Year


Industrial Polluted Fraction=
            42
     Units: percent


Industrial Returnable Waters=
            Desired Industrial Water Withdrawal – Desired Industrial
            Water Consumption
     Units: km*km*km/Year


Industrial Treatment Percentage= INTEG (
            Increase Rate of Industrial Treatment,
            40)
     Units: percent


Polluted Agricultural Water=
```

```
                (Agricultural Polluted Fraction/100) * Agricultural
                Returnable Waters
        Units: km*km*km/Year


Polluted Domestic Water=
                (Domestic Polluted Fraction/100) * Domestic Returnable
                Waters
        Units: km*km*km/Year


Polluted Industrial Water=
                (Industrial Polluted Fraction/100) * Industrial Returnable
                Waters
        Units: km*km*km/Year


Total Returnable Waters=
                Domestic Returnable Waters + Industrial Returnable Waters +
                Agricultural Returnable Waters
        Units: km*km*km/Year


Total Wastewater Reuse=
                SUM(Treated Wastewater Reuse[sector!])
        Units: km*km*km/Year


Treated Domestic Wastewater=
                (Domestic Treatment Percentage/100) * Polluted Domestic
                Water
        Units: km*km*km/Year


Treated Industrial Wastewater=
                (Industrial Treatment Percentage/100) * Polluted Industrial
                Water
        Units: km*km*km/Year


Treated Returnable Waters=
                Treated Domestic Wastewater + Treated Industrial Wastewater
        Units: km*km*km/Year


Treated Wastewater Reuse[sector]= DELAY FIXED (
                (Corrected Wastewater Reuse Percentage/100) * (Wastewater
                Reuse Breakdown by Sector[sector]/100) * Treated Returnable
                Waters, TIME STEP, 1)
        Units: km*km*km/Year


Untreated Agricultural Wastewater=
                Polluted Agricultural Water
        Units: km*km*km/Year


Untreated Domestic Wastewater=
                (1 - (Domestic Treatment Percentage/100)) * Polluted
                Domestic Water
        Units: km*km*km/Year


Untreated Industrial Wastewater=
                (1 - (Industrial Treatment Percentage/100)) * Polluted
                Industrial Water
        Units: km*km*km/Year
```

```
Untreated Returnable Waters=
          Untreated Domestic Wastewater + Untreated Industrial
          Wastewater + Untreated Agricultural Wastewater
     Units: km*km*km/Year

Wastewater Dillution Requirement=
          9
     Units: Dimensionless

Wastewater Reuse Breakdown by Sector[sector]=
          10, 30, 60
     Units: percent

Wastewater Reuse Percentage= INTEG (
          Increase Rate of Wastewater Reuse, 5)
     Units: percent
```
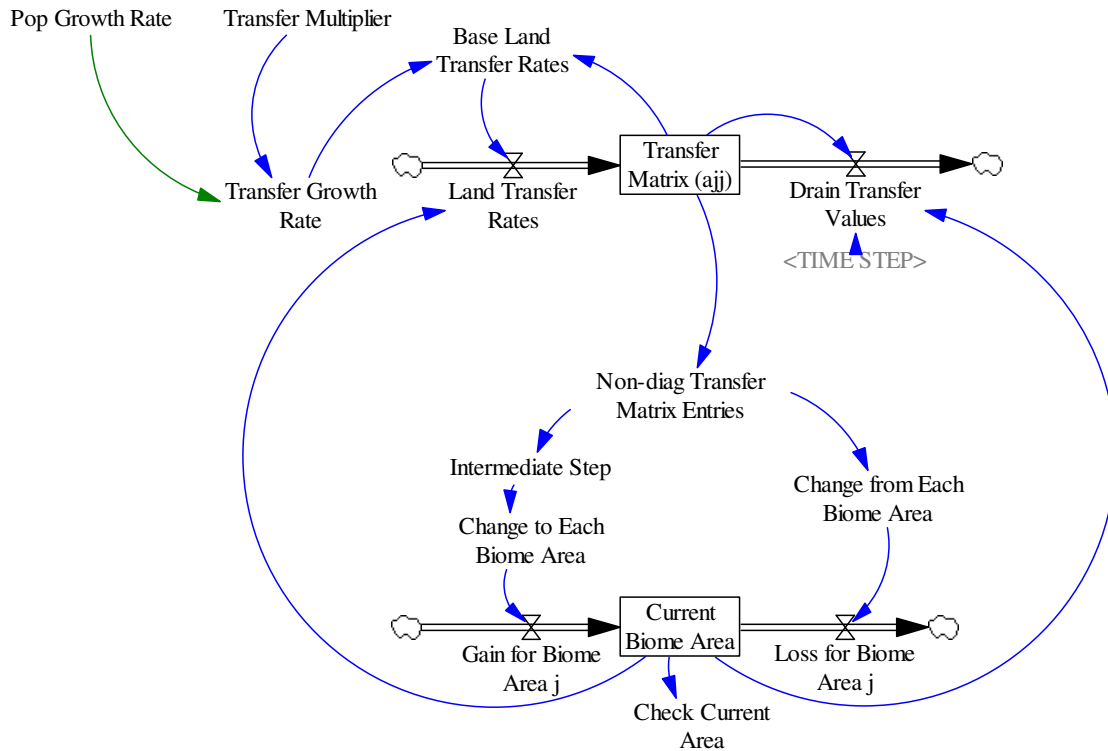
****

.Land

****

The equations for the model's land-use and land-use change sector follow Figure A-30, which illustrates the model layout in Vensim.

Figure A-30: Stocks, Flows, and Variables in Land-use Sector

```
Base Land Transfer Rates[j,q]=
        IF THEN ELSE(j = q, IF THEN ELSE(Transfer Growth Rate >=
        0.01, "Transfer Matrix (ajj)"[j,q]*(((100*Transfer Growth
        Rate)^0.5)/100), "Transfer Matrix (ajj)"[j,q]
        *(((1000*Transfer Growth Rate)^0.5)/1000)), "Transfer
        Matrix (ajj)"[j,q] * (Transfer Growth Rate))
    Units: Mha/Year

"Base Non-diag Transfer Matrix Entries"[j,q]=
        IF THEN ELSE(j=q, 0, "Transfer Matrix (ajj)"[j,q])
    Units: Mha/Year

Biome Area[j]=
        IF THEN ELSE(Current Biome Area[j] > 0, Current Biome
        Area[j] * 1e+010, 0)
    Units: Dimensionless

Change from Each Biome Area[j]=
        SUM("Non-diag Transfer Matrix Entries"[j,q!])
    Units: Mha/Year

Change to Each Biome Area[j]=
        Intermediate Step[q]
```

```
        Units: Mha/Year


Current Biome Area[j]= INTEG (
           Gain for Biome Area j[j] – Loss for Biome Area j[j],
           Init Biome Area[j]/1e+010)
      Units: Mha


Drain Transfer Values[j,q]=
           IF THEN ELSE(Current Biome Area[j] <= 0,
           "Transfer Matrix(ajj)"[j,q]/TIME STEP, 0)
      Units: Mha/Year


Gain for Biome Area j[j]=
           Change to Each Biome Area[j]
      Units: Mha/Year


Init Biome Area[j]=
           3.814e+013, 1.729e+013, 1.782e+013, 1.631e+013, 1.51e+012,
           3.003e+013
      Units: Meter*Meter


"Init Transfer Matrix (ajj)"[j,q]=
           11.305,0,4.023,4.023,0.335,0;  0,1.507,0.67,0,0.335,0;
           0,0,301.47,0,0.67,0;  0,0,0,301.47,0.67,0;  0,0,0,0,0,0;
           0,0,0,1.341,0,0;
      Units: Mha/Year


Intermediate Step[q]=
           SUM("Non-diag Transfer Matrix Entries"[j!,q])
      Units: Mha/Year


Land Conversion by Biome[j]=
           ((1 – Epsilon k[k1]) * "Sigma (Bjk)"[j,k1] * SUM("Non-diag
           Transfer Matrix Entries"[j,q!]) * 1e-005) + ((1 – Epsilon
           k[k2]) * "Sigma (Bjk)"[j,k2] * SUM("Non-diag Transfer
           Matrix Entries"[j,q!]) * 1e-005) + ((1 – Epsilon k[k3] –
           Stem to H) * "Sigma (Bjk)"[j,k3] * SUM("Non-diag Transfer
           Matrix Entries"[j,q!]) * 1e-005) + ((1 – Epsilon L) *
           "Sigma (Lj)"[j] * SUM("Non-diag Transfer Matrix
           Entries"[j,q!]) * 1e-005)
      Units: Gt C/Year


Land Transfer Rates[j,q]=
           IF THEN ELSE(Current Biome Area[j] > 0, Base Land Transfer
           Rates[j,q], 0)
      Units: Mha/Year/Year


Loss for Biome Area j[j]=
           Change from Each Biome Area[j]
      Units: Mha/Year


"Non-diag Transfer Matrix Entries"[j,q]=
           IF THEN ELSE(j=q, 0, "Transfer Matrix (ajj)"[j,q])
      Units: Mha/Year


q: (q1-q6) -> j
```

```
Total Land Conversion=
          SUM(Land Conversion by Biome[j!])
     Units: Gt C/Year

Transfer Growth Rate=
          Pop Growth Rate*Transfer Multiplier
     Units: Dimensionless

"Transfer Matrix (ajj)"[j,q]= INTEG (
          +Land Transfer Rates[j,q]-Drain Transfer Values[j,q],
          "Init Transfer Matrix (ajj)"[j,q])
     Units: Mha/Year

Transfer Multiplier= 1
     Units: Dimensionless
```

****
.Population
****

The equations for the model's population sector follow Figure A-31, which illustrates the model layout in Vensim.

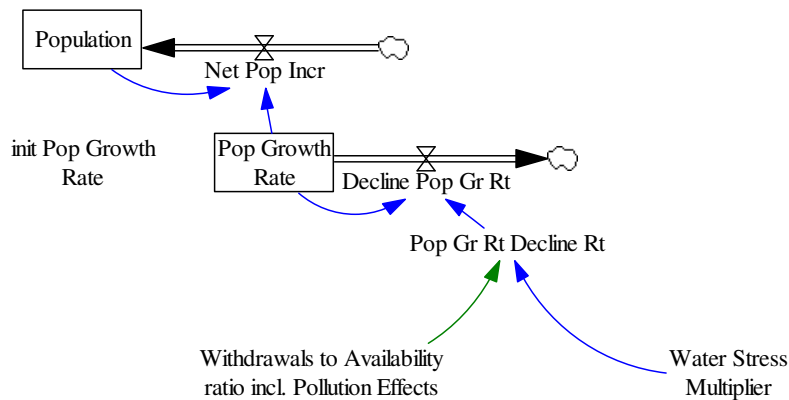**Figure A-31: Stocks, Flows, and Variables in Population Sector**

```
Decline Pop Gr Rt=
          Pop Growth Rate*Pop Gr Rt Decline Rt
     Units: 1/Year/Year

init Pop Growth Rate=
          0.0224
```

```
        Units: 1/Year

Net Pop Incr =
            Population*Pop Growth Rate
        Units: person/Year

Pop Gr Rt Decline Rt=
            Water Stress Multiplier*"Withdrawals to Availability ratio
            incl. Pollution Effects"
        Units: 1/Year

Pop Growth Rate= INTEG (
            - Decline Pop Gr Rt,
            init Pop Growth Rate)
        Units: 1/Year

Population= INTEG (
            Net Pop Incr,
            3.02e+009)
        Units: person

Water Stress Multiplier=
            0.025
        Units: Dimensionless
```

APPENDIX B: CONTENTS OF MODEL CD-ROM

A CD-ROM, which is available from the authors by request, contains a set of models that can be used to reproduce the experimental data described in Davies (2007), the experimental data sets themselves, and the Vensim software required to run the model. Refer to Appendix A for more information on how to use Vensim DSS and the Vensim Model Reader – although Appendix A focuses on Vensim DSS, most of the commands and tools described there apply to the Model Reader as well.

1.   CD-ROM Layout

The CD-ROM contains a hierarchy of folders, as listed below:

- Vensim Installation Software
    - Model Reader
    - Vensim PLE
- Models
    - Complete Model
        - For Use with Model Reader
        - For Use with Vensim DSS
        - Calibration and Validation Version
    - Experimental Data Sets
    - Models for Experiments 1 to 24 (see Davies, 2007)
        - Models for Model Reader
        - Models for Vensim DSS

Vensim Model Reader software is included so that users can open and explore the supplied experimental data and run the models supplied here. Installation instructions are provided in the 'Model Reader' folder.

Vensim PLE is included so that users can familiarize themselves with the basic functionality of Vensim – and system dynamics-based – software. The user guide included with Vensim PLE is comprehensive and many different example models are

included in the software. Installation instructions are included in the 'Vensim PLE' folder. Note that the use of Vensim PLE software is free-of-charge for academic use. We suggest, however, that readers who plan to make more extensive use of the software register with Ventana Systems, Inc., at http://www.vensim.com.

Otherwise, most of the folder contents are clear from the titles. Clearly, readers without a licensed copy of Vensim DSS should install the Model Reader and then focus only on the 'Model Reader'-related folders, while readers with Vensim DSS should use the folders intended for Vensim DSS users. The contents of these version-specific folders are identical except for the version of Vensim required in their use.

- In the 'Complete Model' folder, a generic version of the model is provided for each Vensim version. This generic version has been tidied and documented more clearly than the version used in the experimentation. It lacks non-critical parameters, output variables, and 'logical switches' – see Appendix B for the list of all variables used in the experimentation version. Use this model version to generate the 'base run' data set. The model in the 'Calibration and Validation Version' can only be opened with Vensim DSS. It is what its name suggests, and it has a more complete set of error-checking variables, logical switches, and so on.
- In the "Models for Expts. 1 to 24" folder are twenty-two different versions of the model in both 'Model Reader' and 'Vensim DSS' format, one for each of the experiments described in Chapter 4 of Davies (2007), except for the two sensitivity analysis experiments (the Model Reader cannot perform a sensitivity analysis). Clicking on the 'Run Simulation' button – see Appendix B – will generate the same data output as contained in the 'Experimental Data Sets' folder.

Experimental data in the 'Experimental Data Sets' folder are identical to those used in Davies (2007). Their contents are accessible only *via Vensim software*, through the control panel described in Chapter 3, above.

APPENDIX C: PREVIOUS REPORTS IN THE SERIES

1. Slobodan P. Simonovic (2001). Assessment of the Impact of Climate Variability and Change on the Reliability, Resiliency and Vulnerability of Complex Flood Protection Systems. Water Resources Research Report no. 038, Facility for Intelligent Decision Support, Department of Civil and Environmental Engineering, London, Ontario, Canada, 91 pages. ISBN: (print) 978-0-7714-2606-3; (online) 978-0-7714-2607-0.

2. Predrag Prodanovic (2001). Fuzzy Set Ranking Methods and Multiple Expert Decision Making. Water Resources Research Report no. 039, Facility for Intelligent Decision Support, Department of Civil and Environmental Engineering, London, Ontario, Canada, 68 pages. ISBN: (print) 978-0-7714-2608-7; (online) 978-0-7714-2609-4.

3. Nirupama and Slobodan P. Simonovic (2002). Role of Remote Sensing in Disaster Management. Water Resources Research Report no. 040, Facility for Intelligent Decision Support, Department of Civil and Environmental Engineering, London, Ontario, Canada, 107 pages. ISBN: (print) 978-0-7714-2610-0; (online) 978-0-7714-2611-7.

4. Taslima Akter and Slobodan P. Simonovic (2002). A General Overview of Multiobjective Multiple-Participant Decision Making for Flood Management. Water Resources Research Report no. 041, Facility for Intelligent Decision Support, Department of Civil and Environmental Engineering, London, Ontario, Canada, 65 pages. ISBN: (print) 978-0-7714-2612-4; (online) 978-0-7714-2613-1.

5. Nirupama and Slobodan P. Simonovic (2002). A Spatial Fuzzy Compromise Approach for Flood Disaster Management. Water Resources Research Report no. 042, Facility for Intelligent Decision Support, Department of Civil and Environmental Engineering, London, Ontario, Canada, 138 pages. ISBN: (print) 978-0-7714-2614-8; (online) 978-0-7714-2615-5.

6. K. D. W. Nandalal and Slobodan P. Simonovic (2002). State-of-the-Art Report on Systems Analysis Methods for Resolution of Conflicts in Water Resources Management. Water Resources Research Report no. 043, Facility for Intelligent Decision Support, Department of Civil and Environmental Engineering, London, Ontario, Canada, 216 pages. ISBN: (print) 978-0-7714-2616-2; (online) 978-0-7714-2617-9.

7. K. D. W. Nandalal and Slobodan P. Simonovic (2003). Conflict Resolution Support System – A Software for the Resolution of Conflicts in Water Resource Management. Water Resources Research Report no. 044, Facility for Intelligent

Decision Support, Department of Civil and Environmental Engineering, London, Ontario, Canada, 144 pages. ISBN: (print) 978-0-7714-2618-6; (online) 978-0-7714-2619-3.

8. Ibrahim El-Baroudy and Slobodan P. Simonovic (2003). New Fuzzy Performance Indices for Reliability Analysis of Water Supply Systems. Water Resources Research Report no. 045, Facility for Intelligent Decision Support, Department of Civil and Environmental Engineering, London, Ontario, Canada, 90 pages. ISBN: (print) 978-0-7714-2620-9; (online) 978-0-7714-2621-6.

9. Juraj Cunderlik (2003). Hydrologic Model Selection for the CFCAS Project: Assessment of Water Resources Risk and Vulnerability to Changing Climatic Conditions. Water Resources Research Report no. 046, Facility for Intelligent Decision Support, Department of Civil and Environmental Engineering, London, Ontario, Canada, 40 pages. ISBN: (print) 978-0-7714-2622-3; (online) 978-0-7714-2623-0.

10. Juraj Cunderlik and Slobodan P. Simonovic (2004). Selection of Calibration and Verification Data for the HEC-HMS Hydrologic Model. Water Resources Research Report no. 047, Facility for Intelligent Decision Support, Department of Civil and Environmental Engineering, London, Ontario, Canada, 29 pages. ISBN: (print) 978-0-7714-2624-7; (online) 978-0-7714-2625-4.

11. Juraj Cunderlik and Slobodan P. Simonovic (2004). Calibration, Verification and Sensitivity Analysis of the HEC-HMS Hydrologic Model. Water Resources Research Report no. 048, Facility for Intelligent Decision Support, Department of Civil and Environmental Engineering, London, Ontario, Canada, 113 pages. ISBN: (print) 978-0-7714-2626-1; (online) 978-0-7714-2627-8.

12. Predrag Prodanovic and Slobodan P. Simonovic (2004). Generation of Synthetic Design Storms for the Upper Thames River basin. Water Resources Research Report no. 049, Facility for Intelligent Decision Support, Department of Civil and Environmental Engineering, London, Ontario, Canada, 20 pages. ISBN: (print) 978-0-7714-2628-5; (online) 978-0-7714-2629-2.

13. Ibrahim El-Baroudy and Slobodan P. Simonovic (2005). Application of the Fuzzy Performance Indices to the City of London Water Supply System. Water Resources Research Report no. 050, Facility for Intelligent Decision Support, Department of Civil and Environmental Engineering, London, Ontario, Canada, 137 pages. ISBN: (print) 978-0-7714-2630-8; (online) 978-0-7714-2631-5.

14. Ibrahim El-Baroudy and Slobodan P. Simonovic (2006). A Decision Support System for Integrated Risk Management. Water Resources Research Report no. 051, Facility for Intelligent Decision Support, Department of Civil and Environmental Engineering, London, Ontario, Canada, 146 pages. ISBN: (print) 978-0-7714-2632-2; (online) 978-0-7714-2633-9.

15. Predrag Prodanovic and Slobodan P. Simonovic (2006). Inverse Flood Risk Modelling of The Upper Thames River Basin. Water Resources Research Report no. 052, Facility for Intelligent Decision Support, Department of Civil and Environmental Engineering, London, Ontario, Canada, 163 pages. ISBN: (print) 978-0-7714-2634-6; (online) 978-0-7714-2635-3.

16. Predrag Prodanovic and Slobodan P. Simonovic (2006). Inverse Drought Risk Modelling of The Upper Thames River Basin. Water Resources Research Report no. 053, Facility for Intelligent Decision Support, Department of Civil and Environmental Engineering, London, Ontario, Canada, 252 pages. ISBN: (print) 978-0-7714-2636-0; (online) 978-0-7714-2637-7.

17. Predrag Prodanovic and Slobodan P. Simonovic (2007). Dynamic Feedback Coupling of Continuous Hydrologic and Socio-Economic Model Components of the Upper Thames River Basin. Water Resources Research Report no. 054, Facility for Intelligent Decision Support, Department of Civil and Environmental Engineering, London, Ontario, Canada, 437 pages. ISBN: (print) 978-0-7714-2638-4; (online) 978-0-7714-2639-1.

18. Subhankar Karmakar and Slobodan P. Simonovic (2007). Flood Frequency Analysis Using Copula with Mixed Marginal Distributions. Water Resources Research Report no. 055, Facility for Intelligent Decision Support, Department of Civil and Environmental Engineering, London, Ontario, Canada, 144 pages. ISBN: (print) 978-0-7714-2658-2; (online) 978-0-7714-2659-9.

19. Jordan Black, Subhankar Karmakar and Slobodan P. Simonovic (2007). A Web-Based Flood Information System. Water Resources Research Report no. 056, Facility for Intelligent Decision Support, Department of Civil and Environmental Engineering, London, Ontario, Canada, 133 pages. ISBN: (print) 978-0-7714-2660-5; (online) 978-0-7714-2661-2.

20. Angela Peck, Subhankar Karmakar and Slobodan P. Simonovic (2007). Physical, Economical, Infrastructural and Social Flood Risk – Vulnerability Analyses in GIS. Water Resources Research Report no. 057, Facility for Intelligent Decision Support, Department of Civil and Environmental Engineering, London, Ontario, Canada, 80 pages. ISBN: (print) 978-0-7714-2662-9; (online) 978-0-7714-2663-6.

21. Predrag Prodanovic and Slobodan P. Simonovic (2007). Development of Rainfall Intensity Duration Frequency Curves for the City of London Under the Changing Climate. Water Resources Research Report no. 058, Facility for Intelligent Decision Support, Department of Civil and Environmental Engineering, London, Ontario, Canada, 51 pages. ISBN: (print) 978-0-7714-2667-4; (online) 978-0-7714-2668-1.